AD-752 369

SYMPOSIUM ON RANDOM LOAD FATIGUE

Advisory Group for Aerospace Research and Development
Paris, France

October 1972

AGARD-CP-118

AGARD

ADVISORY GROUP FOR AEROSPACE RESEARCH & DEVELOPMENT

7 RUE ANCELLE 92200 NEUILLY SUR SEINE FRANCE

AGARD CONFERENCE PROCEEDINGS No. 118

Symposium on
Random Load Fatigue

NORTH ATLANTIC TREATY ORGANIZATION

**DISTRIBUTION AND AVAILABILITY
ON BACK COVER**

Fatigue test procedures are discussed and comparison is made with service failures with a description of critical factors such as varying load spectra, differences in random load-time histories, spectrum changes during the life of an aircraft, etc.

Methods for predicting the fatigue life of aircraft structures are reviewed and recent achievements for improved life estimation are reported.

Papers presented at the Structures and Materials Panel 24th Meeting held in Lyngby, Denmark, 13 April 1972.

Fatigue test procedures are discussed and comparison is made with service failures with a description of critical factors such as varying load spectra, differences in random load-time histories, spectrum changes during the life of an aircraft, etc.

Methods for predicting the fatigue life of aircraft structures are reviewed and recent achievements for improved life estimation are reported.

Papers presented at the Structures and Materials Panel 34th Meeting held in Lyngby, Denmark, 13 April 1972.

Fatigue test procedures are discussed and comparison is made with service failures with a description of critical factors such as varying load spectra, differences in random load-time histories, spectrum changes during the life of an aircraft, etc.

Methods for predicting the fatigue life of aircraft structures are reviewed and recent achievements for improved life estimation are reported.

Papers presented at the Structures and Materials Panel 34th Meeting held in Lyngby, Denmark, 13 April 1972.

Fatigue test procedures are discussed and comparison is made with service failures with a description of critical factors such as varying load spectra, differences in random load-time histories, spectrum changes during the life of an aircraft, etc.

Methods for predicting the fatigue life of aircraft structures are reviewed and recent achievements for improved life estimation are reported.

Papers presented at the Structures and Materials Panel 34th Meeting held in Lyngby, Denmark, 13 April 1972.

AGARD Conference Proceedings No.118
North Atlantic Treaty Organization, Advisory Group
for Aerospace Research and Development
SYMPOSIUM ON RANDOM LOAD FATIGUE
Published October 1972
246 pages

Eight papers were presented at this Symposium.
Physical aspects of fatigue damage accumulation and
the significance of theories for the calculation of
fatigue damage accumulation are reviewed. Influence
of test frequencies on crack propagation rates,
measurements of residual stresses in notched speci-
mens, etc. are reported.

P.T.O

AGARD-CP-118
539.43

AGARD Conference Proceedings No.118
North Atlantic Treaty Organization, Advisory Group
for Aerospace Research and Development
SYMPOSIUM ON RANDOM LOAD FATIGUE
Published October 1972
246 pages

Eight papers were presented at this Symposium.
Physical aspects of fatigue damage accumulation and
the significance of theories for the calculation of
fatigue damage accumulation are reviewed. Influence
of test frequencies on crack propagation rates,
measurements of residual stresses in notched speci-
mens, etc. are reported.

P.T.O.

AGARD-CP-118
539.43

NORTH ATLANTIC TREATY ORGANIZATION

ADVISORY GROUP FOR AEROSPACE RESEARCH AND DEVELOPMENT

(ORGANISATION DU TRAITE DE L'ATLANTIQUE NORD)

AGARD Conference Proceedings No.118

SYMPOSIUM ON RANDOM LOAD FATIGUE

THE MISSION OF AGARD

The mission of AGARD is to bring together the leading personalities of the NATO nations in the fields of science and technology relating to aerospace for the following purposes:

-- Exchanging of scientific and technical information;

-- Continuously stimulating advances in the aerospace sciences relevant to strengthening the common defence posture;

— Improving the co-operation among member nations in aerospace research and development;

— Providing scientific and technical advice and assistance to the North Atlantic Military Committee in the field of aerospace research and development;

— Rendering scientific and technical assistance, as requested, to other NATO bodies and to member nations in connection with research and development problems in the aerospace field.

— Providing assistance to member nations for the purpose of increasing their scientific and technical potential;

— Recommending effective ways for the member nations to use their research and development capabilities for the common benefit of the NATO community.

The highest authority within AGARD is the National Delegates Board consisting of officially appointed senior representatives from each Member Nation. The mission of AGARD is carried out through the Panels which are composed for experts appointed by the National Delegates, the Consultant and Exchange Program and the Aerospace Applications Studies Program. The results of AGARD work are reported to the Member Nations and the NATO Authorities through the AGARD series of publications of which this is one.

Participation in AGARD activities is by invitation only and is normally limited to citizens of the NATO nations.

PREFACE

A one day symposium on random load fatigue was held at the 34th meeting of the Structures and Materials Panel in Lyngby, Denmark. Eight lectures were delivered dealing with different aspects of fatigue damage and fatigue testing under random loading. The lectures were presented in English and were followed by vivid discussions.

I had the privilege to chair this symposium and it is my duty and pleasure to thank all speakers for their thoroughly prepared presentations and their cooperation in keeping the time schedule which made the task of the chairman easy.

The local organization of the symposium was in the capable hands of Dr Viggo Tvergaard and other members of the Department of Solid Mechanics at the Technical University of Denmark and I express my appreciation for their devoted work.

Finally, I should like to thank the Structures and Materials Panel of AGARD for sponsoring this symposium on our recommendation.

Frithiof Niordson
Symposium Chairman

iii

CONTENTS

A SHORT SURVEY ON POSSIBILITIES OF FATIGUE LIFE ASSESSMENT OF AIRCRAFT STRUCTURES BASED ON RANDOM OR PROGRAMMED FATIGUE TESTS

By

W. Barrois
Military Chief Engineer (Retired)
Engineer at the Société Nationale Industrielle Aérospatiale
Aircraft Division
Paris, France

SUMMARY

The survey is an attempt to answer the question: "What information is needed in terms of load spectrum and test conditions, to extend the results of laboratory tests to the prediction of service fatigue life of aircraft structures?". After considering designers' needs and detailing the various physical parameters that are significant in the fatigue behaviour of specimens and structures, several types of fatigue tests are reviewed from the view point of their representativeness. A short survey is then made of the present prediction methods of structure fatigue life from fatigue tests of components, assemblies and structures undergoing constant amplitude loadings. Then, after considering fatigue tests under programmed loadings, the case of random loadings is briefly discussed. It is concluded that describing random loadings by their root mean squares is not sufficient to predict the fatigue lives of structures even when the shape of the load power spectrum is known, except in cases of comparative prediction where the only change is the general intensity of the spectrum. The possibility of test acceleration by increasing the general loading intensity is considered. The necessity of a more complete treatment of every partial result of structural fatigue tests is emphasized as well as the usefulness of broad co-operation in this field in order to extend the amount of fatigue data able to be used by designers.

1. INTRODUCTION

For several years, problems in acoustic fatigue and those implied by aircraft dynamic responses to random loadings defined by power spectra, have drawn attention of designers to possibilities of fatigue life assessment from results of fatigue tests under programmed or random loadings that simulate actual random loadings in flight. In these tests, the stress spectrum shapes in relation to statistical frequencies of occurrence and dynamical frequencies may be quite different either due to different excitations or to very different structural responses. Intensity of every loading is defined either by the maximum load or by the quadratic mean load.

Often, these tests are carried out only for purposes of fatigue strength substantiation of particular structures. Their possible use in fatigue life prediction of other structures may entail extensive tests on simple components or elementary assemblies. Before planning costly tests, it may be useful to study how such results might be used by designers.

That leads to the necessity to define designer's requirements and to review briefly fatigue prediction methods using results of conventional tests under constant amplitude loadings, and then to consider two cases of random fatigue tests, either in fatigue at low frequencies or with frequencies within the acoustic range.

2. NEEDS OF THE DESIGNER

In a previous survey[1], we have attempted to show that for technical reasons and due to fundamental and physical causes, it is difficult to assess fatigue life of an aircraft structure sufficiently accurately through elasticity analysis and allowable stress design values related to the particular material. Useful analyses consist only of comparative or interpolative computations based on fatigue test results of structures, assemblies or components. However, even within this restricted field, the computation size is often a heavy burden in practice. Various analytical methods of increasing complexity have been proposed. In order to assess their practical usefulness, two kinds of distinction have to be made:

(i) Firstly, certain methods quickly yield a rough classification of assemblies; they may supply a provisional assessment at the preliminary design stage, at the expense of costly previous analyses on a large number of fatigue test results on actual and similar structures, or assemblies made from the same material through the same manufacturing processes. On the contrary, other more analytical methods imply computations that are tailored for each particular case but can be used only when detailed drawings are available.

(ii) Secondly, the selected method and its degree of accuracy must correspond to the particular needs of the designer.

At the *preliminary design stage*, assembly modes and manufacturing processes that entail the minimum of fatigue problems and a design with geometries that make possible further local reinforcements the incorporatic 1 of which do not imply extended design changes, would be selected. In addition. the structure must be "fail-safe" against fatigue or other causes of damage. The fail-safe requirement may lead to vital attachment being oversize locally, such that the fatigue problem disappears.

At the *prototype design stage*, a *first comparative analysis* should supply a rough classification of the various assembly areas of the structure according to the following degrees of decreasing fatigue strength:

- certainly sufficient,
- doubtful,
- certainly insufficient.

Areas of "certainly insufficient" strength should precipitate immediate design changes. "Doubtful" areas should be assessed again by means of another more accurate computation based on previous fatigue tests. In case of a doubt persisting, development tests on representative assemblies or partial structures should be carried out under the estimated particular loading programme of the aircraft.

At the *production design stage*, an *interpretative third analysis* on development test results might take account of changes in aircraft loading, weights and performances, design and sizing, since the prototype stage. Moreover, some areas previously classified as sufficiently strong may become doubtful, and other development tests should be carried out and analyzed by means of a previously demonstrated computation method.

Finally, after the *full-scale fatigue tests*, interpretative computations are necessary in order to substantiate the fatigue evaluation of operational aircraft, taking into account the latest design changes and inflight load measurements performed in actual operations on the first operational airplanes.

Designers' needs may be summarized as follows:

Interpretative computations that enable re-assessment to be made of the fatigue life of a structure for a new loading programme significantly different from the testing programme.

"A priori" subjective classification of fatigue strength of structural assembly areas with respect to the fatigue strength of structures previously known to be sufficient or insufficient. This implies computations that define the fatigue quality of each structure tested and the quality needed to withstand the particular loading programme that corresponds to the aircraft studied and to its foreseen operational use.

Prediction analysis should take into account detail shapes and sizing. Computations of local stresses near stress raisers and assessment of the allowable intensity value of the load spectrum are needed. Empirical coefficients to use in computations would be obtained by the same computation methods from test results of simple assemblies representative of stress raisers and of current design of joints.

3. REPRESENTATIVENESS OF FATIGUE TESTS

In order to study the possibilities of assessing life in service from test results it is first fitting to examine the representativeness of the tests. Obviously, the service behaviour can be considered to be the most representative test.

(a) Indoor full-scale fatigue tests carried out by the Swiss "Fabrique Federale d'Avions" at Emmen[2] are fairly close to service operation in that *the loads applied to wing, tail surfaces, fuselage and landing gears are controlled by continuous recording which was performed during service operations* for a time long enough for the statistical sampling to be considered as stationary. However, the environment is not so representative from the corrosion point of view. This type of test can begin only after some time of service operations, hence its purpose is only a final verification yielding resulsts after a long time of service operation has elapsed.

(b) *Conventional full-scale fatigue tests* carried out indoors or, better still, in the open, are often performed on a flight-by-flight basis with loading programmes deduced from general statistical data confirmed by sampling measurements carried out on the prototype aircraft or the first production aircraft. The loading programme may be simplified to consist of a reduced number of load levels by means of "equivalent" damage calculation based on fatigue test results of "fairly" representative specimens. It may also be randomized in replacing the continuous curve of the cumulative frequencies of occurrence by a stepped diagram resulting in a discrete number of level classes of flight and ground loads, the application sequence of which is randomized. In some cases the fuselage is immersed into a water tank and filled with water.

Other tests are carried out with air pressurization, the fuselage being filled with rigid plastic foam. Outdoor tests are recommended as being more representative from the corrosion point of view.

(c) *Full-scale fatigue tests of incomplete structures* are carried out in the laboratory, either under a simplified loading programme from service measurements, or more frequently under constant amplitude loadings when it is possible to compare several versions of design, materials or manufacturing processes.

(d) *Systematic fatigue tests of assembly elements* such as sheet joints by means of one or several rivet lines, lug loaded by a pin, etc., are generally performed under constant amplitude loads for several intensities in order to plot a mean $S-N$ curve and to appraise the scatter.

(e) *Systematic fatigue tests of notched specimens* under constant amplitude loads of several intensities and with several values of the alternating-to-steady component ratio and several geometrical notch factors give results which are often used as middle term of comparison to assess the fatigue behaviour of structures under loading programmes differing from those under which they were tested.

(f) *Research fatigue tests* of elementary assembly specimens or notched specimens appraise the influence of different loading programme types assumed to be equivalent in damage when based on the Miner-Palmgren rule.

In order to determine what the representativeness of these types of tests may be, i.e., how realistic they are, and what degree of confidence to ascribe to them, it must be noted which are the parameters of significance in the fatigue behaviour and how these parameters are represented in every fatigue test type.

Broadly considering the initiation phase of fatigue cracking, the governing parameters are as follows:

(i) The alternating component of the surface stress which gives rise to alternating plastic shear strains which modify the cold-worked condition of the surface material and which create clusters of vacancies and pile-ups of dislocations, as well as surface crevices, from which microcracks originate.

(ii) The maximum value of the tensile surface stress which plays an important part in the growth of micro- and macro-cracks.

(iii) The stress gradient in the direction perpendicular to the surface which governs the material depth within which plastic distortions are significant.

(iv) Intensity, gradient and stability of surface residual stresses which, when they are tensile, decrease the duration of the fatigue crack initiation phase, whereas they have a delaying effect when they are compressive.

(v) The geometrical roughness of the surface, and the metallurgical condition of the surface material.

(vi) The beneficial effect of a small enough number of high loads that create favourable residual stresses at notch roots but do not yet create microcracks when applied.

(vii) The corrosion sensitivity of the material and, in assemblies, the fretting behaviour which can create surface damage that may seriously shorten the crack initiation phase.

The fatigue crack propagation phase depends on the stress distribution in the crack area and on the changes in this distribution due to the crack propagation. It also depends on loading sequences through the beneficial effect of rarely occurring overloads. A corrosive environment may also substantially increase the crack propagation rate. Crack propagation may be impeded when the load is transferred from the cracked area into another assemblied part (fail-safe). It may nevertheless give rise to a static fracture. In the case when the propagation of a fatigue crack ceases, further crack propagation may take place due to stress corrosion or intergranular corrosion.

Final static fracture occurs with a smaller and less easily detectable crack the more brittle the material and the thicker the part. It is worth noting that the material is often more brittle in the short transverse direction.

Preceding features imply that to be representative of service behaviour, every full-scale fatigue test should be carried out with a structure made from the same materials, having undergone the same treatments, manufacturing and protection processes, and the same inspection and maintenance procedures as the operational structure. This kind of test is costly and takes too long to complete. Its application is therefore restricted to final fatigue strength substantiations carried out in accordance with the tests of types (b) and (c) previously reviewed.

However, due to discrepancies between the test loading programme and load statistics from measurements performed during actual service operations, or subsequently to a change in operational conditions such as freight weight, aircraft speed, etc., or again after an important development of the aircraft without general modification of the primary structure, a reassessment of the fatigue behaviour may be necessary without the possibility of carrying out a full-scale fatigue test. This raises a problem of selection between partial fatigue tests of weak areas and of systematic tests the results of which will be used in comparative calculations.

All computation methods are based on tests that are performed under conditions more or less representative of actual service environments. Corrosion had no influence in the very rare laboratory tests performed in a vacuum or in a neutral atmosphere, e.g., in dry argon. In normal indoor tests, the corrosion effect is generally fairly small, except during the crack propagation phase in materials susceptible to stress-corrosion. In full-scale fatigue tests performed in the open and in those carried out in water-tanks, the test duration of more than one year achieves a sufficiently severe simulation of the corrosion environment. Corrosion often has a significant but moderate influence on the test duration, measured in real time, and on the fatigue life which is measured in number of cycles, flight hours or number of flights.

Another time effect is due to dynamic resonance of the structure that modifies the stress intensities and distributions. A distinction should be made between random loads at low frequencies which excite vibration modes of the whole structure, and high frequency random loads which excite only local vibration modes of small structure areas.

In discussing prediction methods, the following cases of random loading are to be considered:

— *Very low dynamic frequencies* for which the structure behaves quasi-statically. The loading spectrum mainly depends on the aircraft mission.

— *Frequencies within the range of fundamental vibrations modes of the whole aircraft* which excite structural vibration modes, but for which corrective computations can bring the problem back to the case of quasi-static loading. Loading spectra depend on aircraft missions and dynamical properties on the whole structure. Slow fatigue test results can be used in the assessment of fatigue life, and the number of flights is the more logical fatigue life unit.

— Acoustic frequencies excite locally small structural elements. Stress spectra depend on excitations and local dynamical properties of the structure. They are very different from those applied to the whole structure. Numbers of cycles to consider are generally very large compared with those of loadings that concern the whole structure.

4. PREDICTION AND ANALYSIS METHODS FOR CONSTANT AMPLITUDE LOADINGS

Computation methods which use fatigue test results of notched specimens disregard possible damage by fretting due to relative micro-displacements at the contact surfaces of assembled materials.

Computation methods based on tests of assemblies are also questionable due to the fact that materials, although nominally defined, may differ from those used in the structure. For example, differences may be associated with heat treatment, grain texture, surface condition and corrosion protection.

Computations should, therefore, introduce empirical coefficients resulting from laboratory tests on representative assemblies, which should then be modified after outdoor full-scale fatigue tests and possibly reviewed in the light of service behaviour.

The earlier method of fatigue life assessment of a notched component was based, for comparison, on the higher surface fatigue stress in the notch, so that the favourable effect of the stress gradient in depth was disregarded. This method is very conservative if the data used are from axial fatigue tests on smooth specimens; it is simple and may be used to check whether or not the fatigue strength can definitely be considered sufficient. However, fatigue strength may be overestimated when using rotating bending results of small-diameter smooth specimens. This method fails in the case of fretting or of superimposition of undefined stress raisers.

An improvement of this method was made by taking stress gradients into account and by using fatigue test results of a set of notched specimens with several notch factor values. This permitted curves to be drawn showing fatigue life as a function of alternating and steady components of the higher surface stress for several values of the relative stress gradient, $(1/o)\partial o/\partial n$, in the direction perpendicular to the surface[1,4].

In 1959, Hayes[3] proposed to use fatigue test results of notched specimens with several values of the K_T notch factor in order to define by interpolation an *equivalent notch factor* from one fatigue test of the studied component. Then, the interpolation of curves from test results on notched specimens using this equivalent notch factor enables an assessment to be made of the component fatigue behaviour under any loading programme.

In 1962, an improvement by Deneff[4] was based on the approximate correlation derived for flat specimens between the nominal fatigue stress of a notched specimen and that of smooth specimens. This correlation was found to be independent of the alternating-to-steady stress ratio and to encompass a large range of number of cycles, but was not valid for round specimens. The correlation varies with each notch factor, K_T, but the fatigue notch factor, K_F, varies with K_T and the notch radius, r, according to an empirical relation:

$$K_F/K_T = f(r) .$$

From this, Deneff derived an interpolation method to obtain the diagrams,

$$N = f(\sigma_a, \sigma_m) ,$$

corresponding to fixed values of K_T and r. He applied its method to fatigue strength computation on sheet assemblies where, for the stresses at edges of holes, a distinction was made between stresses resulting from the local load transferred by each fastener and those by-passing the fasteners.

To compute local stresses in a multi-riveted statically-redundant assembly, each assembly sheet was idealized by a system of rectangular meshes according to network lines, the nodes of which were at hole centres. These network lines were assumed to be axially loaded bars transferring shear loads to rectangular sheet elements. Deformations due to bearing stresses in holes and to rivet bending were disregarded. Computation, restricted to the elastic range, yielded nominal stresses applied near each hole and local loads transferred by each rivet. Allowable values of these loads and stresses were drawn from fatigue tests on elementary elements.

In 1969, a first attempt was made by Jarfall[5] to take account of the bending of rivets and hole bearing deformations which vary with sheet thickness, fastener diameter, and with the material. He used elasticity methods of assembly analysis previously investigated from 1944 to 1947 by Vogt[6], Manford et a.[7], and Rosenfeld[8]. In this field it is worth noting a recent paper by Harris et al.[9] that recognizes the possibilities afforded by modern digital computers.

In order to take into consideration the plastic behaviour under fatigue stressing, i.e., changes in stress-strain cycles, creation or relaxation of residual stresses, surface condition in holes, axial tightening and diametral interference or clearance of fasteners, Jarfall introduced two empirical coefficients to be determined in partial fatigue tests. Using these coefficients, he called the "*Stress Severity Factor* – SSF" the ratio of the higher local stress at a hole edge to a reference stress chosen to be the nominal stress near the hole assuming the hole was reduced to a zero diameter.

To determine empirical coefficients, it was postulated that, for a fixed fatigue life of N cycles, the fatigue failure of different elements would occur for the same value of the higher local stress, i.e., for the same value of the product of the nominal stress to failure after N cycles and the SSF-factor. Hence, this factor has some similarity with the fatigue notch factor K_F. It is valid only within a certain range of number of cycles which would have to be determined by experience. It might still be called "Fatigue notch factor equivalent to the assembly detail" and designated $\bar{K}_F$. Three specimens are needed to obtain two ratios each of which supply one coefficient. Jarfall used flat sheet specimens containing a circular hole with three loading modes: axially loaded specimens with free hole or hole filled by a fastener, and specimens fixed at one end and loaded at the hole by means of a pin. Then, in fatigue tests of assemblies, local values of the Stress Severity Factor were determined for each incipient crack. Knowing the SSF of various areas of an assembly, it is possible to compute its fatigue life under any loading programme and then, knowing its service behaviour, to define allowable values of the SSF for each particular class of design and of operational service.

Crichlow and his collaborators[10] have proposed the so-called "*Fatigue Quality Index*" method that comprehensively characterizes the fatigue behaviour of an assembly and implicitly takes account of details and materials. The fatigue quality index is the geometrical notch factor chosen from amongst, or interpoled from, those of a set of simple notched specimens, made from a reference material that has yielded $N = f(\sigma_a, \sigma_m, K_T)$-curves, in order to have same fatigue life as the tested component for the same values of the nominal fatigue stresses, σ_a and σ_m, near the notch or the assembly junction. If the component is tested under a loading programme, fatigue durations of reference specimens are computed and plotted against the loading programme intensity, and, through the point representing the component fatigue test, one interpolation is made to define the K_T-value of the notch factor equivalent to the component. Since the material of the tested component may differ from that of the reference specimens, one no longer speaks of equivalent K_T but only of Fatigue Quality Index K. As in Jarfall's tests, structure tests are carried out considering all intermediate durations until cracks appear, the repair of which allow the fatigue test to continue and more useful results for further prediction purposes to be obtained. This is supported by the fact that in the absence of a "fail-safe" design, the duration for a crack to be detectable is in practice often close to the total fatigue life to failure. For aluminium alloys, 2024-T3 aluminium alloy sheet material is used as the reference.

All previously mentioned prediction methods are fundamentally comparative, comparisons being made through parameters the knowledge of which enables prediction to be made of the fatigue behaviour of another structure or

of an element assumed to be similar to the local area under investigation. In the different cases, attempts are made to describe design and loading conditions of more or less complex structural details in order to bring every problem back to one which has been previously tested. However, because manufacturing processes and metallurgical conditions are playing an important part, it may be expected that the prediction accuracy will be limited by the difficulty to exactly describe all significant conditions. At the very best, it may be hoped that quite good prediction will be possible from a first full-scale fatigue test on the structure being studied when the evaulation aim will be only to appraise the effect of slight changes in sizing and loading on the fatigue life.

The comparisons can be defined along the following lines:

1. *Loading types and their intensities*

Loading may be of three types, namely, constant amplitude, programmed, or random. Intensities of each of them may be measured respectively, as amplitude, higher load and load distribution, and quadratic mean load.

2. *Reference structures*

They may be as follows:

(a) Another structure of same detail design, materials and manufacturing processes.

(b) Structural assembly details having same features.

(c) Notched specimens of same relative stress gradient, material and manufacturing processes.

(d) Smooth specimens made from the same material.

The following comparison parameters may be used:

(i) The "Equivalent notch factor – K_T ", the "Stress Severity Factor – SSF" and the "Fatigue Quality Index – K " are used with reference structures of the types (a) and (b).

(ii) Nominal design stresses around stress raisers are to be used in connection with tests on reference representative details.

(iii) Surface stresses and their relative stress gradients in depth direction.

(iv) Surface stresses alone.

Table 1 shows a simplified description of prediction methods.

A valuable extension of these studies would be the establishment of prediction means, consisting of banks of data on fatigue strengths of conventional structures and elements, and suitable as imput data for digital computers for strength or optimization analyzes. All items of these data would be provided by accurate analyzes of test results on full-scale structures, partial structures, and components and assemblies representative of various designs under constant amplitude loadings. The cases of fatigue life prediction under random loading would be treated by means of the Miner-Palmgren rule.

5. DAMAGE EVALUATION OF FATIGUE LOADINGS ON STRUCTURES BY SIMPLIFIED REPRESENTATION OF THE RANDOM LOAD SPECTRUM

In most full-scale fatigue tests of aircraft structures, the applied load system is simplified with respect to random service loads. The first problem to deal with consists of defining a test load system that is equivalent to service loads with regard to fatigue damage. Figure 1 which concerns the full-scale fatigue test of the "Caravelle" structure, schematizes the general course of computations from gust velocity statistics and one estimate of ground loads to define the load programme to be applied during a test cycle which represents one mean type flight. Figure 1(a) shows gust velocity statistics by sections of altitude, drawn from acceleration recording on an aircraft of comparable type and performances (Comet 1) during a world-round trip. Figure 1(b) illustrates the estimated type flight of the Caravelle with values of airspeed, altitude and aircraft weight that are varying during the flight. For each flight section, constant values are assumed, and partial statistics of acceleration increments, Δn , at the gravity centre are determined. They are corrected to give the same loads when applied to the reference take-off weight. Figure 1(c) shows the sum of these partial statistics as one curve of cumulative frequency in 10^4 flights to reach or exceed Δn-values . Then, it is assumed that the wing structure, in the areas of high stresses, has the same fatigue properties as the notched specimens, the constant amplitude fatigue properties of which are represented in Figure 1(d); in this particular case, these stresses depended on the acceleration increment Δn as follows:

$$S = 8.1 \pm 8.1 \, \Delta n \text{ daN/mm}^2 .$$

The load spectrum of the Figure 1(c) was decomposed into a series of constant amplitude fatigue loads, $S_i = 8.1 \pm S_{ai}$, each of them being applied for N_i cycles and producing a partial damage N_i/N_{Ri}. N_{Ri} is the number of cycles to failure under the load S_{ai}, taken from the Figure 1(d). Numerical data and computation results are reported in Table II.

Partial damage due to ground loads during landing and taxiing, as well as that due to ground-air-ground transition from the lowest negative stress to the highest positive stress can be computed from appropriate load statistics. In the case of the Caravelle, at the beginning of the full-scale fatigue test, the total computed damage was 0.54 for 10^4 flights. The test was carried out for 100,000 cycles without noticeable actual damage. This first test phase was followed by a last phase under a simplified load programme of 21% higher load level for 3,000 cycles corresponding to 4400 flights. It was shown that the test "damage" was lower than 0.1 for 10^4 cycles and that a life of 20,000 flights was substantiated with a scatter factor of 5.

In addition to the fact that the structure under investigation may have a better fatigue strength that the reference notched specimen (here, $K_T = 4$), the discrepancy between damage prediction and full-scale test results is partially explained by the beneficial effect of the supplementary "fail-safe" cycles in which the higher load corresponds to an occurrence frequency of about ten times in 10,000 flights, i.e., to a load defined by $n = 2.56$ and a corresponding maximum stress level of 20.8 daN/mm² , whereas the maximum stress levels in the other test cycles were of 12 daN/mm² in normal cycles applied up to 20,000 cycles, and of 16.2 daN/mm² up to test completion.

In fact, computation had only been used to replace the loads of the average flight in the Figure 1(e) by the "equivalent" test loads of the Figure 1(f), in which the load reached or exceeded on average one time per flight had been kept. In actual service, up to 15,000 flights, the fatigue damages were negligible. Detected damage which did not affect the flight safety was due to unpredicted taxiing loads but such damage concerned only the wing rib at the main landing gear attachment.

This general course of fatigue computation has been retained in France for the Falcon 20 and the Nord 262 civil aircraft, as well as for the military transport aircraft Transall C-160, designed and manufactured in a French-German co-operation. The statistics used for gust loads were those of the RAS Data Sheets. In the case of the Transall aircraft, measurements in flight at low altitude have yielded load statistics used in the interpretation of fatigue test results.

Several causes of error exist in this kind of computation:

(i) Certain load statistics are unknown at the time of test. This was the case for the asymmetrical loads on tail surfaces of the Caravelle type which used thrust reversal after touch-down. In the 707 Boeing aircraft operations, taxiing afforded unpredicted repeated tension stresses in the upper wing skin.

(ii) Fatigue test data from notched specimens or from structures of old design and of war-time manufacture represent badly the properties of the structure under investigation. To cope with this difficulty, some fatigue tests on assembly elements representative of the structure may be carried out under a standardized load spectrum.

(iii) The beneficial effect of design limit loads that could be encountered very clearly in service, or their detrimental effect when applied after a crack initiation, are not represented in tests. The beneficial effect due to a premature application of high loads must be avoided, whereas the detrimental effect would shorten the fatigue life only slightly, due to the exponential course of the crack propagation in fatigue.

(iv) The principle on using an average flight loading is questionable since a number of flights are carried out without noticeable gust loading and also because gust loads concentrated during few flights are less damaging due to the lowering by application of the first high gust of residual tensile stresses created by taxiing loads. When the loading spectrum includes compressive stresses, the damage under a service loading may be less severe than under an average loading programme, as far as the statistics of turbulent and quiet flights are concerned.

As long as the final true load spectrum differs but little from the spectrum used in the structural fatigue test, corrective computations may be made for the areas damaged by the applied loads or, in default of damage, in conservatively assuming damage beginning just at the conclusion of the test.

When the true load spectrum is unknown, comparative experimental investigation of several designs or manufacturing processes may be carried out, or the fatigue strength of a particular structure may be appraised, under a standardized approximate spectrum. In development tests based on a standardized shape of a spectrum of cumulative frequencies of level crossings, a distinction should be made between aircraft components loaded similarly to a wing, i.e., under a loading programme having two mean load values, and components with a loading programme having only one mean load value.

For the first loading case, typical of wings, D.Schütz[12] has proposed the standardized load spectrum shape shown in the Figure 2. It corresponds to a mean load spectrum drawn through flight measurements carried out on DC-9, Boeing 737, BAC-111 and Transall aircraft. Flight loads measured on the Air-France's Caravelles are plotted at the lower limit of the scatter band. It must be pointed out that these loads are deduced from vertical acceleration measurements at the gravity centre by means of a count method in which level crossings are counted only one time between two crossings of the zero acceleration. This method neglects a certain percentage of low level loads but the number of positive maximums is close to that of zero crossings with positive slope. The mean curve of level crossings in flight is quite well represented by a gaussian-logarithmic distribution of the ratio of the alternating load to the mean load, S_a/S_m, of total number of cycles $H_0 = 2 \times 10^7$, passing through the points $P = 0.5$, $S_a/S_m = 0.085$ and $P = 5 \times 10^{-7}$, $S_a/S_m = 1.6$ (see the B-straight line in Figure 4).

Figure 3 shows the level crossing spectrum of vertical accelerations measured at the gravity centres of ten Caravelles of Air-France during 47,000 flights and plotted for 20,000 flights. Positive accelerations, Δn_1, are more severe than the negative accelerations, Δn_2 : that may be due to different pilot responses in presence of severe gusts, and to the asymmetry of manoeuvres. This fact corresponds to a varying mean load. Figure 3 shows the alternating overloads Δn around the mean load, as well as the quantity $1 + S_a/S_m$, where S_a is proportional to Δn and S_m is proportional to $(\Delta n_1 - \Delta n_2)/2$. S_a and S_m are not true stresses since the stress spectrum is not exactly proportional to the spectrum of load factors at the gravity centre of the aircraft. The statistic of level crossings of S_a/S_m values are represented by a straight line 'A' in Figure 4 in assuming for the positive values a total number of level crossings, $H_0 = 2 \times 10^6$, in order to compute the occurrence frequencies. The abscissae scale is the normal Gaussian distribution of probability $P(x \geqslant a)$ such that $\log_{10}(x = S_a/S_m)$ be higher than a fixed value $\log_{10} a$. With $H_0 = 2 \times 10^6$, $H = 10^6$ corresponds to the frequency 0.5. This straight line is easily prolonged, thus permitting an appraisal of the high and very rare overload values as well as frequencies of loads lower than the measurement threshold.

To evaluate the fatigue damage, the load spectrum may be replaced by a stepped diagram or may be broken down into a sum of component spectra for which fatigue results are available. To illustrate the procedure, the Caravelle S_a/S_m spectrum will be broken down into stepped components of constant amplitude or into Gaussian components in order to use LBF results of fatigue tests on notched specimens in the case of constant amplitude loads and in the case of load programmes having a Gaussian distribution of level crossings.

Figure 7 shows $S_a - N_R$ curves for a mean stress $S_m = 8.1$ daN/mm^2, from Mustang wing tests of 2024-T3 aluminium alloy, and LBF fatigue tests on notched specimens $(K_T = 3.1$, $r = 2$ mm$)$[14] made from German 3.1354.5 aluminium alloy. Lockheed results of fatigue tests[15] on notched specimens $(K_T = 4$, $r = 2.5$ mm$)$ made from 7075-T6 aluminium alloy are quite comparable to the Mustang results. With the Caravelle spectrum replaced by a 17-level stepped spectrum, between $H = 10$ and $H = 10^6$, damage computations yield

$$\Sigma n_i/N_{Ri} = 0.224 \text{ from Mustang curves, and}$$
$$= 0.207 \text{ from LBF } S-N \text{ curves for } K_T = 3.1 .$$

Figure 5 illustrates the break-down of the Caravelle spectrum into two Gaussian components, each of them defined by the maximum value, $\bar{S}_a/S_m$, and by their sizes, namely 10^6 for the I-component of maximum level $\bar{S}_a/S_m = 0.9$, and 1.45×10^4 for the II-component of maximum level 1.3. The I-component is tangential to the overall spectrum, while the II-component passes through the point P_1 on the I-component at the distance $\log_{10} 2$ from the overall spectrum. To complete, one stepped rectangular III-component of constant level amplitude, 1.34, and of size 10, is used: it passes through the point P_2 of the II-component at the distance $\log_{10} 2$ from the overall spectrum.

In development fatigue tests of motor-vehicle components that are loaded by the dynamic response to road irregularities, Gassner and W.Schütz[11] have used their standardized LBF programme consisting in eight constant amplitude load steps, the levels of which are interpolated from the binomial distribution C_j^{21} with $j = 0, 1, 2, ... , 10$. The level of each load step is measured by the ratio of its alternating load, S_a, to the highest load value of the programme, $\bar{S}_a$; the mean load, S_m, the same for all steps, is defined by the ratio $R = (\bar{S}_m - \bar{S}_a)/(\bar{S}_m + \bar{S}_a)$. Occurrence frequencies of loads are:

$S_a/\bar{S}_a$ =	1	0.95	0.85	0.725	0.575	0.425	0.275	0.125
ΔN_i =	2	16	280	2720	20,000	92,000	280,000	605,000,

with $H_0 = \Sigma \Delta N_i = 1,000,610 \approx 10^6$, and a RMS stress of the S_a-amplitudes, S_e, such that $(S_e)^2 = 0.055(\bar{S}_a)^2$. For the instantaneous sine-shaped stress S, the quadratic mean would be $\sigma^2 = (S_e)^2/2$. This standardized LBF-distribution is very close to the binomial distribution C_j^{21} which corresponds to $H_0 = 1,048,576$ and to $(S_e)^2 = 0.05357(\bar{S}_a)^2$ or $S_e = 0.231 \bar{S}_a$. It is nearly equivalent to the gaussian distribution of highest level $1.06 S$, and of size 10^6 which is represented by a straight line in a $P(x \geqslant a) - S_a/\bar{S}_a$ diagram: the straight line passes through the points $S_a = 0$, $P = 0.5$ or $H = 10^6$, and $S_a = \bar{S}_a$, $P = 2 \cdot 10^{-7}$ or $H = 4$. The RMS of this distribution is $S_e = 0.230 \bar{S}_a$.

With this Gaussian distribution of programmed loads defined by the highest load, $\bar{S}_a$, LBF's fatigue tests on notched specimens ($K_T = 3.1$) are plotted in Figure 8 and may be represented by straight lines

$$\log \bar{N}_F = a - \bar{k} \log \bar{S}_a ,$$

where N_F is the total number of cycles of all load levels to failure, and $\bar{R} = (\bar{S}_m - \bar{S}_a)/(\bar{S}_m + \bar{S}_a)$ is the fatigue ratio for the highest loads. In case of a same $\bar{S}_m$-value for every programme loading of various $\bar{S}_a$-values, an interpolation has been performed by plotting dotted straight lines through exact points located on $\bar{R}$-curves. With these test results, the break-down of alternating flight loads of the Caravelle spectrum that is illustrated in Figure 6 yields the following "damage" values:

I-component:

$$\bar{S}_a = 0.9 \times 8.1 = 7.3 \text{ daN/mm}^2 , \ H = 10^6, \ N_F = 8 \times 10^6, \ d_t = H/\bar{N}_F = 0.125;$$

II-component:

$$\bar{S}_a = 1.3 \times 8.1 = 10.5 \text{ daN/mm}^2, \ H = 1.45 \times 10^4 .$$

For a size of 10^6, the fatigue would be of $N_F = 1.7 \times 10^6$; the B-curve corresponds to an occurrence frequency of $\bar{S}_a$ equal to 1.45×10^{-4}, i.e., from Gassner and Schütz[11], to a conversion factor 0.22 such as N_F becomes $0.22 \times 1.7 \times 10^6 = 3.75 \times 10^5$. The damage of the II-component would be $d_{II} = 0.0385$;

III-component:

$$S_a = 1.34 \times 8.1 = 10.85 \text{ daN/mm}^2, \ N_F = 4 \times 10^4, \ \text{and} \ d_{III} = 0.00025 .$$

The total computed damage would be $D = 0.1637$.

Taking into account the gaussian-logarithmic distribution of the Caravelle's flight alternating loads, it would have been preferable to compute the damage value from LBF's fatigue tests of notched specimens under this kind of loading programme. This has not been possible in the absence of an exact knowledge of the LBF log-normal distribution.

Consider now the Figure 6 where the distribution of flight alternating loads approximate closely to a straight line component of cumulative occurrence frequencies equal to 2.5 times those of the straight line defined by the points $S_a = 0$, $H_0 = 10^6$, and $S_a/S_m = 1$, $H = 1$. Most of the load spectra of civil and military transport aircraft have a shape which lends itself to a simple approximation by an exponential function represented by a straight line in a diagram $S - \log H$. Therefore, that is this kind of spectrum shape that should be the basis for programmed or random fatigue tests aimed to the design of transport aircraft structures.

On the contrary, for fighter aircraft, flight load spectra are better approached by analysis into Gaussian components, or Rayleigh components such as

$$H = H_0 e^{-(S_a/S_e)^2} ,$$

where H_0 is the total number of zero crossings with positive slope, and $S_e = \sigma\sqrt{2}$ is the RMS of the initial gaussian process when the number of positive maxima equals H_0. The Rayleigh distribution is represented by a straight line in the diagram $(S_a)^2 - \log H$.

Figure 9 illustrates the approximation of the flight load spectrum of the Mirage III RS aircraft measured in Swiss operations[16], by means of only one Rayleigh distribution for positive and negative accelerations. The approximation by a Gaussian distribution is less exact.

Figure 10 and Table III give the shapes and ordinates of the four types of loading spectra previously mentioned. The semi-logarithmic distribution is more suitable for an easy approximation of flight loadings in the case of transport airplanes, due to the possibilities afforded by its variable slope which permit a precise adjustment in the range from medium level to low level loads. The Gaussian distribution of logarithms of load levels (log-normal) might seem better appropriate if it was not often difficult and sometimes not possible to make its adjustment to certain measured loading spectra. The adjustment criteria is that in all points, the approximation curve have a less concavity than the investigated spectrum.

In the case of fighter aircraft, the Rayleigh and the Gaussian distributions may be convenient. However, it is more easy to adjust Rayleigh straight line (in a diagram (load)$^2 - \log_{10} H$) .

However, aircraft flight loads always include the transition at each flight of the mean load from the flight condition to the lower value, negative for the wing, during the taxiing at low speed. The effect of this transition is more to be ascribed to a change in residual stresses than to its direct fatigue damage. The last load just applied before a stress change in sign has a predominant effect on the damage afforded by the following loads (see Schijve[16]). This effect may aggravate the influence of ground loads which produce tensile stresses in the wing upper skin, as is the case of certain transport airplanes having a particularly flexible wing. Figure 11 illustrates the inversion in sign of the loads of upper and lower skins of a wing. In wing upper skins, repeated compressive

stresses due to flight loads tend to create tensile residual stresses at the stress raisers and reinforce the damaging effect of repeated tensile stresses due to ground loads.

In order to take account of ground-air-ground transition, we have proposed[17] to break-down the diagram of loads during one flight into one fundamental component defined by the highest and the lowest loads applied during the flight, and complementary alternating loads. That attributes to the ground-air-ground transition an importance comparable to the actual importance. To our knowledge no other method supported by comparative and statistically significant tests is available to replace this rough mode of assessment.

In full-scale fatigue tests, the following procedures to represent the ground-air-ground transition have been considered.

- Tests of Swiss type[2], controlled by tapes of statistical measurements recorded in actual operations. This method implies that fatigue test results enable, at the very most, late changes to be made in manufactured aircraft and in a number of components under manufacture.

- Tests under random loading with random times for the passage from the flight to the ground conditions. In this case, loads may be generated either by one or several Gaussian processes, or by a program where the sequences of application of individual loads will have been determined randomly.

- Tests under random loads, on a flight-by-flight basis, the overall spectrum being broken down into partial spectra for each flight, the severity of which being distributed according to the extreme values of the loads, on a flight-by-flight basis. In the case of the military aircraft, Transall, Figure 12 illustrates this possibility. Straight lines correspond to a Gaussian distribution between the flights of the logarithms of additional wing bending moments reached or exceeded n times per flight. This result, similar to that obtained by Buxhaum[18,19] from other flights and other measurements on the same aircraft, shows that the individual flight spectra are distributed as the extreme values. This kind of result only concerns gust loads; it would be useful to know if other aircraft behave similarly.

6. FATIGUE TEST ACCELERATION OR INTERPRETATION OF TEST RESULTS IN CASE OF CHANGES IN SERVICE LOAD LEVELS

In the statical strength of aircraft structures, possible service overloading with respect to design loads and the possible weakness of a particular structural component are palliated by a safety factor arbitrarily taken to be equal to 1.5. In the realm of the fatigue strength of these structures, safety is ensured by a life scatter factor quite variable, according to technical circumstances, the Authority and the Country. In France, a value of 5 has been proposed; it is lessened to 3 for secondary structure and for vital components the fail-safe of which has been proved[20]. Its minimum value is 2.

In helicopter components, the very large number of load cycles to consider in service put an obstacle to laboratory tests under the low stresses corresponding to actual number of cycles. Whereas, one should consider service loads applied in the number of cycles range from 10^8 to 10^{10}, fatigue tests are carried out with higher load levels in the range of 10^6 cycles. Test results are extrapolated to a very large number of cycles in order to obtain the so-called endurance limit, S_∞. To compare this fatigue limit strength to applied loads, loads are multiplied by a safety factor the order of magnitude of which may reach 3.

In general, life scatter is fairly constant in ratio along the steeper sloped sections of S-N curves and is rapidly increasing toward the larger number of cycles. Gassmann's tests[21] in axial tension-compression of smooth hour-glass shaped specimens made from a low alloy Cr-Ni-Mo steel in which the static strength was measured by means of tensile specimens taken from the fatigue specimens in the vicinity of the end fittings, have proved that the main part of the fatigue scatter may be ascribed to the scatter in tensile properties, and that the corrected S-N curve was a straight line in a diagram $\log S - \log N$, from $N = 10$ to $N = 10^5$. Then, for $N \geqslant 10^5$, the straight line was lower than test results indicated. For aluminium alloys which have no well-defined endurance limit, it is probable that the straight line would pass through results up to a larger number of cycles. It might be accepted that the scatter in fatigue strength is proportional to that of the static strength, and that it may be better evaluated by means of a regression straight line, except in case of initial damage by fretting.

When a fatigue test has been performed with the loading foreseen for the production aircraft at the time of the prototype manufacture, it frequently happens that the actual loading of production aircraft and, a fortiori, those corresponding to later type developments, are more severe. That implies a need to carry out interpretative analyses by which existent fatigue life margins are transformed into load margins. If life margin is not available, a reinforcement will be substantiated by transforming a lowering of local design stresses into a load margin. In order to be better placed for later interpretation of fatigue test results, and to obtain results more early, it is proposed to reduce the supplementary test duration corresponding to the scatter factor by increasing the general load level, according to this apparent reduction of the scatter factor. This first test phase would permit substantiation of the service operations of the first aircraft, and the test would be possibly resumed to substantiate an actual increase in

operational loads. In the initial phase, inspections should be more frequent, due to the fact that crack occurrence should be detected for smaller crack lengths (divided by the squared factor of load increase). In the following, we make an attempt to evaluate the test duration reduction which would correspond to an increase of 10% in load level.

From fatigue tests performed in Australia on Mustang wings[13], it has been proposed that the results could be considered to be similar to those obtained by the NACA on notched specimens made from 2024—T3 aluminium alloy sheet with a notch factor of 4. This kind of comparison is questionable for the following reasons.

(a) The local fatigue behaviour depends, not only on the stress concentration factor, but also on the stress gradient in the depth direction, particularly in the case of high loads and low fatigue cycles.

(b) In the case of a complex structure, the ratio between the higher stress and the nominal stress is the product of the local stress concentration factor and of the load concentration factor, which is the ratio between the local load and the mean load in the considered area. It stands to reason that the stress gradient corresponding to the local stress concentration should be associated to the overall stress concentration in the prediction of the local fatigue behaviour of the structure.

(c) In actual structures, fretting damage plays a more important part in decreasing the fatigue life in the range of large number of cycles and low stresses; it is absent in tests on notched specimens.

Local shapes of S-N curves may be characterized by their slopes in logarithmic coordinates:

$$ k = -\frac{\partial \log N}{\partial \log S} . $$

This slope varies along the S-N curve; this is likely to be due to the scatter of the material properties as it was the case in the Gassmann's tests. Hence, in tests of assemblies using at the very most two or three specimens per load level, the plotted S-N curve will be questionable, and its slope will be still more questionable. For example, Figure 13 shows fatigue test results from Mordfin and Halsey[22], on box-beams made from 7075—T6 aluminium alloy. From 10^2 to 8×10^4 cycles, with R positive but low, k shows the successive rough values 4.8 — 2.25 and 4.8, of mean value 3.9. Using other test results of the same specimens, a mean straight line of slope k = 4.5 may be plotted, thus showing that the erratic slope variation was due to scatter.

A short survey of published results yields the following values of k.

1. Notched specimens

In tests under constant amplitude of the alternating stress, the mean stress increases the slope of the $\log S_a - \log N$ curve. Round notched specimens made from A—U2GN aluminium alloy thick sheet and tested at the "Établissement Aéronautique de Toulouse", yielded:

$$ K_T = 1.7, \text{ relative stress gradient } g = \frac{1}{S} \partial S/\partial z = -1, \ S_m = 0, \ k = 4.8 ; $$

$$ K_T = 3.3, \ g = -5.7 \, mm^{-1}, \ S_m = 0 \quad 10.5 \quad 2 \ daN/mm^2 $$
$$ k = 4.9 \quad 3.6 \quad 3.1. $$

These values concern the range from 10^4 to 10^5 cycles.

In the same range of number of cycles, tests of LBF (Report 1079) on flat notched specimens made from the German 3.1354.5 aluminium alloy give:

$$ K_T = 3.1 \text{ and } g = -1 \, mm^{-1}: \ S_m = 0 \quad 4.7 \quad 9 \quad 15.15 \, daN/mm^2 $$
$$ k = 3.3 \quad 2.8 \quad 2.4 \quad 2.3. $$

With the same specimens and the same alloy, test results plotted in Figure 8 correspond to: $S_m = 0$, $\bar{k} = 7.6$: $S_m = 8 \, daN/mm^2$, $\bar{k} = 4.8$. It is seen that k is somewhat higher in case of tests under a load spectrum.

2. Riveted or bolted assemblies

Among numerous tests, we will quote some of them on small assemblies made from 2024—T3 aluminium alloy sheet. From 10^4 to 10^5 cycles, test by Schütz (LBF Report F—47) for countersunk rivets yielded:

$$ k = 3 \text{ for constant amplitude loading, and} $$
$$ k = 5.6 \text{ for programmed loading spectrum.} $$

In EAT's tests (Report 8388/MY), $k = 4$ was obtained for countersunk rivets, whereas $k = 7$ for round head rivets.

In NLR's tests (TN M.2104), with round head rivets: $k = 4$ for heat treated sheet with $S_{0.2} = 19.4$ daN/mm² and $k = 2.1$ for cold-worked sheet having $S_{0.2} = 25$ daN/mm² .

It is obvious that the fretting plays a part varying in the different cases, and that this entails a large range of variation of k . Moreover, a part of the variation is due to the scatter and to the small number of specimens tested at each load level.

3. Structures

Under constant amplitude loads, Mustang wings[13] yield between 10^4 and 3×10^5 cycles: $F_{min.} = R = 0$, $k = 5$; $F_m. = 0$, $R = -1$, $k = 6$.

Other results are:

– NACA TN 4137, 2024 aluminium alloy box-beams: $k = 3.7$.

– NACA TN D–547, quoting NACA TN 4132, C–46 wings under constant amplitude loads, between 10^4 and and 10^5 cycles: $k = 3.95$.

– Tests by Mordfin and Halsey on 7075–T6 aluminium alloy box-beams: $k = 3.45$ as shown in Figure 13. Tests by Rosenfeld (ASTM STP 338) yield $k = 4$.

In general, k is quite variable but probably higher than 3 for constant amplitude tests, 4 for programmed tests with zero mean load, and 5 for programmed tests with noticeable mean load.

On condition that a sufficient number of specimens are available for each loading level, the analyzes of tests on various assembly types would permit a better answer to be obtained to the problem. Conservatively, we are assuming that an increase of 10% in load level, in a programmed fatigue test, would correspond to a reduction of 33% in duration.

7. TESTS UNDER RANDOM LOADINGS

The quite recent development of fatigue tests of notched specimens under random loads is first the consequence of practical possibilities afforded by the test devices electronically controlled using imput signals from analogue devices, or from a computer, such as those used by Swanson[23] and by Melcon and McCulloch[24, 15].

Secondly, the prediction of the dynamical response of aircraft in continuous turbulence and to ground irregularities through the power spectral density method give results that are expressed as a sum of Rayleigh distributions weighted by the RMS of each distribution. Melcon and McCulloch have investigated the fatigue life of flat notched specimens ($K_T = 4$, $g = -0.8$ mm⁻¹ and $K_T = 7$, $g = -3.2$ mm⁻¹) made from 7075–T6 aluminium alloy under random or programmed (low-high loads) loading spectra obtained by superimposing elementary spectra. The resulting programme was applied about 10 times. The loadings had the same distribution in cumulative frequency of occurrence in the two test types, random or under programme. These spectra were representative for loadings of fighter aircraft. The discrepancies of results between random or programmed loadings seem ascribable only to the count method applied to the random signal, which disregarded numerous low amplitude variations of the load between two successive zero crossings.

This difference has been avoided in tests by Jacoby[25], in which random or programmed loads were digitally defined by a computer controlling the sequence of their application. Specimens made from 2024–T3 aluminium alloy were of the type with centre notch ($K_T = 3.1$, $g = -1.82$ mm⁻¹) . The loading spectra used were based on flight and ground loads of a transport airplane. The considered sequences were:

(a) Random sequence of maxima and minima, the only condition being that a maximum follows a minimum;

(b) Random sequence of alternating loads around mean loads in flight and on the ground, with random transition from the flight condition to the ground condition;

(c) Flight-by-flight programme with high-low-high sequence of flight loads;

(d) Flight-by-flight programme with low-high-low sequence of flight loads.

Relative durations were:

Sequences	a	b	c	d
Life durations	1	0.9	0.8	1.6 .

We believe that although service loads are not truly alternating and that they often result from multi-modal response giving rise to beating, their representation by alternating loads is likely to represent sufficiently closely actual behaviour when the lower resonance frequencies of the structure are fairly distinct. When the flight alternating load spectrum is known and in the case where the distribution of extreme values per flight is unknown, the most simple test mode consists of creating flight and ground alternating sequences, and to determine randomly the times of the ground-air-ground transition.

If the overall loading spectrum and the extreme value distribution by flight are both known, it will be possible to use random sequences of programmed loads by flight, their intensities being distributed between the flights as extreme values.

The knowledge of the load spectrum computed by means of the power spectral density method as a super-imposition of several Rayleigh distributions (case of gust loads) affords no change in the problem since it does not prejudge on any distribution between flights and the fatigue test on a flight-by-flight basis is certainly fundamental both with programmed and random loadings.

Another problem occurring mainly in fatigue tests at acoustical frequencies related to vibrations of structural sheet panels, is that of the possible definition of a spectrum of cumulative frequency of level crossing by the RMS of a load or a stress.

If the highest value of the load is fixed, if the spectrum is complete, and if its irregularity coefficient H_0/H_1 is known, the RMS, S_e , is a comparison term as valuable as another (H_0 is the number of zero crossings with positive slope, while H_1 is the number of positive maximums). However, S_e , often is only known from an electric measurement on a random signal the maximum values of which are not known. Test results which give place to a S_e-N curve are often obtained from the generation of the random loads by exciting the structure vibrations by a white noise having a power spectral density fairly constant between two cut-off frequencies. It seems difficult to use this kind of result for fatigue life prediction of another different element under an excitation corresponding to a power spectrum having different cut-off frequencies. From Clevenson and Steiner[26], the spectrum shape would have little influence on the fatigue life; the used spectra were well defined, that being not the case in practical problems. Moreover, fretting and ground-air-ground transition were not represented. In the case of aircraft primary structures, the ratios of the highest spectrum loads to the RMS loads vary with the general shape of spectra, therefore vary with the aircraft type, transport or fighter.

Finally, it must be noted that two types of root mean squares of a random load are to be considered, namely:

(a) the time root mean square, σ , which depends on the frequency distribution of oscillating loads and that occurs in computations by the method of the power spectrum, and

(b) the root mean square, S_e , of peak loads.

The relation $S_e^2 = 2\sigma^2$ is only valid when only one gaussian process exists.

8. CONCLUSION ON DESIGNER'S NEEDS RELATIVE TO FATIGUE TEST RESULTS

In the matter of fatigue life prediction, the designer generally lacks reliable data to supplement the laboratory test results on simple notched specimens – few test results may be available on simple riveted or bolted assemblies under constant amplitude load or, more rarely, under programmed loading. The best possibility of prediction still consists of using comparative damage computations using standard fatigue data of notched specimens to analyze a fatigue test result on a structure in order to predict the fatigue life of another structure of some particular design conception and some manufacturing process. The final result depends on the choice of representative structural element to be used in prediction and on the designer judgment, which is unfortunate in case of bad prediction. This state of affairs may be permanent. Any attempt to progress should be international with regard to the importance of test facilities and general means of use.

A practical effort to standardize fatigue tests of components, assemblies and structures has been made by Gassner and his collaborators. Their standardized spectrum is well suitable to represent flight loads of fighter aircraft and general ground loads, its use to represent flight loads of transport aircraft is less convenient. In this latter case, the exponential relation

$$H = H_0 e^{-c(S_a)^2}$$

seems better suited. Hence, it would be possible to perform fatigue development tests by using only two distribution types, namely:

– Gaussian or Rayleigh,

– Exponential.

With each of these distributions, it would be useful to carry out fatigue tests in order to know the influence of the ground-air-ground transition for each type of technological detail. As first proposed by Gassner, each distribution would be defined by the value, $\overline{S}_a$, of the highest load of the spectrum, the value, S_m of the mean load, and the spectrum size, i.e., the total number of mean level crossings. The convenient sizes would be 10^6 for applications to transport aircraft, and 10^4 for fighter aircraft.

The Gaussian-logarithmic distribution is badly suited to adjustment with actual spectra and would be considered only if there were reliable data to demonstrate that the same distribution would be usable for a large class of aircraft. Taking account of the possible application of the Rayleigh distribution to certain problems of acoustic fatigue, it would be judicious to consider this distribution as a substitute of the Gaussian distribution. In this case, the RMS value would be defined by the distribution instead of defining the distribution by the measured RMS of an electrical signal!

Acoustic fatigue tests are excluded from the present short survey, however, if fatigue tests at high frequency concern specimens of stiffness such that the stress distribution depends on the frequency, it would be useful to standardize these tests by defining the highest load and the shape of the level crossing spectrum.

In returning to the designer's needs, it may be stated that before systematic fatigue test results of assemblies under standardized loading spectra become available, a useful fatigue quality classification of assemblies and structures could be carried out along the line of approach used by Crichlow and his collaborators, or by Jarfall.

In the present survey, the general framework of the problem is outlined and tentative suggestions are put forward for discussion, rejection or to be followed-up.

REFERENCES

1. Barrois, W.   *Manual on Fatigue of Structures – Fundamental and Physical Aspects.* AGARD-MAN-8-70, Paris, June 1970

2. Branger, J.   *Ein Simulator der Ermüdungsgeschichte für Grossobjekte (Fatigue History Simulator) im Eidg. Flugzeugwerk (F + W).* Schweizer Archiv für angewandte Wissenschaft und Technik, Heft 8, 1966.

3. Hayes, J.E.   *An Analytical Method for Predicting Aircraft Fatigue Life.* Proceedings of the WADC Symposium 1959 on Fatigue of Aircraft Structures, WADC Report TR 59-107, Wright-Patterson, Ohio, August 1959.

4. Deneff, G.V.   *Fatigue Prediction Study.* Technical Report WADD TR 61-153, Wright-Patterson AF Base, Ohio, January 1962.

5. Jarfall, L.   *Fatigue Cycling of Riveted or Bolted Joints.* FFA Report HF-1239, Stockholm, June 1969.

6. Vogt, F.   *The Load Distribution in Bolted or Riveted Joints in Light-Alloy Structures.* Report SME 3300, Royal Aircraft Establishment, Farnborough, October 1944; also in NACA TM 1135.

7. Manford, B.T.   *Preliminary Investigation of the Loads carried by Individual Bolts in Bolted Joints.*
   Rosenfeld, S.J.   NACA TM 1051, May 1946.

8. Rosenfeld, S.J.   *Analytical and Experimental Investigation of Bolted Joints.* NACA TN 1458, October 1947.

9. Harris, H.G.   *Stress and Deflection Analysis of Mechanically Fastened Joints.* Report AFFDL-TR-
   et al.   70-49, Wright-Patterson AF Base, Ohio, May 1970.

10. Crichlow, W.J.   *An Engineering Evaluation of Methods for the Prediction of Fatigue Life in Airframe*
    et al.   *Structures.* Lockheed California Company, Report ASD-TR-61-434, Wright-Patterson AF Base, Ohio, March 1962, Abstract number N62-12760.

11. Gassner, E.
Schütz, W.
Evaluating Vital Vehicle Components by Programme Fatigue Tests. FISITA, Ninth International Automobile Technical Congress, 1962, Inst. Mech. Engineers, London.

12. Schutz, D.
Establishment of a Standardized Flight-By-Flight Program for Aircraft Wings. ICAF Conference, Stockholm, 1969; also in LBF Report S-81, p.6/20.

13. Payne, A.O.
Determination of the Fatigue Resistance of Aircraft Wings by Full-Scale Testing. Pergamon Press, ICAF-AGARD Symposium proceedings, Amsterdam 1959; edited by Plantema and Schijve.

14. Gassner, E.
Schütz, W.
Assessment of the Allowable Design Stresses and the Corresponding Fatigue Life. Pergamon Press, ICAF-AGARD Symposium, Munich 1965; edited by Gassner and Schütz.

15. McCulloch, A.J.
et al.
Investigation of the Representation of Aircraft Service Loadings in Fatigue Tests. Report ASD-TR-61-435, Wright-Patterson Air Force Base, Ohio, January 1962.

16. Schijve, J.
The Accumulation of Fatigue Damage in Aircraft Materials and Structures. AGARD-AG-157, Jan. 1972.

17. Barrois, W.
Sur la Fatigue des Cellules d'Avions. Métaux-Corrosion-Industries, no. 364, Dec. 1955. See also: *Physical Interpretation of Metal Fatigue.* 5th Conference ICAF, Bruxelles, Oct. 1957.

18. Buxbaum, O.
Betriebsbeanspruchungen des Militar-Transportflugzeuges. Transall A04, LBF Report 1966, not published.

19. Buxbaum, O.
Extreme Value Analysis and its Application to CG Vertical Accelerations Measured on Transport Airplanes of the Type C-130. AGARD Report No.579, March 1971.

20. Barrois, W.
Les Essais Statiques et de Fatigue des Structures des Avions en France et à l'Etranger. First Part, DOC-AIR-ESPACE, No.110, May 1968, Paris.

21. Gassmann, H.
Schädigung und Schadensakkumulation bei hochfestem Stahl. Thesis, Technischen Hochschule Stuttgart, 1966.

22. Mordfin, L.
Halsey, N.
Programmed Manoeuvre-Spectrum Fatigue Tests of Aircraft Beam Specimens. ASTM STP No.338, 1963.

23. Swanson, R.
et al.
Crack Propagation in Clad 7070–T6 Aluminium Alloy Sheet under Constant and Random Amplitude Fatigue Loading. ASTM STP 415, July 1966.

24. Melcon, M.A.
McCulloch, A.J.
Simulation of Random Aircraft Service Loadings in Fatigue Tests. Pergamon Press, ICAF-AGARD Symposium, Rome, 1963.

25. Jacoby, G.H.
Comparison of Fatigue Lives under Contentional Program Loading and Digital Random Loading. ASTM STP 462, Oct. 1968.

26. Clevenson, S.A.
Steiner, R.
Fatigue Life under Random Loading for Several Power Spectral Shapes. NASA TR R-266, Sept. 1967.

TABLE I - FATIGUE PREDICTION METHODS FOR STRUCTURES SUBMITTED TO LOADING PROGRAMMES

STUDIED A-STRUCTURE (LOADING PROGRAMME)	REFERENCE B-STRUCTURE		COMPARISON PARAMETERS	TYPES OF CALCULATION	EXPERIMENTAL DATA	
	TYPE	LOADING			SPECIAL TEST ON B	GENERAL DATA
FULL-SCALE	FULL-SCALE a	PROGRAM.	EQUIVALENT K_T	DAMAGE(A,B)	YES	S-N NOTCH CURVES OF THE MATERIAL
			JARFALL'S SSF	ELASTICITY(A,B)	YES	
			FATIGUE QUALITY INDEX K	DAMAGE (A,B)	YES	S-N-K_T REFERENCE CURVES
ASSEMBLY	LOCAL FITTING b	PROGRAM.	NO	NO ANALYSIS, SAME STRESSES ON A AND B.	YES	NO
			DAMAGE	DAMAGE (A,B)	YES	TESTS OF a, CONSTANT AMPLITUDE LOADS.
		CONSTANT AMPLITUDE	NOMINAL STRESSES	DAMAGE (A,B)	NO	
COMPLEX NOTCHED COMPONENT	NOTCHED SPECIMENS c	CONSTANT AMPLITUDE	SURFACE STRESS AND GRADIENT	ELASTICITY PLOTTING OF S_s-N-RELATIVE GRADIENT CURVES	NO	S-N NOTCH CURVES AND SIZE EFFECT LAW.
K_{TA}-NOTCHED COMPONENT	SMOOTH OR NOTCHED SPECIMENS d	CONSTANT AMPLIT.	SURFACE STRESS	ELASTICITY DAMAGE	NO	S-N CURVES OF SMOOTH OR NOTCHED ($K_T \leqslant K_{TA}$) SPECIMENS.

TABLE II - DAMAGE COMPUTATIONS FOR THE CARAVELLE WING UNDER GUST LOADS.

U, ft/sec., EAS.	7.5	10	15	20	25	30	35	40	45
Δn to P_d	0.242	0.322	0.483	0.644	0.805	0.966	1.128	1.29	1.45
N cumulative	86,600	35,174	6,610	1,584	426	188	66	34.5	1
Δn	0.282	0.402	0.563	0.724	0.885	1.046	1.207	1.37	1.53
N_i	51,426	28,564	5,026	1,158	238	122	31.5	33.5	1
S_{ai} (daN/mm^2)	2.28	3.25	4.55	5.9	7.15	8.45	9.75	11.1	12.4
N_{Ri}	2×10^6	5×10^5	10^5	4.5×10^4	2.5×10^4	1.4×10^4	8.4×10^3	5.4×10^3	3.6×10^2
N_i/N_{Ri}	0.0257	0.0572	0.0503	0.0258	0.0095	0.0087	0.0038	0.0062	0.003

Total gust damage for 10^4 flights $= \sum N_i/N_{Ri} = 0.1875$

TABLE III - DISTRIBUTIONS OF OCCURRENCE OF LEVEL CROSSINGS.

H/H_0	10^{-7}	10^{-6}	10^{-5}	10^{-4}	10^{-3}	10^{-2}	10^{-1}	0.3	0.5	1
EXPONENTIAL	1.167	1	0.833	0.867	0.500	0.333	0.167	0.117	0.083	0
GAUSSIAN	1.085	1	0.906	0.795	0.672	0.525	0.335	0.210	0.136	0
RAYLEIGH	1.08	1	0.913	0.817	0.710	0.580	0.408	0.296	0.224	0
LOG-GAUSSIAN	1.215	1	0.804	0.622	0.470	0.335	0.216	0.162	0.137	0.10

(a) GUST FREQUENCIES

(b) TYPE FLIGHT

(c) CUMULATIVE FREQUENCIES OF LOADS

(d) SPECIMEN FATIGUE LIFE

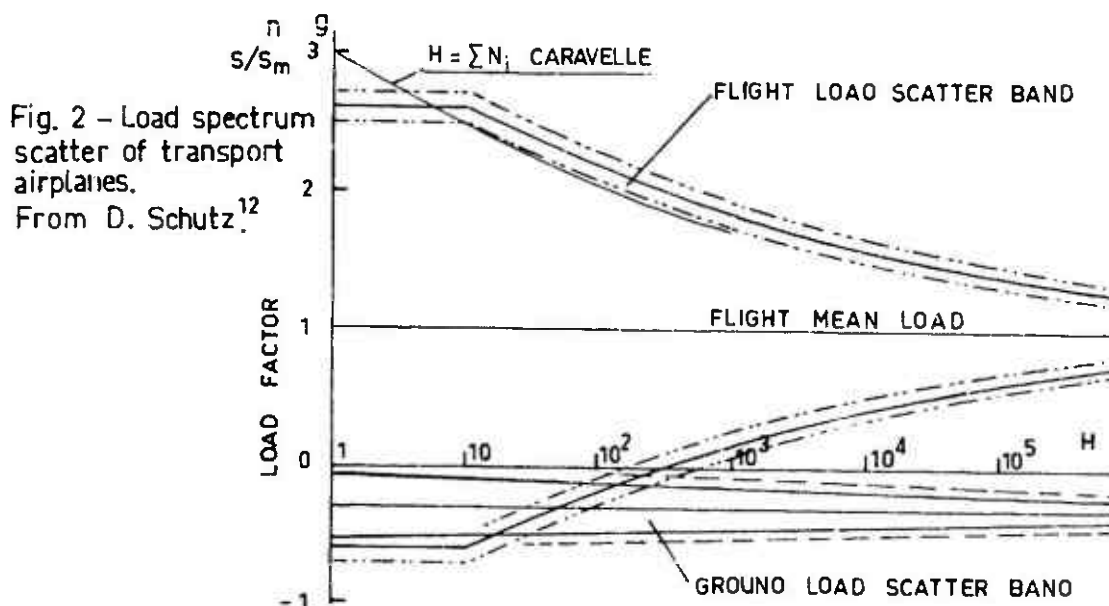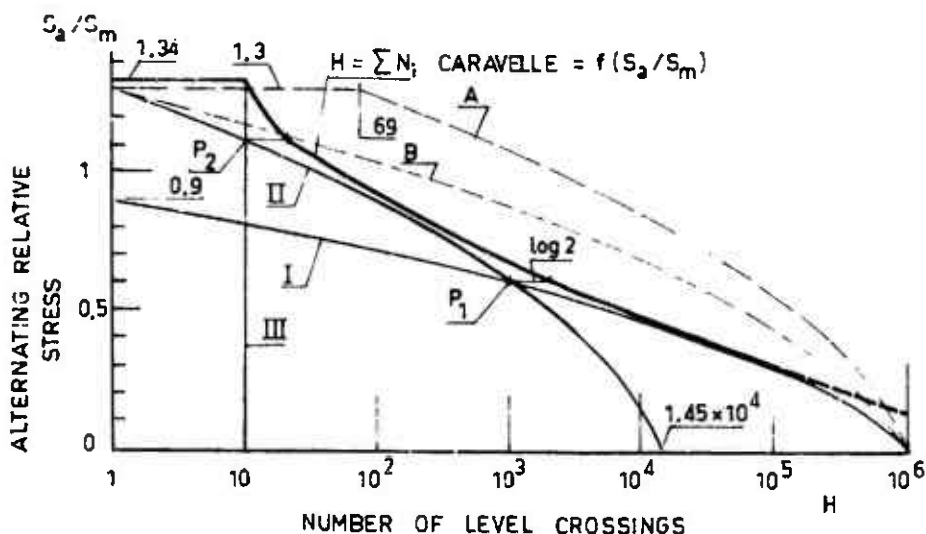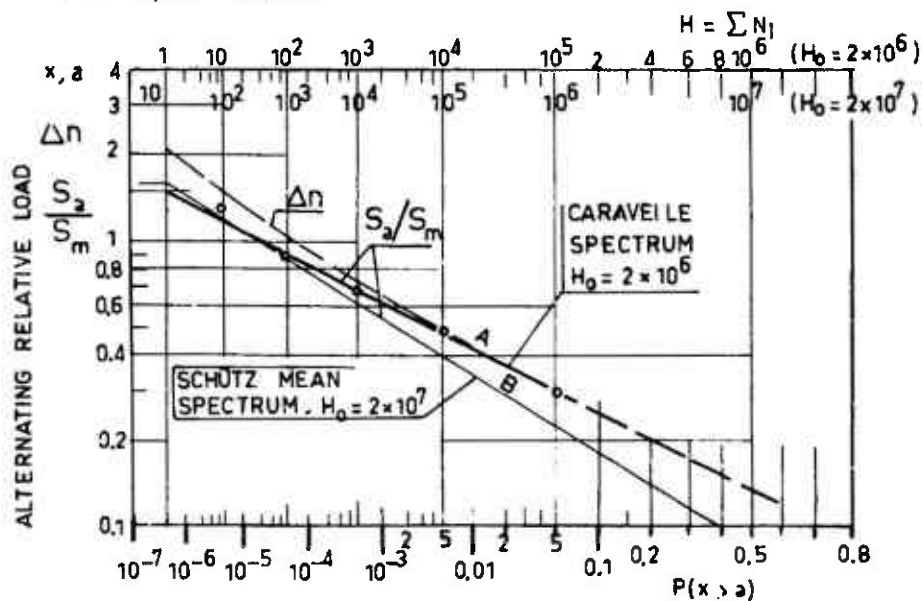(e) LOADS APPLIED DURING A TYPE FLIGHT

(f) LOADS APPLIED DURING A TYPE TEST CYCLE
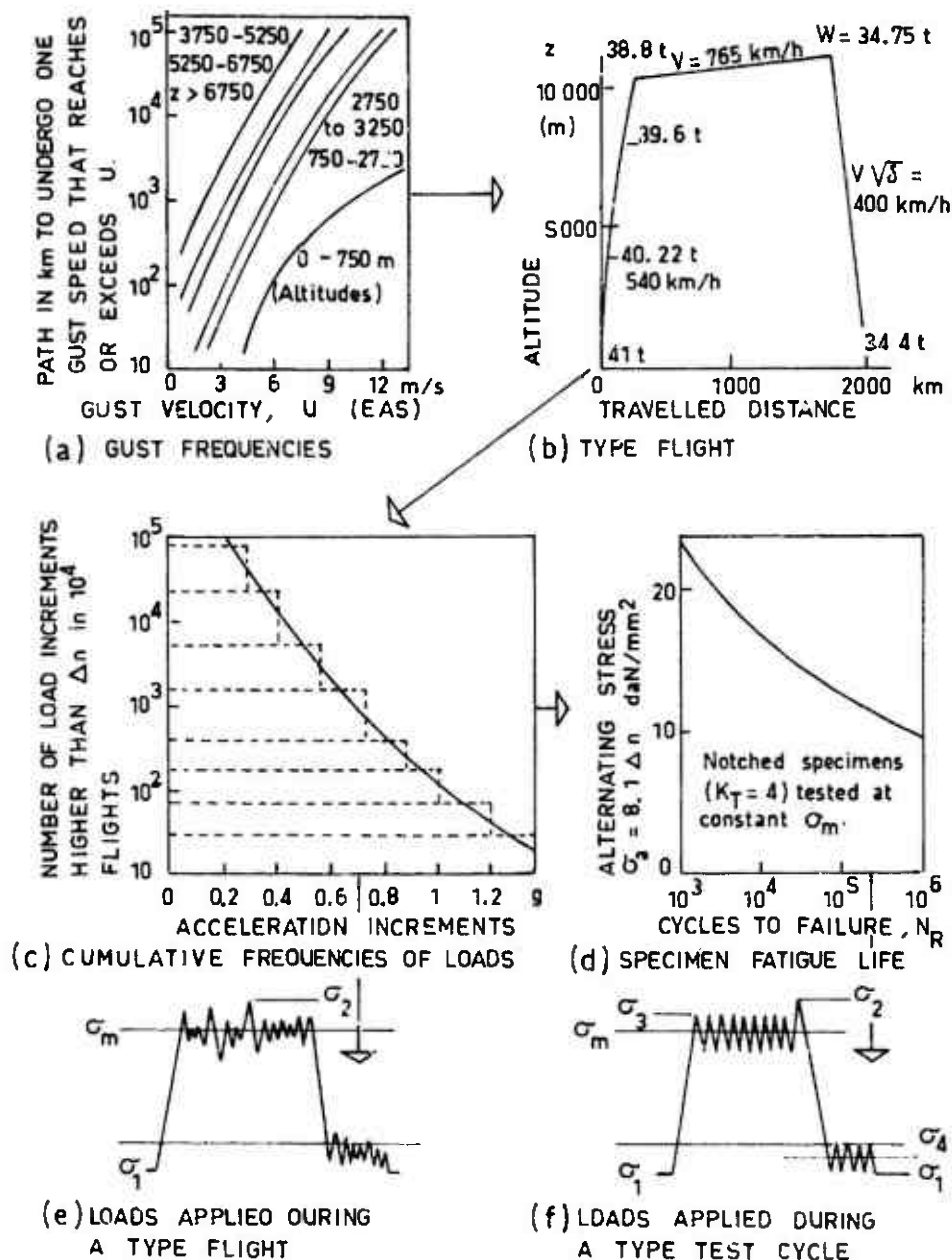
Fig. 1 — Evaluation of fatigue test loads.

Fig. 2 – Load spectrum scatter of transport airplanes. From D. Schutz[12]

FIG. 3 - CARAVELLE FLIGHT LOAD SPECTRUM
FOR 20,000 FLIGHTS.

FIG. 4 - LINEAR PLOTTING OF LOG-NORMAL DISTRIBUTIONS.
CARAVELLE DATA FOR 20,000 FLIGHTS.

FIG. 5 - GAUSSIAN COMPONENTS OF THE CARAVELLE SPECTRUM.
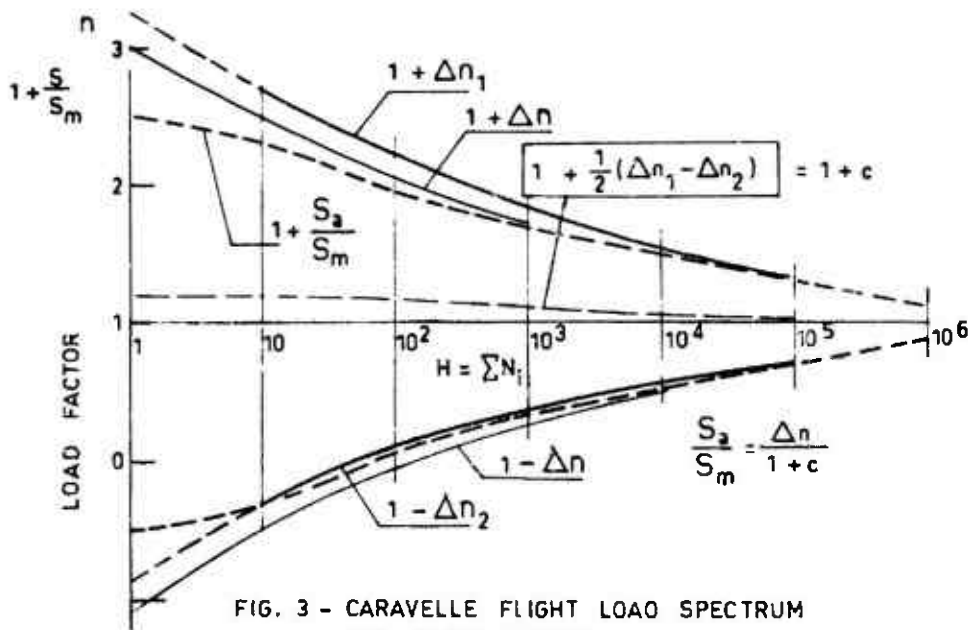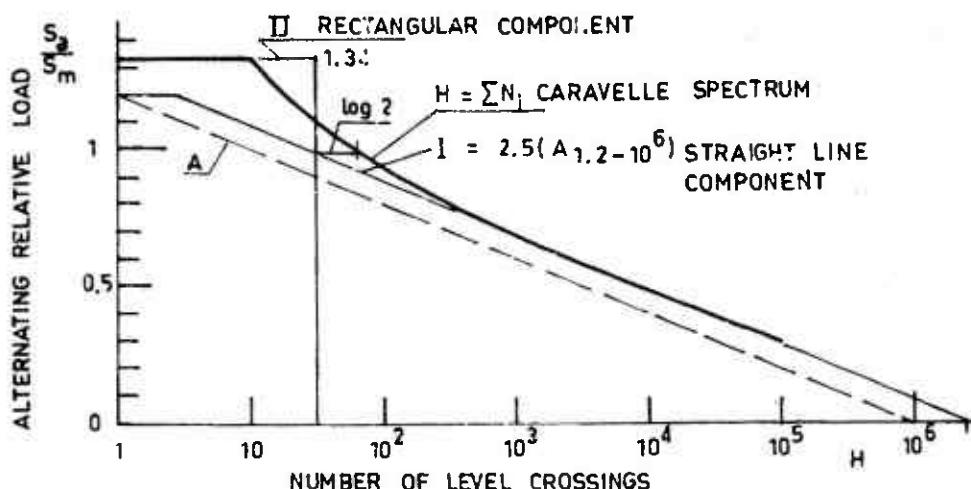
FIG. 6 - STRAIGHT LINE COMPONENT OF THE CARAVELLE SPECTRUM.

FIG. 7 - CONSTANT AMPLITUOE FATIGUE TEST RESULTS
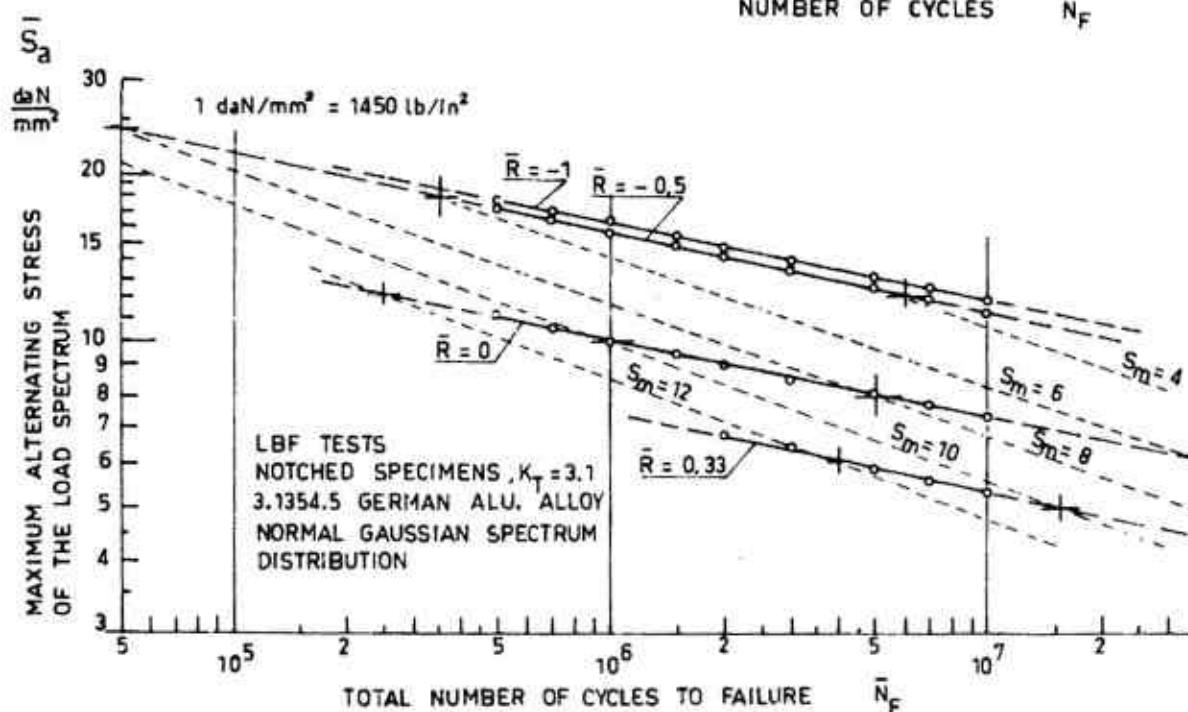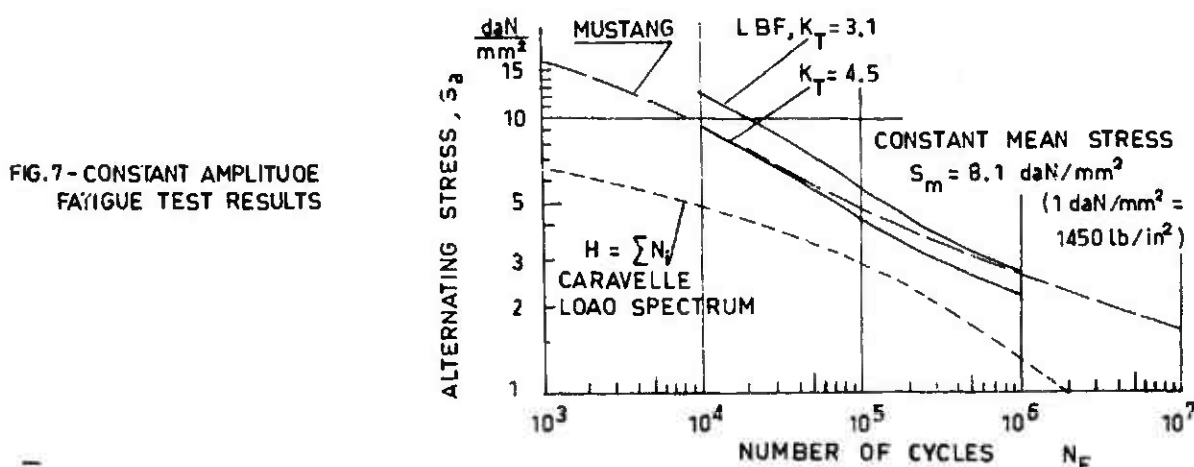
FIG. 8 - LBF $\overline{S}_a$-$\overline{N}$ CURVE OF 3.1-K_T NOTCHED SPECIMENS UNDER GAUSSIAN LOAD DISTRIBUTION
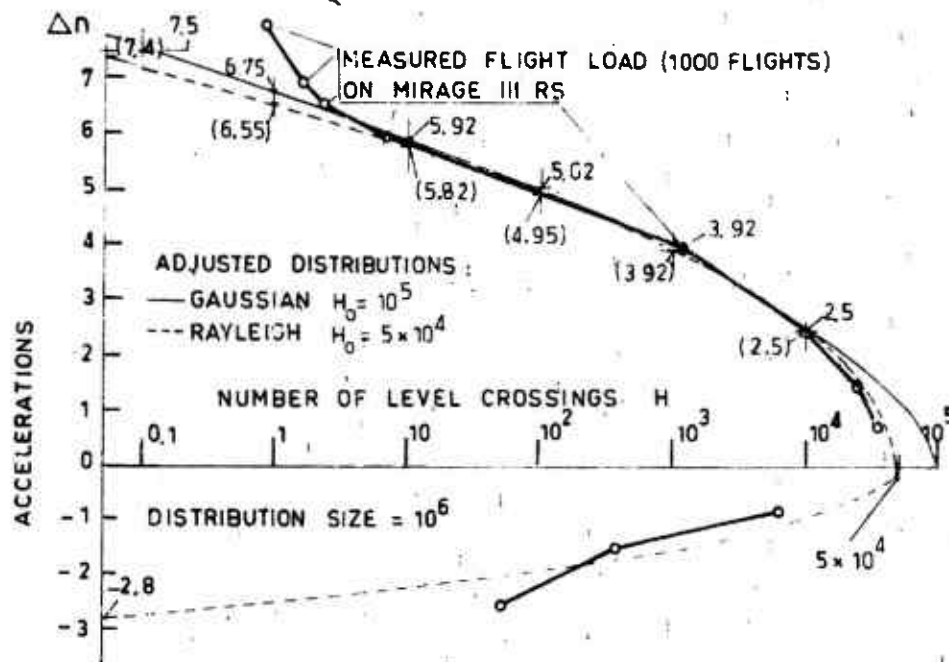
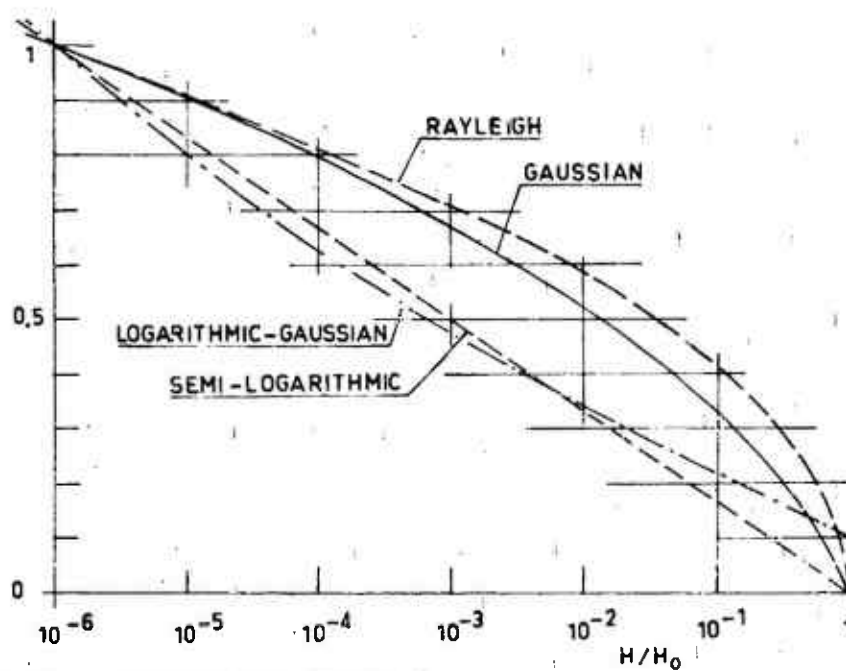FIG 9 - FLIGHT LOAOS ON A FIGHTER AIRCRAFT.
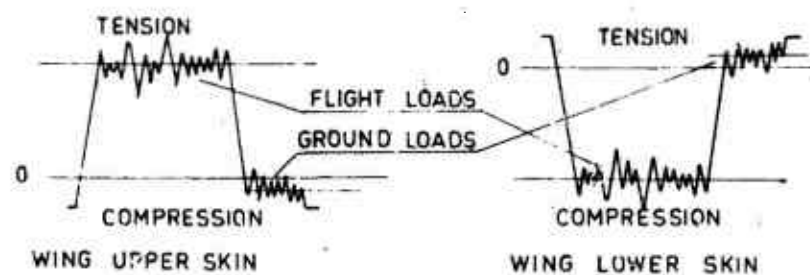

FIG. 10 - DISTRIBUTION SHAPES.

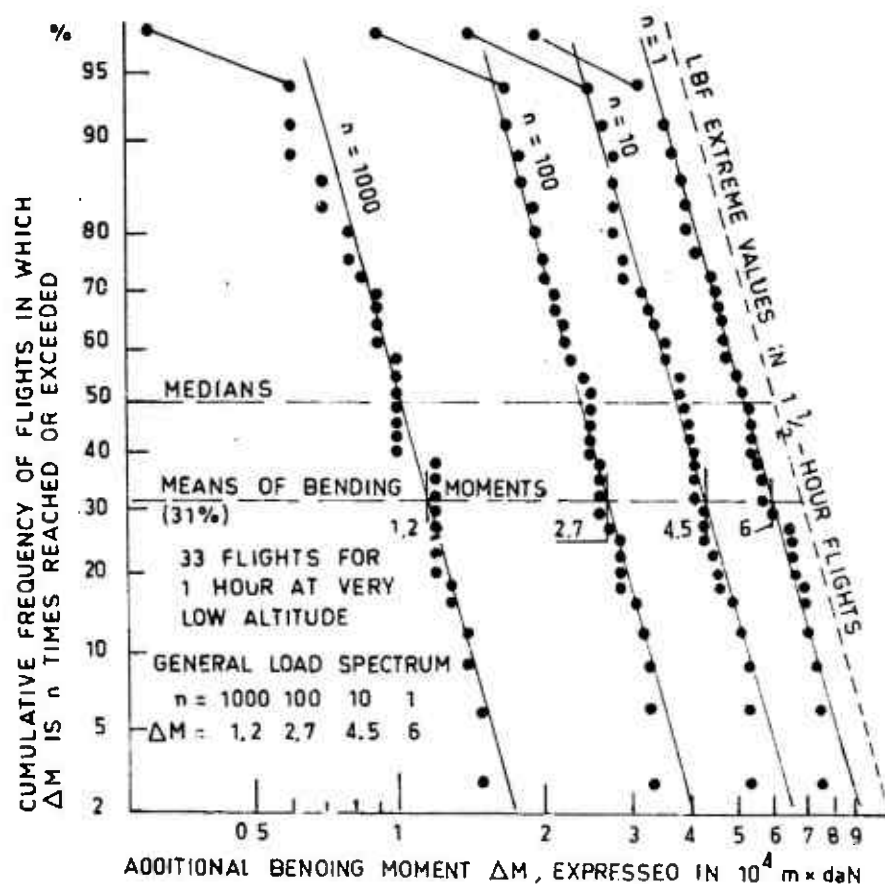FIG. 11 - SERVICE STRESSING OF WING UPPER AND LOWER SKINS.

FIG 12 – FLIGHT DISTRIBUTION IN SEVERITY OF FLIGHT LOAD
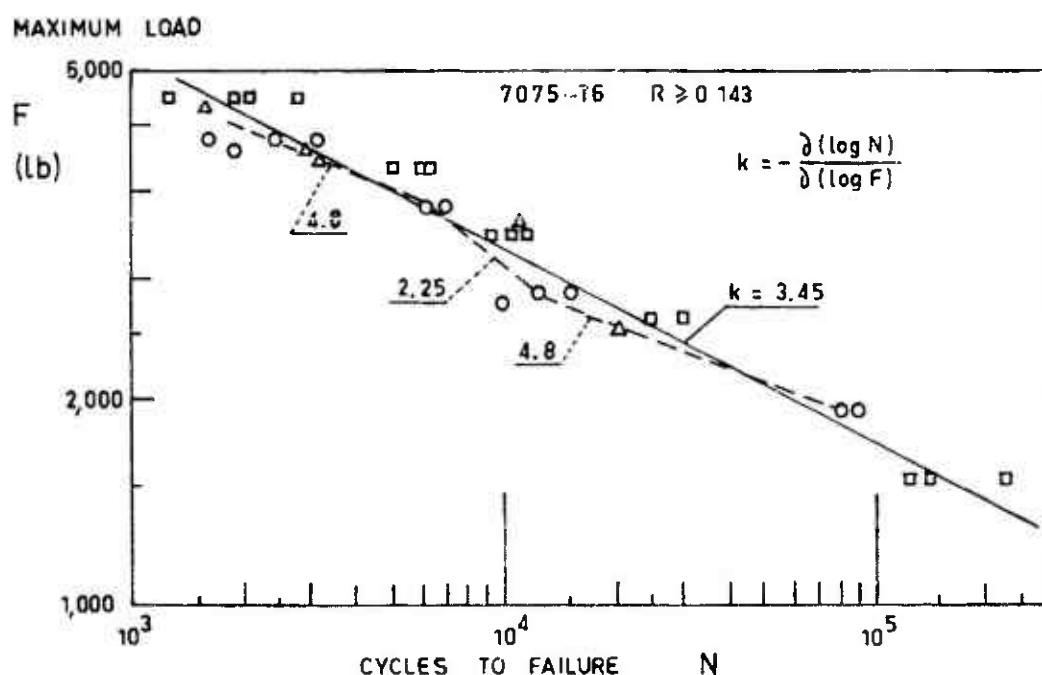SPECTRA OF TRANSALL AIRCRAFT AT LOW ALTITUDES.

FIG. 13 – FATIGUE TEST RESULTS OF 7075-T6 ALUMINIUM ALLOY BEAMS,
FROM MOROFIN AND HALSEY[22].

SOME EFFECTS OF CHANGE IN SPECTRUM SEVERITY AND SPECTRUM
SHAPE ON FATIGUE BEHAVIOUR UNDER RANDOM LOADING

by

W. T. Kirkby
Structures Department, Royal Aircraft Establishment,
Farnborough, Hants., England

SUMMARY

In this paper consideration is given to the problem of re-assessing the fatigue life of an aircraft
structure when it is found that the spectrum of loads experienced in service differs from the load spectrum
applied in test. Results obtained during fatigue tests on structural elements under random load spectra
are used to illustrate some of the important considerations involved. It is shown that the use of an
improved method of life prediction, now issued in Data Sheet form, will generally lead to improved accuracy
in following the procedure for re-assessing life.

In the concluding sections of the paper attention is turned to the corresponding problems of
re-assessing crack growth rates in fail-safe structures, when service experience differs from test
conditions. The need for further work on this problem is emphasised.

1   INTRODUCTION

The problems of the planning and interpretation of fatigue tests to give accurate prediction of life
in service are manifold and work directed to the associated problems has been in progress in several
countries, including the United Kingdom, for more than two decades. Each country concerned has developed
its own fields of expertise and has made particular contributions on one, or more, of the many problems
that arise - it is only by the sharing of the knowledge obtained that significant overall progress towards
adequate understanding has been made. The object of this paper is to summarize some of the more important
findings from cumulative fatigue damage studies made in the UK in recent years, with emphasis on aspects
of the work which are relevant to the interpretation of full scale fatigue tests on component parts and
complete airframe structures. The paper is offered as a contribution to general discussion of the subject
and no attempt is made to summarize the overall state-of-the-art.

A considerable proportion of the fatigue research conducted in the UK in the aircraft field has been
aimed broadly at obtaining a better understanding of the way in which fatigue damage develops and grows in
aircraft structures and is influenced by various aspects of the environment. More specifically, the
objectives of the work have been twofold - firstly to provide a basis for the development of better methods
of full scale fatigue testing and secondly to help with the development of improved methods of fatigue life
prediction. Much of the above work has been conducted on specimens, referred to as 'structural elements'
which represent in a simplified way the essential features of structural joints in aircraft. Such elements
are chosen for study because fatigue damage in aircraft structures generally originates in joints - the
elements may therefore be used to establish basic principles of behaviour though it is recognised that
care must be taken in 'reading across' the knowledge gained to anticipate behaviour in relatively complex
full scale structures. Three types of structural element have generally been used - notched specimens, to
represent stress concentration effects in isolation, and pinned-lug and clamped-lug specimens which include
fretting as well as stress concentration effects.

The influence of several parameters, such as loading waveform, load spectrum shape, load spectrum
severity and exposure to heat, on the development and growth of fatigue damage has been studied using
structural elements, and much has been learned.

This paper is written against the background of one particular, and important, problem which commonly
arises in the interpretation of fatigue tests on aircraft structures - the problem of re-assessing life
when it is found that the spectrum of loads experienced in service differs from the loading spectrum
applied in test. In the sections which follow, the procedure which has been in use in the UK for several
years to meet this problem is outlined and it is shown how the results of the work on structural elements
under random load spectra have contributed to recent improvements in the accuracy of the procedure. The
greater part of the paper is concerned with re-assessment of overall fatigue life to failure and as such
is particularly relevant to safe-life structures. However, towards the end of the paper some evidence is
presented of behaviour during nucleation and propagation of cracks under variable amplitude loading. The
evidence presented on crack propagation, when considered together with the much larger body of evidence
from research centres outside the UK, may contribute to the solution of the particular problem of
re-assessing crack growth rate in fail-safe aircraft under revised loading spectra.

2   BACKGROUND

Fatigue tests form an essential part of the procedure generally adopted in the UK to establish the
airworthiness of an aircraft. The general approach that is adopted in design, testing and operation of
military aircraft in order to meet the fatigue requirements is described in Ref.1. Though civil require-
ments may differ in emphasis and detail, the basic principles are much the same. In order to provide a
setting for the presentation of the results of cumulative fatigue damage studies which are given below it
is necessary to outline, in simple terms, some aspects of the overall approach adopted.

When designing an aircraft the designer must estimate the spectrum of loads to which the aircraft
will be subjected in its service lifetime, from the detailed specification of intended usage of the
aircraft. For many types of aircraft the ground-air-ground cycle is the most important fatigue loading

action though there may be significant additional contributions to the overall loading experience from cabin pressurisation loads, gust loads, manoeuvre loads and landing/taxying loads - for certain types of military aircraft the manoeuvre loads dominate the spectrum. The load spectrum so derived will then be translated into stress spectra for a number of components in the aircraft structure which are considered likely to be the most critical from fatigue considerations. An initial prediction will then be made of the fatigue performance of the components concerned using Miner's rule together with S-N curves appropriate to the type of component and material considered. Redesign may follow if the estimated fatigue life is inadequate or, indeed, if the component is evidently over-designed. In marginal cases fatigue tests may be made on the components concerned under the estimated load spectrum. At a somewhat later stage of development of the aircraft a full scale fatigue test will be carried out on the complete structure, or on major components (complete wing, fuselage, empennage etc.). The test loads will generally be applied on a flight-by-flight basis with manoeuvre and/or gust loads applied in random order within ground-air-ground cycles and will include pressurisation cycles where appropriate.

Any failures of components within the structure that have occurred under the known load spectrum applied in test are then related, in terms of fatigue endurance, to the performance predicted in the design phase. For each component, where failure has occurred, the S-N curve used in the design phase is adjusted by factoring the stress scale until the revised life estimation agrees with the life achieved in test. It should be noted here that the error in the original life calculation for a particular component may be due in part to error in predicting the load distribution throughout the airframe under the applied load spectrum and it may also be due in part to error in the cumulative damage hypothesis used in estimating life.

The concept of adjusting the S-N curve is important as it is this adjusted S-N curve which is used in revising the fatigue life estimates for aircraft of the type concerned, when information becomes available on the load spectra actually experienced in service. Differences between the spectrum assumed in design and testing from the spectra actually experienced by individual aircraft in service may be associated with statistical variation in load history between aircraft of the same type flying in nominally similar conditions - more gross variations may stem from radical changes in the operational rôle assigned to such aircraft. In either event, as discussed further below, the accuracy of the procedure for monitoring life consumption will be improved if the fundamental accuracy of the cumulative damage hypothesis used is increased.

The foregoing observations are drawn from the procedures applicable to safe life aircraft which may fail without prior warning. Much the same procedures apply to the clearance of fail-safe structure, but, from the airworthiness standpoint, there is particular emphasis on ensuring that any fatigue cracks that occur will not grow to catastrophic proportions before detection and subsequent remedial action. From considerations of economical operation of the aircraft it is, of course, desirable that the aircraft shall have a reasonably long crack free life. Thus for fail-safe structures it is necessary to understand, or to make allowances for, the extent to which the nucleation period and subsequent crack growth rates will be affected by deviations of the load spectrum actually experienced in service from the estimated for design and applied in the full scale test.

There are, of course, other important aspects of the overall clearance procedure, such as load monitoring in service, and residual strength requirements, which lie outside the scope of this paper and have not been discussed. However, sufficient has been said to demonstrate the important part that the method of life prediction plays in re-assessing life, and the need for further understanding of the way in which initiation and growth of fatigue cracks may be affected by changes in the loading environment. In the sections which follow an outline is given of the insights which have been gained and the progress that has been made in the above fields in the course of cumulative fatigue damage studies in the UK.

3   EFFECTS OF LOAD INTERACTIONS ON FATIGUE LIFE TO FAILURE

The importance of interaction effects when load cycles of differing magnitudes are applied to a specimen undergoing fatigue tests have been recognized for many years. Experience in tests using preloading, block programme loading and more realistic forms of loading such as flight-by-flight loading have provided much qualitative evidence of behaviour. Many of the associated studies in the UK in recent years have been conducted on pin-lug and simple bolted joint specimens under random loading. In this work evidence has been obtained of the effects on cumulative damage of changes both in load spectrum severity and in shape of spectrum - this evidence is used, in the paragraphs which follow, to highlight some aspects of behaviour which are relevant to the problems of relating test conditions to service experience.

3.1   Outline of results to be considered

The results which form the basis of discussion in this section were obtained in the course of an investigation[2] of a method of life prediction using data obtained under random loading conditions. Lug specimens in aluminium alloy (Fig.1) loaded through steel pins were used. The tests were conducted in fluctuating tension both under constant amplitude loading and under random loading. In the latter tests, narrow band random loading was used firstly to apply a simple Rayleigh distribution - Fig.2a shows a typical loading waveform and Fig.2b shows the probability distribution of peak amplitudes. These tests were conducted over a range of average (rms) levels and were followed by 'random programmed' tests in which a gust spectrum was synthesised by the repetitive application of three different rms levels of the Rayleigh distribution to give the required overall peak distribution (analogous to block programme loading). The gust spectrum chosen was taken from RAeS/ESDU Data Sheets[3]. Tests under this latter spectrum were run at three overall average spectrum levels, designated A, B and C in the table below.

Table 1

Step No.	% of total number of peak counts	Spectrum A	Spectrum B	Spectrum C
		Alternating stress level ksi (rms)		
1	77	0.98	1.38	1.66
2	21	1.76	2.50	3.00
3	2	2.90	4.05	4.90
Overall average spectrum level ksi (rms)		1.25	1.76	2.13

In all the above tests a minimum of four tests were conducted at each loading condition - the results are illustrated in Figs.3a snd 3b. For convenience in subsequent discussion the results of the tests under random losding may be summarised as follows:-

Table 2

Spectrum shape	Spectrum level ksi (rms)	Endursnce log mean - cycles 10^6
Rayleigh distribution	1.37	2.68
	2.57	0.713
	3.75	0.308
	4.9	0.213
RAeS Gust spectrum	1.25 (A)	5.54
	1.76 (B)	4.40
	2.13 (C)	3.12
	1.68 (B^+)	1.85

The spectrum B^+ listed above diffeied from B in that the Rayleigh distribution of Step 3 was omitted - this was the highest rms level in the synthesis but it only accounted for 2% of the totsl number of peak counts in the overall spectrum.

It is of interest in relation to the problems of interpretation of lsboratory tests in terms c^f service experience to exsmine the above reaults in the context of the general procedure currently followed for full scale structures and components as outlined in section 2 above. For example the result of a particular test under apectrum loading could be considered to represent the only avsilable result from, ssy, a full scale test. This result, together with the basic S-N curve (Fig.3a), could then be used to establish an adjusted S-N curve and, on the basis of this latter curve, life under one, or more, of the other test spectra could be re-estimated. Comparison of the re-estimated life with the lives actually achieved under the spectra concerned would give some indication of the magnitude of the errors which may be involved in following the procedure. It should be remembered that such a simplified examination only explores the sources of error associated with inaccuracy of the cumulstive damage rule employed - as discussed in section 2 another potential source of error, when dealing with full scale structures, is associated with incorrect assumptions regarding rhe load distribution on individual component psrts of the structure. This latter sspect is not considered in this paper.

In the following paragraphs an examination is carried out firstly to consider errora arising when the rms level, rather than the shape of the spectrum, is changed snd, secondly, when the shape of the spectrum is changed with little chsnge in level.

It will be recollected that the first step in the procedure for re-assessing life described in section 2 ia to observe the ratio between the life achieved in the test under spectrum losding and the life predicted from the originsl S-N curve. The original S-N curve is then repositioned by scaling the stress axis so thet the ratio becomes equal to unity. In the analysis of the pinned-lug test results this ratio may siwply be referred to as the value of $\Sigma(n/N)$, since there is no uncertsinty regarding the magnitude of the fatigue losds applied. In considering the results it would be informative to note the values of $\Sigma(n/N)$ under the various loading conditiona, as deduced from the original S/N curve (Fig.3a):-

Table 3

Spectrum shape	Spectrum level ksi (rms)	$\Sigma(n/N)$
Rayleigh distribution	1.37	1.12
	2.57	2.03
	3.75	2.20
	4.9	2.38
RAeS gust spectrum	1.25 A	2.39
	1.76 B	5.03
	2.13 C	5.51
Modified RAeS gust	1.68 B^+	1.71

3.2 Effect of change of spectrum level

Considering first the effects of changing spectrum level, it is apparent from Table 3 above that broadly speaking the higher the rms level the greater the value of $\Sigma(n/N)$. Fig.4 illustrates this trend - it is clearly evident for the Rayleigh distribution and it is even more marked for the gust spectrum. Thus when applying the procedure of section 2 to these particular results in order to give some indication of the validity of the procedure, the following pattern of error was found to apply to the results of the re-assessment of life. If the level of the loads experienced 'in service' was less than that anticipated and applied in test, then the revised prediction of life was optimistic (unsafe). This is because there is an implicit assumption in the procedure that the value of $\Sigma(n/N)$ does not change with spectrum level and thus having been brought to unity at the (higher) spectrum level in test, by adjusting the S-N curve, it will also be equal to unity at the lower level experienced 'in service'. In fact $\Sigma(n/N)$ was lower. If, conversely, the loads experienced 'in service' were of greater overall severity than those applied in test, then the inverse was true, i.e. the life achieved 'in service' was longer than the prediction based on the adjusted S/N curve had suggested.

Specific examples may be taken to illustrate the above trends. The first examples are taken from the results of the tests under the Rayleigh spectrum; let it be supposed that the log mean life of 0.308×10^6 cycles obtained at a spectrum level of 3.75 ksi rms (Table 2, page 2-3) represents the single full scale test result. If subsequent service experience were to show that the spectrum level was 2.57 ksi rms - some 30% lower than anticipated - with no change in spectrum shape, then applying the procedure to adjust the original S/N curve and re-assess life would result in an estimate of life of 0.77×10^6 cycles compared with the life of 0.71×10^6 cycles actually achieved. Thus, the life achieved 'in service' would be approximately 90% of that predicted. If the level measured in service were to be 1.77 ksi rms - approximately 65% lower than anticipated - the error would be much more serious: the predicted life would be 5.28×10^6 cycles compared with an achieved life of 2.68×10^6 cycles, so that service life would only be some 50% of that expected. On the other hand, if the service experience indicated more severe loading - 4.9 ksi rms compared with the test loading of 3.75 ksi rms - then the revised life estimate would be conservative (safe), since the life achieved would be approximately 10% greater than anticipated.

A similar trend may be demonstrated from the results of the tests under the gust load spectrum. However, with this form of load spectrum the errors in life re-assessment may be considerably greater for a given percentage different between the severities of the 'full scale test' and 'service' spectra than was the case with the Rayleigh distribution. For example, if the test result under the gust spectrum at 1.76 ksi rms (Table 2, page 2-3) is taken as the single full scale test result, it may be shown that this life achieved in service will be somewhat less than 50% of that predicted on the basis of a service spectrum some 30% lower in severity than assumed for the full scale test loading. Conversely, if the spectrum in service were to be approximately 10% higher than anticipated for full scale test purposes then the life in service would be about 10% greater than the service life prediction would suggest.

The above examples have served to illustrate the magnitude of the errors that may arise in re-assessing life in service when it is found that the spectrum of loads in service differs in overall severity but not in shape, from the spectrum of loads applied in the full scale test. In the section which follows attention is turned to errors that may arise in re-assessing life when the shape of the spectrum of loads experienced in service, rather than the overall severity of load spectrum, differs from that applied in test.

3.3 Effect of change of spectrum shape

Considering now the effect of change of spectrum shape on fatigue endurance at a given overall level, it is immediately evident from Fig.3b that large changes in endurances can occur at the same spectrum level. Generally, over the range of levels considered the endurance under the gust spectrum is some 2 to 3 times greater than the endurance under the Rayleigh distribution, for the same rms stress level, the higher ratios being associated with the higher spectrum levels.

It is evident from the above evidence that spectrum level alone is an inadequate guide to endurance when reading across from one spectrum to another of appreciably different shape. Further examination of the results shows that even a comparatively small change in spectrum shape can produce a dramatic effect on endurance at the same average level. For example, from Fig.3b, it may be seen that at an rms level of 1.68 ksi that the endurance under spectrum B was reduced by a factor of approximately 2.5 in changing to spectrum B⁺. It will be recollected that the difference in spectrum shape was small - some 2% of the total number of peak counts, associated with the highest step in the programme B being omitted. Since the life was reduced by deletion of the highest peaks it is evident that these high peaks were, in fact, beneficial. Use of the procedure of section 2 to re-assess life with the modified spectrum would in fact have indicated approximately 5% increase of life in contrast with the severe reduction which occurred.

3.4 Further investigations

The results discussed above refer to the behaviour of pin-lug elements under fluctuating tensile loadings and it would be unwise to generalise too widely from these particular results. It should be borne in mind that, when considering other forms of variable amplitude loading (such a flight-by-flight loading) in which values of $\Sigma(n/N)$ closer to unity may occur, the magnitude of the errors in life re-assessment would not necessarily be so great. However, the results have served to illustrate some of the problems inherent in re-assessing life and, in particular, they have highlighted the need for a more accurate cumulative damage rule.

Following the investigation[2] from which the above test data were taken, a large body of evidence has been obtained from subsequent work under variable amplitude loading. Cumulative damage studies have been made on several other forms of structural elements such as notched specimens[4], clamped lug (simple bolted joint) specimens[5] and more complex bolted joints[6]. The studies have included observations of the effects on cumulative damage behaviour of preload, mean stress[7] and exposure to heat[4]. The results of all this

work taken together with information from many other sources, have helped to build up a background of evidence within which improved methods of life prediction have been developed and assessed.

In the course of the foregoing studies an assessment[7] has been made of the relative importance of several factors which may affect the accuracy of fatigue life prediction under variable amplitude load spectra. In this assessment consideration has been given to the variation of relative damage rate with stress level, effect of low level stress cycles, effect on life of the load at which a component fails, effects of fretting, and the effects of residual stresses associated with plastic deformation at stress concentrations. Of the factor considered, it was shown that residual stresses at stress concentrations could have a large influence on the rate of growth of fatigue damage - consideration of the effects of such stresses could explain, in many cases, large departures of $\Sigma(n/N)$ from unity when applying Miner's rule.

In the light of this assessment, work followed to obtain a better quantitative understanding of the magnitude of the residual stresses under various loading conditions, using the 'companion specimen' technique[8]. Such studies have been made on structural elements containing a circular notch[9] and, very recently, on loaded holes in pin-lug specimens. This work was aimed at providing further information to be used, together with evidence from similar studies in Germany[10] and the USA[8], in the evolution of an improved method of life prediction in which some allowance would be made for residual stress effects. Such a method has now been developed and issued[11] in Data Sheet format by the Engineering Sciences Data Unit of the Royal Aeronautical Society. It is believed that the use of this improved method of life prediction will signif- icantly reduce the errors of the nature discussed above, when re-assessing life under a change spectrum of loads. Some evidence to support this view follows in the next section.

3.5 The RAeS/ESDU method of life prediction

In applying the method of the ESDU Data Sheet, the cumulative damage principle of Miner's rule is broadly followed but allowance is made for residual stress effects which modify the local mean stress when local yielding occurs at the stress concentration. In following this procedure, use is made of a simple model of the stress strain curve for the material concerned. It is necessary to consider not only changes in local mean stress under the variable amplitude spectrum loading but also to consider deviations from the nominal local mean stress under the constant amplitude loading of the basic S-N data.

Table 4 - Comparison of life prediction using Miner's rule and RAeS/ESDU method

Type of member	K_t	Material	Load sequence	Number of specimens	Mean endurance cycles × 10^{-6}	$\Sigma(n/N)$ Miner	$\Sigma(n/N)$ RAeS/ ESDU	Ref.
Notched strip	4.0	7075-T6	high-low	4	1.27	4.00	1.04	13
Riveted lap joints	3.75	7075 clad	low-high	7	0.81	1.01	1.01	14
			"	7	0.94	0.94	0.94	
			"	7	0.66	1.04	1.04	
			"	7	1.01	0.73	0.73	
			"	3	10.10	12.50	1.60	
			"	4	4.88	5.90	0.76	
			"	5	4.87	5.90	0.76	
			high-low-high	7	0.51	0.71	1.85	
			"	7	0.71	0.86	2.50	
			"	7	3.03	3.70	0.48	
			low-high	7	0.95	1.26	1.12	
			low-high	7	0.78	1.06	0.93	
			high-low	7	0.74	1.01	0.88	
			low-high-low	7	0.72	0.97	0.86	
			high-low	7	3.48	4.11	0.55	
			low-high	7	0.72	1.03	0.93	
Riveted lap joints	3.75	2024 clad	low-high	7	13.30	2.60	1.07	14
			high-low	7	7.11	1.40	0.55	
			low-high-low	7	10.40	2.08	0.83	
			low-high	7	6.31	1.23	0.67	
			low-high	7	18.60	1.92	0.78	
			high-low-high	7	5.40	1.07	0.71	
			high-low-high	7	35.2	6.67	1.60	
Notched strip	3.95	OTD 363A bar	low-high-low	6	0.14	1.30	0.61	15
			"	6	0.12	1.06	0.74	
				5	0.11	2.04	0.89	
Notched strip	3.5	2024-T4	low-high-low	10	1.75	0.25	0.95	16
			low-high-low	13	7.00	1.00	1.18	
Notched strip	4.0	2024-T3	random	6	0.20	2.30	1.25	17
Loaded lugs	3.2	BS 2L65	random	5	0.22	2.38	1.00	2
			"	4	0.32	2.18	1.14	
			"	5	0.82	2.04	0.84	
			"	4	2.80	1.08	1.08	
			"	4	5.66	2.38	0.55	
			"	8	4.80	5.25	0.85	

The method is broadly similar to that developed independently by Impellizzeri[12] in the United States - the RAeS method is however somewhat simpler in concept and application as it is assumed that the residual stress state remains unchanged until yielding next occurs at the stress concentration. This contrasts with the method of Impellizzeri in which some allowance is made for decay of residual stress state between cycles in which yielding occurs.

A considerable body of data from variable amplitude fatigue tests obtained from several sources[2,13-17] has been reexamined in order to assess the improvement in accuracy obtained when the RAeS/ESDU method is used in place of Miner's rule. Table 4, on reverse side of this page, gives details of specimen type, loading conditions, and other relevant information - it includes figures of $\Sigma(n/N)$ using the two methods of life prediction. The results are illustrated in Fig.5. It will be seen that most of the data examined relates to block programme loading tests, only a small proportion of the data being obtained under random loading conditions. The results of the assessments of accuracy which have been completed to date are encouraging. Based on the 36 results listed in Table 4, page 2-5, the following statistical assessment has been made:-

<p align="center">Table 5</p>

	Miner's rule	RAeS/ESDU
Mean summation	$\Sigma \frac{n}{N} = 2.42$	$\Sigma \frac{n}{N} = 0.97$
Standard deviation of $\Sigma \frac{n}{N}$	2.38	0.40
Coefficient of variation of $\Sigma \frac{n}{N}$	0.98	0.41

On the basis of the above analysis it is evident that there is a marked improvement in the accuracy of life prediction when using the RAeS/ESDU method and also, and equally important, there is a significant reduction in variability. It is considered that the magnitude of the improvement is more than sufficient to justify the use of this method despite the increased computational effort involved.

It should be noted that, in the life prediction method, quantitative allowance is made for residual stress effects at the surface at the point of maximum stress concentration where fatigue damage will generally nucleate. It is implicitly assumed that the corrections made to the cumulative damage calculation to allow for residual stress behaviour in the vicinity of damage nucleation also apply throughout damage growth to failure. Since local stress conditions and metallurgical conditions during nucleation of fatigue damage differ markedly from conditions during crack growth there is no fundamental reason to suppose that such an assumption is justified. However, the fact that the method appears to work reasonably well suggests that, broadly speaking, load interaction effects are comparable, qualitatively and quantitatively, during nucleation and crack propagation. This is not to say that the underlying load interaction mechanisms are the same - attention is paid to some aspects of the associated problems in the section which follows.

4 LOAD INTERACTION EFFECTS DURING CRACK NUCLEATION AND PROPAGATION

4.1 Preamble

In the preceding sections attention has been directed to the problems involved in re-assessing fatigue endurance to failure when the spectrum of loads experienced in service differs from that applied in test. Such re-assessment is a primary consideration for components or structures designed on a safe-life basis. However, in the case of structures designed on fail-safe principles consideration other than simply life to failure must also be borne in mind. Two important objectives of a full scale fatigue test on a fail-safe structure are to demonstrate a reasonable life free from the onset of cracking and also to demonstrate that any cracks which may occur will not grow to dangerous proportions before detection. To meet the latter requirement, fatigue tests on such structures will have included observation of the growth rates of any cracks in the structure ('natural' or artificially induced), and such observations will subsequently be related to frequency of inspection in service. If it is subsequently found that the spectrum of loads actually experienced in service differs from that applied in test, then re-assessment of fatigue performance should include re-assessment of life to the appearance of damage and also, and perhaps more importantly from an airworthiness standpoint, re-assessment of crack growth rates.

The majority of the cumulative damage investigations conducted in the UK on structural elements have been aimed primarily at observing and understanding the effects of load interactions on life to failure. Nevertheless, in the course of these investigations, valuable insight into some aspects of crack nucleation and propagation under variable amplitude loading have been gained. Some of the UK experience is set out in the paragraphs below. The evidence presented is somewhat fragmentary and serves rather to highlight the complexity of the problems rather than to indicate a coherent overall pattern of behaviour. It is therefore offered primarily as a contribution to wider discussion from which, it is hoped, clearer guidelines may be established for re-estimation of crack rate after change in load spectrum.

4.2 Evidence of the relative importance of load interaction effects during crack initiation and during crack propagation

In this section evidence is presented which was obtained during tests on pin-lug specimens to examine the relationship between the residual static strength of the element and the proportion of fatigue life consumed. Tests were made under both constant amplitude and random loading conditions. The results are important as they suggest, in contrast to the broad indications of section 3.5, that load interaction effects may have more influence on the rate of growth of fatigue damage during the nucleation phase of the fatigue process than in the subsequent crack growth phase.

The results are taken from an extensive investigation[7] of cumulative fatigue damage in pinned-lug specimens in DTD 5014 aluminium alloy. The design or the specimen is the same as that shown in Fig.1. The technique used was to establish average life to failure (log-mean endurance) at a particular stress level and to perform a series of tests subsequently in which the fatigue loading was stopped at a chosen percentage of the average life; the specimen was then removed from the fatigue machine and a static strength test was performed. By carrying out such static tests at different chosen percentages of fatigue life, a curve could be drawn showing residual static strength *vs.* percentage of fatigue life consumed. When using this technique it was found that there was considerable scatter in static strength at any chosen percentage of the average fatigue life, probably because of scatter in the individual lives to failure, relative to the average life to failure. Indeed, it was difficult to acquire results for endurance beyond 75% of average life without experiencing an unacceptable number of fatigue failures, prior to achieving the intended percentage of average life. Nevertheless, despite the scatter problem, trends can be discerned from the results which are of considerable value in understanding the overall fatigue damage process.

In Figs.6a and 6b results are shown for residual strength tests at three rms stress levels under both constant amplitude (sinusoidal) and random loading with a Rayleigh distribution of peak amplitudes. It may be seen that, under constant amplitude loading, there is a significant difference in the shapes of the curves at the three stress levels - for example, at a stress level of 1.5 ksi rms the specimens have fallen to 80% of their original strength when 50% of the fatigue life has been consumed, whereas at 6.5 ksi rms the specimens retain approximately 80% of their strength at 80% of life. The tendency for the original strength to be maintained to a higher percentage of fatigue life, as stress level is increased, is believed to be associated partly with the beneficial residual stresses associated with local yielding. The yield strength (0.1% proof) of the material used in the foregoing residual strength tests was approximately 51 ksi and, with a stress concentration factor K_t of 2.96, local yielding would occur at and beyond alternating stresses of 1.1 ksi (peak) when superimposed on a mean stress of 16 ksi. Local yielding will therefore occur over the range of alternating stresses illustrated and the residual stress effects will become more significant as stress level is increased. This observed pattern of behaviour may be explained if it is assumed that load interactions have a more beneficial affect during the nucleation phase of the fatigue damage process than in the subsequent crack propagation phase and that there is no significant reduction in static strength of the specimen until cracking occurs on a macro-scale. There is a considerable body of evidence to support the latter assumption[18,19] and if the first assumption is accepted it would follow that beneficial residual stress effects would lead to retention of the original static strength to a higher percentage of life to failure.

The results obtained from the residual strength tests under variable amplitude loading - Fig.6b - differ markedly from those under constant amplitude loading. There is a tendency for the curves for variable amplitude loading at the three stress levels to group more closely together and the general shape corresponds to the curve for the highest constant amplitude stress - 6.5 ksi rms. This is broadly in keeping with the effects of residual stresses discussed above since the higher peaks in the variable amplitude load spectra would be expected to cause a more local yielding than would occur under constant amplitude loading at stresses appropriate to the same life to failure. Results which are qualitatively similar have also been obtained on such specimens at other mean stress levels.

It will be noted that the hypothesis that load interaction effects are more significant during the nucleation phase than in the subsequent crack propagation phase is apparently somewhat at variance with the general observation at the end of section 3.5 which suggested that load interaction effects were much the same throughout life.

In considering such an apparent anomaly it should be remembered that the so-called nucleation period in the pin-lug joints includes the complex process of initiation of damage, probably by a combination of fretting and stress cycling effects, and the subsequent development and growth of micro-cracks. Moreover the damage develops and grows through the stress gradient associated with the stress concentration at the hole. In such a complex situation it would certainly be unwise to generalise from the particular results obtained but, equally, such results must be borne in mind when endeavouring to establish a model of cumulative damage behaviour under spectrum loading that can be widely applied.

4.3 Some evidence concerning fretting behaviour under random loading

It is generally recognised that in specimens in which fretting occurs, such as the pin-lug specimen discussed above, the effect of fretting is to reduce substantially the nucleation phase of the overall damage process. In seeking further understanding of the observed prolongation of the nucleation period relative to the crack propagation phase, discussed in section 4.2 above, consideration has been given to the possibility that the build up of fretting damage under variable amplitude loading conditions may have been significantly slower than during the associated constant amplitude tests.

A series of tests is currently in progress to examine this possibility using plain aluminium alloy (BS 2L65) specimens and using steel (S98) fretting pads. Tests are being conducted under both sinusoidal loading conditions and random loading conditions - firstly to determine life without fretting, secondly to determine life with fretting pads fitted throughout the total life and, finally, to observe life with the fretting pads removed at differing proportions of the nominal (fretted) life of the specimen. Such tests will indicate the percentage of life at which the fretting process may be regarded as being complete. Some preliminary results are now available[20] which have been obtained over a range of alternating stresses about zero mean load. These are presented in Figs.7a and 7b.

It will be seen that these preliminary results, in fact, strongly indicate that the completion of fretting damage is more rapid in the random loading case than under sinusoidal loading. For example, in the endurance range $10^6 - 10^7$ cycles it appears that the fretting process is completed (from the point of view of reducing life) somewhere between 10% and 30% of life under sinusoidal loading whereas under random loading the damage process is virtually complete at 5% of life.

It is evident that these results do not explain the observed extension of the nucleation phase and other explanations must be sought. The fact that crack propagation (in this case including micro-cracking)

may occupy 95% of the life of structural elements under random loading, if fretting occurs from the start of the loading, emphasises the need for further understanding of load interaction effects throughout the whole crack growth process. Such knowledge will be necessary if the effects of change in loading spectrum on the behaviour of such elements are to be fully understood and, in the section which follows, results are outlined which provide some further evidence on this topic.

4.4 Values of $\Sigma(n/N)$ for life to failure, and for crack propagation under the same load spectra

The results which are outlined in this section are taken from experiments made in connection with the evaluation of a method[6] of monitoring the severity of the fatigue loads experienced by a structure. The monitoring device consists of a pre-cracked coupon which is attached to the aircraft structure so as to experience a strain history corresponding to that experienced by the structure under the applied fatigue loads. The principle of the method is that the growth of the crack in the coupon provides a measure of the severity of the fatigue loads applied to the parent structure. Tests have been made in the course of a preliminary investigation of the method using a double-ended bolted joint specimen with a centre cracked rectangular panel (Fig.8) attached to the aluminium alloy boom of the specimen. The length of the starter crack in the coupon was 0.5 in and the coupon was replaced periodically, throughout the fatigue life of the bolted joint, as the crack in each coupon reached approximately 1 inch in length. The chemical composition of the sheet material from which the coupon was cut was virtually identical to that of the aluminium alloy boom. Tests were made on such bolted joint specimens, with a series of coupons attached, under sinusoidal loading, block programme loading and under random loading. The tests were made predominantly in fluctuating tension — the block programme loading represented a gust spectrum for a short haul transport aircraft and the random loading was a flight-by-flight representation of a gust spectrum for a long range transport aircraft with ground-air-ground cycles.

From the results of the tests under constant amplitude loading a conventional S-N curve for the joint was obtained and, also, an 'S-N curve' for crack growth in the coupons — in the latter case N was the number of cycles required under an alternating stress S to grow the crack from 0.5 in to 1.0 in. The S-N curve for the joint and the curve showing crack behaviour in the coupon are shown in Fig.9. From these curves, values of $\Sigma(n/N)$ at failure were calculated for the joint under the two differing load spectra and also, on the basis of the observed crack growth rates under each of the two load spectra, corresponding value of $\Sigma(n/N)$ were calculated for crack growth from 0.5 in to 1.0 in. In the above calculations simple summation of damage (Miner's rule) was used. The results of the analysis were as follows:-

Load spectrum	Spectrum severity ksi rms	Overall life		Cracked coupon behaviour	
		Endurance cycles $\times 10^{-6}$	$\Sigma \frac{n}{N}$	Growth rate cycles $\times 10^{-6}/0.5$ in	$\Sigma \frac{n}{N}$
Gust spectrum – short haul transport	2.78	3.51	2.42	0.465	3.19
Gust spectrum + GAG – long range transport	3.83	1.07	1.89	0.302	2.03

It will be seen that $\Sigma(n/N)$ for the growing crack did not differ very greatly from the value of $\Sigma(n/N)$ for life to failure of the parent member over the range of crack length concerned. Again it would be unwise to generalise from this particular result as it is probable that the value of $\Sigma(n/N)$ for a crack growing under variable amplitude loading will not only depend on the spectrum shape and severity but also on the mean length of crack for which the value of $\Sigma(n/N)$ is derived. Setting aside interaction effects, crack growth will not occur under a particular load cycle in the applied spectrum unless the resultant stress intensity at the crack tip exceeds a certain threshold value. The stress intensity is a function of both the average stress in the vicinity of the crack and also the length of the crack; it follows that at very short crack lengths a proportion of the stress cycles in the applied spectrum may be causing no crack growth whereas, at longer crack lengths, all of the stress cycles may be contributing to growth. However, in the example that we have considered above, the length of the starter crack was such that, for both spectra, the crack growth threshold was exceeded by the lowest stress cycles applied so the observed differences in $\Sigma(n/N)$ for crack growth under the two differing spectra are almost certainly due to load interaction effects.

Although detailed correlation with results from other sources is outside the scope of this paper, it may be observed that there is a large body of evidence, principally from investigations at the NLR in Holland[21,22] and at NASA (Langley)[23] which also show that values of $\Sigma(n/N)$ for crack growth considerably in excess of unity may occur under fluctuating tensile loading - values of $\Sigma(n/N)$ greater than 3 have been noted[21] for crack growth in sheet material under random loading spectra.

4.5 General comments on crack initiation and growth under variable amplitude loading

In the preceding sections results have been given which illustrate the complexity of the general problem of understanding and predicting crack growth under variable amplitude loading. Certain anomalies have become apparent in seeking a coherent pattern of behaviour. Bearing in mind the exponential nature of crack growth, a large proportion of life may be spent in the micro-macro growth range. Growth in this range therefore will play an important part in determining life over which no significant damage occurs and over which residual static strength is not seriously impaired. This growth regime is of significance in safe-life aircraft though generally it does not receive specific attention in design and airworthiness clearance – such aircraft are cleared broadly on endurance to failure as outlined in section 2 above. Further research work is necessary in this regime in order to obtain a better understanding of interaction

effects - however, there is no immediate urgency in relation to airworthiness problems and the studies may be conducted on a relatively long-term basis. The problems, as mentioned in the concluding paragraph of section 4.2 above, appear to be more daunting than at relatively long crack lengths. Evidence has recently emerged from work currently in progress in the UK on clad and non-clad aluminium alloy sheet materials[24] which suggests that there may be radically different load interaction behaviour in the nucleation-micro cracking phase for the clad and non-clad material. The significance of this finding in relation to the overall behaviour of clad and non-clad material under variable amplitude loading has yet to be assessed.

In the case of fail-safe aircraft growth in the micro-macro range is of economic importance insofar as also it influences the life to the development of damage which may necessitate repair. However, from the point of view of safety of fail-safe aircraft it is generally the growth of relatively long cracks, measured in inches rather than thousandths of an inch, that is of current concern.

In this latter regime the only results from UK work that may be said to be relevant to discussion of crack propagation under variable amplitude load spectra are those of section 4.4 above. These results indicated values of $\Sigma n/N$ considerably in excess of unity and were in general accord with the much larger body of evidence obtained at research centres outside the UK, principally at NLR. Several hypotheses have been, and are being, considered to explain load interaction effects during crack propagation - they involve consideration of residual stress effects, crack blunting, cyclic strain hardening effects, and effects due to incomplete crack closure associated with irregularities of the crack surfaces following plastic deformation. All the above effects may be, to a greater or lesser extent, dependent on material properties, crack length, thickness of component, and the nominal stress field. Though much qualitative understanding of interaction effects during crack growth has been obtained in recent years, as far as the author is aware, no specific guidelines have been firmly put forward to predict effects on crack growth rate of change in spectrum shape or severity. Further work in this area is clearly essential and is a matter of immediate concern in relation to the associated airworthiness problem of fail safe aircraft.

5   TO SUMMARISE

Results of work carried out in the UK in recent years, aimed at providing deeper understanding of cumulative fatigue damage under variable amplitude load spectra, have been presented. In particular, the observed variation of fatigue endurance of structural elements, with change in spectrum severity and spectrum shape, has been examined. The insights gained in this work have been related to the general problem of the re-assessment of fatigue life when it found that the spectrum of loads experienced in service differs from the load spectrum applied in full scale (or component) tests. The use of a cumulative damage rule forms an essential part of the process of re-assessing life and until recently Miner's rule has been used in the UK. It has been demonstrated that a considerable proportion of the overall error, which may arise in re-assessing life, may be associated with the errors arising from the simple assumptions of Miner's rule and that the use of an improved method of life prediction, recently issued in Data Sheet form by the Royal Aeronautical Society, Engineering Sciences Data Unit, will generally lead to a significant improvement in accuracy in re-assessing life.

A small amount of evidence has been presented also relating to nucleation and propagation of fatigue cracks under variable amplitude loading. Certain anomalies become apparent when considering the results and the evidence has served to emphasise the complexity of the problem of predicting crack growth behaviour. The need for further work to study load interaction effects during nucleation, macro-cracking and subsequent grosser crack growth has been stressed with particular emphasis on the need for understanding of such effects at relatively long crack lengths. Such understanding is necessary for re-estimating crack growth rates in fail-safe structures, when service load histories are found to differ from test loading conditions.

REFERENCES

1   R.D.J. Maxwell, 'The practical implementation of fatigue requirements to military aircraft and helicopters in the United Kingdom'. Presented at the Sixth ICAF Symposium, Miami Beach, Florida, USA, May 1971

2   W.T. Kirkby, P.R. Edwards, 'A method of fatigue life prediction using data obtained under random loading conditions'. RAE Technical Report 66023 (1966)

3   'Royal Aeronautical Society/Engineering Sciences Data Unit'. Data Sheet No.A02.01(A)

4   J.R. Heath-Smith, Judy E. Aplin, 'The effect of the application of heat on the fatigue performance under random loading of a notched specimen of DTD 5014 (RR 58) material'. RAE Technical Report 71209 (1971)

5   W.T. Kirkby, P.R. Edwards, 'Cumulative fatigue damage studies of pinned-lug and clamped lug structural elements in aluminium alloy'. ARC CP 1089, HMSO 1970

6   W.T. Kirkby, P.H. O'Neill, 'An evaluation of a method of fatigue damage indication'. RAE Technical Report in preparation.

7   P.R. Edwards, 'Cumulative damage in fatigue with particular reference to the effects of residual stresses'. ARC CP 1185, HMSO 1971

8   J.H. Crews, H.F. Hardrath, 'A study of cyclic plastic stresses at a notch root'. SESA Paper No.963, May 1965

9   P.R. Edwards, 'An experimental study of the stress histories at stress concentrations in aluminium alloy specimens under variable amplitude load sequences'. RAE Technical Report 70004 (1970)

REFERENCES (concluded)

10   D. Schütz, 'The study of elasto-plastic behaviour at the root of a notch, as an alternative to purely empirical methods of fatigue research'. RAE Library Translation 1394 (Laboratorium für Betriebsfestigkeit Report TB-80 (1968)

11   'Royal Aeronautical Society/Engineering Sciences Data Unit'. Data Sheet 71028

12   L.F. Impellizzeri, 'Cumulative damage analysis in structural fatigue. Effects of environment and complex load history on fatigue life'. ASTM STP 462 (197) pp.40-68

13   E.C. Naumann, H.F. Hardrath, D.E. Guthrie, 'Axial load fatigue tests of 2024-T3 and 7075-T6 aluminium alloy sheet specimens under constant and variable, amplitude loads'. NASA TN D-212, December 1959

14   J. Schijve, F.A. Jacobs, 'Program fatigue tests on notched light alloy specimens of 2024 and 7075 material'. NLR TR M2070 (1960)

15   W.A.P. Fisher, 'Programme fatigue tests on notched bars to a gust load spectrum'. ARC CP 498, HMSO 1960

16   E. Gassner, E.C. Horstmann, 'The effect of ground-to-air-to-ground cycle on the life of transport aircraft wings which are subjected to gust loads'. RAE Library Translation 933 (1961)

17   E.C. Naumann, 'Evaluation of the influence of load randomization and of ground-to-air cycles on fatigue life'. NASA TN D-1584, October 1964

18   A.W. Cardrick, 'Comparative fatigue performance of pinned-lug and clamped lug specimens in L65 and in Al 5% N 4% Zn alloy under constant and variable amplitude loading'. RAE Technical Report in preparation

19   J.R. Heath-Smith, F. Kiddle, 'Influence of ageing and creep on fatigue of structural elements in an Al 6% Cu alloy'. RAE Technical Report 67093 (1967)

20   R.J. Ryman, 'Investigation of the fretting fatigue strength of BS L65 aluminium alloy under narrow band random loading and under programmed random loading'. Testwell Ltd., Daventry UK, Report No.FAT 44, March 1972

21   J. Schijve, F.A. Jacobs, P.J. Tromp, 'Crack propagation in aluminium sheet materials under flight simulation loadings'. NLR TR 68117 U, December 1968

22   J. Schijve, F.A. Jacobs, P.J. Tromp, 'Crack propagation in 2024-T3 alclad under flight simulation loading. Effect of truncating high gust loads'. NLR TR 69050 U, June 1969

23   W. Elber, 'The significance of fatigue crack closure'. Presented at the 1970 Annual Meeting of the American Society for Testing and Materials, Toronto, Canada. June 21-26, 1970

24   P.R. Edwards, 'A comparison of cumulative damage behaviour of clad and non-clad notched aluminium alloy specimens'. RAE Technical Report in preparation

ACKNOWLEDGMENTS

Fig.1

Holes
reamed to
0·50 dia

1 in

6 in

1 in

1·26 in

0·2 in
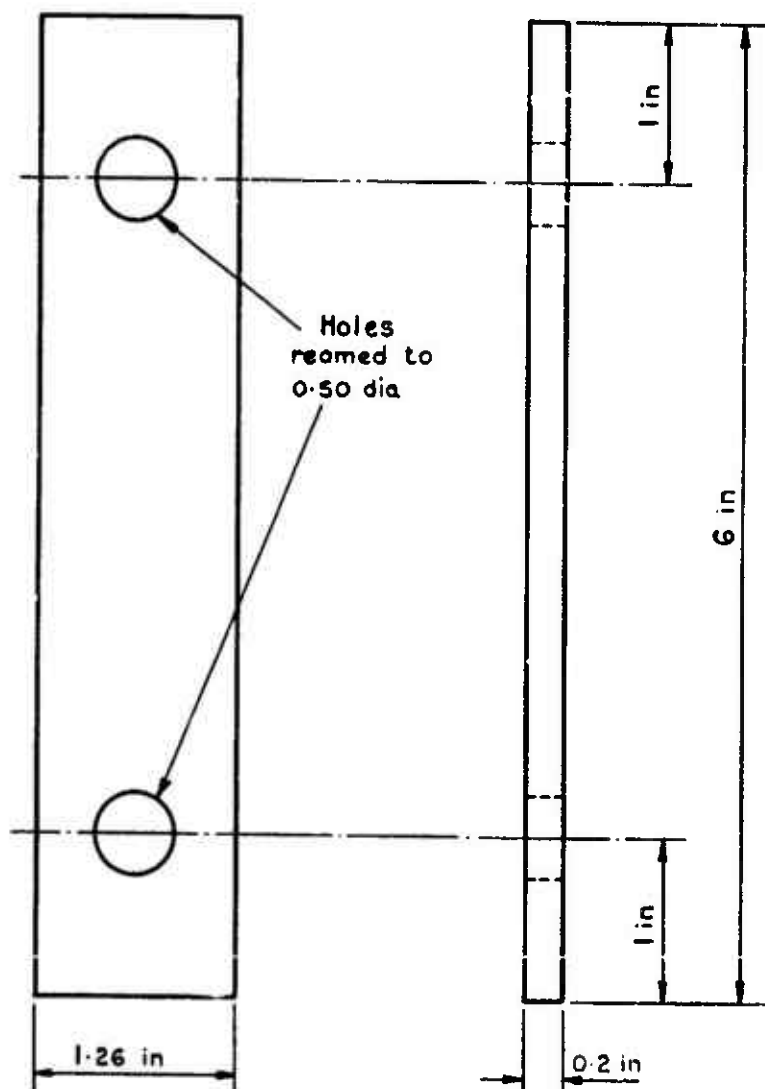
Material : BS 2L65

Fig.1   Lug specimen (Ref 2)
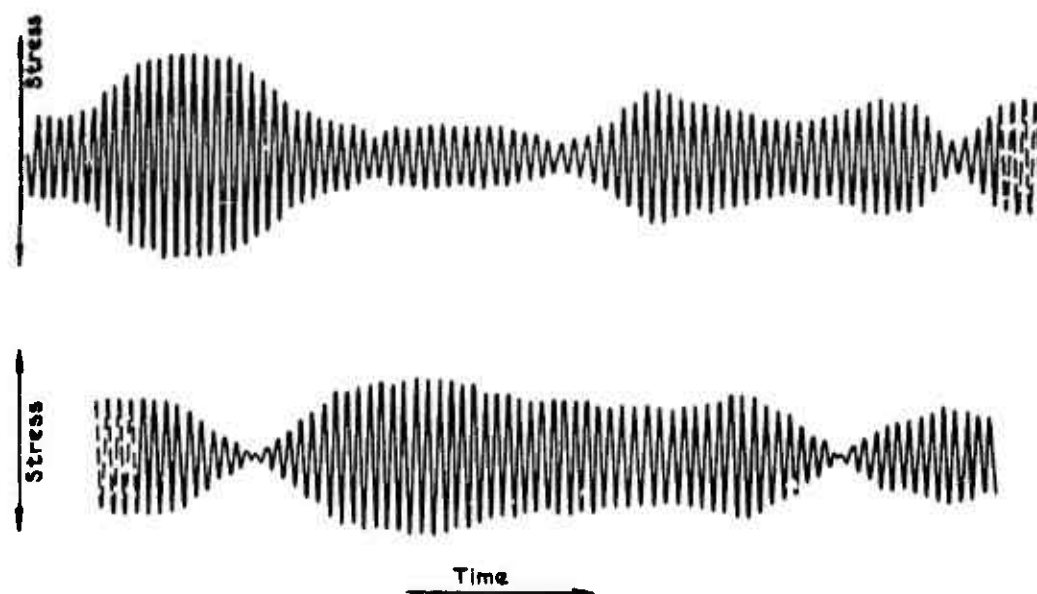
Fig.2 a & b

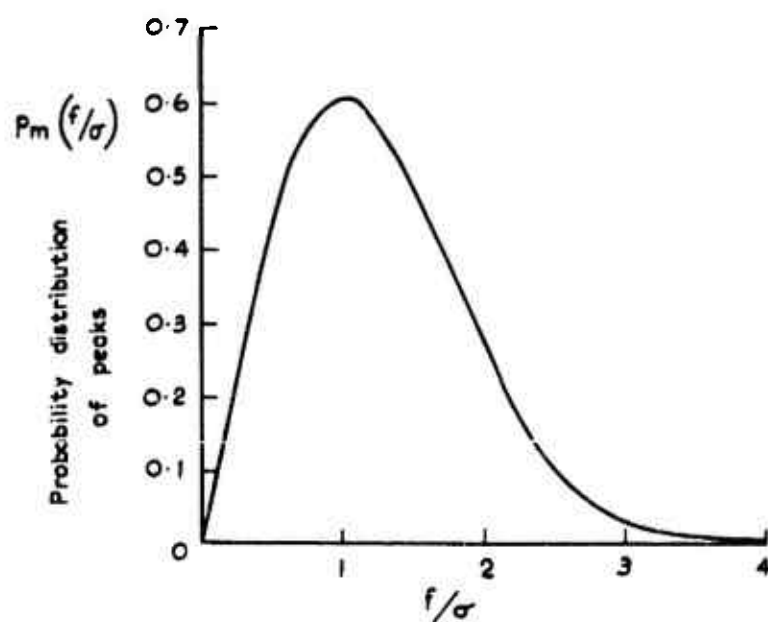
Fig.2a Random stress – time waveform
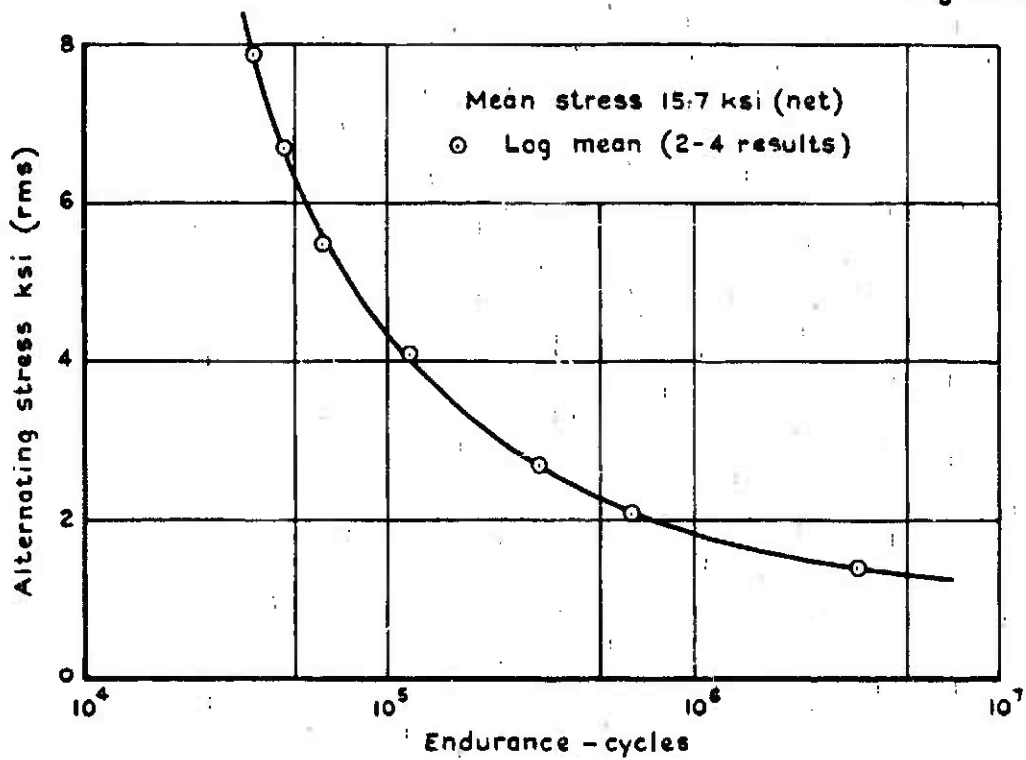

Fig.2b Rayleigh distribution (Ref 2)

Fig.3 a & b

Fig.3a Constant amplitude loading –S/N curve

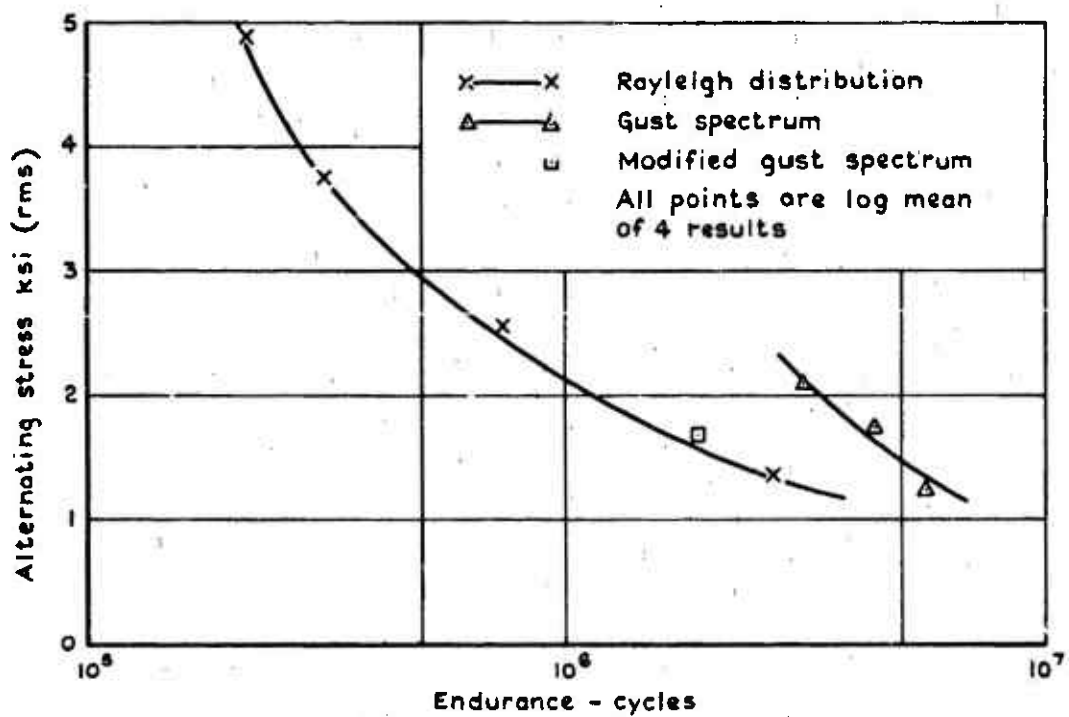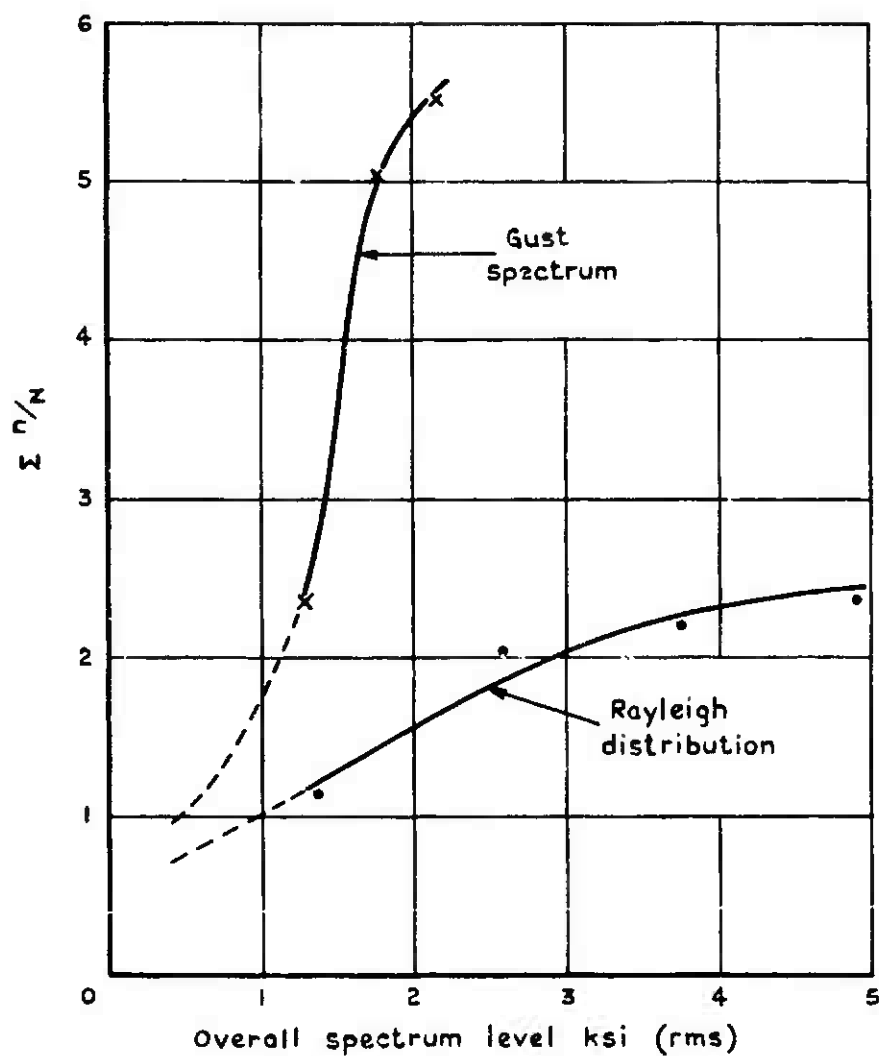Fig.3b. Random loading – σ/N curve

Fig. 4

Fig. 4   General   trend of $\Sigma \, {}^n/_N$ with change in
spectrum   level (fluctuating tensile   loading)
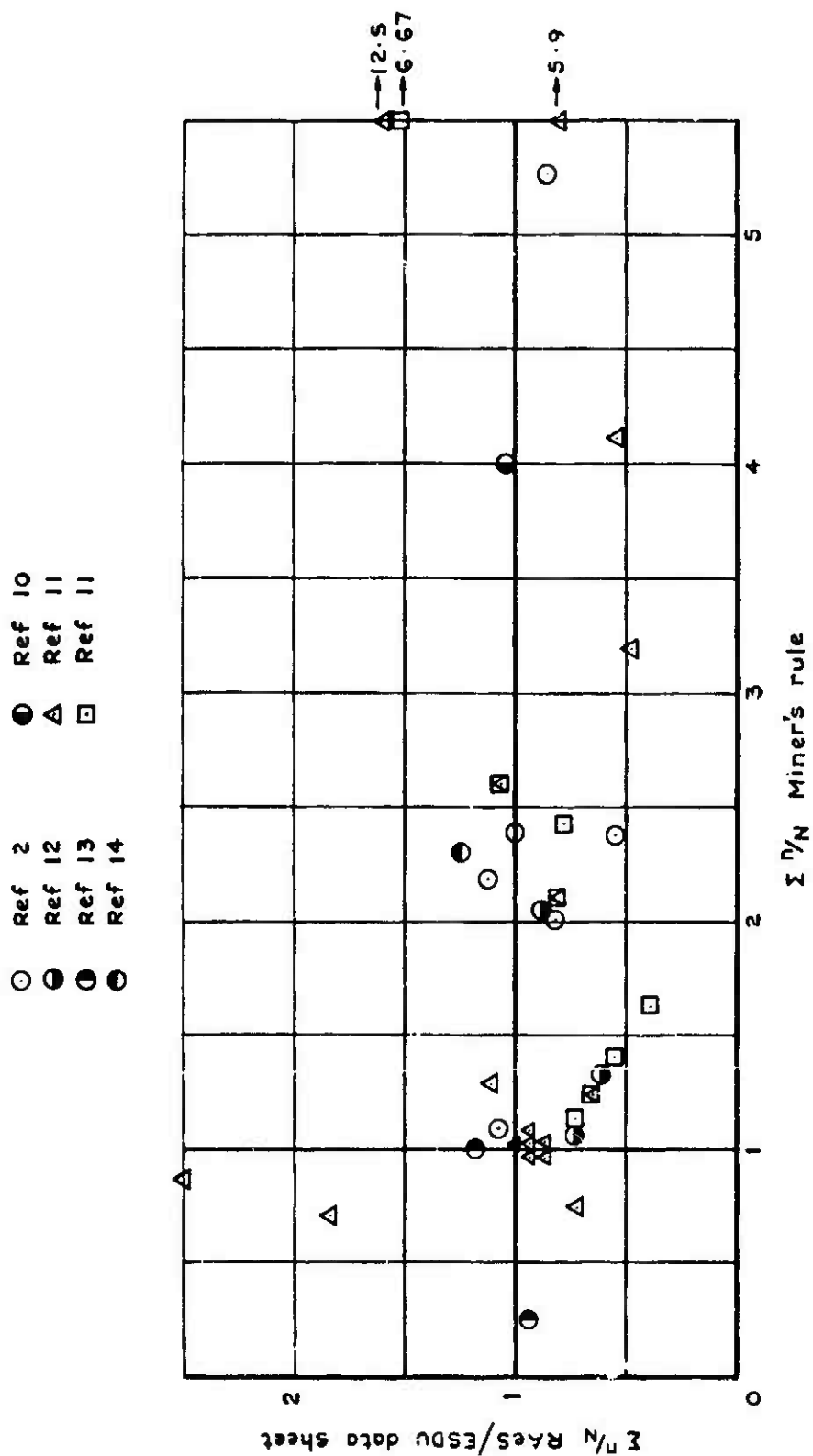
Fig.5

Fig 5 Comparison of life estimation using Miner's rule and RAeS/ESDU data sheet

Fig.6a & b

All alternating stresses are rms

a   Constant amplitude loading (Ref 5)

Alternating stresses and lives
- ▣ 6·5 ksi (4·5 10⁴)
- + 3·5 ksi (2·1 10⁵)
- ⊙ 1·5 ksi (2·5 10⁶)
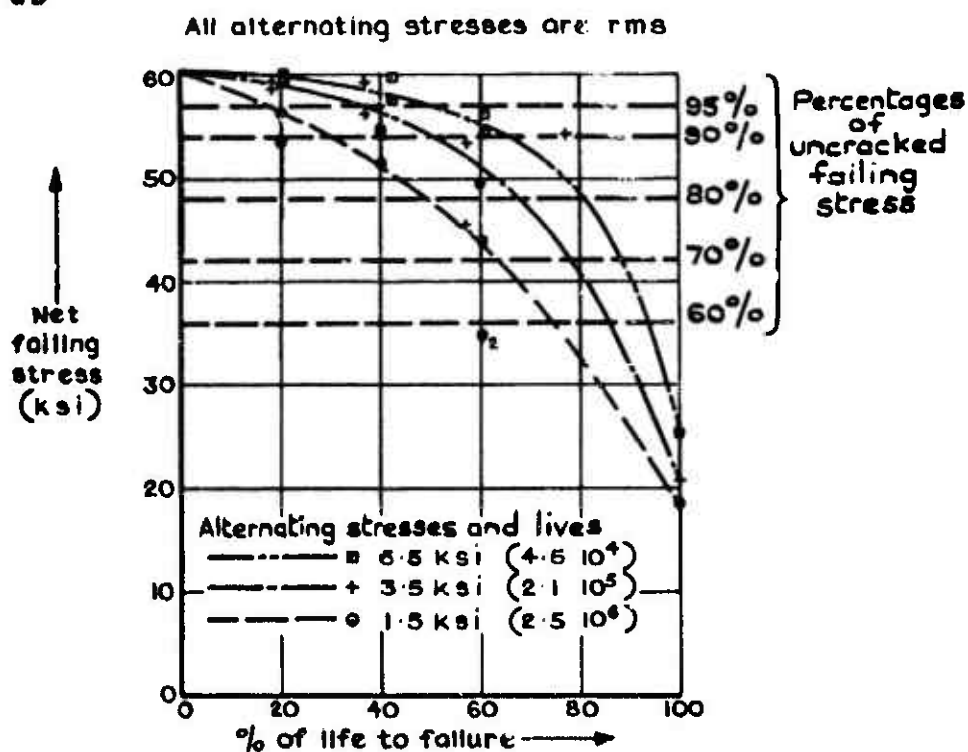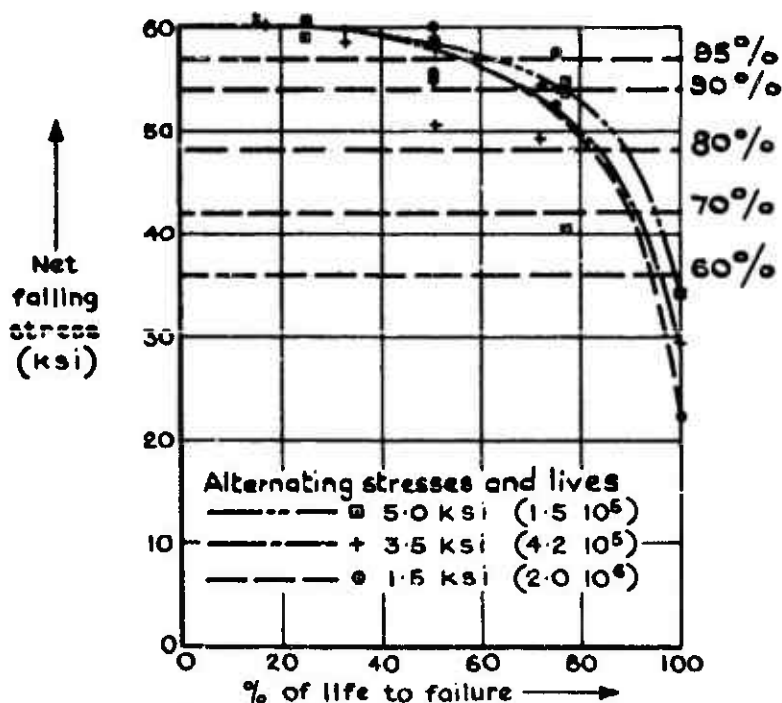
b   Stationary random loading (Ref 5)

Alternating stresses and lives
- ▣ 5·0 ksi (1·5 10⁵)
- + 3·5 ksi (4·2 10⁵)
- ⊙ 1·5 ksi (2·0 10⁶)

Fig.6a & b Partial damage tests—16 ksi mean stress—DTD 5014 lugs

Fig.7a & b

Fig.7a Effect af fretting-constant amplitude loading

Fig.7b Effect af fretting -random loading

Fig.8

Centre cracked coupon
(4 in × 2 in × 0.050 in)

3.33 in

24.5 in

0.80 in
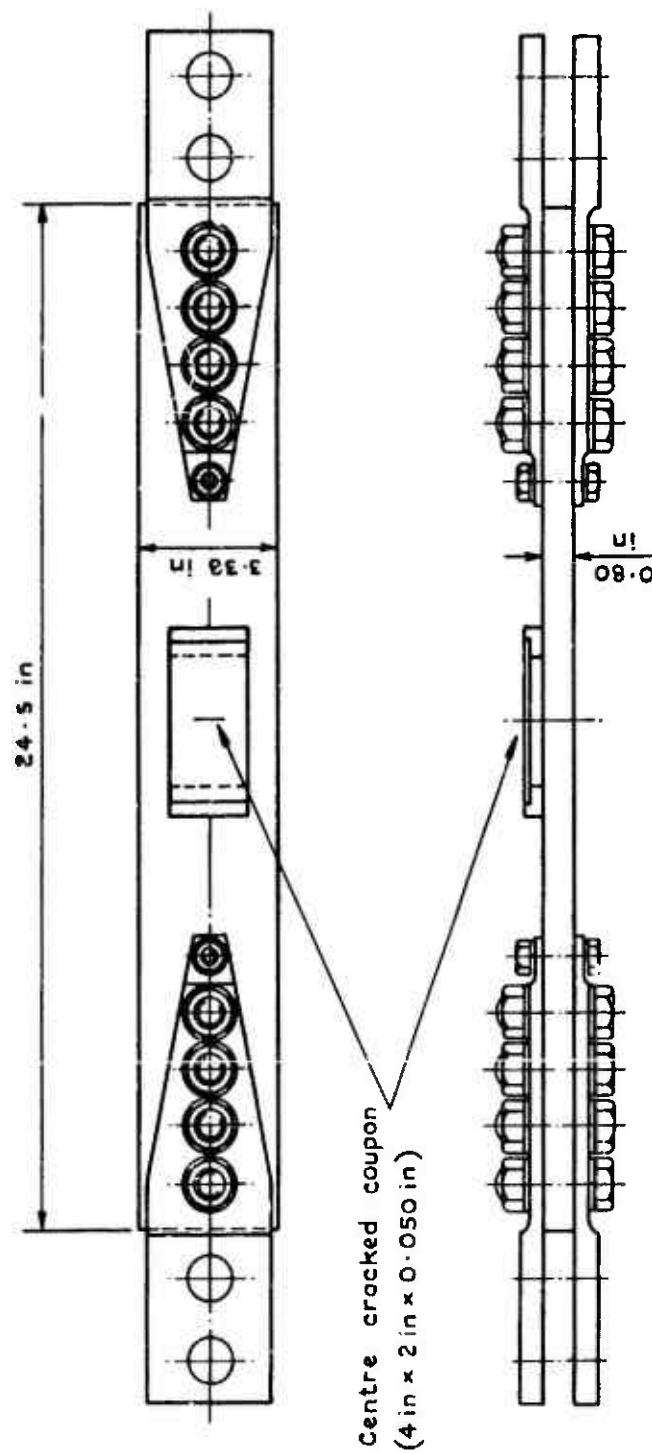
Fig.8   Bolted joint with cracked coupon attached
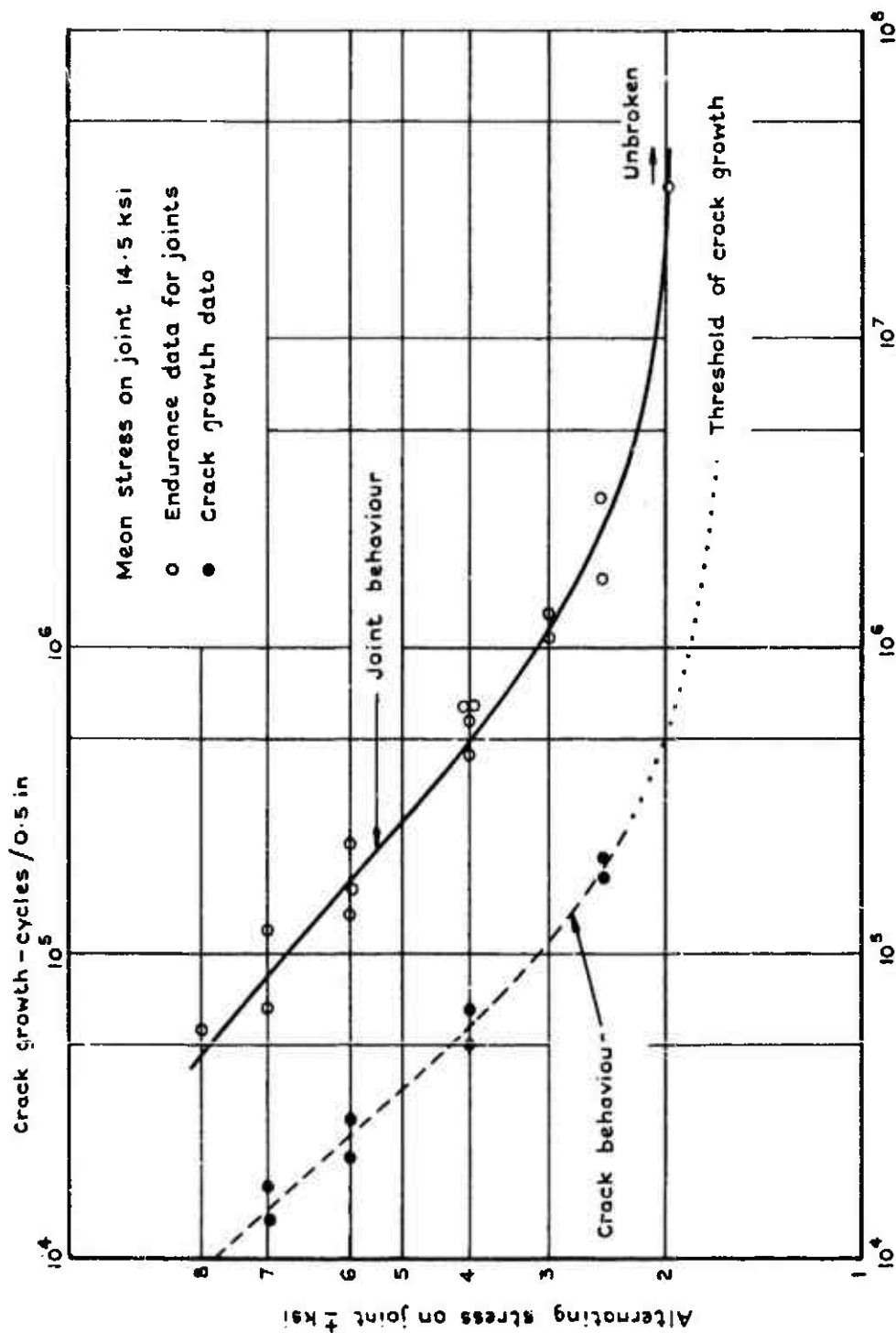
Fig.9

Fig.9 Comparative behaviour of joint and coupon

THE ACCUMULATION OF FATIGUE DAMAGE IN AIRCRAFT

MATERIALS AND STRUCTURES

by

J.Schijve

National Aerospace Laboratory NLR
Sloterweg 145, Amsterdam (17), The Netherlands

SUMMARY

The available literature is surveyed and analysed. Physical aspects of fatigue damage accumulation are discussed, including interaction and sequence effects. Empirical trends observed in variable-amplitude tests are summarized including the effects of a high preload, periodical high loads, ground-to-air cycles and the variables pertaining to program loading, random loading and flight-simulation loading. This also includes results from full-scale fatigue test series. Various theories on fatigue damage accumulation are recapitulated. The significance of these theories for explaining empirical trends as well as for estimating fatigue properties as a design problem is evaluated. For the latter purpose reference is made to the merits of employing experience from previous designs. Fatigue testing procedures are discussed in relation to various testing purposes. Emphasis is on flight-simulation tests. Finally several recommendations for further work are made.

LIST OF SYMBOLS

D	damage
ΔD	damage increment
kc	kilocycles (1000 cycles)
K	stress intensity factor
K_t	theoretical stress concentration factor
ℓ	crack length for edge crack
	semi crack length for central crack
$\Delta \ell$	increment of ℓ
$d\ell/dn$	crack propagation rate
n	number of cycles
n'	number of cycles of a particular load spectrum
N	fatigue life
N'	fatigue life in program test or random test
N_ℓ	fatigue life to obtain a crack of length ℓ
P	load
r	radius
R	stress ratio (S_{min}/S_{max})
S	stress
S_a	stress-amplitude
$S_{a,max}$	maximum S_a in a variable-amplitude test
$S_{a,min}$	minimum S_a in a variable-amplitude test
S_m	mean stress of stress cycle
S_{max}	maximum stress of stress cycle
S_{min}	minimum stress of stress cycle
S_{rms}	root-mean square value of stress in random load test
S_u	ultimate tensile stress
$S_{0.1}, S_{0.2}$	yield stresses for 0.1 and 0.2 percent permanent yield
S_{1g}	mean stress in flight
ΔS	stress range $(S_{max} - S_{min})$
t	sheet thickness
ε	strain
κ	exponent in S-N relation $(SN^\kappa = \text{constant})$
μ	micron = 0.001 mm

THE ACCUMULATION OF FATIGUE DAMAGE IN AIRCRAFT MATERIALS AND STRUCTURES

J. Schijve

1. INTRODUCTION

In a classic fatigue test the load is varying sinusoidally with a constant mean load and a constant load amplitude. The fatigue load on a structure under service conditions, however, generally has a more or less arbitrary or random character. Nevertheless it may well be assumed that the accumulation of fatigue damage under such an arbitrary fatigue load is a process which occurs in the material in a similar way as in the classic fatigue test. It is just one step further to state that the fatigue life for an arbitrary load-time history can be predicted from fatigue life data obtained in classic fatigue tests. The well-known Palmgren-Miner rule ($\Sigma n/N = 1$) was based on such assumptions, which also applies to more complex laws proposed by others.

It has to be admitted, however, that a rational law for the calculation of fatigue damage accumulation is not yet available. There is an abundant literature on fatigue which has revealed several characteristic features of the fatigue process in metallic materials. Fatigue tests with a varying load-amplitude were also carried out by many investigators. This has indicated many empirical trends for which physical explanations were sometimes given. Moreover, calculation rules for the accumulation of fatigue damage were published from time to time. Nevertheless the present situation is far from satisfactory, even from an engineering point of view.

The purpose of this report is to survey the various aspects of fatigue damage accumulation and to analyse the problems associated with this phenomenon. The implications of the present knowledge for making life estimates in the design phase of an aircraft and for pla nning fatigue tests will be considered also.

In summary the aims of the report are:
a To review the present state of knowledge about fatigue damage accumulation (Chapters 2 and 3).
b To summarize the empirical trends obtained in tests with variable-amplitude loading and to see whether they can be explained (Chapter 4).
c To survey the various life calculation theories (Chapter 5).
d To analyse the design problem of estimating fatigue lives and crack propagation rates (Chapter 6).
e To assess the merits and the limitations of various fatigue testing procedures adopted for fatigue life evaluations (Chapter 7).
The report is completed (Chapter 8) by sections giving a summary of the present study and recommendations for future work.
It should be pointed out that aspects associated with elevated temperature due to aerodynamic heating have been excluded from the survey.

It is hoped that this report will provide a background to those dealing with fatigue life problems in the aircraft industry. On the other hand, it is also hoped that it will give a better picture of the real problem to scientists in universities and laboratories when approaching fatigue damage accumulation from a more theoretical point of view.

2. THE FATIGUE PHENOMENON IN METALLIC MATERIALS

Our present knowledge about fatigue in metals has to a large extent been obtained by means of the microscope. In 1903 Ewing and Humfrey observed that fatigue cracks were nucleated in slip bands. Around 1930 classical studies were conducted by Gough and his co-workers, who further emphasized the significance of slip systems and resolved shear stresses. After 1945 the number of microscopical investigations has considerably increased and the information becoming available has broadened for a variety of reasons. It turned out that the observations could be dependent on the type of material, the type of loading and

and the level of magnification. The electron microscope has added a number of details unknown before. It will be tried in this chapter to recapitulate briefly the main points of the numerous phenomenological investigations. More detailed surveys are given in references 1-6.

Three phases in the fatigue life

An important observation is that cracks may nucleate relatively early in the fatigue life. As an illustration figure 2.1 shows results of optical microscopy during fatigue tests on aluminum alloy specimens (Ref.7). Cracks of 0.1 millimeter (100 μ) were present after 40 percent of the fatigue life had elapsed. The electron microscope has revealed cracks at earlier stages, almost from the beginning of a fatigue test. Nevertheless the lower part of figure 2.1 suggests that nucleation is relatively more difficult at stress levels near the fatigue limit.

It appears useful to divide the fatigue life into three phases, namely: crack nucleation, crack propagation and final failure, see figure 2.2. A difficulty thus introduced is that of the definition of the transition from the nucleation phase to the propagation phase.

Slip

It is well established that fatigue requires cyclic slip. The present state of our knowledge about dislocations and metal physics leave no doubt about the essential contribution of slip to fatigue.

Fatigue on the atomic level, decohesion

If there were no decohesion there would be no fatigue. In principle decohesion may occur by sliding-off, by cleavage or by vacancy diffusion. Disruption of atomic bonds is involved in any case.

Although it is difficult to rule out cleavage type conceptions, it is thought that sliding-off is the more plausible mechanism for relatively ductile materials. Sliding-off implies that dislocations are cutting through the free surface which may also be the tip of a fatigue crack. A second possibility is that dislocations are generated at the tip of a crack. In the latter case the tip of a crack acts as a dislocation source rather than a dislocation sink. In general terms fatigue may be visualized as the conversion from cyclic slip into crack nucleation and crack growth.

Chemical attack may facilitate the decohesion process but the environmental affect on the atomic level is not well understood.

Fatigue on the microscopic level, striations

Cross sections of fatigue cracks, as viewed through the optical microscope, usually show the crack to be transgranular. The path of the crack appears to have a fairly irregular orientation at this level of magnification.

Replicas from the fatigue fracture surface studied in the electron microscope have revealed the so-called striations, see for an example figure 2.3. Such striations clearly prove that crack extension occurred in every load cycle. This type of evidence was mainly obtained for macro-cracks, while for micro-cracks striations cannot be observed for several reasons. However, if crack propagation occurs as a cyclic sliding-off mechanism it appears reasonable to assume that crack growth of a microcrack also occurs in every load cycle.

For aluminium alloys evidence is available that strongly suggest crack extension and striation formation to occur as a co-operative sliding-off on two differently oriented $\{111\}$ slip planes (Refs.9,10).

Type of loading (tension vs. torsion)

Brief reference may be made here to the work of Wood et al. (Ref.11) concerning torsion fatigue tests on copper specimens. It turned out that crack nucleation occurred by the forming of pores and this was a process of a relatively long duration. It appears that the process may be essentially different from fatigue under cyclic tension because in pure tension the planes with a maximum shear stress have a zero tensile stress. It is thought that this will allow a much slower crack nucleation and even a different dislocation mechanism may be applicable. Since fatigue in aircraft structures is associated with cyclic tension, torsion will not be considered in the present report.

Nucleation sites

In fatigue tests on unnotched specimens the probability to observe more than one fatigue crack in the same specimen is increasing at higher stress amplitudes. At low stress levels near the fatigue limit quite frequently only one crack nucleus is observed. This observation may inspire statisticians to develop a weakest-link theory to explain size effects. Another consequence, not generally recognized, is that special fatigue sensitive conditions apparently exist at the site of crack nucleation. Grosskreutz and Shaw (Ref.12) in this respect have studied crack nucleation at intermetallic particles in an Al alloy (see also Ref.13). Nucleation at inclusions in high strength steels were also reported. Other special conditions can easily be thought of, such as cladding layer, surface scratches, local inhomogeneity of the material.

Plane strain vs. plane stress conditions

Macroscopically a slowly propagating fatigue crack is growing in a plane perpendicular to the maximum tensile stress (main principal stress). However, if the crack rate is accelerating the growth will continue on a plane at 45° to the maximum tensile stress. This transition occurs gradually, see figure 2.4, starting at the free surface of the material with the development of shear lips. It is generally accepted that this is to be related to the transition from plane-strain conditions to plane-stress conditions at the tip of the crack. After the transition has occurred, it is more difficult to observe the striations but there are still indications that crack extension occurs in every load cycle.

The transition from the tensile mode (plane strain) to the shear mode (plane stress) and Forsyth's Stage I/Stage II (Ref.2) proposition should not be confounded. Stage I was associated with the initial and very slow growth along a slip plane and Stage II with later growth perpendicular to the tensile stress. Stage II should correspond to the tensile mode. Stage I, however, is thought to occur only at the free surface of the material at both low and fast propagation rates (Ref.6). It is promoted by the lower restraint on slip at the free surface.

Cyclic strain-hardening (and softening)

Since fatigue and crack growth are a consequence of cyclic slip, cyclic strain-hardening (or softening) will occur. That means that the structure of the material will be changed. The spatial configurations of the dislocations will change. Dislocation multiplication may occur as well as dislocation reactions and pinning. According to Grosskreutz, a cel structure will be formed (Ref.14).

If the material was already work-hardened, re-arrangement of the dislocation distribution may lead to cyclic strain softening. Anyhow, crack growth will occur in a material that will not have the same dislocation structure as the virgin material or the material in the "as received" condition.

A major problem is to define quantitatively the structure of the cyclically strain-hardened material in terms of dislocations. Secondly the significance for crack growth is not fully clear.

Rate effects

Fatigue being a consequence of cyclic slip may well be a loading rate sensitive phenomenon, because slip itself may be a function of the loading rate (creep). Fatigue as it is considered in this report, is outside the creep domain. However, there are more reasons why rate effects may occur. Chemical attack from the environment may be significant at the surface of the material (nucleation) but also in the crack at its very apex (propagation). Secondly, diffusion in the material may affect the mobility of the dislocations and the fracture mechanism.

It is very difficult to get beyond speculative arguments. However, a few empirical trends seem to be well established. Decreasing the loading frequency of a sinusoidal loading may decrease fatigue lives and increase crack rates. These effects will depend on the type of material and on the environment. Especially crack propagation in aluminium alloys got much attention. It was clearly observed that the crack rate was reduced if the humidity of the environment was lower, while this effect was dependent on the loading frequency (Refs.15,16).

Type of material

It can hardly be a surprise that fatigue does not manifest itself as exactly the same phenomenon in all materials. Striations have been noticed on many materials, but differences were found, such as ductile

striations in the 2024 alloy and brittle striations in the 7075 alloy (Ref.2). There are also materials (some types of steel) where striations are hard to observe.

Since fatigue is a consequence of cyclic slip, it will be clear that fatigue is dependent on the possibilities for slip (available slip systems, ease of cross slip), the hardening mechanisms present in the matrix, the break-down of such mechanisms, cyclic strain-hardening (or softening), etc. This implies that the picture can be different for different materials. Crack nucleation may also depend on the material due to the presence of second phase particles or inclusions, that means on the cleanness of the material.

Concluding remarks

It is trivial to state that various details of the fatigue mechanism will be different for different conditions. At this stage, it is more relevant to see whether fatigue in technical alloys under various conditions has still enough features in common to postulate a simple fatigue model, that could be useful for a discussion of fatigue damage accumulation under variable-amplitude loading. It is thought that a model with the following characteristics could satisfy this need, while still being in agreement with the observations discussed before.

1. Since we are concerned with "finite life" problems, this implies that crack nucleation starts early in the life. Hence the nucleation period may be neglected.

2. Crack growth occurs by sliding-off at the tip of the crack, either by dislocations moving into the crack or by dislocations emitted by the crack, that means it occurs by slip, which is local plastic deformation.

3. As a consequence, the growth rate is dependent on the amount of cyclic slip and on the effectivity of converting cyclic slip into crack extension. Obviously, the amount of slip is a function of the local condition of the material and the local stresses. The condition of the material is dependent on the preceding strain history, while the local stress is a function of the applied stress and the geometry of the specimen, including the length of the crack.

4. The conversion of cyclic slip into crack extension will also depend on the local tensile stress (fracture mechanism, disruption of bonds, strain energy release). This stress should include residual stress induced by the preceding fatigue loading.

More comments on fatigue damage accumulation will be given in the following chapter.

3. FATIGUE DAMAGE ACCUMULATION

In the previous chapter the fatigue phenomenon has been discussed in qualitative terms, tacitly assuming that the fatigue loading did not vary during the test (constant mean, constant amplitude). If the fatigue load does vary, how will this picture be affected? This will be discussed in the present chapter. Pertinent questions are:

a Is fatigue under a variable fatigue loading still the same process as fatigue under constant amplitude loading?

b How does fatigue damage accumulation occur under a variable fatigue loading?

c To answer the previous question, the following question has also to be answered:
How do we describe fatigue damage?

With respect to the first question it has to be expected that the qualitative description of fatigue given in chapter 2 is still valid. It does occur in the same material, again as a consequence of cyclic slip. This does not imply that the fatigue process will also be the same in a quantitative way. It need not even be the same in constant-amplitude tests at high and low amplitudes (high-level fatigue and low-level fatigue). The discussion of quantitative aspects first requires a definition of fatigue damage.

3.1 Fatigue damage

Fatigue damage is most generally defined as being the changes of the material caused by fatigue loading. The amount of cracking, apparently, is the most prominent aspect of these changes. However, there are other changes in the material than cracking alone, for instance cyclic strain-hardening and the development of residual stresses.

Geometry of the crack

It should be recognised that the crack is not completely defined by giving a crack length or a cracked area. Considering a crack as a separation in the material its size, as a first approximation, can be defined by the position and the orientation of the crack front. The crack front need not be a single straight line or a circular arc. On a microscopic level it certainly will not be a straight line through the various grains. At a macroscopic level the orientation of the crack front will be different for a plane-strain crack (tensile mode) and a plane-stress crack (shear mode) (Fig.2.4).

The geometry of the crack tip is another aspect to be considered. On the atomic level a detailed picture is a matter of imagination, but even on a microscopic level this is a difficult problem. It has to be expected that the tip will be blunted after application of a high tensile load, while reversing the load will induce resharpening of the crack tip. Blunting and resharpening both will depend on the local ductility of the material and on the magnitude of the load applied.

If a cracked sheet is loaded in compression the crack will be closed. Hence it will be no longer a severe stress raiser since it can transmit compressive loads. This argument was suggested by Illg and McEvily (Ref.17) who confirmed it by comparing crack propagation data obtained in tests with the same S_{max}, but with $S_{min} = 0$ in one case ($R = 0$) and $S_{min} = - S_{max}$ in the other case ($S_m = 0$, $R = -1$). Approximately the same crack rates were found. This result was more applicable to 7075-T6 sheet material than to 2024-T3 sheet material. The latter was explained by the higher ductility of the 2024 alloy, implying more crack opening due to plastic deformation in the crack tip area. Hence a larger compressive stress was required before crack closure occurs.

Recently, Elber (Refs.18,19) observed that crack closure may occur while the sheet is still loaded in tension. According to Elber plastic elongation will occur in the plastic zone of the growing crack. This plastic deformation will remain present in the wake of the crack and it will cause crack closure before complete unloading of the specimen. This phenomenon was confirmed in an exploratory investigation at NLR. The data in figure 3.1 illustrate the conception. As a consequence of crack closure the crack opening as a function of applied stress shows a non-linear behaviour. For increasing stress, the crack is gradually opened until at $S = S_o$ it is fully open. During the fatigue tests 1 and 2, see lower graph of figure 3.1, the crack was partly closed during a considerable part of the stress cycle. For tests 3 and 4, the S_o-level could only be determined after unloading the specimen below S_{min}.
The above aspects of the crack geometry have been listed in figure 3.2.

Strain-hardening effects

As said in chapter 2, cyclic slip will affect the structure of the material. In view of the stress concentrating effect of the crack, changes of the structure will have a localized character with large gradients. Since it is already difficult to describe the changes in a qualitative way, it will be clear that a quantitative description is a termendous problem.

Residual stress

Plastic deformation at the tip of the crack will occur in the ascending part of a load cycle. If this deformation is not fully reversed in the descending part it will leave residual stresses in the crack tip region. In the fatigue model outlined in the previous chapter, the efficiency of converting slip into crack extension is dependent on the tensile stress in the crack tip region. Residual stresses have to be added to the stresses induced by the applied loads. As a consequence, residual stresses will affect the fatigue damage accumulation and for this reason they are an essential part of fatigue damage.
A calculation of the distribution and the magnitude of the residual stresses will be extremely difficult in view of the cyclic plastic behaviour of the material, the large strain gradients and the crystallographic nature of the material.
The picture is further complicated by crack closure as described above. It will turn out later that several empirical trends, attributed to residual stresses in the crack tip region, may also be explained by crack closure.

3.2 Fatigue damage accumulation. Interaction

Aspects of the previous discussion are summarized in fig.re 3.2 which will be discussed further in this section. In general terms fatigue damage may also be formulated as follows:

$$\text{Fatigue damage} = \left(\begin{array}{c} \text{changes of the material} \\ \text{due to cyclic loading} \end{array} \right) = \left| \begin{array}{c} \text{crack geometry} \\ \text{cyclic strain hardening} \\ \text{residual stresses} \end{array} \right| , \qquad (3.1)$$

Fatigue damage accumulation means an accumulation of damage increments in every load cycle. A damage increment according to equation (3.1) involves incremental changes of the crack geometry, the cyclic strain-hardening and the residual stress. If these three aspects were uniquely correlated, fatigue would be the same process irrespective the magnitude of the fatigue loading. The damage could then be fully described by one single damage parameter, for instance the crack length. Unfortunately such a unique correlation does not exist. Compare as an example high-level fatigue and low-level fatigue. Crack propagation occurs in both cases, but the amount of cyclic strain-hardening and the residual stress at e certain length of the crack will be different. Even the crack will not be the same. It may be a shear mode crack for high-level fatigue and a tensile mode crack for low-level fatigue. This implies that quantitatively, fatigue is not the same process, irrespective of the magnitude of the fatigue loading. Consequently, it is impossible to describe the damage by a single damage parameter.

For a variable fatigue loading, the problem is still more complex than for constant-amplitude loading. A crack propagation test with a constant-amplitude loading and a few intermittent high loads is a relatively simple case, while at the same time it is a very illustrative example.
As shown in figure 3.3, three upward peak loads had a large delaying effect on the crack propagation, compare C and A. If the upward peak load was immediately followed by a downward one (sequence B), the delaying effect is much smaller, but nevertheless the increase of life is noticeable. Some comments on these results may now be made.
During the peak load crack extension does occur. Although, being small from a macroscopic point of view the extension could be observed. The question is whether this increment of the crack length would have been the same if the crack had been grown up to the same length by peak loads only (compare also A and C in Fig.3.2). There are various reasons to believe that this is not true.
1. The orientation of the crack front would be different because peak load cycles would produce a shear mode fracture, whereas the low-amplitude cycles produced a tensile mode fracture. In other words the peak loads in figure 3.3 are faced with an orientation of the crack front that is not compatible with their own magnitude. This incompatibility or mismatch between load amplitude and crack front orientation is illustrated by figure 3.5 for some simple load sequences.
2. The low-amplitude cycles will produce a sharper crack tip than cycles of the peak load magnitude would have done. This may also affect the crack extension of a single peak load.
3. The cyclic strain history is obviously different for low-amplitude cycles and high-amplitude cycles. It is extremely difficult to quantify these three aspects.

Let us now consider the crack growth during the low-amplitude cycles after a peak load was applied, that means during the delayed growth period. The delay can also be explained by various mechanisms.
1. The high peak load in test C induced compressive residual stresses in the crack tip region. This will not necessarily restrain clic slip but according to the model outlined in the previous chapter, it will suppress the conversion into crack extension. In test B, the subsequent downward peak load reversed the sign of the residual stress but this occurs in a smaller plastic zone because the crack is closing under compression. Hence the crack tip is surrounded by a small zone with tensile residual stresses and a larger zone with compressive residual stresses, see figure 3.4 In agreement with this picture the crack growth started faster, then slowed down and finally resumed normal speed.
2. The observations in figures 3.3 and 3.4 can also be explained by Elber's crack closure argument. This was recently studied by Von Euw (Ref.21). The argument is that the delaying effect of the positive peak load caused by crack closure should occur after the crack has penetrated the plastic zone with the residual compressive stresses. Consequently the crack rate should reach a minimum after some further growth.

Von Euw could substantiate this view by fractographic observations (see also Ref.26).

3. Crack blunting might qualitatively explain the delay in test C. However, the delay would be very large for a crack that is blunted on a microscopic scale only, whereas it is still a sharp crack on a macroscopic scale. Further, it is difficult to see that crack blunting can explain the delay in test B since the downward peak load should resharpen the crack tip again.

4. Strain-hardening in the crack tip region is also a mechanism to explain the observations, although in this case it also is difficult to reconcile the large differences between the delays in tests B and C. It would require a more detailed picture about strain-hardening under cyclic load.

Another example is given in figure 3.5b. The crack extension due to the batch of low-amplitude cycles was smaller than in a constant-amplitude test with the same low amplitude. Arguments mentioned before, such as residual stress, crack closure, incompatible crack front orientation, cyclic strain hardening and crack blunting may all be relevant in this case. It is indeed difficult to design a test and means for observation such that just one mechanism can be studied separately.

Interaction effects

As illustrated by the above tests, crack extension in a load cycle is depending on the fatigue damage being present. This damage is again dependent on the load history that produced the damage. In other words, a damage increment in a certain load cycle will be a function of the damage done by the preceding load cycles. A recapitulation of the various aspects is given in figure 3.2.

It may also be said that the damage produced in a certain load cycle will affect the damage produced in the subsequent load cycles. These effects were labelled in the past as interaction effects, as it was supposed to be an interaction between the damaging effects of load cycles of different magnitude. We will still use the word "interaction effect" in order to refer to damage accumulation under variable fatigue loading as being different from damage accumulation under constant-amplitude loading.

3.3 Fatigue damage at final failure

The end of the fatigue life could be defined as the presence of a specified amount of fatigue cracking. In most theories, however, the end of the fatigue life is associated with complete failure. Obviously, the length (or the area) of the fatigue crack will then be a function of the highest load occurring in the test, as indicated by Valluri (Ref.23). This applies to both constant-amplitude tests as well as variable-amplitude tests. For the former type of testing it is illustrated by figure 3.6, which has been drawn for this illustrative purpose only. Unfortunately this aspect is ignored by most cumulative damage theories to be discussed in chapter 5.

In a variable-amplitude test the occurrence of the final failure will be dependent on the maxima of the load history and the size of the growing crack. One may ask whether the condition of the material at the tip of the crack could also affect the occurrence of the final failure. Broek's work (Ref.24) suggests that this will hardly be true. The final failure (unstable crack growth) will be preceded by a small amount of stable crack growth. Moreover, he found that saw cuts and fatigue cracks gave similar residual strength values. It thus appears to be justified to apply the fracture toughness conception for the prediction of the final failure, i.e. the end of the fatigue life.

3.4 Micro and macro aspects

The various possibilities for interaction effects during the accumulation of fatigue damage are summarized in figure 3.2. It is good to realize how we arrived at the knowledge or the recognition of the existence of such interaction mechanisms. It then has to be admitted that macroscopic concepts (stress and strain e.g.) were quite frequently employed. Microscopic observations (striations) were usually obtained for macrocracks. Crack growth delays were also observed for macrocracks. For microcracks the growth rate is so low that detailed observations are extremely difficult. Nevertheless, it is thought that the damage accumulation picture outlined before will qualitatively apply in the micro range also. However, since the

picture for macrocracks is also largely qualitative it will be clear that there is a good deal of intuitive speculation involved in our conceptions. It is expected that our knowledge for a long time will still have a qualitative character.

4. EMPIRICAL TRENDS OBSERVED IN VARIABLE-AMPLITUDE TESTS

As explained in the previous chapter, fatigue damage accumulation is a fairly complex phenomenon characterized by various mechanisms for interaction effects. In this chapter it will be analysed whether variable-amplitude tests have revealed systematic trends with respect to interactions. For this purpose we will first consider the methods for measuring interaction effects. Secondly various types of variable-amplitude loading will be listed. The major part of the chapter is covered by summarizing empirical trends observed in various test series (Secs.4.3-4.18). It is not the intention to give a complete compilation of all available data. Representative data will be shown, however, to illustrate the various trends.

4.1 How to measure interaction effects?

In chapter 3 the interaction effect was defined as the effect on the damage increment in a certain load cycle as caused by the preceding load-time history. It can be similarly defined as the effect of the damage being present on subsequent damage accumulation.

Fractography

In view of the significance of cracking for fatigue damage, the best method for measuring interaction effects would be by fractographic means. With the electron microscope striations can be observed, that means crack length increments of individual load cycles. It is beyond any doubt that fractography is the most direct method to measure interaction effects. However, there are limitations because striations cannot always be observed, especially in the microcrack range. Moreover, interpretation problems may also arise. Reference may be made here to the work of McMillan, Pelloux, Herzberg (Refs.25,26) and Jacoby (Ref.4). More investigations of this nature are thought to be very worthwhile.

Visual crack growth observations

The examples of interaction discussed in the previous chapter (Sec.3.2), were studied by visual observation of the crack growth. The effects could still directly be observed because there were considerable crack growth delays. A similar observation was made (Refs.27,28) after changing the stress amplitude from a high to a low value (two-step test), as illustrated by figure 4.1a. When changing the amplitude from a low to a high value, the crack apparently resumed immediately the propagation rate pertaining to the high stress amplitude, see figure 4.1b. In other words, macroscopically an interaction effect could not be observed in the second case. Nevertheless, a significant interaction effect during a small number of cycles could easily escape such visual crack growth observations. Electron fractography is then required and there are indeed some indications (Ref.21) that the crack rate immediately after a low-high step was higher during a few cycles.

Fatigue life

In the majority of variable-amplitude test series reported in the literature, observations on crack growth were not made. Since favourable interaction effects increase the life, whereas unfavourable effects will shorten it, interaction effects can also be derived in an indirect way from fatigue life data.

Damage values $\Sigma n/N$

Since the value of $\Sigma n/N$ at the moment of failure may be considered as a relative fatigue life, this value may also be adopted for studying interaction effects. We may expect $\Sigma n/N > 1$ to be the result of a favourable interaction effect, whereas $\Sigma n/N < 1$ would indicate an unfavourable interaction effect. Other reasons for deviations from $\Sigma n/N = 1$ are defined in section 5.3.2.

The value of $\Sigma n/N$ can give an indication of interaction only if the fatigue load is varied no more than once in a test, see figure 4.2, A1 and A2. If the fatigue load is changed more than once, see for a

simple example figure 4.2B, a value $\Sigma n/N > 1$ may again be interpreted as an indication of favourable interaction effects. However, it is impossible to say whether it was a favourable interaction of the high-amplitude cycles on subsequent damage accumulation during low-amplitude cycles or the reverse. It is even possible that there were unfavourable and favourable interaction effects both, with the latter ones predominating. Hence, in general, the $\Sigma n/N$ value will only indicate some average of all possible interaction effects.

4.2 Various types of variable-amplitude loading

There is obviously a multitude of load-time histories deviating from the fatigue load with constant mean and constant amplitude. A survey of several types applied in test series reported in the literature and the nomenclature to be used, are given in figures 4.2 and 4.3. The more simple ones are presented in figure 4.2. The number of variables is small and the variables can easily be defined. For the more complex load-time histories shown in figure 4.3, a statistical description of the loads has to be given. This may be the distribution function of the load amplitudes. The function may be a stepped one, as for instance for the programloading F and the randomized block loading G in figure 4.3. An example of such a stepped function is given in figure 4.22.

Program loading was proposed in 1939 by Gassner (Ref.29), while the randomized block loading was advised by NASA (Refs.30,31) as a variant of program loading. In a program test, the blocks with load cycles of the same magnitude are applied in a systematic sequence, whereas this sequence is a random one for the randomized block loading.

If random loading is a stationary Gaussion process, it is fully described by its power spectral density function (PSD-function). Other statistical parameters characterizing the random load are the root mean square value of the load (S_{rms}) and the ratio between the number of peaks and the number of mean-load crossings. For a narrow-band random loading, the latter ratio is approaching one, while the distribution function of the amplitudes is a Rayleigh distribution. Aspects of describing random loads are discussed in the literature (for instance Refs.32-34).
The sequence of peak loads of a quasi-random or pseudo-random loading is derived from random numbers, in such a way that there is no correlation at all between the magnitude of successive load cycles.

In a realistic flight simulation test (M in Fig.4.3), flight loads are applied in sequence which are different from flight to flight, see also figure 7.3. The load-time history may be a calculated one, whereas actual load records obtained in flight can be adopted if available (Branger, Ref.35). In the past, many full-scale structures have been tested with simplified flight-simulation loadings such as shown in figure 4.3, all flights being identical.

In figures 4.2 and 4.3, only the major types of fatigue loadings are given. The list is not complete since many variants on the examples shown can be thought of. For instance in a program test, the mean load need not be constant but may vary from block to block. As another example in a random load test, the S_{rms} need not be constant but can be varied from time to time as proposed by Swanson (Ref.33). Nevertheless, the list is complete enough for the discussion in the following section on systematic trends in the results of variable-amplitude loading. The merits of several testing methods are discussed in more detail in chapter 7.

4.3 Trends observed in tests on unnotched specimens

If an unnotched specimen is axially loaded, the stress distribution will be homogeneous. Exceeding the yield limit will not induce residual stress on a macro scale. This is an important difference as compared to notched specimens. Consequently, a significant mechanism for interaction effects will not occur in axially loaded unnotched specimens.
If unnotched specimens are loaded in rotating bending, the mean stress is equal to zero and the sign of the stress will change in each cycle. This is again an important difference with notched specimens

loaded at a positive mean stress.

As a consequence, we have to expect that the cumulative damage behaviour of unnotched specimens especially if loaded at $S_m = 0$, may be significantly different from the behaviour of notched specimens loaded at a positive mean stress. For instance it may be said that $\Sigma n/N < 1$ is a fairly common observation for unnotched specimens loaded in rotating bending, whereas $\Sigma n/N > 1$ is a relatively common observation for notched specimens loaded at a positive mean stress. An example of different sequence effects in unnotched and notched specimens is given in figure 4.4. It is thought that the explanation for the sequence effect of the unnotched specimens is mainly a matter of crack nucleation. Nucleation will more readily occur with the high stress amplitude at the beginning of the tests. Subsequently, cycles with a lower amplitude may then carry the crack to failure. For the notched specimens, residual stresses are responsible for the reversed sequence effect, see the following section.

Unnotched specimen data were reviewed in references 38,39. In view of their limited practical significance the data will not be further considered in this report.

4.4 The effect of a high preload

Various investigators have studied the effect of a single high preload on the subsequent fatigue life of notched elements. A survey is given in table 4.1 which shows that the effect of preloading was studied for a variety of materials and specimens including built-up structures, while the fatigue loading encompasses constant-amplitude loading, program loading and random loading.

Without any exception an increased fatigue life due to the preload was found in all the investigations. This was generally attributed to residual stresses at the root of the notch. Already Heyer in 1943 (Ref.41) attributed the increased life to compressive residual stresses. It is shown in figure 4.5 how these stresses are introduced by a high load. The compressive residual stress at the root of the notch implies that the local mean stress in subsequent fatigue testing will be reduced with an amount equal to the residual stress. Two examples of the effect of a preload on the S-N curve are shown in figure 4.6, one for constant-amplitude loading and one for random loading.

As a general trend, the investigations mentioned in table 4.1 also indicate that the preload effect is larger for higher preloads. This is illustrated by Heywood's results in figure 4.7.

In some investigations the effect of a negative preload (compressive load) was also studied (Refs.41-43, 47,49) and reductions of the life were found indeed, see figure 4.7. These losses are to be attributed to tensile residual stresses.

4.5 Residual stresses

Compressive residual stresses will increase the life for reasons discussed in chapter 3. Unfortunately residual stresses may be released by subsequent cyclic loading. Crews and Hardrath introduced a new technique for measuring the residual stresses at the root of a notch by means of very minute strain gauges (Refs.52,53). With the strain gauges the local strain history is measured. The corresponding stress history is then deduced from tests on unnotched specimens to which the same strain history is applied. Some results from Haibach, Schütz and Svenson (Refs.54,55) for a simple flight simulation loading, are given in figure 4.8. After the peak load F the local mean stress is lower than before the peak load and this will reduce the damage rate. However, the downward load A (ground-to-air cycle) has a reversed effect and hence it is unfavourable for a long fatigue life. Similar measurements were reported by Edwards (Ref.56).

The residual stresses at a notch will remain present only if the local stress range does not cause local yielding. This is obviously depending on the fatigue load applied, the geometry of the specimen (including cracks) and the cyclic stress-strain behaviour of the material. When cyclic plastic deformation occurs, either at the root of the notch or in the crack tip region, relaxation of residual stresses will occur. Obviously the residual stress can be restored by a new high load. Consequently periodic repetition of high loads will have a much larger effect on the fatigue life than a single preload of the same magnitude. Examples will be discussed later on.

Imig (Ref.49) performed fatigue tests on edge-notched Ti-alloy specimens and he found a life increase from 25000 to 145 000 cycles due to a preload of 70 kg/mm^2 (cyclic stress range 0-35 kg/mm^2). He could largely

eliminate the residual stress induced by preloading, by applying a new heat cycle ($288^{\circ}C$) to the specimens. This reduced the life from 145 000 cycles to 55000 cycles.

t might be expected that residual stresses can fade away if given enough time. This could apply to strain-ageing materials, such as mild steel. However, it has not been observed in aluminium alloys. Smith (Ref.45) found the same fatigue life for preloaded 7075 T6 specimens when tested immediately after preloading or tested half a year later. Preloading had more than doubled the life. Program tests of Gassner (Ref.57) on a tube with 3 holes may also be mentioned here. Frequent interruptions of these tests for two days rest periods did not systematically affect the life.

4.6 Periodic high loads and residual stresses

Investigations on this topic have been listed in table 4.2. Fatigue tests are interrupted from time to time for the application of a high load (Fig.4.2D). The general trend is that these periodic high loads are considerably more effective in increasing the life than a single preload. An illustration of this observation is presented by figure 4.7. The delaying effect on crack propagation was already discussed in chapter 3, see figure 3.3. The effect will be larger for higher periodic loads (Refs.26,60,62).

The relaxation and restoration of residual stresses is illustrated by the results of reference 39. Riveted lap joints were tested under program loading, see figure 4.9. The periodic high loads considerably increased the life. If the application of the high loads was stopped after the 50th period (series 6a), the residual stresses could be relaxed by the subsequent fatigue loading and failure occurred after 8 additional periods. Similarly, applying the high loads after each 2 periods (series 6b) also allowed more relaxation of residual stress and gave a three times shorter life. It is also noteworthy that the application of the program loading in the Hi-Lo sequence (series 17) instead of the Lo-Hi sequence, gave a much shorter lif Apparently, applying the maximum amplitude immediately after the periodic high load reduced the residual stresses and the subsequent lower amplitude cycles could be more damaging than in test series 6.

In some investigations, listed in table 4.2, it was studied whether a high negative load would reduce the life increasing effect of a high positive load. This was true in all cases. An illustration concerning crack propagation was already discussed in chapter 3, see figure 3.3 Another example for the fatigue life of riveted joints is shown in figure 4.10. If a single load cycle with a very high amplitude is applied, it is apparently very important whether this cycle starts either with the positive peak or the negative peak. The last peak load applied has a predominant effect on the damage accumulation, see discussion in section 3.2.

Hudson and Raju (Ref.62) also performed constant-amplitude tests with intermittent batches of 5, 10, 20 or 28 high load cycles. The effect of crack propagation in aluminium alloy sheet material was studied and it turned out that the crack growth delays were larger than for single high loads. It may be assumed that more high load cycles will further increase the compressive residual stresses in the plastic zone. It may also be assumed that the size of the plastic zone will still become larger. Another explanation is to attribute the increased growth delay to a more intensive strain hardening in the crack tip zone. It is difficult to indicate the significance of the various contributions. It is noteworthy that Haywood (Ref.42) found a few test results indicating that 10 high preloads on a notched element induced a larger increase of the fatigue life than a single high preload.

4.7 The damaging effect of periodic negative loads on GTAC

For wing structures, ground-to-air cycles (GTAC), also called ground-air-ground transitions (GAG), are frequently recurring load cycles. A survey of investigations on the effect of GTAC on fatigue life is presented in table 4.3. The GTAC has the reputation to be very damaging. It is true indeed that GTAC are reducing the life considerably, that means to a much greater extent than the Palmgren-Miner rule predicts (see for summaries Refs.76 and 79). In flight-simulation tests, life reduction factors in the range 2-5 are common.

A GTAC may be damaging for two reasons. First, it generally is a severe load cycle which certainly will contribute to crack growth. Second, it will partly eliminate compressive residual stresses as explained in section 4.5, see also figure 4.8. These two arguments explain the results of Barrois (Ref.70) in figure 4.11, which illustrates that the life in cycles is shorter if there are more GTAC.

From the above arguments it has to be expected also, that the damaging effect will be larger if the minimum load in the GTAC is going farther down into compression. This is illustrated by results of Naumann (Ref.67) and Imig and Illg (Ref.80), see figure 4.12.

The effect of GTAC was also studied for macrocrack propagation. The effect in simplified flight-simulation tests was observed to be small (see Ref.72). It was more significant with realistic flight simulation loading (Refs.77,78) as shown by the results in figure 4.13. The reduction factors for the crack propagation life are nevertheless noticeably smaller than the usual values for notched specimens and structures (range 2-5). Hence the damaging effect of the GTAC appears to be smaller for crack propagation. Reversing the load on a notched element implies that the stress at the root of the notch is also reversed and may thus reverse the sign of the residual stress if plastic deformation occurs. The reversion would also occur if small microcracks are present. However, for a macro crack, reversing the load from tension to compression implies that the crack will be closed thus being able to transmit compressive loads as discussed in section 3.2. The crack then is no longer a stress raiser.

As a consequence of the above reasoning, it appears that GTAC are more damaging for crack nucleation (including micro-crack growth) than for macrocrack propagation.

4.8 Sequence effects in two-step tests

In the previous sections the effects of high loads were discussed and it turned out that residual stresses could well explain the trends observed. As a consequence, a high peak load cycle could extend the life if it started with the negative half cycle and ended with the positive half cycle. Reversing the sequence of the two high loads had a detrimental effect on the fatigue life.

Another example of a sequence effect is given in figure 4.4b. In this figure the first block of high-amplitude cycles apparently exerted a favourable interaction effect ($\Sigma n/N = 5.35$) on the remaining life under the second block of low-amplitude cycles. This effect may again be due to residual stresses, although cyclic strain hardening and other interaction effects may also have been active.

The following illustrative example has been drawn from Wallgren (Ref.81). In figure 4.14 results are shown from two series of two-step tests that are almost identical, since the same S_m and S_a values apply to the first and the second block. The only difference is in the transition from the first block to the second one, which had a significant effect on the life. The life is relatively short if the first block ends up with S_{min} and relatively long if the block ends with S_{max}, which is just a matter of one additional half cycle. This observation is strongly in favour of residual stress as the major mechanism for interaction. The observation is also in good agreement with Edwards' measurements of residual stresses at the root of a notch (Ref.56), showing that the sign of the residual stress may change in each cycle if the applied stress range is large enough.

With respect to macrocrack propagation in sheet specimens, crack growth delays after a high-low amplitude step have been mentioned before (Section 4.1). It was also emphasized that an interaction effect after a low-high step, being significant during a few cycles only, could easily escape macro observations, but it can be detected by electron fractography. Crack growth acceleration after such a low-high step was successfully explained by Elber (Ref.19), using the crack-closure argument. During the low-amplitude cycling little plastic deformation is left in the wake of the crack. Consequently, after changing over to the high amplitude there is less crack closure and more crack opening as compared to crack growth at the high amplitude only. After some further crack extension the crack closure is again representative for the high amplitude (Ref.21).

4.9 Sequence effects in program tests

In a two-step test the stress amplitude is changed only once. In a program test it is changed many times, both by increasing and decreasing its value. As a consequence, results of two-step tests will not necessarily allow a direct interpretation of sequence effects in program tests.

There is another reason why explaining sequence effects in program tests may be problematic. In most program tests a change of S_a is supposed to occur stepwise. If this were true, it is important whether the change is made either after the minimum or after the maximum of the last cycle of a step, see the previous section and figure 4.14. Unfortunately this information is rarely given in the literature for those cases where the change is really step-wise (manual operation, slow-drive machine, closed-loop machine with load control on individual cycles). Many program tests were carried out on resonance fatigue machines, which implies that changing the amplitude from one level to another level did occur gradually, that means in a rather large number of cycles. Apparently, there is a poor definition of details of the load sequence in program tests although these details could be important for interaction effects and hence for the fatigue life.

Gassner proposed the program test in 1939 (Ref.29) and shortly afterwards he studied already the effect of period size (number of cycles in one period, see figure 4.3F) and the effect of the sequence of amplitudes in a period (Ref.82). A survey of investigations on the methods of program testing is given in table 4.4.

Size of period

The investigations listed in table 4.4 indicate that the fatigue life may depend on the size of the period but unfortunately a clearly systematic trend was not found in all cases. Reducing the size of the period in several but not in all cases, reduced the life.

Reducing the size of the period to relatively small numbers of cycles while maintaining the same load spectrum, implies that the highest amplitudes occur less than once in a period. The amplitudes then have to be applied in a limited number of periods. Adopting this procedure, Lipp and Gassner (Refs.94,95) and Breyan (Ref.98) reported a systematic effect on the program fatigue life. The results, as shown in figure 4.15, indicate that the effect was far from negligible. In an NLR study (Refs.96,97) on crack propagation, a similarly large effect of the period size was found, see figure 4.16, while the load spectrum of amplitudes was exactly the same for the short and the long period.

Sequence of amplitudes

Sequences frequently applied are:

a increasing amplitudes (Lo-Hi)

b increasing-decreasing amplitudes (Lo-Hi-Lo)

c decreasing amplitudes (Hi-Lo)

d randomized sequence of blocks with the same amplitude.

Various comparative studies are reported in the literature. The effect of the sequence is illustrated by the NASA results in figure 4.17, and for crack propagation by the NLR results in figure 4.16. The results are generally systematic in a way that the life for the Lo-Hi-Lo sequence is always in between that of the Lo-Hi and the Hi-Lo sequence. Unfortunately, the results are not systematic with respect to the comparison between the Lo-Hi and the Hi-Lo sequence. In both figures 4.16 and 4.17, the fatigue life was longer for the Hi-Lo sequence, a trend also confirmed by tests on wings reported by Parish (Ref.91). However, results of Gassner (Ref.81) and NLR tests on riveted joints (Refs.39,58) showed the opposite trend, that means longer fatigue lives for the Lo-Hi sequence. As said before, the way of changing from one amplitude to another one may be important for having either favourable or unfavourable interaction effects.

Both the effect of the size of the period and the effect of the sequence of amplitudes indicate that the damage accumulation rate is a function of the frequency of changing the amplitude (period size) and the pattern of changing the amplitude (sequence). From a fatigue point of view it cannot be surprising that these variables will affect the damage accumulation and hence the fatigue life. However, a detailed

picture about how interactions could explain the data, would eak a good deal of speculation.

4.10 High-amplitude cyclee in program tests

In a program test the statistical distribution function of the amplitudes is usually based on an assumed load spectrum. Aseessing the maximum value of the stress amplitude to be applied in a program test, ia making e more or lees arbitrary choice. Sometimes the choice is dictated by the possibilities of the available fatigue machine. In view of the large effect that periodic high loads could have on the fatigue life (see Sec.4.6), it has to be expected thet the assessment of $S_{a,max}$ in a program test may be a critical issue. A survey of relevant investigations has been given in table 4.4.

High-amplitude cyclee may either extend or reduce the fatigue life for the following reesons:
a These cycles will be damaging since they will substantially contribute to crack nucleation and propagation. They may contribute to crack growth even more than in a constant-amplitude test carried out et $S_{a,max}$, because of unfavoureble interactio..s caused by cycles with lower S_a values.
b High-amplitude cyclee will also reduce the life because final failure will occur at a shorter crack length.
c On the other hand, high-amplitude cycles may extend the life if they introduce compressive residual stresses which is not unlikely. The crack closure argument also appears to be applicable.
In view of these arguments it will be clear thet fully systematic results cennot be expected. The trend could be depenuent on the question whether there ars relatively many high amplitude cycles (manoeuvre spectrum) or juet a few (gust spectrum). Secondly, the question whether compressive oi tensils residual stresses are introduced will bo dependent on $S_{a,max}$, the detailed load sequence, the geometry of the notch and ths matariel. Consequently, it should not be surprising that datu from the litereture indicete both life extension and reductions if higher amplitudes are applied in a program test. Illustrations of both are given in figure 4.18. The results of the tailplanes reported by Rossnfeld (Ref.48), were obtained with S_{min} = + 13.3 % P_L (P_L = limit load) end hence the increeeed life obteined by adding higher load cyoles may well be due to introducing compressive residual stress, which epparently outweighed the damaging effect of these cyclee per ee. In Naumann's tests (Ref.87) on the edge notchsd specimens, the addition of higher load cycles was coupled to negative minimum loads which may have eliminated compressive residual stress and thus the cycles werc damaging only. Effecte as found in other investigations were generally smaller then those in figure 4.18.

Kirkby and Edwards carried out narrow-band rendom load tests on lug type specimens (Ref.99). They also performed test seriee with three S_{rms} valuss in a programmed sequence, see figure 5.2. Omission of the highest S_{rms} reduced the life 2.5 times. Apparently, the higher-amplitude cycles had a beneficial effect in the first teats. Comments on high-amplitude cvcles in flight-simulation teata are given in section 4.13.

4.11 Low-amplitude cyclss in program tests

In aircraft structures fetiguc load cycles with a low amplitude usually occur in relatively large numbers. Consequently, if such cycles could be omitted from a test a large nroportion of the testing time would be seved. This topic was studied in several investigations employing program loading, see for a survey table 4.4.
Low-amplitude-cycles may bs damaging for more than one reason:
a Due to the large numbers, they may induce fretting corrosion damage and thue enhance crack nucleation.
b Low-amplitude cyclee may contribute to crack growth as eoon es a crack has been crested by higher-amplitude cyclee. This implies thet cycles with an amplitude below the fatigue limit cen be damaging.
c Low-amplitude cycles may enhance the crack growth at subsequent cycles with a higher amplitud, see the discussion in section 4.8.

It ie well-known that fretting corrosion can have a most detrimentel effect on the fatigue limit and on the lower part of the S-N curve. However, ths effect is relntively small at high S_e-valuee becauee crack nucleation does occur quite early and is less dependent on the aeeietance of fretting corroeion. Similarly,

we may expect fretting corrosion to be less important in program tests. Nevertheless, Gassner (Ref.100) still found a 50 percent life reduction if fretting was applied at the root of a notched 2024-T4 specimen. Jeomans (Ref.89) also in program tests, found a life reduction of about 65 percent when comparing dry and greased bolted joints of the 2014 alloy.

Program tests from which low-amplitude cycles were omitted, always indicated either a negligible effect on the fatigue life (in periods) or an increase of the life. In other words the available data confirm that cycles with amplitudes below the fatigue limit may be damaging. An example is given in figure 4.19 with results reported by Wallgren (Ref.83). The last column of the table illustrates the reduction of testing time obtained when omitting low-amplitude cycles.

4.12 Comparison between the results of program tests and random tests

In comparison to a random load test, the variation of the stress amplitude in a program test occurs in a simple and systematic way. For random loading the amplitude (as well as S_{max} and S_{min}) may be significantly different from cycle to cycle. In a program test, however, the amplitude may remain unchanged during large numbers of cycles. The number of amplitude changes is relatively small. In view of the present knowledge about interaction effects, it has to be expected that the fatigue damage accumulation rate may be different for the two types of loading. Any similarity between the results of random tests and program tests cannot be claimed on physical arguments but has to be shown by tests.

A second aspect of the comparison between random and program loading is concerned with the concept "random". A random signal may be stationary or non-stationary, it may be Gaussian or non-Gaussian (Refs.32-34). If it is a stationary Gaussian process, the sequence is still dependent on the power-spectral density function (PSD-function). An illustration is given in figure 4.20 by two record samples of Hillberry (Ref.101). The effect of the shape of the PSD-function on the random load fatigue life was studied in some investigations, see table 4.5. As a general trend, it was found that the effect was either small or negligible. It is thought, however, that these data are still too limited to justify a generalization.

The importance of the "randomness" for fatigue life has also been studied under different pseudo random loading conditions. In figure 4.21, results of Naumann (Ref.67) illustrate that the fatigue life is apparently depending on the question whether we consider full cycles (starting and ending at S_m) or half cycles (also starting and ending at S_m). It should be pointed out that the statistical distribution functions of the maxima and the minima were exactly the same for all test series in figure 4.21. It should also be pointed out that the statistical distribution functions of stress ranges (differences between successive values of S_{max} and S_{min}) are not the same for these test series, which will be evident after a closer look at the sequence samples in figure 4.21.

A second example of sequence effects in random load tests is shown in figure 4.16, giving data from NLR tests on crack propagation. In two test series exactly the same random sequence of complete load cycles were applied. In the first series the cycle started with the positive half cycle, whereas in the second series it started with the negative one. Also here it is true that the statistical distribution functions were the same for the peak values but different for the stress ranges, which apparently has some effect on the crack propagation life, although the effect was small.

A comparison between the results of random tests and program tests was recently published by Jacoby (Refs.107,108). Some new results became available since then. A survey of comparative investigations is given in table 4.6. As Jacoby pointed out, there is no unique relation between the fatigue lives for random loading and for program loading. He mentioned (Ref.109) various aspects that could affect the comparison. Some important ones are the type of random loading, the type of program loading, the maximum stress in the test, the mean stress and the shape of the load spectrum.

It is difficult to draw general trends from the investigations listed in table 4.6. In general, the life in the "equivalent" program test is larger than in the random test. In several investigations the difference is not very large. However, Jacoby (Ref.107) arrived at program fatigue lives that were about six times longer than in random load tests. In figure 4.16, NLR results on crack propagation indicate about

three times longer lives if the comparison is made with program loading with 40000 cycles in a period. Fractographic observations also indicated different cracking modes. For the short period (average 40 cycles), the difference between random and program loading was small. This is in agreement with the observation that the sequence effect in the program tests (Lo-Hi, Lo-Hi-Lo and Hi-Lo) was small for the short period (although still systematic). Gaesner's and Lipp's results (Refs.94,95, see fig.4.15) also point to a small difference between random and program test results if the period of the program is short. There are some indications that the differences may also be smaller for a more severe load spectrum. Unfortunately the large differences mentioned above still give some uneasy feelings about the equivalence of random tests and program tests.

4.13 Trends observed in flight-simulation tests

A survey of investigations on flight-simulation testing is presented in table 4.7. In these investigations several trends were observed that are qualitatively more or less similar to those discussed before.

Sequence effects

Naumann's tests on the effect of the random sequence of either complete cycles or half cycles also included flight-simulation tests. As the results in figure 4.21 show, a similar sequence effect was found in the random tests and in the flight-simulation tests. However, the effect was much smaller in the flight-simulation tests. A similar observation was made by Jacoby (Ref.107).
The sequence effect in flight-simulation tests was one of the topics studied in a recent NLR investigation (Refs.77,78) on crack propagation in 2024 and 7075 sheet material. The gust load spectrum applied is shown in figure 4.12, while different sequences are presented in figure 4.23. In these tests 10 different types of weather conditions were simulated in different flights. Apart from test series H the gust sequence in each flight was random, while the sequence of the various flights was also random. In figure 4.23 a comparison is made between a random sequence of complete cycles, the same sequence of "reversed" complete cycles and a Lo-Hi-Lo programmed sequence. As the data in the figure show, the sequence effect was practically negligible. This result is in good agreement with the small sequence effect found in figure 4.16 when comparing random loading and program loading with a short period.
A small sequence effect was also found by Gasener and Jacoby (Refs.66,73), and by Imig and Illg (Ref.80) with one exception. Gasener and Jacoby, testing 2024-T3 specimens ($K_t = 3.1$), found fatigue lives of 2500, 2800 and 5800 flights for a random gust sequence, a Hi-Lo-Hi gust sequence and a Lo-Hi-Lo gust sequence, respectively. The latter result is considerably higher than the former two results. They applied 400 gust cycles in each flight which is a relatively high number.

Low-amplitude cycles

As said in section 4.11, low-amplitude cycles may be significantly damaging in a program test. In such a test these cycles are applied in blocks of large numbers of cycles. In random loading the low-amplitude cycles are randomly dispersed between cycles with higher amplitudes. This implies that the information from program tests is not necessarily valid for random loading.
Some investigations on flight-simulation testing have also explored this aspect, see table 4.7. Average results are collected in figure 4.24. Naumann (Ref.67) found a very small increase of the fatigue life when omitting low-amplitude gust cycles, while Branger (Ref.110) found a small reduction of the life. Gaesner and Jacoby (Ref.73), however, found a significant increase. They omitted 370 low-S_a cycles from 408 cycles in each flight. Both numbers are large, which may have contributed to the result. The NLR results on crack propagation are recapitulated in figure 4.25. Here also it is evident that omitting low-S_a cycles increases the life.
With respect to omitting taxiing loads from the ground-to-air cycles, the trend appears to be that this has a minor effect on life. It is thought that the taxiing cycles were hardly damaging because they occurred in compression. Consequently the low damaging effect of the taxiing loads will not be applicable if the mean stress of the GTAC is a tensile stress (upper skin of wing structure).

High-amplitude cycles

In section 4.6 it turned out that periodically applied high loads could considerably increase the fatigue life. It then may be expected that high-amplitude cycles in a flight-simulation test may also have a similarly large effect, if applied now and then in a few flights. This aspect was not intensively studied so far, see table 4.7. Gassner and Jacoby (Ref.73) reported 25 percent longer life if increasing the maximum stress amplitude from 0.55 S_m to 1.1 S_m (S_m is mean stress in flight). In these tests the gust loads in each flight were applied in a programmed sequence. Branger (Ref.111), employing a manoeuvre spectrum, found 10 to 40 percent longer lives when raising the maximum peak loads with 15 percent. At the NLR we performed one test series on a sheet specimen with a central hole and several series on crack propagation in sheet specimens (Refs.77,78). The results of the hole notched specimens are shown in figure 4.26. Load sequences were similar to those shown in figure 4.25 (sequence B), while the load spectrum given in figure 4.23 was applicable. In three comparative test series the spectrum was truncated at $S_{a,max} = 4.4$, 6.6 and 8.8 kg/mm^2 respectively. Truncation implies that cycles, which should have higher amplitudes according to the load spectrum, were applied with an amplitude equal to $S_{a,max}$ (truncation level). Figure 4.26 clearly shows a systematic effect of the truncation level on both the nucleation period and the crack propagation life. Both periods are longer for higher $S_{a,max}$ values. More data from the crack propagation tests are collected in figure 4.27, which clearly confirms the longer fatigue life if higher amplitudes are included in the flight-simulation test. In one test on a 7075-T6 specimen the gust spectrum from figure 4.22 was applied without truncation, that means $S_{a,max} = 12.1$ kg/mm^2. The crack rate was extremely low and decreased as the crack grew longer. The test had to be stopped in view of excessive testing time.

It is thought that the predominant effect of high gust load cycles, as illustrated by figures 4.26 and 4.27), has to be explained by the effect of compressive residual stresses on crack growth and by crack closure. Practical aspects of the effect of the truncation level are discussed in chapter 7.

Some remarks on the effects of loading frequency and environment as observed in flight-simulation tests are made in section 4.17.

4.14 The effects of the design stress level and the type of load spectrum

The design stress level will obviously affect the fatigue life of an aircraft. Empirical studies for a long time could only be made by program tests. Gassner started the work about 30 years ago (Refs.29,57, 82); another early publication is from Wallgren (Ref.83), see also table 4.4 The major part of this type of work was carried out in Gassner's laboratory at Darmstadt. Much of this work was recently summarized by W. Schütz (Ref.115).

From a large amount of program data obtained with standardized load spectra (Ref.116), Gassner found a linear relation between log stress level and log program fatigue life. This trend is illustrated by figure 4.28. The relation can be written as:

$$N' \, S_{a,max}^{\kappa} = \text{constant} \tag{4.1}$$

Many tests indicated the trend for κ to be in the order of 5-7. In equation (4.1), N' is the program life and $S_{a,max}$ is the maximum amplitude of the standardized load spectrum which is truncated at a level occurring once in 500 000 cycles.

Since $S_{a,max}$ as well as S_m are linearly related to the ultimate design stress level, the merit of the above relation is that it immediately indicates the change of life associated with a certain percentage change of design stress level. The question is, however, whether equation (4.1) would also be valid for realistic service load-time histories. This could not be checked empirically until the electrohydraulic fatigue machine with closed loop load control became available. As pointed out in section 4.12 it remains to be explored whether trends valid for program tests are also applicable to random loading.

In the more recent literature some test results are presented regarding the effect of design stress level on fatigue life in flight-simulation tests, see table 4.7. These, by now, are apparently the most

realistic deta availeble to judge this effrct. The data are eummarized in figure 4.29. It should be
pointed out thet for each test series in this figure changing the streee 'evel did not affect the shape
of the load time history. Hence the shape of the load spectrum elso remeined the same. Changing the
stress level only implied thet all load levels were multiplied by the same factor. Evidently, the deta
in figure 4.29 are too limited for deriving e general trend. The reletion of equation (4.1) is not
appliceble to the NLR crack propaṛation date. In the other graphs the slope factor κ is outside the
range 5-7 usually found for program tests. Three graphs indicate a ʾigher value (everage 8), while the
data of Branger and Ronay indicate e very low κ-value . Further comments on this topic are made in
section 5.3.7.

In varieble-amplitude tests based on a service load spectrum, a gust spectrum or a manoeuvre spectrum was
usuelly adopted. The investigations, in general, do nct allow a direct comparisicn between the two spectre,
since there were more variables than the spectʳum shape alone (for instance stress ratios, truncation
level).
Nevertheless, manoeuvre spectra are generally considered to be more severe than gusx spectra, because the
prcportion of higher-amplitude cycles is larger.
The effect of the spectrum shape was systemetically studied in one investigation only, namely by
Ostermann (Ref.117). He performed program teste on notched 2024-T3 specimens and kept all variables
constant except the spectrum shape. The number of cycles in one period was also constant. The test
results indeed confirmed that the life became snorter if the proportion of high-amplitude cycles in-
creased (and the proportion of low-amplitude cycles decreased). Some further comments on this work ere
mede in section 5.3.5.

4.15 Observations from full-scale fatigue test series

This section is partly similer to Appendix J of referencs 76, entitled "The influence of the loeding
history on the indication of fatigue-critical components".
As explained before, high loads will introduce local stress redistributions around notches end the effect
on the fatigue life may be different for different ncteheе, depending on K_t, stress gradient and nominal
stress lᵉvel. The consequence ie that the indications of the most fatigue-critical componɛnt in e
structure may depend on the selected load spectrum and the truncation level. Fatigue tests cn lerge
structures reported in the literature give some informetion on this question. ʾhey ere summᵤrized below.

Tests on Muetang wings

Results of an extensive test program on ꝹuꜱꞇꜺnꞡ winge were reported in references 44,74 end 118. The
following types of tests were carried out:
(1) Constant-amplitude testᵉ, various P_a and P_m values
(2) Program tests with 3 amplitudee, $P_{max} = 33 \% P_u$
(3) Random loed tests, ḡust spectrum, $P_{max} = 63 \% P_u$
(4) Random load tests with CTAC, same gust spectrum, P_{min} for CTAC $ = - 24 \% P_u$
(5) Rardom ioad tests, manoeuvre spectrum, including negetive manoeuvre loads, $P_{max} = 75 \% P_u$.
The 1-g load level for test series 2-5 was 20 $\% P_u$. The stresses at P_u were in the oᵣᵈer of 28 kg/mm^2.
Crecks were meinly found in two areas, indicated as the tank bay area and the gun bay area. For the two
ereas intersecting S-N curves were found in test series no.1, both for initial cracking and final feilure.
Thie showe that a certain compᵤnent, which under constent-amplitude loading is more fatigue-criticel than
another component, car be less criticel at another ioad level.
In test series 2-5 the initiel feilure was alwaye first observed in the gun bay area. However, cracking
in the tank bay aree could be more serious. The final feilure occurred in both areas in teet series 2
(lower P_{max} value) and in the tank bay aree only ᵢn test series 3, 4 and 5. In the random ꝛust tests
without CTAC the gun bay area was then in an advanced stage of cracking, whereas this failure ꭓas almost
completely suppreeeed in the random ꝝuet tests with CTAC. The latteʳ wae partly true aleo for test series 5.

Tests on Commando wings

Results of tests on Commando wings were reported by Huston in reference 119. Three types of tests were conducted, viz.:

(1) Constant amplitude tests (P_{max} values $\leqslant$ 5.5 % P_u)

(2) Program tests with a gust spectrum ($P_{max} \sim 75$ % P_u)

(3) Program tests with a manoeuvre spectrum ($P_{max} \sim 78$ % P_u) .

A limited amount of service experience was available. The program tests were randomized step tests. The stress at P_u was low, viz. about 19 kg/mm^2.

Constant-amplitude tests revealed only 1 or 2 fatigue-critical locations, which were different for high and low amplitudes. In test series 2 and 3, cracks were found at 7 different locations. With respect to the first crack that appeared, the crack at location F (code of Ref.119) was the most frequent one in test series 2 and 3, whereas this location was not very important in the constant-amplitude tests. The most critical crack with respect to final failure was found at location B in the constant-amplitude tests and at location III in the program tests.

A comparison between the cracks found in service (4 aircraft) and in the program tests (gust spectrum), yielded a reasonable agreement regarding the locations at which cracks were found.

Tests on Dakota wings

In reference 71 Wickworth reported the results of testing 4 Dakota wings and a comparison with service experience.

The following four tests were carried out:

(1) Gust cycles only, constant amplitude, P_a corresponding to 12 ft/sec gust.

(2) Simplified flight simulation, 15 gust cycles (as applied in test 1) per flight.

(3) Same as test 2, except 5 instead of 15 gust cycles per flight.

(4) GTAC only, P_{max} at 1-g level, $P_{min} < 0$.

Cracks occurred at three different locations, A, B and C. The most critical crack in tests 1 and 2 occurred at location A and in tests 3 and 4 at location C. Cracks at location B were found in all tests. In service cracks were predominantly found at location B and cracks at location A did not occur. Cracks were also found in service at a location at which no cracks were found in the tests. It cannot be said that a fair agreement between service experience and testing was obtained. This may be partly due to the simplified flight-simulation load sequence adopted for the tests.

Tests on a swept back wing

Results of constant-amplitude tests and program tests on a wing of a fighter were reported by Rosenfeld (Ref.48). In the program tests two different manoeuvre spectra were used. In one test series GTAC were inserted (in batches), which in this case were upward loads rather than downward loads. Values for P_{max} from 55 to 100 % P_L (P_L is limit load) were used in the constant-amplitude tests and from 35 to 125 % P_L in the program tests. P_{min} was 13.3 % P_L in all tests.

In each wing, failure always occurred at a bolt hole. In the program tests (4 different programs) failures occurred at locations A (6 times), C (once), E (twice) and F (once). In the constant-amplitude tests, failures occurred at locations A (7 times), especially at the higher load levels), B (twice), C (once) and D (twice, at the lowest load level only).

Tests on the pre-mod F-27 center section wings

Random and program tests were carried out, both with and without ground-to-air cycles (Ref.76). Constant-amplitude tests were carried out representing GTAC loading and gust load cycles. In the random and the program tests a very severe gust spectrum was adopted, the maximum load being $P_{max} = 65$ % P_u where P_u is the ultimate design load. In the constant-amplitude tests, P_{max} values covered a range from 35 to 47 % P_u.

Although the same type of crack was the most critical one in all tests, considerable differences were found between the random and the program tests at the one hand and the constant-amplitude tests on the other hand. Contrary to Huston's findings, the number of locations at which cracks were found was larger in the constant-amplitude tests. Secondly, some types of cracks occurred predominantly if not exclusively in the random and the program tests, whereas other types of cracks were found in the constant-amplitude

tests only.

Tests on Venom wings

Branger (Refs.120,121) has reported interesting data on the indication of fatigue critical locations in the structure. Information was available from:

(1) One constant-amplitude test ($P_{max} = +1g$)

(2) Two program tests ($P_{max} = 7.25$ g, $P_{min} = -0.87$ g)

(3) Six half wings tested with a most realistic flight-simulation loading ($P_{max} = 6.5$ g, $P_{min} -30\% P_{max}$)

(4) Service experience.

In the flight-simulation tests, two explosive failures occurred. One of these failures had not been detected in the constant-amplitude test and the program tests. Initial cracking corresponding to this failure was observed in service. On the other hand, five main failures occurring in the constant-amplitude test and the program tests did not occur in the flight-simulation tests and in service.

One general trend emerging from the available evidence is that the picture of fatigue-critical elements in an aircraft structure is significantly depending on the load-time history applied. This emphasizes the need for realistic load-time histories for application to full-scale testing, see chapter 7.

4.16 Fatigue by two superimposed sinusoidal loads with different frequencies

The superposition of two cyclic loads with different amplitudes and frequencies may occur in certain components under service conditions. This especially applies if a component is subjected to high-frequency vibrations, while at the same time a low-frequency fatigue loading occurs. Even gust loads and taxiing loads may be considered as high-frequency loads superimposed on the ground-to-air cycle.

Apart from the technical significance, the superposition of two cyclic loads is an intrigueing variable-amplitude load sequence to check certain assumptions about fatigue damage accumulation. Two examples are shown in figure 4.30, which can be written as

$$S = S_m + S_{a1} \sin \omega_1 t + S_{a2} \omega_2 t \qquad (4.2)$$

with $\omega_1 \ll \omega_2$, ω being the angular frequency.

Investigations on superimposed cyclic loads have been listed in table 4.8 which shows that there is a good deal of variety between the various studies. Nevertheless some general findings may be reported. If S_{a2} is small enough to be below the fatigue limit, the Palmgren-Miner rule would suggest the cyclic load $S_{a2} \sin \omega_2 t$ to be non-damaging. Consequently the life should be N_1 if N_1 is the fatigue life associated with S_{a1}. However, it turns out that the life is shorter. This has to be expected since the cyclic load $S_{a2} \sin \omega_2 t$ will anyhow increase the stress range of the low-frequency component from $2 S_{a1}$ to $2 (S_{a1} + S_{a2})$, see figure 4.30a. In other words, a life N_1 associated with an amplitude $S_{a1} + S_{a2}$ should be expected at most. Usually a shorter life is found depending on the ratios S_{a1}/S_{a2} and ω_2/ω_1. Apparently, apart from increasing the stress range, the high-frequency cyclic load itself is also contributing some damage.

The example shown in figure 4.30b has more the character of a cyclic load ($S_{a2} \sin \omega_2 t$) with a slowly varying mean. Available results indicate this varying mean to be damaging, implying that the life will be shorter than N_2, if N_2 is the life associated with S_{a2}. Here also the stress range is increased to $2 (S_{a1} + S_{a2})$ and even in case that $S_{a1} \ll S_{a2}$, the material will remember this to some extent depending on ω_2/ω_1.

In some investigations the low-frequency component was cyclically changed step-wise or following a triangular wave form. With respect to the high-frequency component, a randomly varying S_{a2} value has been applied (Ref.129). This is further complicating the picture but it is more similar to practical conditions. Such complex load histories raise the problem of how to define a load cycle. This already applies to the examples in figure 4.30. A cycle with a range $2 (S_{a1} + S_{a2})$ does in fact not occur in these examples, although the range has still some meaning for the fatigue life. The problem how to define cycles for more complex load-time histories is given more attention in chapter 6. It may be noted here that fatigue under superimposed cyclic loads is also being studied by following the strain histories (Refs.128,129).

4.17 Effects of environment and loading frequency

In chapter 2 brief reference was made to the possible effects of environment and loading frequency. Effects were observed in constant-amplitude tests and although the humidity of the environment appears to be important, a full understanding of these effects has not yet been obtained. Only a few investigations have been made under variable-amplitude loading.

Environment

In a comparative investigation at NLR (Ref.106) on 2024 and 7075 sheet material, crack propagation was simultaneously studied in an indoor and an outdoor environment. Program loading and random flight-simulation loading were used. The results indicated a negligible effect for the 2024 material, but for the 7075 alloys the crack growth outdoors was 1.5 to 2 times faster than indoors. Figge and Hudson (Ref.130) in a recent study found a similar trend. Branger (Ref.111), testing two-hole specimens under flight-simulation loading, found a doubling of the life when testing in pure nitrogen instead of air. The specimens were produced from 7075-T6 bar material.

Loading frequency

In a recent NLR investigation crack propagation tests have been carried out on 2024 and 7075 sheet speci-mens under flight-simulation loading. The variables being studied are of the design stress level and the loading frequency. Three frequencies have been adopted, namely 10 cps, 1 cps and 0.1 cps. The investiga-tion is not yet complete, but abailable data (see Ref.64) indicate a rather small and not fully systemat-ic influence. Although such a small effect is a very convenient result, it is not yet justified to generalize this empirical observation.

Branger (Ref.111), in flight-simulation tests on light alloy specimens notched by two holes, found a slightly lower life at 96 cpm (cycles per minute) as compared to 173 cpm (1.6 cps and 2.9 cps respect-ively). Surprisingly enough he found a reversed frequency effect in another test series with frequencies of 210, 40 and 5.4 cpm (3.5, 0.7 and 0.09 cps respectively). The longer life was obtained at the lower frequency.

4.18 Aspects related to the type of material

The majority of variable-amplitude tests was performed on aluminium alloy specimens and structures. There is some work available on titanium alloys and low-alloy steels. (Table.4.1-4.8). The question now is whether these materials show empirical trends similar to those of the aluminium alloys. Indications of a significantly different behaviour have not been obtained so far.

There are some reasons why certain materials may show a similar cumulative fatigue damage behaviour. The accumulation of fatigue damage has been described in chapter 3. The interaction mechanisms, see figure 3.2, were related to cracking, residual stress at the tip of the crack due to local plastic deform-ation, crack closure, crack blunting, cyclic strain-hardening, etc. All these mechanisms are related to the ductility of the material. Consequently it is thought that materials with a similar plastic behaviour could show a cumulative damage behaviour that is qualitatively similar. With respect to preloading notch-ed elements this was clearly confirmed (Refs.41,46,49).

A qualitative similarity, however, does not yet imply a quantitative similarity. This can be illustrated by comparing data for the two well-known aluminium alloys 2024 and 7075. Both alloys are neither extreme-ly ductile nor brittle, but the ductility of the 7075 alloy is certainly smaller than that of the 2024 alloy. Favourable interaction effects have been noted for both alloys. Nevertheless, Hardreth, Naumann and Guthrie (Refs.30,31,88) found systematically higher $\Sigma n/N$ values for the 7075 alloy. Similarly figure 4.27 shows that the 7075 alloy is indeed more sensitive to the effect of high-amplitude cycles. Larger favourable interaction effects are also confirmed by the NLR crack propagation data in figure 4.29, the more so since constant-amplitude data suggested a much longer life for the 2024 alloy as compared to the 7075 alloy. An increasing ductility will imply that the residual stresses will be smaller and that relaxation of residual stresses due to cyclic straining will be easier.

As a general conclusion, similar qualitative trends may be expected within certain limits. The similarity should no longer be expected if the material has a significantly different ductility, for instance a very high ductility (low strength alloys) or responds to unstable yielding (mild steel). Brittle materials for

which a very small crack may be disastrous and for which the life is mainly occupied by crack nucleation, may also behave differently.

5. THEORIES ON FATIGUE DAMAGE ACCUMULATION

5.1 Introduction

In the literature a variety of cumulative damage theories have been presented. The question now is whether these theories can account in a realistic way for the trends described in the previous chapter. In this chapter an attempt will be made to give a systematic survey of the various aspects characterizing the theories. In view of this goal, some salient features of fatigue damage will be summarized first (section 5.2). Secondly, damage theories will be discussed in three groups, each group being character- ized by a certain similarity of the damage accumulation model adopted (section 5.3). Finally the physical and practical limitations of the theories are discussed in section 5.4. The significance of the limita- tions for practical applications is a topic also covered by chapter 6.

5.2 Fatigue damage

Fatigue and damage accumulation in metallic materials have been discussed in chapters 2 and 3. The fatigue life was divided in some periods, for instance (see also figure 2.2):
- crack nucleation
- crack propagation
- final failure.

These periods are recognized by some theories but certainly not by all. An obvious difficulty is the definition of the termination of the first period and the start of the second period. This problem does not occur in those theories that assume crack growth to start in the very beginning of the fatigue life. Since the most essential part of fatigue damage was described in chapter 3 as decohesion of the material, a physical theory should incorporate crack growth as a minimum requirement.

However, it was explained in chapter 3 that the amount of cracking alone could not give a complete des- cription of the state of fatigue damage. Several additional damage aspects were mentioned, see figure 3.2. From these aspects only residual stress has been incorporated in a few theories. The other aspects have been mentioned in the literature to explain certain trends observed in tests, but these aspects are not an explicit part of a quantitative theory.

The occurrence of the final failure should be a function of the crack length and the applied maximum stress. A few theories try to account for this aspect by employing fracture toughness criteria. Several theories predict fatigue life only, without any reference to the physical damage occurring between the beginning and the end of the fatigue life. Moreover, the end of the life in most theories means "complete failure" without any further specification.

5.3 Theories

5.3.1 General survey

The number of cumulative fatigue damage theories is large. This is certainly true if we keep in mind that the theories try to solve the same problem, which is to predict the fatigue life (or crack propagation life) under variable-amplitude loading from available data. For a good appreciation of the various theories, three different approaches may be recognized, as listed in table 5.1.

In the incremental damage theories it is assumed that each cycle or each batch of cycles causes a certain damage increment. This increment is quantitatively equal to the percentage of fatigue life consumed by those cycles. The complete life expires and failure will occur at the moment that the sum of all damage increments becomes equal to one.

The similarity approach refers to those theories, which presume that similar loading conditions at the fatigue-critical locations in two different specimens should produce similar fatigue lives. The stress history or the strain history could be adopted for characterizing the loading condition. For crack propagation the similarity approach implies that similar stress intensity factors should produce the same crack rates.

The interpolation methods appear to be the most direct approach, since interpolation is made between available fatigue data. Nevertheless, the interpolation procedure may be a critical issue. Interpolation can be made for a large variety of variables, such as S_m, K_t, load spectrum shape, etc.
More details of the theories are given in the following sections. An evaluation of the theories is given in section 5.4.

5.3.2 The Palmgren-Miner rule

This rule is the most well-known representative of the incremental damage theories. Palmgren (Ref.131), as early as 1923, assumed that n_i load cycles with the same mean load and load amplitude will consume a portion of the fatigue life equal to n_i/N_i where N_i is the life to failure in a constant-amplitude test with the same mean and amplitude. Secondly, Palmgren assumed that failure will occur if the sum of the consumed life portions equals 100 percent. This implies that the condition for failure is:

$$\sum n_i/N_i = 1 \qquad\qquad (5.1)$$

Without any detailed knowledge about fatigue in metals, Palmgren's assumptions are the most obvious ones to be made. One might well ask how many times the assumptions were made independently afterwards. Well-known is the publication of Miner in 1945 (Ref.132) and curiously enough less well-known is the earlier publication by Langer (Ref.133) in the same journal. The assumptions were also independently made in a Dutch publication in 1940 by Biezeno and Koch (Ref.134).

Langer should be especially quoted, since he already made the refinement to divide the life into a crack nucleation period and a crack propagation period. Langer suggested

$$\sum n_i'/N_i' = 1 \quad\text{and}\quad \sum n_i''/N_i'' = 1 \qquad\qquad (5.2)$$

where n_i' and n_i'' are numbers of cycles spent in the crack nucleation period and the crack propagation period, while N_i' and N_i'' are the corresponding crack nucleation life and crack propagation life. Obviously the problem is how to define and to determine the moment that the first period terminates and the second one starts. Langer's assumptions were also repeated, namely by Grover in 1960 (Ref.135) and by Manson et al in 1966 (Ref.136).

In the literature, the Palmgren-Miner rule is also referred to as the linear cumulative damage rule. Miner indeed assumed that the damage in a constant-amplitude test is a linear function of the number of cycles. However, Bland and Putnam (Ref.137) in the discussion on Miner's paper, indicated that the linearity was not required in order to obtain $\sum n/N = 1$. It was sufficient to assume that the damage rate was a function of n/N which is independent of the magnitude of the cyclic stress. Moreover, these authors emphasized that the material should be insensitive to load cycle sequences. A similar assumption was made by Nishihara and Yamada (Ref.138) by stating that the degree of fatigue damage D was a function of the cycle ratio n/N, independent of the stress amplitude (affine damage curves after Shanley, Ref.139):

$$D = f\,(n/N) \qquad\qquad (5.3)$$

In reference 140 the present author argued that $\sum n/N = 1$ requires that:
1 The fatigue damage is fully characterized by a single fatigue damage parameter D.
2 The damage D is indeed a single valued and monotonously increasing function of the cycle ratio n/N, which is the same in any constant-amplitude test (stress independent after Kaechele, Ref.141). Hence

failure will always occur at the same amount of damage.

A consequence of the first statement is that interaction effects will not exist. The second one implies
$\Sigma \, n/N = 1$ at failure.

5.3.3 Incremental damage theories

Theories based on constant-amplitude data, ignoring sequence effects

Several objections have been raised against the Palmgren-Miner rule, associated with interaction effects,
sequence effects, damage due to cycles below the fatigue limit, favourable effect of positive peak loads,
etc., which all lead to $\Sigma \, n/N \neq 1$. These effects have been illustrated in chapter 4. Moreover, from a
physical point of view it appears incorrect to state that a single damage parameter can uniquely indicate
the state of fatigue damage. This has been discussed in chapter 3.

The short-comings of the Palmgren-Miner rule have stimulated several new theories which still preserve
the idea of progressive damage accumulation and also the concept of summing damage increments cycle by
cycle. A survey of the theories is given in table 5.2.

It is not the purpose of this report to give a complete list and full details of all theories. Several
surveys have been given in the literature, see for instance references 47, 142, 143. A recent survey has
been given by O'Neill (Ref.144). It will be tried here to indicate essential features of the main groups
of theories. There are two important questions in this respect, see table 5.2. The first question is
whether the theory employs constant-amplitude fatigue data or variable-amplitude fatigue data. The
majority still employs the first type of data. A second question is whether fatigue damage accumulation
is sensitive to variations of th load sequence.

The first group of theories to be mentioned is characterized by some kind of adjusted S-N curves.
Freudenthal and Heller (Refs.145,146) started from the idea that damage increments in a random load test
will be affected by stress interaction effects. They finally arrive at formulas which they call a
"quasi-linear rule of cumulative damage". Their failure criterion can be written as

$$\Sigma \, \frac{n_i}{N_i/\omega_i} = 1 \tag{5.4}$$

where the "interaction factor" ω_i is either constant or a simple function of S_{ai}, to be determined from
fatigue tests. It may also depend on the type of load spectrum. Equation (5.4) indeed implies the
application of the Palmgren-Miner rule to adjusted S-N curves. Since these authors assume $\omega_i > 1$, the
curves are reduced life curves.

Marsh (Ref.147) suggests to adopt a hypothetical S-N curve with a different slope and a lower fatigue
limit (80 %) as compared to the original curve. He recognizes the problem of arriving at such an adjusted
curve in order to match the empirical data with $\Sigma \, n/N_a = 1$, where N_a is derived from the adjusted curve.

Haibach (Ref.148) also allows for load cycles below the fatigue limit by stating that the fatigue limit
is continuously decreasing as a result of increasing fatigue damage. For random and program loading his
analytical evaluation is equivalent to applying $\Sigma \, n/N = 1$ to a S-N curve, which is adjusted below the
fatigue limit only, see figure 5.1.

Henry (Ref.149) assumes that fatigue damage may be described as a notch in the material which will
proportionally lower the S-N curve over the entire stress range. A damage increment is an incremental
shift of the S-N curve.

Smith (Ref.45) suggested that $\Sigma \, n_i/N_i = 1$ could not be valid for a program test because residual stresses
introduced at the higher amplitudes affected the damage accumulation at the lower stress amplitudes. He
therefore proposed that N_i in the Palmgren-Miner rule should be replaced by the fatigue life of the
specimen preloaded to the maximum stress occurring in the program test. The preloading should induce the
same residual stress being present in the program test. This presumes that a relaxation of the residual

stress will not occur.

In later publications (Refs.150,151) Smith proposed two other theories. In the "linear strain theory" it is assumed that the strain at the root of the notch will be $K_t \cdot \varepsilon_{nominal}$, also after local plastic deformation. With the aid of a stress-strain curve the residual stress at the root of the notch may then be determined. The stress at the root of the notch is then $S = K_t \cdot S_{nominal} + S_{residual}$. Employing this stress-value, corresponding N-values are obtained from unnotched S-N curves for different R-values. These N-values are used for the Palmgren-Miner rule.

The second theory ("Smith method") starts from the idea that the maximum stress at the root of a notch in a program test will be of the order of the yield stress, provided local plastic deformation occurs. The residual stress is now determined indirectly from a constant-amplitude test on the component, tested at the maximum load cycle to be applied in the variable-amplitude test. The fatigue life obtained in this test and the assumption about S_{max} at the root of the notch in conjunction with the unnotched S-N data, will then indicate the applicable R-value and hence S_{min} at the root of the notch. This is sufficient for determining the complete stress history at the root of the notch for the variable-amplitude test. Knowledge of the K_t-value is not required. Again the Palmgren-Miner rule and the unnotched fatigue data are used for the life calculation.

In both proposals Smith has assumed that the material at the root of the notch behaves elastically after the residual stress has been introduced by plastic deformation induced by the maximum load cycle. Secondly, a relaxation of the residual stress should not occur. Since he adopts the Palmgren-Miner rule sequence effects are ignored.

Several authors were reasoning that damage accumulation is progressive crack growth. Shanley (Ref.139) assumes an exponential crack growth law for each constant-amplitude test:

$$\ell = \alpha \ e^{C \ S_a^\beta \ n}$$ (5.5)

where α, β and C are constants and n is the number of cycles. Failure should occur at a constant crack length ℓ_c independent of the cyclic stress

$$\ell_c = \alpha \ e^{C \ S_a^\beta \ N}$$ (5.5a)

Damage accumulation was assumed to be the summing of crack length increments without interaction effects. Equation (5.5) and (5.5a) can be written as

$$\ell / \ell_c = (\ell_c/\alpha)^{(\frac{n}{N} -1)}$$ (5.6)

which is of the type of equation (5.3). Consequently, Shanley's formulas imply the validity of the Palmgren-Miner rule. More comments on Shanley's formulas are given in reference 38.

Valluri (Ref.23) also adopted the idea that damage accumulation was a cumulative process of crack growth increments without interaction effects. However, he stated that the crack length at failure was depending on the highest stress amplitude applied, see section 3.3. Since the N-values in $\Sigma \ n/N = 1$ are in fact related to different amounts of cracking depending on the stress cycle, Valluri does not arrive at the Palmgren-Miner rule.

Corten and Dolan (Ref.152) included interaction effects in their crack propagation concept. They postulated that in a program test the maximum load cycle will be decisive for the initial damage, since it will determine the number of loci at which crack growth will start. After this number has been established crack growth is again assumed to be a cumulative process without any interaction. For a program test they arrive at the formula

$$N_g = \frac{N_1}{\sum a_1 \ (\frac{S_{a1}}{S_{a1}})^d}$$ (5.7)

where N_g is the program fatigue life, S_{a1} is the maximum stress amplitude with the corresponding constant-amplitude fatigue life N_1, α_i is the percentage of cycles applied at amplitude S_{ai} and d is a constant, that should follow from tests. Since $\alpha_i N_g = n_i$ equation (5.7) can be rewritten as:

$$ \sum \frac{n_i}{N_i} \left[\frac{N_i}{N_1} \left(\frac{S_{a1}}{S_{ai}} \right)^d \right] = 1 \qquad (5.8) $$

Note the similarity with equation (5.4). Further, if the S-N relation could be written as $N_i \, S_{ai}^{-d} =$ constant, equation (5.8) reduces to the Palmgren-Miner rule.

In the last 10 years high-level low-cycle fatigue got much attention. Many constant-strain amplitude tests were carried out involving large amounts of plastic strain. Ohji, Miller and Marin (Ref.153) have suggested that the Palmgren-Miner rule should apply to variable-strain-amplitude tests. In this case n_i is the number of cycles with strain amplitude ε_{ai}, while N_i is the constant-strain amplitude fatigue life associated with ε_{ai}. The same concept has recently been adopted by Dowling (Ref.129), but he first splits up the life in a nucleation period and a propagation period, similar to Langer's treatment, see section 5.3.2.

Incremental damage theories based on constant-amplitude data, including sequence effects
For several years sequence effects were almost exclusively attributed to residual stresses only, these stresses being caused by local plastic yielding at the root of a notch or the tip of a crack. Consequently a theory predicting sequence effects should include the evaluation of the residual stresses during a variable-amplitude test. Presently available theories are deriving residual stresses from the strain-history at the root of a notch. This work was started by Crews and Hardrath (Refs.52,53) as discussed in section 4.5.

A few theories for life calculations employing the above concept have now been published. The basic line of reasoning includes the following steps:
1 The starting data are: a The load-time history, b the material and c the geometry of the specimen.
2 The second step consists of calculating the strain history and the stress history for the fatigue critical location of the specimen. For a notched specimen this is the root of the notch. The strain history will include plastic strains and the stress history will include the local residual stress.
3 The strain history or the stress history calculated in the previous step is split up into individual cycles. Each cycle is assumed to cause a damage increment ΔD equal to $1/N$, where N is the corresponding constant-amplitude life. The failure criterion is again $\Sigma \Delta D = 1$.

The second step is a difficult issue. The strain history may be measured and the stress history may then be derived from the strain history by additional testing. This was discussed in section 4.5, see also figure 4.8. However, a life calculation theory requires that these data be obtained by means of calculation rather than experiment. Morrow and co-workers (Refs.51,154,155) at the University of Illinois are working on this topic. They adopt the Neuber equation, relating the stress and the strain at the root of the notch by:

$$ K_\sigma \cdot K_\varepsilon = K_t^2 \qquad (5.9) $$

where K_σ is the stress concentration factor including plasticity, K_ε is the strain concentration factor, also including plastic strain, and K_t is the well-known stress concentration factor for elastic behaviour. Equation (5.9) seems to be satisfactorily substantiated. Morrow et al. then adopt the cyclic stress-strain behaviour from unnotched material. For aluminium alloys this appears to be justified by the observation that the stress-strain hysteresis loop rapidly stabilises, also after a change of amplitude. The strain history and stress history can then be calculated. Morrow et al. also carried out test series to check the theory and the data reported look promising. The evaluation of this concept is still not yet complete and further work is going on.

Impellizzeri (Ref.156) has been reasoning along similar lines. However, since results as shown in figure 4.9, indicate a relaxation of residual stress, he introduces the relaxation into his calculation.

The rate of change of residual stress $d\,S_{res.}/dn$ in each cycle is assumed to be equal to:

$$\frac{d\,S_{res.}}{dn} = a\,S_{res.}\,\epsilon_R\,\frac{S_R}{S_{yield}}$$

where $S_{res.}$ is the residual stress, ϵ_R and S_R are the applied strain and stress range at the root of the notch, and "a" is an empirically determined constant of proportionality. With a computer program Impellieserri has treated program fatigue test data from NLR, NASA and his own data. He found a very good agreement. In a recent publication (Ref.157) Martin, Topper and Sinclair also introduced stress relaxation. Moreover, their stress-strain model also allows cyclic strain hardening or softening to be accounted for. Agreement with low-cycle variable-amplitude data was good.

With respect to the third step, both Morrow et al., Martin et al. and Impellizerri adopt $\Sigma\,n/N = 1$. Morrow and Martin prefer constant-strain amplitude data whereas Impellizzerri employs constant-stress amplitude data. In fact, the former are mainly working in the low-cycle fatigue range whereas Impellizzerri applies his calculations to high-cycle fatigue data.
One difficulty in calculating $\Sigma\,n/N$ may still be mentioned here. For a variable-amplitude loading, a load-time history in general will not consist of a sequence of complete load cycles. This also applies to the stress and strain history at the root of a notch if residual stresses are included. The definition of n in $\Sigma\,n/N$ then becomes a problem. This issue is discussed in section 6.2.

Incremental damage theories based on variable-amplitude data, ignoring sequence effects

In the Palmgren-Miner rule $\Sigma\,n/N = 1$, the values of N are derived from constant-amplitude fatigue data. However, it is also possible to adopt variable-amplitude fatigue data for this purpose. Gassner (Ref.158) proposed to use program fatigue test data while Kirkby and Edwards (Ref.99) suggested to adopt narrow-band random load fatigue data. The basic idea comprises the following steps:

<u>1</u> A load spectrum for a variable-amplitude test should be standardized.

<u>2</u> Variable-amplitude tests with this load spectrum should be carried out for different intensities of the load spectrum. The results can be plotted as $S'-N'$ curves, where S' is a stress value characterizing the intensity of the load spectrum and N' is the fatigue life in cycles obtained in the variable-amplitude tests.

<u>3</u> An arbitrary load spectrum can now be decomposed into the sum of a number of the standardized load spectra. If n_i' is the number of cycles of the spectrum characterized by S_i' the failure criterion is

$$\sum\,\frac{n_i'}{N_i'} = 1 \tag{5.10}$$

The procedure is illustrated by figure 5.2 for narrow-band random load fatigue data, although the principle is essentially the same for program fatigue test data (Ref.159). In a narrow-band random load test, the load spectrum of the stress peaks is in accordance with a Rayleigh distribution. This distribution is the standardized load spectrum mentioned in step 1 above. The characteristic stress value S' is most conveniently taken as the root-mean-square value S_{rms} of the variable stress. Kirkby and Edwards carried out tests on lug specimens and the results have been plotted in figure 5.2a (step 2). In subsequent tests, the S_{rms} was varied periodically, see figure 5.2b. This was done in such a way that the sum of the three spectra A, B and C was approximately similar to a gust spectrum (step 3). In other words, the gust spectrum can be decomposed into the three spectra A, B and C all obeying a Rayleigh distribution. For the tests in figure 5.2b, both $\Sigma\,n'/N'$ and the classical $\Sigma\,n/N$ values were calculated, see figure 5.2c. From these results the authors drew the following conclusions:

<u>a</u> Damage calculations according to the proposed method ($\Sigma\,n'/N'$) gave results superior to the classical Palmgren-Miner $\Sigma\,n/N$ values, i.e. the values were deviating less from 1.

<u>b</u> The $\Sigma\,n'/N'$ values still deviate considerably from 1.

As shown in figure 5.2b, the S_{rms} value was programmed in a Lo-Hi sequence. However, some tests carried out in a Hi-Lo sequence gave similar fatigue lives. It should be noted that the calculation of $\Sigma\,n'/N'$ still ignores the sequence.

Kirkby and Edwards also performed some tests from which the most severe step C was omitted. As mentioned in chapter 4, this reduced the life 2.5 times. Unfortunately also the Σ n'/N' value was considerably affected, see fig.5.2d. This implies that the new concept in this case does not well account for the change in load spectrum.

5.3.4 The similarity approach

<u>The similarity approach based on stress</u>
In section 5.3.1 the similarity approach was defined as the conception that similar loading conditions at the fatigue critical locations in two different specimens of the same material should produce similar fatigue results. This concept is easily illustrated by referring to the notch effect under constant-amplitude loading.
Compare a notched and an unnotched specimen. If the cyclic stress at the root of the notch is the same as in the unnotched specimen, the same fatigue life may be expected. This had led to the well known $K_f = K_t$ relation, where K_f is the fatigue strength reduction factor and K_t is the theoretical stress concentration factor assuming elastic behaviour. The shortcomings of this relation are also well recognized. Part of them are due to plasticity effects and another part may be attributed to differences between the volumes of highly stressed material (stress gradient effect). Actually, these arguments imply that the conditions at the fatigue critical locations were not really the same.
With respect to plasticity effects an improvement was the work of Crews and Hardrath, and Morrow et al. mentioned before. By accounting for the plastic deformation at the root of the notch, the cyclic stress at that location could be described more accurately. This cyclic stress was again compared with the same stress in an unnotched element.

For joints and other complicated components, K_t values are usually unknown. For such cases effective stress concentration factors, K_{eff} have been adopted in the literature. A survey was given by Schütz (Ref.115). The background is in fact a similarity approach. It is assumed that a component to which a certain K_{eff}-value applies, will show the same fatigue life as a simple notched specimen for which the K_t-value is equal to K_{eff}. This should be valid for any cyclic stress. The empirical determination of K_{eff} for a certain component should therefore be made by comparative testing of the component and of simple notched specimens with a sufficient range of K_t-values.
Obviously the conception again ignores the effects of size and plasticity. Moreover, the fact that different components may exhibit intersecting S-N curves, see figure 7.2, is not easily reconciled with this K_{eff} concept. It requires that for a component having a lower K_{eff} than another component, the S-N curve should be superior at all stress amplitudes.

The K_{eff} conception need not be restricted to constant-amplitude loading conditions. Gassner and Schütz (Ref.159) have proposed the application to the results of program fatigue tests. They performed numerous tests of this type on 2024-T3 specimens with a range of K_t-values. They suggest to use the data for estimating the program fatigue life of a component by assuming some K_{eff}-value for the component. The life is then obtained by interpolation between the specimen data for adjacent K_t-values.

<u>The similarity approach based on strain</u>
The similarity approach based on strain was adopted in the measurements described in section 4.5, see also figure 4.8. The assumption made was that similar strain history, i.e. at the root of a notch and in an unnotched specimen, should produce similar stress histories. Another assumption is that similar strain histories should also produce similar fatigue lives.
For practical application the similarity approach based on strain is not yet easily used. The strain history has to be either measured or calculated. Subsequently, life data for a similar history if not available, should be determined empirically.

The similarity approach for crack propagation

The application of the stress intensity factor K to the correlation of fatigue crack propagation data is a most outstanding example of the similarity approach.

The stress distribution around the tip of crack can be written in the following form (Ref.160)

$$S_{ij} = \frac{C\, S\sqrt{\ell}}{\sqrt{2\pi r}}\; f_{ij}(\theta) \qquad (5.11)$$
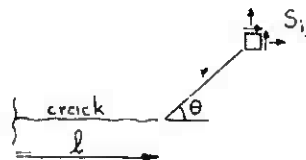
S is the nominal stress on the specimen, ℓ is the crack length and r and θ are polar co-ordinates. The geometry of the specimen is accounted for by the non-dimensional constant C. It should be pointed out that equation (5.11) is essentially a solution for linearized elasticity. Moreover it is asymptotically valid only for small values of r/ℓ, that means for the crack tip region. Further, different values of $f_{ij}(\theta)$ apply to the three crack opening modes. It is sufficient here to consider only the tension opening mode (tensile mode, $90°$ mode in fig.2.4).

Equation (5.11) can be written as

$$S_{ij} = \frac{K}{\sqrt{2\pi r}}\; f_{ij}(\theta) \qquad (5.12)$$

with the stress intensity factor $K = C\, S\sqrt{\ell}$ $\qquad (5.13)$

Equation (5.12) implies that the stress distribution at the crack tip is fully determined by K.

The similarity approach can now be defined. Compare two different specimens, with different geometry, crack length and loading stress, but the same stress intensity factor. Then the stress distribution at the crack tip according to equation (5.12) will be the same. For a cyclic stress, Paris et al. (Refs.161, 162) proposed that equal K-values should imply equal crack propagation rates, and consequently the crack rate should be a unique function of the stress intensity factor

$$\frac{d\ell}{dn} = f(K) \qquad (5.14)$$

A cyclic stress is determined by two of the quantities S_{max}, S_{min}, S_{a}, S_{m}. The ratios between these quantities are constant for fatigue tests with a constant stress ratio R ($= S_{min}/S_{max}$). Hence it should be expected (Ref.163) that f(K) in equation (5.14) is dependent on R:

$$\frac{d\ell}{dn} = f_{R}(K) \qquad (5.15)$$

There is now abundant evidence from constant-amplitude tests confirming the applicability of equation (5.15). The similarity approach here implies that crack growth in a certain type of specimen can be predicted from relation (5.15) determined empirically on another type of specimen. The latter may be a simple sheet specimen.

Available data mainly comes from macrocrack growth observations. It was stimulating to see, however, that the concept was still applicable to corner cracks in different 2024-T3 specimens with sizes as small as $\ell = 0.2$ mm, see figure 5.3. Nevertheless, there should be a lower limit to the validity of the K concept, which implies that it cannot be used in the crack nucleation period (Ref.163).

Limitations should also be expected from other arguments. The K-value is essentially an elastic conception, whereas fatigue crack propagation is due to cyclic plastic strain. If the plastic zone is small, as compared to the region where equation (5.12) is still approximately valid, the stress intensity factor may also be a characteristic value for the amount of plasticity in the small plastic zone. However, for large plastic zones the validity of equation (5.15) should get lost. Nevertheless, it is surprising to see that crack rates at fairly high values of stress and crack length could still be correlated by K, despite the fact that the transition from a $90°$-mode crack to a $45°$-mode crack had occurred already.

Another stimulus was offered by comparing results of two differently loaded specimens, see figure 5.4 (Ref.164). One specimen was stressed at the ends, whereas the other specimen was loaded at the opposite edges of the crack. For crack growth under constant-amplitude loading this implies that K will increase in the former specimen, whereas K will decrease in the latter one, see figure 5.4b. This is clearly confirmed by the two crack propagation curves shown in figure 5.4a. Nevertheless, the two types of specimen loading produced the same $d\ell/dn-K$ relation, as illustrated by figure 5.4c.

The crack rate in each cycle of a variable-amplitude test could be drawn from equation (5.15), that means from data obtained in constant-amplitude tests. However, this is only allowed if there are no interaction effects. Since there are such effects this procedure cannot be valid. Crack growth delays, as discussed in chapter 3, amply illustrate this point.

The similarity approach could still be applied to variable-amplitude tests by comparing crack rate data obtained in different variable-amplitude tests. Paris (Ref.162) suggested that K should be applicable to random load tests if S_{rmf} is substituted in equation (5.13). Limited evidence available (Refs.165-167) seems to confirm this viewpoint. A recent NLR test program is concerned with crack propagation under flight-simulation loading (Ref.64) with the design stress level as a variable. It was tried to correlate the data for different design stresses with the stress intensity factor. Unfortunately the attempt was unsuccessful. In fact the similarity approach is not satisfied by similar K-values alone in order to predict similar crack rates. A second requirement should be that the crack tip regions should have gone through similar K-histories. In general the two requirements are incompatible. For constant-amplitude tests, the second requirement apparently is not important. It may be more important for variable-amplitude tests due to interaction effects. Further investigations are required to solve this problem. It would indeed be of practical significance if the K-concept could be applied to random loading and flight-simulation loading.

5.3.5 Interpolation methods

Interpolation, extrapolation and generalization of empirical trends may be illustrated by some proposal made by Gassner and Schütz in reference 159. The type of information employed has already been discussed in section 4.14. Figure 5.5a is illustrating equation (4.1) once again. The relation can be written as:

$$\log N' + \kappa \log S_{a,max} = C \tag{5.16}$$

where N' is the program fatigue life, $S_{a,max}$ is the maximum stress amplitude of the standardized load spectrum applied in the test and C is a constant. This linear relation was confirmed by many tests. From a graph as given in figure 5.5a, the program fatigue life can be read for any value of $S_{a,max}$, either by interpolation or extrapolation. Usually the slope factor κ had a value in the order of 6.

In figure 5.5b the slope of figure 5.5a has been adopted to draw the line through a single available data point. Obviously, this is a generalization of an empirical trend.

The effect of the shape of the load spectrum has also been mentioned in section 4.14. Results from Gassner's group for four different shapes shown in figure 5.5c, (spectrum D is a constant-amplitude loading) produced a curve as plotted in figure 5.5d. Curves shown in figure 5.5a can now be adjusted to another load spectrum by generalizing the applicability of figure 5.5d (Ref.159). If figure 5.5a is valid for spectrum A, it can be adjusted to spectrum B by multiplying the N' values with a life reduction factor N'_B/N'_A drawn from figure 5.5d. This implies a horizontal shift of the curve over a distance $\log N'_B - \log N'_A$, while the slope remains the same. This is another case of generalizing an empirical trend.

Employing empirical trends is similar to applying past experience. It is better justified if more experience is available. It is fully justified only if the trend is obeying a recognized physical law. Unfortunately such laws are not yet established for fatigue. The quality of the results obtained will therefore depend on the amount of available information and the personal ability of interpreting and judging the validity of the data.

The comparison between the results of random load tests and program tests, as discussed in section 4.12, is an example where generalising trends is apparently unjustified. Trends indicated by one type of tests are not necessarily valid for the other type of testing. For flight-simulation tests the trends may again be different, at least quantitatively. In fact figure 4.29 is already illustrating this point.

Obviously, the safe way of handling available information is to interpolate between data rather than to extrapolate data by generalising empirical trends. For the purpose of making life estimates, interpolation will produce only relevant information if we start from realistic test data. It is now believed that the most realistic data should come from flight-simulation tests. As a consequence of this position, the present author in references 64 and 96 has proposed the following concept, which might be labelled as the "flight-simulation interpolation method". In order to avoid extrapolation extensive data obtained in flight-simulation tests should be compiled. The data should cover the main variables of this type of testing. Life estimates can then be made by interpolation. The following test program was proposed: Random flight-simulation tests for a certain structural material should be carried out, including the following variables:

a Specimens. Representative riveted and bolted joints should be used.

b Shape of load spectrum. Some typical shapes should be used, for instance representing gust spectra and manoeuvre spectra.

c Design stress level. Some values should be adopted in order to study the effect of the stress level in a similar way as Gassner has done for program tests.

d Ground-to-air cycle. The number and the magnitude may be varied.

Taking for example four cases for each item a-d this would imply $4^4 = 256$ test conditions if all possible combinations are made.

Evidently it is a large test program, but it would serve more than one purpose. Firstly, the data could indeed be used in the design stages for making life estimates by interpolation between the data. Secondly, the results would reveal the effects of several variables under flight-simulation conditions, which are not well known up to now. Thirdly, without actually having to design a standardized test one could use the data as a standard for comparison when checking the fatigue quality of a new component. A handbook with this type of data could be extended from time to time.

Of course the above flight-simulation interpolation method will not exclude all extrapolations, mainly because the geometry of an actual component will deviate from those of the specimens tested. However, some additional flight-simulation tests on the actual component may indicate the applicability of the available data. Moreover, this will add to the compilation of flight-simulation test data.

5.4 Evaluation of the theories

In the introduction of this chapter the question was asked whether one of the proposed theories could account in a realistic way for the trends described in chapter 4. Actually, if one of the theories could do so the present report would not have been prepared. Nevertheless, some theories can account for one or a few trends because these theories were based on those trends. The principal question now is: What do we expect from a theory, which requirements should it satisfy, which questions should it answer, accepting the fact that it will be unable to answer all questions.

There are two different approaches to this question, the physical one and the practical one. With respect to the first approach it is important that the theory has a physical base which appears to be sound rather than speculative. The theory as a physical model should be in agreement with the phenomenological observations on crack nucleation and crack growth. The agreement may be qualitative, but anyhow the model should make sense.

With respect to the practical approach the question is whether a theory can give reasonable answers to life prediction problems as they occur in aircraft design or in service.

The two approaches are specified in some more detail by a number of questions listed in the table 5.3. More questions could easily be formulated, but those in the table are pertinent ones for a discussion on the significance of the theories presented in the previous sections.

5.4.1 Physical significance of the theories

Most incremental damage theories in table 5.2 ignore the existence of crack nucleation and crack growth and for that reason these theories are to be labelled as non-physical. In fact most theories ignore all aspects a-d from table 5.3.

Fatigue damage in some theories (Shanley, Valluri and Corten and Dolan), is associated with a fatigue crack, while the accumulation of damage is then similar to crack growth. However, these theories do not explain such simple sequence effects as illustrated in figures 3.3, 4.4 and 4.14. The effect of single overloads may be qualitatively explained by Elber's argument, which is the plastic deformation left in the wake of the crack. Recently Von Euw showed this argument to be applicable (see section 3.2). However, a quantitative treatment of the delay has not yet been achieved. This would require the solution of extremely difficult problems related to cyclic stress-strain distributions around cracks.

A residual stress concept was introduced by Smith in a simplistic way. A more advanced approach is the prediction of stress strain histories at the root of a notch (Crews and Hardrath, Jo Dean Morrow et al., Impellizzerri). This is indeed a refinement of the description of the load history at the fatigue critical location which then appears to be sensitive to load sequences. The effect of high preloads on the fatigue life of notched elements are well predicted by this approach. However, for more complex sequences the translation of the stress-strain history into fatigue lives is just another problem.

According to the incremental damage theories, the damage increment per cycle ΔD equals $1/N$, if N is the constant-amplitude life associated with the magnitude of the individual strain cycles or stress cycles. The N-value is derived from adjusted S-N curves in some theories. From a physical point of view, $\Delta D = 1/N$ is at most "plausible" but in fact it is pure speculation. It also implies that interaction effects on the damage accumulation are accounted for only by adopting the real stress-strain history at the root of the notch, which includes residual stress. Other interaction effects and damage parameters as outlined in chapter 3 are ignored. Moreover, the nucleation and the growth of cracks do not form a part of these theories.

In conclusion it has to be admitted that available theories are physically speaking rather incomplete and hence fairly primitive. The complexity of fatigue damage accumulation as a physical phenomenon is much better recognized than in the early days. At the same time this offers tremendous problems for postulating a quantitative physical theory.

5.4.2 Practical significance of the theories

If a life prediction is made for a practical problem, the reliability of the result may be limited for several reasons. These reasons are only partly associated with the validity of the cumulative damage rule, adopted, as will be discussed in chapter 6. Here the discussion is restricted to the cumulative damage theory itself and the fatigue data required for its application.

The majority of the incremental damage theories are based on constant amplitude data, see table 5.2. Frequently, it is tacitly assumed that these data are available or can easily be estimated. Since practical questions are associated with components and joints, this is incorrect. Moreover, an empirical determination of S-N data of joints is usually costly and time consuming. Apparently, the S-N data are a weak link in the application of the incremental damage theories. More comments on this aspect are given in chapter 6.

Prediction of fatigue life until visible cracks (topic e table 5.3)

Most theories do not pay much attention to the definition of the end of the fatigue life. In general it should be understood to be the life until a visible crack is present, or the life until complete failure of a small component. It is not realistic to consider the life until complete failure of the entire aircraft structure, unless it is a safe-life structure. In a fail-safe structure the propagation of the visible crack should be treated separately.

Assuming that S-N data are available, the Palmgren-Miner rule is the most simple rule to be used. Many

investigations were carried out to check the validity of the rule and considerable deviations were found. Although the deviations do not show a clear pattern, it may be said that most values of $\Sigma n/N < 1$ were found for zero mean stress and for unnotched material (Ref.168). For positive mean stress and notched elements, quite a lot of $\Sigma n/N$ values are in the range 0.5 - 2.0 (Refs.168,169). It was concluded elsewhere (Ref.78) that the Palmgren-Miner rule in many practical applications will be good enough for a rough life estimation, provided realistic S-N data are available.

If unconservative estimates have to be feared, for instance in case of zero mean stress or many cycles below the fatigue limit, the application of the Palmgren-Miner rule to an adjusted S-N curve, such as proposed by Haibach (see figure 5.1), may be recommended. For the combination of flight loads with GTAC some conservatism could be added by simply starting from $\Sigma n/N = 0.5$.

A comparison between a number of incremental damage theories was made by several authors (Refs.47,142,170). In general the conclusion was that it is hard to prefer one of the rules to the Palmgren-Miner rule. Better predictions were sometimes found by the Corten-Dolan theory if the constant "d" in equation (5.7) could be adapted to the test results. Actually, a more accurate validity for practical loading conditions until now, cannot be claimed by any of the incremental damage theories based on constant-amplitude fatigue data.

It may be expected that theories based on stress-strain histories at the root of a notch have the potentiality to give more accurate life predictions. This is thought to be true because they may account for residual stress effects, which probably play an important part in fatigue damage accumulation. Even relaxation of residual stress could be incorporated. Results published by Impellizzerri look promising but a wider exploration is required before definite conclusions can be drawn. One improvement of the situation may be mentioned here. Present computers allow damage calculations to be made from cycle to cycle, even if the total life is a high number of cycles.

Another improvement, as compared to the Palmgren-Miner rule, appears to be obtained by the procedures proposed by Gassner and by Kirkby and Edwards ($\Sigma n'/N' = 1$). Also here a general validity will probably not apply. Similar to the application of the Palmgren-Miner rule, the availability of relevant fatigue curves (S'- N' data) may be a problem. Moreover, the advantage of these procedures may be weakened by the problem of how to account for deterministic loads such as the ground-to-air cycles. The most logical consequence then appears to be to start from data obtained in flight-simulation tests. This is the proposal discussed in section 5.3.5. The purpose is indeed to minimize extrapolation as far as possible. More comments are given in chapter 6.

Prediction of macro-crack propagation (topic e2, table 5.3)

The most logical approach appears to be an estimation by employing the stress-intensity factor. A crack growth curve may be calculated by integrating $\Delta \ell$ for each cycle, where $\Delta \ell$ is derived from $d\ell/dn = f_R (K)$ (Eq.5.15) as obtained in constant amplitude tests. Interaction effects are ignored by this procedure and since such effects are predominantly favourable to macro-crack growth, a conservative result will be obtained. Moreover, it will be necessary to calculate K-values for the structure as a function of crack length. The relevance of this procedure was recently proven (Refs.171,172) for cracks in stiffened panels. A good agreement between prediction and test results (constant-amplitude loading) was found. More comments on predicting crack growth are made in section 6.4.

Complicated sequence affects (topic f, table 5.3)

In section 4.13 it was indicated that a change of the load sequence in a flight-simulation test probably had a small effect on life only. This is a convenient trend because almost all incremental damage theories do not account for different sequences. The exceptions are theories based on stress strain histories which, however, are not yet sufficiently checked for practical load histories.

Effect of a change of the load spectrum (topic g, table 5.3)

If an aircraft is used for two different missions, two different load spectra will apply. It is a practical question to ask how the fatigue lives associated with these missions will compare. A similar problem

occurs if the service load spectrum turns out to be different from the load spectrum adopted in design calculations and full-scale fatigue tests.

If the lives for load spectre A and B are L_A and L_B respectively, the ratio L_B/L_A may be calculated by means of the Palmgren-Miner rule. It is sometimes suggested that the invalidity of the rule, which could lead to misleading values of both L_A and L_B, would have a smaller effect on the accuracy of the calculated ratio L_B/L_A. This suggestion is unjustified.

Although the rule may give rough life estimates it is in fact unable to give indications of the damage contributions of the various load amplitudes S_{ei}. Some may be larger than n_i/N_i, others may be smaller. If the modification of the load spectrum is in a range of S_e-values, where n_i/N_i gives a false indication of the damage contribution, the ratio L_B/L_A will also be a false indication.

The so-called "level of maximum damage", was defined in reference 173 (see also Ref.168) as the load amplitude of a load spectrum giving the largest contribution to $\Sigma\, n_i/N_i$. However, it is far from sure that it will indeed give the largest contribution. All the misleading suggestions tacitly assumed the absence of interaction effects, which do exist, however.

Some simple examples of misleading indications were discussed in chapter 4. If a gust spectrum is changed by having some more high-amplitude cycles the Palmgren-Miner rule predicts a slightly shorter life. In reality the life may be much longer. A second simple example is offered by modifying the spectrum in the low-amplitude range. According to the Palmgren-Miner rule this will have no effect at all, contrary to test results.

Unfortunately, the fact that the Palmgren-Miner rule is unreliable to account for modifications of the load spectrum, also applies to the other incremental damage theories. The only way out is testing, that means comparative flight-simulation tests with different load spectra. Once again we arrive at the proposal for systematic flight-simulation tests made in section 5.3.5. Curves similar to the curves in figure 5.5d, determined by Gassner and co-workers for program fatigue tests, would be required.

Effect of a few high-amplitude cycles (topic h, table 5.3)

According to most theories the effect of a few high-amplitude cycles will be negligible, whereas in reality it may be very large. Theories including a residual stress concept try to account for the effect of a few high-amplitude cycles. This applies to the Smith theory and the theories based on the strain-history at the fatigue critical location. As said before, a satisfactory solution has not yet been obtained but a further exploration is certainly worthwhile.

Effect of many low-amplitude cycles (topic j, table 5.3)

If low-amplitude cycles are below a fatigue limit, most incremental damage theories will predict these cycles to be non-damaging. The exceptions are the theories that include a reduced fatigue limit. Unfortunately these theories do not account for the effect of a few high-amplitude cycles.

In summary

With respect to making life estimates, a theory that is distinctly superior to the Palmgren-Miner rule, is not available. Secondly, a life estimate obtained with the Palmgren-Miner rule is a rough life estimate only. Its accuracy is not only dependent on deviations from the rule but also on the reliability of the S-N curves used. Thirdly, for the purpose of estimating the effect of modifications of the load spectrum the Palmgren-Miner rule is unreliable. The same applies to the other rules.

There is some prospect for the theories based on stress-strain histories at the fatigue critical locations, but a further evaluation and empirical checking is necessary.

Until now most theories had the character of incremental damage theories. The similarity approach, in principle, is a fully justified approach, but unfortunately there are still considerable limitations. The $\bar{K}_{eff}$-method being the most prominent exponent for life estimates is not satisfactory. For crack propagation, the stress-intensity factor is successful for constant-amplitude tests. There are indications that the stress-intensity factor will not work for service load-time history, but a further exploration is desirable.

The interpolation approach will probably give the most accurate life predictions, provided that it can be based on realistic flight-simulation tests data. Such data are still largely to be collected.

6. ESTIMATING FATIGUE PROPERTIES AS A DESIGN PROBLEM

6.1 Survey of aircraft fatigue problems

A large variety of empirical trends has been reported in chapter 4. Cumulative damage theories have been discussed in chapter 5 and it has to be admitted that the picture of theories, in view of explaining the empirical trends, is not a bright one. There is some qualitative understanding of the trends, but the possibilities for quantitative predictions is still rather limited as yet.

It should now be analysed how this affects the determination of fatigue properties of aircraft structures, both in the design stage and later on. It cannot be the purpose of this report to discuss all aspects of fatigue in aircraft structures. It is sufficient here to list the most prominent aspects and this has been done in table 6.1 drawn from reference 78. The list is not necessarily complete, but sufficient for the present analysis. It is important to note that there are three phases in the history of an aircraft, namely, the design phase, the construction of the first aircraft and the performance of test flights, and finally, the utilisation of the aircraft in service.

In the first phase the designer has to start with the actual design work, including general lay-out of the structure, joints, detail design specification of the materials, etc. He then has to estimate the fatigue performance of the structure, which broadly outlined involves the steps indicated in table 6.2.

The description of the fatigue environment is a complex problem, not only because it involves a good deal of guesswork but also in view of the large variety of aspects. This is illustrated by table 6.3. Several topics in the table will be briefly touched upon when discussing the merits of life calculations and fatigue tests.

The second step of table 6.2 includes the dynamic response of the structure to arrive at the fatigue loads in the structure. A modern trend in this area is the application of power spectral density (PSD) methods. The calculation of the fatigue loads in the structure is beyond the scope of this paper, but it has to be said that the aircraft response may be a significant source of uncertainties. It can be partly circumvented by direct load measurements in flight.

The last step in table 6.2 is concerned with the estimation of fatigue lives and crack propagation. In the present chapter comments will be made on the statistical description of service load-time histories (Sec.6.2), while the problem of estimating fatigue lives and crack propagation data is dealt with in the remainder of the chapter. Aspects of testing procedures, in order to get relevant information, are discussed in chapter 7.

6.2 The description of the service load-time history

In general service load-time histories are described by statistical means. There are two different approaches, namely:

1. Counting methods
2. The power spectral density method.

Before making comments on these methods some thought should be given to the definition of a load cycle.

Definition of a load cycle

In constant-amplitude tests the fatigue life N is given as a number of cycles until failure. In the Palmgren-Miner rule, $\Sigma \, n_i/N_i = 1$, the meaning of n_i also is a number of cycles applied at a certain cyclic load. Mathematically it may seem attractive to define the size of the load cycle by specifying its mean and amplitude, for instance S_m and S_a (Fig.6.1a). However, considering fatigue as a damaging phenomenon in the material, the moments of reversing the loading direction are the more important milestones of the load-time history. In other words, the load peaks, i.e. minima and maxima, are the characteristic occurrences of the cyclic load. Consequently from a physical point of view it would be better to define a cycle by its minimum and maximum, see figure 6.1b. In order to complete the definition of a load cycle it should be said that it consists of a rising and a falling part, that means it

consists of two half cycles. For the time being the loading rate will not be considered.

A few variable-amplitude load sequences are given in figure 6.1 c-f. Figure 6.1c shows the case where the amplitude is reduced, while maintaining the same minimum. The definition of load cycles 1-4 gives no problem.

If the amplitude is reduced while the mean remains the same, this can be done in two ways, see figures 6.1d and e. Clearly enough cycle 3 in figure 6.1d and cycle 2 in figure 6.1e cannot be defined by a single value for S_{max} and S_{min}. As shown by the empirical trends in figure 4.14, the difference between the two cases is not irrelevant for fatigue damage accumulation.

Another problem is illustrated by figure 6.1f. The small intermediate load fall BC implies an additional maximum and minimum. Hence one might say that there are two cycles in this figure, although the material from a damaging point of view will respond to it as a single cycle ADE. Considering the two gust load records in figure 6.2 it will be clear that a definition of load cycles in these practical cases is far from simple.

Counting methods

The aim of counting methods is to give a statistical distribution of characteristic magnitudes of the load-time histories. Whether useful data can be produced in this way will be discussed later. In the following a survey of some counting methods is given to illustrate the type of data obtained. Characteristic occurrences of a load-time history adopted for counting may be either peaks, level crossings or ranges. This has led to a variety of counting methods (Refs.174-176). Examles are illustrated by figure 6.3, while a more complete list is given by Van Dijk (Ref.176).

In methods a and b peaks are counted. In the second one only the most extreme peak between two mean-crossings is counted. The purpose of this is to ignore smaller load variations which are thought to be irrelevant to fatigue. The VGH records were evaluated with this peak-between-mean crossings count method. In method c leven crossings are counted. One might assume that the number of maxima above a certain level is equal to the number of crossings of that level (with positive slope). This, however, is incorrect although it is approximately valid under certain conditions.

Method d is a variant of method c involving a second condition to be met before a level-crossing count is made. A level-crossing in the upward direction is counted only if the load has gone downwards to a lower level. This eliminates level crossings from smaller load variations. The well-known Fatiguemeter is operating according to this method.

In the simple range count method (Fig.6.3e), positive and negative ranges between successive peak values are counted. The basic idea is that ranges are more important for fatigue than the absolute peak values. The range count method has one serious disadvantage. The counting result is extremely sensitive to the smallest load variations still to be considered. In figure 6.1f, the range AD will not be counted, but instead of one large range three smaller ranges AB,BC and CD have to be counted.

With the range-pair exceedance count method, range exceedances are counted in pairs of equal magnitude and opposite sign. The disadvantage of the range count method is thus eliminated.

Recently, De Jonge (Ref.177) proposed the NLR counting method (referred to as the range-pair-range count method by Van Dijk (Ref.176). This method is a further development and extension of the range-pair-exceedance counting method. It also gives information on the mean of the range counted. This implies that peak load levels can also be derived from the counting result. Moreover, counts for a relatively small time interval can be processed separately. As a consequence, the "memory" for pairing positive and negative ranges has now been set to certain limits. Hence the method is thought to give more relevant information from a fatigue damaging point of view as compared to previous methods. It should be noted that the rain-flow counting method (Ref.129) can produce similar information as the NLR counting method.

The power spectral density concept

The application of power spectral analysis to randomly varying loads, especially to gust loads, is being explored to an ever-increasing extent. The mathematical frame work for application to random loads cannot be discussed here. It may be found, for instance, in references 32-34,178. It is assumed that the external load, for instance turbulent air, may be considered to be a stationary Gaussian process during a certain period. Such a process is fully described by its power spectral density function $\phi_e(\omega)$, where ω is an angular frequency. If the response of the structure to the external load is linear, the power spectral density function of the internal load $\phi_i(\omega)$ can be calculated from $\phi_e(\omega)$ and the transfer function of

ths structure. This is an elegant way to account for the dynamic behaviour of the structure.
It is possible to calculate from $\phi_i(\omega)$ the statistical distribution functions for level crossings and
peak loads. The weakness is that all crossings and all peaks are obtained, also if they are caused by
very small load fluctuations. Results obtained by counting methods based on ranges, cannot be calculated.
Nevertheless, $\phi(\omega)$ is fully characteristic for a random sequence and any information that cannot be
calculated mathematically can be determined by measurements from a signal with the same spectral density
function. The effect of $\phi(\omega)$ on the irregularity of the random load was already illustrated by
figure 4.20. It may be emphasised here that the power spectral density method requires the external load
to be a Gaussian phenomenon.

The usefulness of the counting methods

The question about the usefulness has to be related to the purpose of the data being collected. Three main
objectives may be mentioned here.
1. Collecting data for load spectra to be used for future aircraft design.
2. Establishing data for the application to a full-scale fatigue test.
3. Collecting data for estimating the consumed life of individual aircraft.
The first topic is of interest to the designer, the second one to the test engineer, while the third one
is important for the aircraft operator.
Starting with the last objective there is a fairly extensive literature on collecting in-flight data for
this purpose. A discussion would be beyond the scope of this report. Reference may be made here to a
recent publication by De Jonge (Ref.177). He made a proposal for a fatigue load monitoring system. Two
essential features are: (1) Load statistics should be derived from strain records instead of acceleration
measurements. (2) The strain record should be analysed by the NLR counting method. The first recommenda-
tion was made because the relation between accelerations and loads in the structure is not unequivocal
in many cases. The second recommendation is made because it is thought that the NLR counting method gives
more appropriate indications about the fatigue load environment.
The second objective mentioned above is discussed in chapter 7. Some comments will be given there. The
first objective is important for estimating fatigue lives which is the subject of the present chapter.

Various counting methods were compared for the application to gust load records (Ref.174) and manoeuvre
load records (Ref.176). It turned out indeed that the range method was fully inadequate in view of its
sensitivity to small load fluctuations as mentioned before. Also the simple level-crossing count method
and the simple peak count method are believed to count toomany irrelevant occurrences.
The restricted-level-crossing count method (Fatiguemeter) and the peak-between-mean crossings count method
(VGH records) give more relevant information. Moreover, the two methods show reletively small differences
between their counting results. The range-pair exceedance count method appears attractive but the disad-
vantage is that no information is obtained about peak values of the load-time history. This disadvantage
is eliminated in the NLR counting method. Unfortunately, almost no data obtained with this method are
available as yet.

The question whether a counting method gives useful information for calculating fatigue lives does not
yet allow a definite answer. If statistical data obtained with some counting method could give a realist-
ic estimation of the actual load-time history, we are still left with another problem. This is how to
calculate the fatigue life from this load-time history. In the previous chapter it had to be admitted
that this problem is not yet solved. As a consequence, a comparison between service life and calculated
life can neither prove nor disprove the quality of the counting method since the uncertainties about the
life calculation method are involved also. At best we may ask whether statistical counting results allow
a relevant estimation of the service load-time history. The estimation is considered to be relevant if
tests with the real load-time history and the estimated one would produce similar fatigue lives. Keeping
in mind this criterion some more comments will be made later.

Sequence of loads

It should be pointed out that all counting methods do not give any information about the sequence of the
loads counted. (Some information about possible sequences will be retained by the NLR counting method).

The results of statistically counted loads are usually presented as arceedance curves, such as shown in figure 6.4 for gusts and for manoeuvres. For gusts it is assumed that the load spectra for positive and negative gusts are symmetric which allows a presentation by a single curve. For manoeuvre loads the same procedure cannot be adopted since positive manoeuvre load increments are usually much more severe than negative increments. A presentation by two curves is necessary, see figure 6.4b.

Since curves as shown in figure 6.4 do not contain information about the sequence of the loads, the usual procedure for estimating fatigue lives is to combine upward peak loads and downward peak loads, that have the same frequency of occurrence, in order to form complete load cycles. This is illustrated for a single cycle in both figures 6.4a and b. Actually, load records such as shown in figure 6.2 do not justify this procedure. However, it is generally thought to be conservative since it has the character of maximizing load cycle amplitudes. The counting results produced by Van Dijk (Ref.176) suggested that it most probably will be conservative for manoeuvre loadings.

Ground-to-air cycles

Contrary to gusts and manoeuvre loads, the ground-to-air cycle has a more or less deterministic character. Several loads occur once per flight such as the transition from the static load on the ground to the static load in flight, fuselage pressurisation, flap loads and empennage loads during take-off and landing, etc. The flight-load profile thus consists of a mixture of these deterministic loads and other loads that are mainly statistical in nature with respect to occurrence and magnitude.

Flight-load profiles

The assessment of flight-load profiles for a certain type of aircraft requires an analysis of the various missions to be performed by the aircraft. Both deterministic and stochastic loads can then be estimated. As a result of combining these loads, synthetical flight-load profiles will be obtained. Two simplified examples applying to wing bending, are shown in figure 6.5. A number of comments on this figure should be made:

1. Those portions of the flight during which the load is not varying have been omitted.
2. Gusts manoeuvres and tariing loads were assumed to occur as complete cycles. As said before this is probably a conservative procedure.
3. The sequence of gusts, manoeuvres and tariing loads was assumed to be random without any sequence correlation. For gust loads the PSD-method might allow a more realistic determination of the sequence.
4. Flight-load profiles may be different from flight to flight. For gusts this has to be expected since flights both in good weather and in poor weather will occur.
5. The two examples in figure 6.5 show that there may be one important additional cycle per flight. Basically it is the static ground-air-ground transition, but it is enlarged by additional loads both at the ground and in flight. The minimum and the maximum of this additional cycle are indicated in figure 6.5. The magnitude of this cycle may vary from flight to flight. In view of the discussion in the previous chapters this cycle may well be expected to give a significant damage contribution. Duxbaum (Ref.179) measured the maximum load cycle of each flight of a transport aircraft and he made a statistical evaluation of its magnitude.

In summary: The assessment of flight-load profiles implies the prediction of the sequence of various fatigue loads from flight to flight, i.e. the service load-time history. It is flying the aircraft by imagination at a moment that it still has to go into service. This is necessary for planning a realistic full-scale test, see chapter 7. However, it is also necessary in view of defining the cycles associated with the ground-air-ground transition. Such cycles are certainly important enough to be considered in making life estimates.

6.3 Methods for estimating fatigue lives

The fatigue life in this section should be understood to be the life until a visible crack is present, or the life until complete failure of a small component. If life estimates as accurate as possible are required, realistic flight-simulation tests are essential. This will be discussed in chapter 7. However, if provisional estimates have to be made several procedures can be adopted. The basic elements involved in such estimates have been listed in table 6.4. The first topic of the table is the estimated service load-

time history. This aspect was discussed in the previous section. The second element is the structure or component for which a life estimate is requested. It will be assumed that the dimensions and the material have been chosen already. Insufficient fatigue life could of course modify these data.

The third element of table 6.4 includes a variety of possibilities concerning available fatigue data. A survey is given in table 6.5. As an example of similar materials one may adopt fatigue data from 2024-T3 material for applications where 2024-T8 or 7075-T6 material was selected. Obviously, this may affect the quality of the life estimate to be based on the data.

The type of specimen for which data are available may vary from the unnotched specimen to the component itself. This implies that it may vary from a highly unrealistic representation to the most realistic representation of the component for which the life estimate has to be made. Also for the type of loading the qualification of available data may vary from a low similarity (constant-amplitude loading) to a high similarity (experience in service).

The fourth topic in table 6.4 is the fatigue life calculation theory. This subject has been analysed in chapter 5. It was made clear that there were no reasons to be optimistic with respect to the accuracy of available theories.

For completeness, additional fatigue tests have been mentioned as the last aspect in table .4. It will be clear that the quality of a life estimate can be improved by additional tests.

Several procedures for making life estimates can now be specified. A survey is given in table 6.6 which will be discussed below. For all cases it is assumed that estimated service load statistics were collected already.

Methods based on available data

As illustrated by table 6.6, the calculated life will depend on the type of available data, on corrections made to these data by accounting for deviating aspects and on the life calculation theory. Apparently there may be several weak links.

The most simple type of fatigue data would be S-N curves for unnotched specimens. The S-N curves for the component under consideration have to be derived from these data and this will introduce unknown inaccuracies. The reliability of the required S-N data would be improved by starting from S-N data for notched specimens, while data for components could be a still better starting point. Methods for obtaining optimal S-N data, improved by accounting for material, S_m , K_t, size, etc., are beyond the scope of this report (see for instance Refs.180,181). It may be said here that the relevance and the quality of S-N data to be obtained are a matter of judgement and ability to evaluate available information.

As said in chapter 5, a better cumulative damage rule than the Palmgren-Miner rule does not appear to be available yet. Starting from fatigue data obtained under a more complex fatigue loading, such as program loading, random loading or flight-simulation loading, has as its aim to reduce or eliminate uncertainties about the life calculation theory (methods 1c,1d,1e in table 6.6). This approach is still hampered by insufficiently available fatigue data. Other aspects have been discussed in chapter 5.

Methods based on service experience from previous designs

A new design may have a high similarity with a previous design. It even may be a further development of the previous one. In this situation it will be clear that most valuable information should come from the service record of the older design (see for instance Ref.182). This information can be utilized in a rather general way by adopting the stress level, that for a certain material allowed a satisfactory service behaviour in the past (method 2a in table 6.6). If cracks did not occur in the previous design, the life drawn from its service experience is a lower limit. The life should be longer. Obviously it is necessary to prove that the new design is at least as good as the previous one. The proof could be given analytically, for instance by considering K_t-values for improved detail design. For joints the stress severity factor proposed by Jarfall (Refs.183,184) may turn out to be a useful criterion for judging the fatigue quality (Ref.185). The alternative to the analytical comparison is comparative testing, see section 7.4.

A further evaluation of past experience, method 2b in table 6.6, includes a consideration of all relevant conditions instead of considering the stress level only. This implies that service experience is now considered to be a fatigue test on specific components. The conditions for the old design have

now to be translated to the new design by accounting for deviating aspects. This offers similar problems as correcting S-N data, and in addition one new problem, which is accounting for a different load spectra. As said before, the Palmgren-Miner rule is unreliable for the latter purpose. Comparative testing, see section 7.4, is the best solution. If this is not feasible conservative assumptions may be made. The attractive feature of employing past experience is that we start from data obtained under most realistic conditions. Secondly, the information may come from a large number of aircraft, which increases the statistical confidence. Limitations already mentioned are associated with deviations between the new and the old design. Another limitation is that the load-time history for the old design, in many cases, will not be accurately known, which requires estimates to be made.

Testing of a new component or a complete structure

This method (method 3 in table 6.6) will be advisable in many cases. Nevertheless it appears to be fully justified only if a realistic load-time history will be applied in the test. That means that a flight-simulation test should be carried out. This topic is discussed further in chapter 7.

Comparison of the methods

Speaking in general terms there are three alternatives apart from new methods still under development:
1. Estimates based on S-N data employing the Palmgren-Miner rule.
2. Estimates based on the evaluation of the experiences obtained with previous designs.
3. Estimates based on flight-simulation tests.

The first method will give rough life indications only. It would not be fair to say that the Palmgren-Miner rule is the only weak link in this method. The estimated S-N curves may also be a source of inaccuracies. Obviously additional constant-amplitude component testing could improve the situation. The second method has a good appeal for reasons mentioned above. There are also limitations. However, if a careful analysis is incorporated into this method it should be preferred to the first method. Comparative flight-simulation tests may significantly add to the value of the second method. The third method, still to be discussed in chapter 7, is to be recommended only if a carefully planned flight-simulation test will be carried out. The method is certainly preferable to the first method. In comparison to the second method, testing the component or structure itself implies a more realistic simulation in this respect. This may also apply to the load-time history adopted in the test. The second method, however, may be more realistic with respect to the environment (corrosive effects, rate effects), while the statistical confidence may also be superior. It is difficult to say which of the two methods will give the best answers. An evaluation of past experience should be recommended in any case. However, a realistic flight-simulation test on a component need not be a relatively costly effort if a modern fatigue machine is available. Hence in many cases such tests are recommendable as well. A full-scale fatigue test with a realistic flight-simulation should anyhow be recommended, since such a test serves more purposes than obtaining life indications only (see chapter 7).

6.4 Methods for estimating crack propagation rates

Problems of estimating crack propagation rates are to a large extent similar to those involved in estimating lives. Some specific features will be discussed.

Information about the propagation of macro-cracks is desirable in view of judging the safety of an aircraft. For assessing the quality of a fail-safe design this information is even indispensable. It may be tried to give a similar survey as given in table 6 for estimating fatigue lives. This has been done in table 6.7.

The amount of available data from constant-amplitude tests is steadily increasing and as discussed in section 5.3.4, such data allow a presentation as

$$d\ell/dn = f_R(K) \tag{6.1}$$

It should be pointed out that almost all data in the literature were obtained by testing sheet material under axial loading. However, in thick sections with predominantly plane-strain conditions the crack

rate may be higher. The crack rate in a pressurized fuselage will also be higher in view of bulging of the crack due to the pressure on the edges of the crack.

The most simple case would be to predict the crack propagation rate in an axially loaded sheet metal structure for which K-values can be calculated. Tests on stiffened panels have shown that equation (6.1) is indeed capable of correlating the crack propagation rates obtained under constant-amplitude loading (Refs.171,172). For a service load-time history the crack rate could be estimated by the formula:

$$\frac{d\ell}{dn}(\ell = \ell_j) = \frac{\sum\limits_i n_i \frac{d\ell_j}{dn}(K_{ji})}{\sum\limits_i n_i} \tag{6.2}$$

where the subscript i is referring to the various stress levels involved.

Equation (6.2) gives a weighted average crack rate, but the same formula is obtained if the Palmgren-Miner rule is applied to the fatigue lives required for an incremental crack length extension. This implies that equation (6.2) is ignoring any interaction effect between successive stress cycles with different magnitudes. Since interaction effects are predominantly favourable for macro-crack growth, equation (6.2) will produce a conservative result and it even may be very conservative depending on the type of load spectrum (see for instance Ref.186).

More realistic estimates will be obtained if data from flight-simulation tests can be adopted. Such tests were recently carried out at NLR (see table 4.7), but so far this appears to be the only source.

Additional testing is to be recommended because crack propagation may be sensitive to the type of alloy. Different crack rates may even be found for the same alloy produced by different manufacturers while also batch to batch variations have been noted (Ref.163). The recommendation for additional testing is easily made since simple and inexpensive specimens can be used for this purpose.

Service experience from previous designs with respect to crack propagation will in general not be available. It is common practice to repair a crack in service immediately after it was found. However, data from full-scale tests on previous designs may give useful indications about crack rates to be expected in a new design. Testing the new design itself obviously should give the most direct information. This is discussed in chapter 7.

6.5 The significance of life estimates

The significance of a life estimate and the accuracy required or desirable will depend on the consequences that the estimated life values may have. This part of the problem has several aspects. Some aspects are briefly mentioned below in order to further complete the picture of the practical problem.

The consequences of the life estimate will obviously depend on the result obtained. The estimated life may be highly insufficient, it may be of the correct order of magnitude, and it also may be much larger than required. Obviously these three cases will ask for different actions to be taken. It will be clear that the follow-up of the estimate should also depend on the quality and reliability of the estimate. Moreover, scatter of fatigue properties has to be considered.

Decisions to be made will also depend on design aspects. If the design is an entirely new type for which no experience is available, a realistic life estimate seems desirable. Another aspect is the question whether the structure has a fail-safe or a safe-life character. In the latter case accurate life estimates are again requested. For coming to decisions it may also be important whether a redesign is easily possible. Test facilities available are another aspect of the problem in view of complementary testing.

The question whether the result of a life estimate should be considered as being satisfactory, in many cases, will not allow an easy answer due to the many aspects involved. The problem will not he discussed any further here. It may be said, however, that the philosophy of the aircraft firm with respect to designing for safety and economics, airworthiness requirements and requests of the aircraft operator may also affect the answer.

7. FATIGUE TESTING PROCEDURES

7.1 Survey of testing procedures and testing purposes

With respect to testing purposes, the main aspects characterizing a fatigue test are the type of specimen and the type of fatigue load applied. From a testing point of view the fatigue testing machine is important. In this connection the question is whether available fatigue equipment is capable of handling the specimen and of applying the fatigue load sequences required. Some general comments on the above aspects will be made in this section, while the usefulness of various testing methods for specific testing purposes will he discussed in subsequent sections.

Test purposes

Being confronted with the vast amount of literature on fatigue investigations, it is useful to recognize some categories of purposes. In general terms three groups may be mentioned.
1. Basic fatigue studies.
2. Empirical investigations to explore the effect of various factors on fatigue life.
3. Test series to provide specific data for design purposes.
The purpose of the first group is to increase our physical understanding about fatigue, to describe the fatigue phenomenon qualitatively, and if possible also quantitatively. Investigations to improve our knowledge about fatigue damage accumulation are in this group.
The second group comprises the investigations on the effects of notches, metallurgical conditions, surface treatment, fretting corrosion, production aspects, etc. Experience obtained in such investigations provides useful qualitative information for the designer with respect to the selection of materials, dimensions, production techniques, etc.
The main purpose of test series in the third group is to provide test data for estimating fatigue properties of structures and its components. This type of data was referred to in tables 6.6 and 6.7. Some more specific testing purposes of the third category are indicated in figure 7.1.
Since basic fatigue studies are important here with respect to damage accumulation, some comments on testing procedures for this purpose will he made in section 7.2. The second category is largely outside the scope of the present report. Planning fatigue tests for the third category requires knowledge about trends in damage accumulation under variable-amplitude loading. Tests will be discussed in sections 7.3 - 7.7.

Type of specimen

A survey of different types of specimens is given in table 7.1. Specimens with simple notches may reveal the notch sensitivity of a material. Since most cracks in a structure are starting in joints, a simple notched specimen is not yet a relevant representation of a fatigue critical location in a structure. In a joint fretting corrosion is generally significant. This can be simulated in simple joint specimens. The advantage of a component over a simple joint specimen is that all dimensions and the production technique are fully realistic. Testing a full-scale structure is obviously still more realistic. This may eliminate questions about the correct loads for the various components of the structure. Moreover, unknown eccentricities of the loads on the various components are automatically simulated.

Load sequences in fatigue tests

A survey of possible load sequences has previously been given in figures 4.2 and 4.3, while examples of variants are given in several other figures. With respect to design purposes the discussion will be restricted to constant-amplitude tests, program tests, random tests and flight-simulation tests, see figure 7.1. For basic studies on damage accumulation simple variable-amplitude load sequences may be attractive.

Fatigue testing machines

For a long time fatigue machines were primarily designed for carrying out constant-amplitude tests. If the machine was designed as a resonance system, high loads and high loading frequencies could relatively easily be obtained. Such machines were not well suited for variable-amplitude tests but a slow variation of the amplitude was possible. Hence program tests could be carried out. A major difficulty was to apply small numbers of high-amplitude cycles. This had to be done either manually or by non-resonant slow-drive loading mechanisms.

In some laboratories resonance fatigue machines have been successfully adapted for carrying our narrow-band random load fatigue tests (Refs.99,187).

A break-through in this situation was the development of the electro-hydraulic fatigue machine with closed-loop load control. (Refs.33,188). Each load-time sequence that could be generated as an electrical signal could be applied. By now several fatigue machines of this type are commercially available. In many full-scale tests hydraulic jacks operating according to the same principles have been employed. It is true, however, that a test in such a machine will be more expensive then a constant-amplitude test in an old machine. The problem may then be whether the more relevant information from a complex load sequence is worth the price.

7.2 Tests for basic fatigue studies

In chapter 3 fatigue has been described as a cumulative process. Although cracking was the most prominent feature of fatigue damage, the accumulation of damage turned out to be a complex phenomenon. Under variable-amplitude loading a number of different interaction mechanisms could be operating. Although there is some qualitative understanding it is not free from speculation. In fact there is still ample room for studying the damage accumulation phenomenon. Partly this should occur by refining our knowledge about local stress-strain history. For another part microscopical observations on damage accumulation should be very worthwhile.

Load sequences for basic fatigue studies should be simple sequences in order to bring out the observations to be made as explicitly as possible. Two-step tests, interval tests and tests with periodic high loads may be most appropriate. With a more complex sequence the risk of mixing up a variety of favourable and unfavourable interaction effects is present. It may be impossible then to distinguish the various effects. It will be clear that for detailed observations the electron microscope and fractography are indispensable tools. It should also be said here that basic studies will not immediately solve the life estimating problems of the designer. However, a basic understanding is a prerequisite for arriving ultimately at qualitative improvements of the present situation.

7.3 Determination of fatigue data for making life estimates

As illustrated by fig.7.1, different types of tests could be adopted for the determination of basic data for life estimates. The merits and limitations of constant-amplitude tests, program tests and random tests have been discussed in section 6.3. Further is was indicated that data from flight-simulation tests could provide the most relevant information for this purpose, see also section 5.3.5.

From the discussion in chapter 4 it follows that the test results of program tests, random tests and flight-simulation tests will depend on some variables associated with the loads applied. The main variables are listed in table 7.1. The need for standardising is apparent and in fact Gassner has made proposals for as program test. Standardizing is justified only if we know the effect of the variables

to be standardized on the test result. In this respect the program test, the random test and the flight-simulation test are all sensitive to the maximum load amplitude allowed in the test. With respect to the sequences, the effect is probably small for random loading and flight-simulation loading, whereas it may be significant for the program test. This aspect and the uncertain ratio between the results of program tests and random load tests have led to a preference for random loading instead of program loading (see also section 4.12).

For a narrow-band random load test, the distribution function of the load peaks is a Rayleigh distribution, while for broad-band random load the same distribution is approximately valid except for the lower amplitudes.

A flight-simulation test can be carried out only on a fatigue machine with closed loop load control. This implies that any load spectrum can still be adopted. Standardizing a flight-simulation test at this stage appears to be somewhat premature, since the influence of several variables has still to be explored in greater detail. For this purpose the test program in section 5.3.5 was proposed. Nevertheless, some recommendations can be made already now, for instance with respect to sequence and truncation. This is discussed later in this chapter.

Finally, some unbalanced approaches with respect to determining fatigue data for life estimates may be mentioned here. It is not realistic to carry out flight-simulation tests on unnotched specimen. This is combining an advanced testing method with a primitive and unrepresentative specimen. Similarly, it is an unbalanced approach to apply a constant-amplitude test on a full-scale structure, which is the most simplified test on the most realistic simulation of the structure.

7.4 Comparative fatigue tests

Many people still feel that constant-amplitude tests are a good means for comparing alternative designs, production techniques, etc. However, the possibility of intersecting or of non-parallel S-N curves is making this very dubious. In figure 7.2 comparative tests at stress level S_{a1} would indicate design A to be superior to design B. At stress level S_{a3} the reverse would apply, whereas at S_{a2} both designs would be approximately equivalent. Some comments on this issue were made in section 5.3.4 when discussing the K_{eff} concept. Fretting corrosion is one aspect where constant-amplitude tests may give a misleading of its effect in service.

The numerous test series with program loading carried out by Gassner and his co-workers suggest that the risk of a misjudgement would be smaller if program loading were adopted for comparative testing. This will apply also to random loading. Nevertheless, if flight-simulation loading can be adopted it appears that it is the most preferable solution. Real problems should be tackled with realistic testing methods if possible. Recently, Ronay (Ref.189) adopted random flight-simulation loading for exploring the fatigue behaviour of a high-strength steel. Imig and Illg (Ref.80) adopted this test method for studying the effect of temperature on the endurance of notched titanium alloy specimens. Schütz and Lowak (Ref.190) studied the effect of plastic hole expansion on the fatigue life of an open hole 2024 alloy specimen by employing flight-simulation loading. At the NLR, as part of an ad-hoc problem, we compared two alternative types of joints with random flight-simulation loading. Some aircraft firms have already started comparative testing for design purposes employing a kind of flight-simulation loading.

As an illustration of different answers to the same question, a recent investigation (Ref.64) indicated that the crack propagation in 7075-T6 was four times faster than in 2024-T3 according to constant-amplitude loading. However, under flight-simulation loading the ratios were only 1 to 2 (see Fig.4.29).

7.5 Direct determination of fatigue life and crack propagation data by flight-simulation testing

In the previous chapter it was concluded that life estimates based on available data may have a low accuracy. If a better accuracy is required, a realistic test is necessary. This implies that both the specimen and the load sequence should be representative for service conditions. For the specimen this means that the test should be carried out on the actual component or a complete part of the structure.

With respect to the fatigue load, a flight-simulation test representative for service loading is required. An exact simulation of the load-time history in service would be the preferable solution. Usually a service record will not be available, but in case that it can be measured before the fatigue test it is the best starting point as advocated by Branger (Ref.35). For reasons of time and economy, periods during which the load does not vary could be left out.

In general, a load-time history will have to be designed on the basis of mission analysis and load statistics obtained with other aircraft. It is thought that it is possible to compose a representative load-time history (see the discussion in section 6.2). A good knowledge of the empirical trends is essential for this purpose. As an illustration, figure 7.3 shows a sample of a load record from the test on the F-28 wing. Different types of weather conditions were simulated in accordance with statistical information. The sequence of the gust loads in each flight was a random sequence without any sequence correlation. This may be a deviation from the random sequence in service, but fortunately the deviation will probably have a minor effect as discussed in section 4.13.

A major problem is the assessment of the highest load level to be applied in the flight-simulation test. As discussed before, this level may have a predominant effect on the life and the crack propagation. If the load level that will be reached (or exceeded) once in the target life of the aircraft is applied in a test, we know that it may have a favourable effect on the fatigue life. It then should be realized that this load level is subject to statistical variations, that means some aircraft will meet this load more than once in the target life, whereas other aircraft will never be subjected to it. In view of this aspect and the flattering effect of high loads, it was proposed elsewhere (Refs.58,76) that the load spectrum should be truncated at the load level exceeded ten times in the target life (see Fig.7.4 for illustration).

In reference 76 a similar recommendation was made for crack growth studies, but then, instead of the aircraft life, one has to consider the inspection period. The predominant influence of high loads on crack growth was illustrated by the results presented in sections 3.2 and 4.6. If a full-scale structure with cracks is tested to study the crack rate, high loads will considerably delay the crack growth. The application of high loads may again considerably flatter the test result. Therefore a truncation is necessary to avoid unsafe predictions for those aircraft of the fleet that will not meet the high loads.

Sometimes fail-safe loads are applied at regular intervals during a full-scale fatigue test to demonstrate that the aircraft is still capable of carrying the fail-safe load. If this load exceeds the highest load of the fatigue test, the result may be that a number of cracks that escaped detection so far, will never be found because of crack growth delay. In other words, this procedure could eliminate the possibility of obtaining the information for which the fatigue test is actually carried out. The crack growth delay in a full-scale structure was recently confirmed (Refs.63,64) in additional tests on the F-23 wing. The certification test was completed after simulating 150 000 flights. Then fail-safe loads (limit load) were applied. In a subsequent research program it turned out that several cracks did not grow any further as shown in figure 7.5. New artificial cracks, however, showed a normal growth.

The significance of low-amplitude cycles has been discussed in section 4.13. Leaving out these cycles from a flight-simulation test will considerably reduce the testing time. For the F-28 wing, omitting the gust cycles with the lowest amplitude reduced the testing time per flight from 116 seconds to 46 seconds. However, since such cycles may contribute to crack nucleation (fretting) and crack growth, the cycles were not omitted during the certification tests.

Taxiing load cycles can be omitted under certain conditions. In fact it appears admissable only if the cycles occur in compression for the components being tested (see section 4.13). Care should be taken that the ground-to-air cycle reaches the most extreme minimum load occurring on the ground, including dynamic loads (see Fig.6.5).

The development of hydraulic loading systems with closed-loop load control has considerably affected the present state of the art. By now it seems inadmissable to simplify the loading program in a flight-simulation test for experimental reasons to a sequence of the type shown in figure 4.31.

The result of a flight-simulation test will be a fatigue life in numbers of flights or a crack propagation rate in millimeters per flight. There are limitations to the meaning of these data, which are discussed in the section 7.7.

7.6 Full-scale fatigue tests

A full-scale test on a new aircraft design is an expensive test. Hence there should be good reasons to carry out such a test (Refs.191-194). In most general terms the test is carried out to avoid fatigue trouble in service. Reference may be made to table 7.2 giving a survey of several types of fatigue problems and possible consequences. In view of these consequences and the costs of the test there is every reason to require that the test gives realistic and relevant information. As said before, a full-scale fatigue test should be carried out with a carefully planned realistic representation of the service load-time history.

Comments on the application of high-amplitude and low-amplitude cycles were made in the previous section (see also Ref.76). It may be emphasized once again that the application of a high pre-load for static testing purposes (strain measurements for instance) or high fail-safe loads during the test, should be prohibited. Such loads may have a large flattering effect on fatigue lives and crack rates, and quantitative indications from the test may become worthless. Some more information from test series in full-scale structures bearing on this aspect were recapitulated in section 4.15.

Several aspects can be mentioned that make full-scale testing of a new aircraft structure desirable. It is thought that the most important ones are listed below (Ref.76).
(1) Indication of fatigue critical elements and design deficiencies.
(2) Determination of fatigue lives until visible cracking occurs.
(3) Study of crack propagation, inspection and repair methods.
(4) Measurements on residual strength.
(5) Economic aspects.
Items 4 and 5 are beyond the scope of the present discussion.

With respect to the first purpose mentioned above, Harpur and Troughton (Ref.191) observed that in several cases fatigue cracks occurring in service were not found in the full-scale test, because the structure tested was not sufficiently representative. This was not only due to manufacturing differences and modifications, but also to simplifying the test article. Due consideration should therefore be given to the structural completeness of the specimen.
Fatigue critical elements will only be indicated in the correct order if the fatigue lives obtained in the full-scale tests are correct indications of the service life. The test should not indicate component A to be more critical than component B if service experience indicate the reverse order. This risk can be avoided only by a realistic and representative test. In section 4.15, several examples of misleading information obtained in full-scale tests due to unrealistic fatigue loadings have been mentioned.
It will be clear that a representative fatigue loading also implies, that due consideration has to be given to simulate all types of fatigue loads that may be significant for certain parts of the structure.

The full-scale test is also a training experiment with respect to inspection techniques. This problem will not be discussed in this report. If a structure is a good design, inspecting for cracks during a full-scale test is a tough job because cracks will hardly occur.
In order to obtain information about crack propagation rates it is common practice to apply artificial cracks to the structure for initiating fatigue crack growth. Usually this is done by making saw-cuts. The information about crack growth is needed in order to establish safe inspection periods. As suggested in the previous section, the truncation level of the load spectrum should be lowered after application of the artificial cracks. This was in fact done during the certification tests on the F-28 wing.

The limitations of the information obtained in a full-scale test are discussed in the following section.

7.7 Limitations of flight-simulation tests

Assuming that the load-time history to be applied in a flight-simulation test was carefully planned, there are still some limitations to the information obtained in the test. Aspects to be briefly mentioned here are associated with loading rate, corrosive influences, scatter and deviating load spectra in service.

Loading rate

A full-scale test on a structure is an accelerated flight simulation that may last for 6 to 12 months, while representing 10 or more years of service experience. A flight-simulation test on a component in a modern fatigue testing machine may take no more than a week.

Considering loading rate effects, one should not simply compare testing time with flying time, but rather the times that the structure is exposed to the high loads. Orders of magnitude are given in figure 7.6. This argument is speculating on the fact that any effect of the loading rate is a matter of some time-dependent dislocation mechanisms occurring at high stresses. It might imply that the effect is relatively small for a full-scale test but it could have some effect in a component test in a fatigue machine running at a relatively high load frequency (see also the discussion in section 4.17).

Corrosive influences

Differences between testing time and service life also imply different times of exposure to corrosive attack. Therefore, if corrosion is important for crack nucleation (corrosion fatigue) one certainly should consider this aspect. In practice cracks frequently originate from bolt holes and rivet holes where the accessibility of the environment is usually poor and the corrosion influence probably not very significant. However, as soon as macro-cracks are present the environment will penetrate into the crack and the effect on crack growth should be considered. Safety factor should be applied to inspection periods depending on the material and the environment (see also the discussion in section 4.17).

Scatter

Testing a symmetric structure generally implies that at least two similar parts are being tested. However, fatigue properties may vary from aircraft to aircraft because the quality of production techniques and materials will not remain exactly constant from year to year. It will not be tried here to speculate on the magnitude of the scatter, although some interesting data are available in the literature. It is recognized, however, that the shortest fatigue lives in a large fleet of aircraft, in general, will be shorter than the result of the full-scale test as a consequence of scatter.

Deviating load spectrum

Load measurements in service may indicate that the service load history is significantly deviating from the load history applied in the test. Suggestions were heard in the past that the test result could be corrected for such deviations by calculation, employing the Palmgren-Miner rule and some S-N curves. However, as explained in section 5.4.2 this rule is highly inaccurate for this purpose.

If the structure has good fail-safe properties, the question of deviating load spectra in service is probably less important. This is certainly true if the impression is that the service load spectrum is less severe than the test spectrum. However, if one feels that the service loading could be more severe than the test loading, it appears that additional testing is indispensable for a safe-life component.

Comparison between test and service experience

After having summarized several limitations of a full-scale flight-simulation test, the proof actually is the comparison between service experience and test results. A few papers on this issue have been presented in the literature (Refs.120,191,196,197) and some comments will be made.

As far as data are available, the service life is usually shorter than the test life, although there are some cases where the agreement is reasonable. However, if the service life is from 2 to 4 times shorter than the test life, further clarification is obviously needed.

There are a number of reasons why discrepancies between test results and service experience may occur. Several of them have been listed above, for instance scatter and environmental effects. Secondly, a fair comparison requires that the test is a realistic simulation of the service load history and this is a

severe restriction on the comparisons that could be made in the past. Thirdly, if a test reveals a serious fatigue failure it is likely that the aircraft firm will modify the structure, thus eliminating the possibility of a comparison.

In summary: The accuracy of the quantitative results from a full-scale test is limited by the above aspects. It is difficult to quantify these aspects. Depending on the possible consequences associated with the fatigue indications obtained in the test, scatter factors or safety factors may be applied. The selection of these factors is again a matter of philosophy, as briefly commented on in section 6.5.

8. SURVEY OF PRESENT STUDY AND RECOMMENDATIONS

8.1 Survey of the present study

Several features of the fatigue phenomenon have been recapitulated in chapter 2. The fatigue process was described as a sequence of crack nucleation, micro-crack growth, macro-crack growth and final failure. Subsequently, it was tried in chapter 3 to describe fatigue damage and damage accumulation. In most general terms fatigue damage is a change of the material as caused by cyclic loading. Fatigue cracking, i.e. decohesion, is the most prominent feature of fatigue damage. However, the amount of cracking alone is insufficient to describe the damage. A definition of the fatigue damaged material should include a description of all aspects of the fatigue crack geometry and the condition of the material around the fatigue crack, including cyclic strain-hardening and residual stress distributions. A survey is given in fig.3.2. Damage accumulation in a certain load cycle therefore implies incremental changes of all these aspects. The incremental changes will depend on the intensity of the load cycle, but at the same time they will be a function of the damage already present. This has led to the definition of inter-action effects, which in general terms means: the damage increment due to a certain load cycle will depend on the damage caused by the preceding load cycles. This also implies that the damage caused by a certain load cycle will affect the damage increments of subsequent load cycles. Interaction effects may be either favourable or unfavourable, which means that they may either decelerate or accelerate the damage accumulation. As a consequence, it is important for the damage accumulation in which sequence load cycles of various magnitudes will be applied. Such sequence effects have been observed in many test series.

Various examples of interaction effects and sequence effects are presented in chapter 4, which gives a survey of empirical trends observed in tests with a variable fatigue load. This includes the effects of high preloads, periodically applied high load cycles, ground-to-air cycles and the effects of several variables of program loading, random loading and flight-simulation loading. The investigations are summarized in tables 4.1 - 4.8, while various illustrative test results are shown in figures 4.1 - 4.30. The empirical trends can sometimes be explained qualitatively, fatigue cracking and residual stresses being the main arguments. Nevertheless, the trends clearly confirm that fatigue damage accumulation is a complex phenomenon which will not easily allow a satisfactorily quantitative treatment.

Some thought was given to the comparison between fatigue under program loading and random loading. In a random load test the load amplitude is varied from cycle to cycle. The load amplitude in a classic program test, however, is varied infrequently and in a systematic way, i.e. in a programmed sequence. Consequently sequence effects on the damage accumulation may be different, which implies that a strict correlation between the fatigue lives in the two types of tests may not be expected. Empirical evidence has substantiated this view. In fact, a realistic simulation of fatigue damage accumulation as it occurs in service, requires a test that preserves the essential features of the service load-time history. With the present knowledge it can be concluded that a flight-simulation test may satisfy this requirement, whereas a more simple test will not do so.

A survey of theories for life calculations has been given in chapter 5. An important question is whether the theories are capable of predicting the empirical trends as summarized in chapter 4. The theories were grouped in three categories, which are (1) the incremental damage theories, (2) theories based on a

similarity approach and (3) interpolation procedures. Most theories are in the first group, see table 5.2. However, they poorly satisfy the picture about fatigue damage accumulation and it is not surprising that the prediction of empirical trends is also poor. Also the similarity approach, although being less dependent on knowledge about fatigue damage, does not yield accurate life prediction. The quality of predictions with the interpolation methods is apparently dependent on the quality of the data from which the interpolation is made. In view of the knowledge of interaction effects and sequence effects, interpolations should preferably be based on results of flight-simulation tests. Since such data are hardly available, a proposal is made for a systematic test program that could fill this gap.

In chapter 6 the consequences of the present state of the art for estimating fatigue lives and crack propagation rates in the aircraft design phase are analysed. First a survey is given of the various aspects of designing an aircraft from the point of view of fatigue. This indicates that the fatigue theory is not the only weak link in predicting fatigue properties. One aspect briefly discussed is the definition of load cycles if the load is varying in some random way as occurs in service. Attention is then paid to estimation methods based on available fatigue data and, as an alternative method employing service experience from previously designed aircraft. The advantages and limitations of both approaches are emphasized. Reliable and accurate information of fatigue properties in many cases can be obtained only by carrying out relevant tests.

Several testing methods are discussed in chapter 7. Different testing purposes are listed first, which are: (1) basic fatigue damage studies, (2) test series exploring the effects of various factors on fatigue life and (3) estimation problems with respect to fatigue life and crack propagation as a design effort. Some comments are made on the first topic, but major emphasis is on the last one. Four types of tests are considered, which are constant-amplitude loading, program loading, random loading and flight-simulation loading. Specific goals are: (1) compiling basic data for life estimates, (2) comparative design studies and (3) determination of direct estimates of life and crack propagation. The conclusion is that the flight-simulation tests should be preferred to the other types of tests. It is emphasized that comparative tests on different designs may give unreliable information if constant-amplitude tests are used. Actually, if realistic answers are required realistic testing procedures have to be adopted. This appears to be a trivial conclusion. Nevertheless, it is well substantiated by present day knowledge of fatigue damage accumulation and by empirical evidence from a vast amount of variable-amplitude test series.

For a full-scale fatigue test, a realistic flight-simulation loading is a necessity. If a simplified fatigue loading is adopted, the test may give incorrect indications of fatigue critical components and misleading information about fatigue lives and crack propagation rates. Relevant evidence from test series on full-scale structures was summarized in chapter 4 (section 4.15). It is also emphasized that the application of fail-safe loads during a full-scale test may fully obliterate the relevance of the test results. By introducing residual stresses, such a high load may considerably increase the fatigue life and it may completely stop the growth of fatigue cracks. Comments are also made on the significance of truncating the load spectrum, omitting low-amplitude cycles and other aspects of flight-simulation testing.

In 1965, Herbert Hardrath (Ref.198) presented a review on cumulative fatigue damage. He then came to the conclusion that new break-throughs of our knowledge should not be expected in the near future. In fact this has been true for the past six years. Hardrath's review is still relevant to day but some aspects have become more clear since then. These aspects are listed below in view of making recommendations for future research.

1 Electro-hydraulic cylinders and fatigue machines with closed-loop load control are now being used in many laboratories. Actually this is some sort of a break-through with respect to the possibilities of performing fatigue tests with any required load-time history. Advantages already exploited are related to an increasing knowledge about fatigue damage accumulation and to more realistic testing methods for practical problems.

2 Our phenomenological knowledge about fatigue damage accumulations is steadily increasing. The phenomenon appears to be more complex than thought before, but this trend is not uncommon in science.

3 Sequence effects and interaction effects are better recognized than before.

4 Progress has been made with respect to predicting the strain and stress history at the root of a notch. Calculations to be made from cycle to cycle are no longer objectionable in view of computer capabilities.

8.2 Recommendations for future work

Basic research and empirical research are still required both. Basic research cannot be neglected because the evaluation of trends, as observed in empirical studies, requires a physical understanding of the phenomenon occurring in the material. Empirical investigations on the other hand are necessary because we simply cannot wait until our physical understanding is good enough to answer a number of practical questions. Apparently we are learning slowly and extensive efforts have to be made to improve our knowledge. Therefore, it has to be emphasized that all laboratories should be fully aware of the various aspects of the practical problem. We should avoid to look for solutions of problems that do not exist by outlining what the real problems are. It is hoped that the present report will prove to be helpful in this respect. Some more specific recommendations will now be made.

Basic research

1. Microscopic studies

The phenomenological picture of fatigue damage accumulations is still highly qualitative in nature. Microscopic studies providing quantitative data about the various aspects of the damaging process should therefore be welcome. Studies with both the optical and the electron microscope can be useful. There is still ample room for fractographic observations of crack growth under variable-amplitude loading. At the same time thin-foil studies of fatigue damaged material appear to be worthwhile. It then should be kept in mind that fatigue is a highly localized occurrence, that means that the local state of the material may differ from that of the bulk material.

2. Stress-strain histories at the notch

In this report reference was made to investigations on the prediction of stress-strain histories at the root of a notch under variable-amplitude loading. Such studies included speculative assumptions about incremental damage accumulation. Nevertheless the stress-strain histories at a notch root may be considered in its own right. As such it is a more detailed description of the fatigue environment for the material at the critical location. Without this information it is difficult to see how a rational cumulative fatigue damage theory for notched elements could be formulated. Already for this reason alone this type of investigations should be recommended.

3. Crack closure

Crack closure as described by Elber, has recently entered our picture of fatigue crack growth. More quantitative information about this phenomenon under various conditions should be welcomed.

4. Plastic stress-strain distributions

Theoretical calculations of stress-strain distributions around notches and cracks, including plasticity, is a difficult problem. It is even more difficult for cyclic loading since the cyclic stress-strain behaviour of the material can usually not be described in a simple way. It should be recommended to exploit the potential usefulness of finite element methods to this problem.

5. Environmental effects

Laboratory results to be extrapolated to service conditions are still afflicted by the possibility of unknown environmental effects. Investigations to improve our physical knowledge about the mechanisms of environmental effects are to be recommended.

Empirical investigations

6. Flight-simulation testing

For many practical problems, flight-simulation testing was recommended in this report. Our knowledge of the effects of several variables pertaining to flight-simulation testing, is still insufficient. For that reason investigations on notched elements exploring these effects should be advised. Such investigations may be somewhat similar to test series carried out by NLR on fatigue crack propagation (section 4.13).

7. Compilation of flight-simulation test data

In this report the compilation of flight-simulation test data was advocated. A test program for this purpose was described in section 5.3.5. A handbook with this type of data may be useful for estimating fatigue properties. Moreover, it could be a reference for comparative testing in order to judge the fatigue quality of a new design.

8. Service experience

In chapter 6 it was emphasized that experience on fatigue in service gives most useful information. Such data are obtained under highly realistic conditions with respect to load-time histories and environment. The statistical reliability may be high if many aircraft are involved. In would be extremely useful if such data could be collected and analysed, and be made generally available.

9. Statistical analysis of service load-time histories

The prediction of fatigue properties in the design phase, the performance of realistic flight-simulation tests, and the monitoring of fatigue life in service all require information about service load-time histories. Investigations on the question how relevant information can be obtained should be recommended. Problems involved are partly associated with measurement techniques, while another aspect is the statistical analysis in relation to fatigue damage accumulation.

10. Fatigue machines

A flight-simulation test requires a fatigue machine with closed-loop load control. Electro-hydraulic machines of this type are now available. It would certainly stimulate more realistic testing procedures if these machines could be produced at a lower price. Secondly, the generation of electrical signals for controlling the load in such a machine is also a topic where a development of new and cheaper apparatus is desirable.

A final recommendation is related to the dissemination of information. Several times it was noticed that good solutions were not reached because of insufficient knowledge about the real problems, although the information was available elsewhere. Equally regretful is the situation where prejudice prevents improved solutions. In this respect, flight-simulation testing is sometimes labelled as a "sophisticated" type of testing. Actually a flight-simulation test is a rather trivial solution because it is aiming at a simulation of service loading. A constant-amplitude test on the other hand, being a convenient type of test from an experimental point of view, is in fact a highly artificial simulation of service loading. We should be careful that progress is not hampered by historical traditions starting at the time of August Wöhler. The problem is partly a matter of education and dissemination of information. It is hoped that the present report may be helpful also in this respect by outlining the various aspects of the aircraft fatigue problem and by the analysis of and cross references to the literature.

9 REFERENCES

1. Barrois, W.G.   Manual on fatigue of structures. Fundamental and physical aspects. AGARD-MAN.8-70, 1970.

2. Forsyth, P.J.E.   The physical basis of metal fatigue. Blackie and Son, London 1969.

3. Grosskreutz, J.C.   Fatigue mechanisms in the sub-creep range. Am.Soc.Teeting Mats, STP (to be published).

4. Jacoby, G.H.   Application of microfractography to the study of crack propagation under fatigue stresses. AGARD Report 541, 1966.

5. Plumbridge, W.J.   The metallography of fatigue. Metallurgical Reviews, Vol.14, Review 136, 1969,
   Ryder, D.A.   pp 119-142.

6. Schijve   Analysis of the fatigue phenomenon in aluminium alloys. NLR TR M.2122, Amsterdam 1964.

7. Schijve, J.   Fatigue crack propagation in unnotched and notched aluminium alloy specimens.
   Jacobs, F.A.   NLR TR M.2128, Amsterdam 1964.

8. Broek, D.   Systematic electron fractography of fatigue in aluminium alloys. NLR TR 68002,
   Van der Vet, W.J.   Amsterdam, 1968.

9. Pelloux, R.M.N.   Mechanisms of formation of ductile striations. ASM Trans.Quarterly, Vol.62, p.281, 1969.

10. Bowles, C.Q.   On the formation of fatigue striations. To be published in Int.J.of Fract.Mech.
    Broek, D.   Also NLR MP 69014, Amsterdam 1969.

11. Wood, W.A.   Systematic microstructural changes peculiar to fatigue deformation. Acta Met.,
    Cousland, S.   Vol.11, 1963, p.643.
    Sargant, K.R.

12. Grosskreutz, J.C.   Critical mechanisms in the development of fatigue cracks in 2024-T4 aluminum,
    Shaw, G.G.   Fracture 1969, Ed.P.L.Pratt, p.620, Chapman and Hall, London 1969.

13. Bowles, C.Q.   The role of inclusions in fatigue crack initiation in an aluminum alloy.
    Schijve, J.   NLR MP 70019, Amsterdam 1970.

14. Grosskreutz, J.C.   Microstructures at the tips of growing fatigue cracks in aluminum alloys.
    Shaw, G.G.   Fatigue crack propagation, Am.Soc.Test.Mats, STP 415, p.226, 1967.

15. Hartman, A.   On the effect of oxygen and water vapor on the propagation of fatigue cracks in 2024-T3 Alclad sheet. Int.J.of Fract.Mech., Vol.1, 1965, p.167.

16. Bradshaw, F.J.   The influence of gaseous environment and fatigue frequency on the growth of
    Wheeler, C.   fatigue cracks in some aluminum alloys. Int.J.of Fract.Mech., Vol.5, 1969, p.255.

17. Illg, W.   The rate of fatigue crack propagation for two aluminum alloys under completely
    McEvily, A.J.   reversed loading. NASA TN D-52, 1959.

18. Elber, W.   Fatigue crack closure under cyclic tension. Fracture Mechanics, Vol.2, 1970, p.37.

19. Elber, W.   The significance of fatigue crack closure. Paper 1970 Annual Meeting ASTM, Toronto, June 1970.

20. Schijve, J.   Some tests on Elber's crack closure. NLR report, Amsterdam, to be issued shortly.
    Groep, F.F.

21. Von Euw, E.F.J.   Effect of overload cycles on subsequent fatigue crack propagation in 2024-T3 aluminum alloy. Doctor Thesis, Lehigh University, March 1971.

22. Schijve, J.   Fatigue damage interaction due to incompatibility between crack front orientation and stress amplitude. NLR report, Amsterdam, to be issued shortly.

23. Valluri, S.R.   A unified engineering theory of high stress level fatigue. Aerospace Eng., Vol.20, 1961, p.18.

24. Broek, D.   The residual strength of high alloy sheets containing fatigue cracks. Aerospace Proceedings 1966, p.811. McMillan 1967.

25. McMillan, J.C.   Fatigue crack propagation under random and program loads. Fatigue Crack Propaga-
    Pelloux, R.M.N.   tion. Am.Soc.Test.Mats, STP 415, 1967, p.505.

26. McMillan, J.C.   The application of electron fractography to fatigue studies. Electron Fracto-
    Hertzberg, R.W.   graphy, Am.Soc.Test.Mats, STP 436, 1968, p.89.

27. Schijve, J.   Fatigue crack propagation in light alloy sheet material and structures. Advances in Aeronautical Sciences, Vol.3, Pergamon Press, 1961, p.387. Also NLR MP 195, Amsterdam 1960.

28. Hudson, C.M.   Effects of changing stress amplitude on the rate of fatigue crack propagation in
    Hardrath, H.F.   two aluminum alloys. NASA TN D-960, 1961.

29. Gassner, E.   Festigkeitsversuche mit wiederholter Beanspruchung im Flugzeugbau. Luftwissen, Vol.6, p.61, 1939. Translation: NACA TM 1087.

30. Hardrath, H.F.   Variable-amplitude fatigue tests of aluminum alloy specimens. Am.Soc.Test.Mats,
    Naumann, E.C.   STP 274, 1960, p.125.

31. Naumann, E.C.   Axial-load fatigue tests of 2024-T3 and 7075-T6 aluminum alloy sheet specimens
    Hardrath, H.F.   under constant- and variable-amplitude loads. NASA TN D-212, 1959.
    Guthrie, E.C.

32. Bendat, J.S.   Principles and applications of random noise theory, John Wiley and Sons, New York, N.Y. 1958.

33. Swanson, S.R.   Random load fatigue testing: A state of the art survey. Materials Research and Standards, Vol.8, No.4, p.11, April 1968.

34. Kowalewski, J.   Beschreibung regelloser Vorgänge. Fortschritt Berichte, VDI-Z, Reihe 5, Nr.7, 1969.

35. Branger, J.   Second seminar on fatigue design. Columbia Un., Institute for the study of Fatigue and Reliability, TR No.5, 1964.

36. Macro, S.M.   A concept of fatigue damage. Trans.ASME, Vol.76, 1954, p.627.
    Starkey, W.L.

37. Schijve, J.   Fatigue tests on notched and unnotched Clad 24 S-T sheet specimens to verify the
    Jacobs, F.A.   cumulative damage hypothesis. NLR Report M.1982, Amsterdam 1955.

38. Schijve, J.   Research on cumulative damage in fatigue of riveted aluminum alloy joints.
    Jacobs, F.A.   Nat.Aeronautical Research Inst., Amsterdam, Report M.1999, January 1956.

39. Schijve, J.   Program fatigue tests on notched light alloy specimens of 2024 and 7075 material.
    Jacobs, F.A.   Nat. Aeronautical Research Inst., Amsterdam, Technical Report M.2070, 1960.

40. Forrest, G.   Some experiments on the effects of residual stresses on the fatigue of aluminium alloys. J.Inst.Metals, Vol.72, 1946, pp 1-17.

41. Heyer, K.   Mehrstufenversuche an Konstruktionselementen. Lilienthal-Gesellschaft für Luftfahrtforschung, Bericht 152, 1943.

42. Heywood, R.B.   The effect of high loads on fatigue. Colloquium on Fatigue. Ed. by W. Weibull and F.K.G. Odquist. Springer Verlag 1956, p.92.

43. Heywood, R.B.   The influence of preloading on the fatigue life of aircraft components and structures. RAE Report Structures 182, June 1955.

44. Payne, A.O.   Determination of the fatigue resistance of aircraft wings by full-scale testing. Fatigue Testing of Aircraft Structures, ICAF Symp., Amsterdam 1959, ed. by F.J.Plantema and J.Schijve. Pergamon 1961, p.76.

45. Smith, C.R.   Fatigue-service life prediction based on tests at constant stress levels. Proc. SESA, Vol.16, No.1, 1958, p.9.

46. Boissonat, J.   Experimental research on the effects of a static preloading on the fatigue life of a structural components. Fatigue of Aircraft Structures, ICAF Symp., Paris 1961, ed. by W.Barrois and E.L.Ripley, Pergamon, 1963, p.97.

47. Mordfin, L.   Programmed maneuver-spectrum fatigue tests of aircraft beam specimens. Symp.
    Halsey, N.   Fatigue Tests of Aircraft Structures, Am.Soc.Test.Mats, STP 338, 1963, p.251.

48. Rosenfeld, M.S.   Aircraft structural fatigue research in the Navy. Symp. Fatigue Tests of Aircraft Structures, Am.Soc.Test.Mats, STP 338, 1963, p.216.

49. Imig, L.A.   Effect of initial loads and of moderately elevated temperature on the room-temperature fatigue life of Ti-8Al-1Mo-1V titanium alloy sheet. NASA TN D-4061, 1967.

50. Kirkby, W.T.   Variable-amplitude loading approach to material evaluation and component testing
    Edwards, P.R.   and its application to the design procedure. Proc.ICAF Symp., Stockholm 1969, ed. G.Wallgren and S.Eggwertz, FFA. Also RAE TR 69182.

51. Morrow, J.D.   Laboratory simulation of structural fatigue behavior. Symp.Effects of Environment
    Wetzel, R.M.   and Complex Load History on Fatigue Life. Am.Soc.Test.Mats, 1970, STP 462,
    Topper, T.H.   pp 74-91.

52. Crews, J.H.   A study of cyclic plastic stresses at a notch root. J.Soc.Ex.Stress Analysis,
    Hardrath, H.F.   Vol.6, 1966, p-313.

53. Crews, J.H.   Elastoplastic stress-strain behavior at notch roots in sheet specimens under constant-amplitude loading. NASA TN D-5253, 1969.

54. Schütz, D.   Die Betrachtung der elastischen-plastischen Beanspruchung in Kerbgrund als Ausweg aus einer phänomenologisch betriebenen Schwingfestigkeitsforschung. LBF-Colloquium May 1968, LBF Bericht TB-80, Darmstadt 1968.

55. Heibach, E.   Zur Frage des Festigkeitsverhaltens regellos im Zug-Schwell-Bereich beanspruchter
    Schütz, D.   gekerbter Leichtmetallstäbe bei periodisch eingestreuten Druckbelastungen.
    Svenson, O.   LBF Bericht FB-78, Darmstadt 1969.

56. Edwards, P.R.   An experimental study of the stress histories at stress concentrations in aluminium alloy specimens under variable-amplitude loading sequences. RAE TR 70 004, 1970.

57. Gassner, E.   Ueber bisherige Ergebnisse aus Festigkeitsversuchen im Sinne der Betriebsstatistik. Lilienthal Gesellschaft für Luftfahrtforschung, Bericht 106, 1.Teil, 1939. Translation NACA TM 1266, 1950.

58. Schijve, J.   The endurance under program-fatigue testing. Full-scale Fatigue Testing of Aircraft Structures, 1st ICAF Symposium, Amsterdam 1959, ed. by F.J.Plantema and J.Schijve, Pergamon 1961, p.41. Also NLR MP 178, Amsterdam 1959.

59. Schijve, J.   Fatigue-crack propagation under variable-amplitude loading. NLR Report M.2094,
    Broek, D.   Amsterdam 1961.
    De Rijk, P.

60. Hudson, C.M.   Investigation of the effects of variable-amplitude loadings on fatigue crack
    Hardrath, H.F.   propagation patterns. NASA TN D-1803, August 1963.

61. Smith, S.H.   Random-loading fatigue crack growth behavior of some aluminum and titanium alloys. Symp. Structural Fatigue in Aircraft, Am.Soc.Test.Mats, STP 404, 1966, p.76.

62. Hudson, C.M.   Investigation of fatigue-crack growth under single variable-amplitude loading,
    Raju, K.N.   NASA TN D-5702, 1970.

63. Schijve, J.   Crack propagation in a full-scale wing structure under random flight-simulation
    De Rijk, P.   loading. NLR TR 71043, Amsterdam 1971.

64. Schijve, J.   Fatigue tests with random flight-simulation loading. Paper 6th ICAF Symp., Miami, May 1971. Also NLR MP 71008, Amsterdam 1971.

65. Gassner, E.   Einfluss der Start-Lande Lastwechsels auf die Lebensdauer der böenbeanspruchten
    Horstmann, K.F.   Flügel von Verkehrsflugzeugen. Advances in Aero.Sc., Vol.4, Pergamon 1961, p.763.

66. Gassner, E.   Betriebsfestigkeitsversuche zur Ermittlung zulässiger Entwurfsspannungen für die
    Jacoby, G.   Flügelunterseite eines Transportflugzeuges. Luftfahrttechnik-Raumfahrttechnik, Vol.9, Jan.1964, p.6.

67. Naumann, E.C.   Evaluation of the influence of load randomization and of ground-to-air cycles on fatigue life. NASA TN D-1584, 1964.

68. Melcon, M.A.   Simulation of random aircraft service loadings in fatigue tests. ICAF Symp. 1963:
    McCulloch, A.J.   Current Aeronautical Fatigue Problems, ed. by J.Schijve, J.R.Heath-Smith and E.R.Welbourne, Pergamon 1965, p.347.

69. McCulloch, A.J.   Investigation of the representation of aircraft service loadings in fatigue tests.
    Melcon, M.A.   ASD TR 61-435, Sep.1961.
    Crichlow, W.J.
    Foster, H.W. and Rebman, J.

70. Barrois, W. — Physical interpretation of metal fatigue. Minutes 5th ICAF Conference, Brussels 1957.

71. Winkworth, W.J. — Fatigue behavior under service and ground test condition. RAE TN Structures 306, 1961.

72. Schijve, J. De Rijk, P. — The effect of ground-to-air cycles on the fatigue crack propagation in 2024-T3 Alclad sheet material. NLR TR M.2148, Amsterdam 1966.

73. Gassner, E. Jacoby, G. — Experimentelle und Rechnerische Lebensdauerbeurteilung von Bauteilen mit Start-Lande-Lastwechsel. Luftfahrttechnik-Raumfahrttechnik, Vol.11, 1965, p.138.

74. Mann, J.Y. Patching, C.A. — Fatigue tests on Mustang wings and notched aluminium alloy specimens under random gust loading with and without ground-to-air cycles of loading. Note ARL/SM.268, Melbourne 1961.

75. Finney, J.M. Mann, J.Y. — Fatigue behavior of notched aluminium alloy specimens under simulated random gust loading with and without ground-to-air cycles of loading. ICAF Symp.1961: Fatigue of Aircraft Structures, ed. by W.Barrois and E.Ripley, Pergamon 1963, p.151.

76. Schijve, J. Broek, D. De Rijk, P. Nederveen, A. Sevenhuijsen, P.J. — Fatigue tests with random and programmed load sequences with and without ground-to-air cycles. A comparative study on full-scale wing center sections. NLR Report S.613, Amsterdam 1965. Also AFFDL-TR-66-143, Oct. 1966.

77. Schijve, J. Jacobs, F.A. Tromp, P.J. — Crack propagation in aluminium alloy sheet materials under flight-simulation loading. NLR TR 68117, Amsterdam 1968.

78. Schijve, J. — Cumulative damage problems in aircraft structures and materials. The 2nd F.J.Plantema Memorial Lecture, ICAF Conference, Stockholm 1969. The Aeronautical Journal, Vol.74, 1970, p.517. Also NLR MP 69005, Amsterdam 1969.

79. Jacoby, G. — Comparison for fatigue life estimation processes for irregularly varying loads. Proc. 3rd Conf. on Dimensioning and Strength Calculations, Hungarean Ac.of Sc., Budapest 1968, p.81.

80. Imig, L.A. Illg, W. — Fatigue of notched Ti-8Al-1Mo-1V titanium alloy at room temperature and 550°F (560°K) with flight-by-flight loading representative of a supersonic transport. NASA TN D-5294, 1969.

81. Wallgren, G. — Review of some Swedish investigations on fatigue during the period June 1959 to April 1961. FFA-TN-HE-879, Stockholm 1961.

82. Gassner, E. — Auswirkung betriebsähnlicher Belastungsfolgen auf die Festigkeit von Flugzeugbauteilen. Doctor Thesis, Darmstadt 1941. Also Bericht der DVL, Cf 407/5, 1941.

83. Wallgren, G. — Fatigue tests with stress cycles of varying amplitude. FFA Report No.28, Stockholm 1949.

84. Wallgren, G. Petrelius, S. — Program utmattningsprov med bultförband. FFA Report HU-429:2, Stockholm 1954.

85. Fisher, W.A.P. — Some fatigue tests on notched specimens with programme loading for a "ground-attack" aircraft. RAE TN Structures 235, 1958.

86. Fisher, W.A.P. — Programme fatigue tests on notched bars to a gust load spectrum. RAE TN Structures 236, 1958.

87. Naumann, E.C. Schott, R.L. — Axial-load fatigue tests using loading schedules based on maneuver-load statistics. NASA TN D-1253, 1962.

88. Naumann, E.C. — Variable-amplitude fatigue tests with particular attention to the effects of high and low loads. NASA TN D-1522, 1962.

89. Yeomans, H. — Programme loading fatigue tests on a bolted joint. RAE TN Structures 327, 1963.

90. Corbin, P.L. Naumann, E.C. — Influence of programming techniques and varying limit load factors on maneuver load fatigue test results. NASA TN D-3149, 1966.

91. Parish, H.E. — Fatigue test results and analysis of 11 piston Provost wings to determine the effect of programmed load. Min.of Tech., U.K., S and T Memo 5/67, 1967.

92. Parish, H.E. — Fatigue test results and analysis of four piston Provost wings tested in an ascending-descending order of loading. Min. of Aviation, S and M Memo 1/68, 1958.

93. Dunsby, J.A. — Fatigue tests on notched specimens of 2024-T351 aluminum alloy under a low altitude load spectrum. Nat.Res. Council Canada, NAE LR-504, 1968.

94. Lipp, W. — Unterschiede in der Lebensdauerangabe nach Betriebsfestigkeitsversuchen gegenüber den Ergebnissen aus Fahrversuchen. LBF Bericht Nr. TB-80, Darmstadt 1968, p.67.

95. Gassner, E. — Betriebsfestigkeit gekerbter Stahl- und Aluminiumstäbe unter betriebsähnlichen und betriebsgleichen Belastungsfolgen. Materialprüfung, Vol.11, 1969, p.373. Also ICAF Symp., Stockholm 1969.

96. Schijve, J. — Load sequences for fatigue testing of components and full-scale aircraft structures. ICAS Congress Rome 1970, Paper No. 70-32. Also NLR MP 70012, Amsterdam 1970.

97. Schijve, J. — The effect of load sequence on fatigue crack propagation under random loading and program loading. NLR TR 71014, Amsterdam 1971.

98. Breyan, W. — Effects of block size, stress level, and loading sequence on fatigue characteristics of aluminum-alloy box beams. Effects of Environment and Complex Load History on Fatigue Life, ASTM STP 462, 1970, p.127.

99. Kirkby, W.T. — Constant-amplitude or variable-amplitude tests as a basis for design studies. ICAF Symp., Munich 1965. Fatigue Design Procedures, ed. by E.Gassner and W.Schütz, Pergamon 1969, pp 253-290.

100. Gassner, E. — On the influence of fretting corrosion on the fatigue life of notched specimens of an AlCuMg2 alloy. Fatigue of Aircraft Structures, ICAF Symp., Paris 1961, ed. by W.Barrois and E.L.Ripley, Pergamon 1963, p.87.

101. Hillbery, B.M. — Fatigue life of 2024-T3 aluminum alloy under narrow- and broad-band random loading. Effects of Environment and Complex Load History on Fatigue Life. ASTM STP 462, 1970, p.167.

102. Kowalewski, J. — On the relation between fatigue lives under random loading and under corresponding program loading. Full-Scale Fatigue Testing of Aircraft Structures, 1st ICAF Symp., Amsterdam 1959, ed.by F.J.Plantema and J.Schijve, Pergamon 1961, p.60.

103. Fuller, J.R. Research on techniques of establishing random type fatigue curves for broad band sonic loading. SAE Paper 671 C, April 1963 (see also ASD-TDR-62-501, Oct. 1962).

104. Naumann, E.C. Fatigue under random and programmed loads. NASA TN D-2629. Febr. 1965.

105. Clevenson, S.A. Fatigue life under random loading for several power spectral shapes. NASA TR
     Steiner, R. R-266, 1967.

106. Schijve, J. The crack propagation in two aluminum alloys in an indoor and an outdoor environ-
     De Rijk, P. ment under random and programmed load sequences. NLR TR M.2156, Amsterdam 1965.

107. Jacoby, G. Comparison of fatigue lives under conventional program loading and digital random loading. Effects of environment and complex load history on fatigue life. ASTM STP 462, 1970, p.184.

108. Jacoby, G. Vergleich der Lebensdauer aus Betriebsfestigkeits-, Einzelflug- und digital programmierten Random-Versuchen sowie nach der linearen Schadsnakkumulations-hypothese. Fortschritt Bericht VDI-Z, Reihe 5, Nr. 7, 1969, p.63.

109. Jacoby, G. Beitrag zum Vergleich der Aussagefähigkeit von Programm- und Random-Versuchen. 1970 Zeitschrift für Flugwissenschaften, Vol.18, 1970, p.253.

110. Branger, J. A review of Swiss investigations on aeronautical fatigue during the period June 1965 to April 1967. Eidgenössisches Flugzeugwerk, Emmen, F+W, 1967, S.196.

111. Branger, J. The influence of modifications of a fatigue history loading program. Paper 6th ICAF Symposium, Miami, May 1971.

112. Branger, J. Investigation of high strength steels under history program fatigue. Columbia Un.,
     Ronay, M. Institute for the Study of Fatigue and Reliability, TR No.56, 1968.

113. Schijve, J. Crack propagation in 2024-T3 Alclad under flight-simulation loading. Effect of
     Jacobs, F.A. truncating high gust loads. NLR TR 69050, 1969.
     Tromp, P.J.

114. Schütz, D. Einzelflugversuchs und Einstufenversuche an Augenstäben aus AlZnMgCuHg (3.4354.7) zur Ueberprüfung der linearen Schadsnakkumulation. LBF TM 53/70, Darmstadt 1970.

115. Schütz, W. Ueber eine Beziehung zwischen der Lebensdauer bei konstanter und bei veränder-licher Beanspruchungsamplitude und ihre Anwendbarksit auf die Bemessung von Flugzeugbauteilen. Doctor Thesis Technische Hochschule München, October 1965. A shorter version is published in Z.für Flugwissenschaften, Vol.15, 1967, p.407.

116. Gassner, E. Effect of variable load and cumulative damage on fatigue in vehicle and airplane structures. Int.Conf.Fatigue of Metals, The Inst.of Mech.Eng., London 1956, p.304.

117. Oatermann, H. Einfluss der Kollektivform auf die Schwingfestigkeit der Aluminiumlegierung 3.4354.5 (AlCuMg2). LBF TM 36/68, Darmstadt 1968.

118. Jost, G.S. The fatigue of 24 S-T aluminium alloy wings under asymmetric spectrum loading. Report ARL/SM.295, Melbourne, Febr. 1964.

119. Huston, W.B. Comparison of constant-level and randomized step tests of full-scale structures as indicators of fatigue-critical components. Symp. Full-scale Fatigue Testing of Aircraft Structures, Amsterdam 1959. Pergamon 1961, p.193.

120. Branger, J. Life estimation and prediction of fighter aircraft. Int.Conf.Structural Safety and Reliability, April 1969, Smithsonian Institution, Washington D.C. Also Eidgenössisches Flugzeugwerk, Emmen, F+W, S.207.

121. Branger, J. Private communication.

122. Locati, L. Essais de fatigue par flexion avec fréquences superposées. Colloquium on Fatigue, Stockholm 1955, ed. by W.Weibull and F.K.G.Odquist, Springer Verlag, 1956. p.160.

123. Starkey, W.L. Effects of complex stress-time cycles on the fatigue properties of metals.
     Macro, S.M. Trans.ASME, Vol.79, 1957, p.1329.

124. Nishihara, T. Fatigue life of metals under varying repeated stresses. Proc.6th Japan Nat.Congress
     Yamada, T. for Appl. Mech., 1956, p.61.

125. Gassner, E. Einfluss von Störschwingungen auf die Ermüdungsfestigkeit. Stahl und Eisen, Vol.82,
     Svenson, O. 1962, p.276.

126. Jacoby, G. Observation of crack propagation on the fracture surface. ICAF Symp. Current Aero. Fatigue Problems, Rome 1963, ed. by J.Schijve, J.R.Heath Smith and E.R.Welbourne, Pergamon 1965, p.165.

127. Yamada, T. Fatigue strength of aluminium alloy under actual service loads. Proc.12th Japan
     Kitagawe, S. Congress on Mats Res., 1969, p.56.

128. Nowack, H. Biharmonische Beanspruchungsabläufe zur Beurteilung der Schädigung unregelmässiger Beanspruchungen, VDI-Z, Fortschritt Berichte, Reihe 5, No.7, 1969, p.91.

129. Dowling, N.E. Fatigue failure predictions for complicated stress-strain histories. Un.of Illinois,
     T. and A.M.Report 337, 1971.

130. Palmgren, A. Die Lebensdauer von Kugellager. Z.V.D.I., Vol.68, 1924, pp 339-341.

132. Miner, M.A. Cumulative damage in fatigue. J.Appl.Mech., Vol.12, 1945, pp A159-A164.

133. Langer, B.F. Fatigue failure from stress cycles of verying amplitude. J.Appl.Mech., Vol.4, 1937, pp A160-A162.

134. Koch, J.J. Over een verkorte methode ter bepaling van den kerffactor β bij wisselende buig-
     Biezeno, C.B. en wringbelasting. De Ingenieur, 1940, No.46.

135. Grover, H.J. An observation concerning the cycle ratio in cumulative damage. Symp. on Fatigue of Aircraft Structures, Am.Soc.Test.Mats, STP 274, 1960, pp 120-124.

136. Manson, S.A. Application of a double linear damage rule to cumulative fatigue. Fatigue Crack
     Freche, J.C. Propagation, ASTM STP 415, An.Soc.Testing Mats, 1967, p.384.
     Ensign, C.R.

137. Bland, R.B. Cumulative damage in fatigue. Discussion on Ref.132. J.Appl.Mech., Vol.13, 1946,
     Putnam, A.A. pp A169-A171.

138. Nishihara, T. The fatigue strength of metallic materials under alternating stresses of varying
     Yamada, T. amplitude. The Japan ScienceReview, Vol.1, No.3, 1950, pp 1-6.

139. Shanley, F.R. A proposed mechanism of fatigue failure. Colloquium on Fatigue, ed.by W.Weibull and F.K.G.Odquist. Springer Verlag, 1956, pp 251-259.

140. Schijve, J. Critical analysis of the fatigue damage concept and some consequencies for fatigue testing of aircraft structures. Minutes 4th Conf. of the Int.Comm.on Aero.Fatigue, Zürich 1956, Appendix 2.

141. Kaschele, L.   Review and analysis of cumulative-fatigue-damage theories. The Rand Corp.
                           Memo RM-3650-PR, 1963.

142. Crichlow, W.J.   An engineering evaluation of methods for the prediction of fatigue life in air-
     McCulloch, A.J.   frame structures. ASD-TR-61-434, Wright Patterson AFB, 1962.
     Young, L.
     Melcon, M.A.

143. Edwards, P.R.   Cumulative damage in fatigue with particular reference to the effects of residual
                           stresses. RAE TR 69 237, 1969.

144. O'Neill, M.J.   A review of some cumulative damage theories. Aero Res.Labs, Melbourne, Peport
                           ARL/SM 326, 1970.

145. Freudenthal, A.M.   Accumulation of fatigue damage. Proc.Int.Conference on Fatigue on Aircraft
     Heller, R.A.   Structures, Academic Press, 1956, p.146.

146. Freudenthal, A.M.   On stress interaction in fatigue and a cumulative damage rule. J.Aerospace Sc.,
     Heller, R.A.   Vol.26, 1959, pp 431-442.

147. Mareh, K.J.   Direct-stress cumulative fatigue damage tests on mild-steel and aluminium alloy
                           specimens. Nat.Engineering Lab. Glasgow, NEL Report No.204, 1965.

148. Haibach, E.   Modifizierte lineare Schadensakkumulations-Hypothese zur Berückeichtigung des
                           Dauerfestigkeiteabfalls mit fortschreitender Schädigung. Laboratorium für
                           Betriebsfestigkeit, TM Nr.50/70, July 1970.

149. Henry, D.L.   A theory of fatigue damage accumulation in steel. Trans.ASME, Vol.77, 1955, p.913.

150. Smith. C.R.   Small specimen data for predicting life of full-scale structures. Symp.Fatigue
                           Tests of Aircraft Structures: Low-Cycle, Full-Scale and Helicopters, Am.Soc.
                           Testing Mats, STP 338, 1963, pp 241-250.

151. Smith, C.R.   Linear strain theory and the Smith method for predicting fatigue life of struc-
                           ures for spectrum-type loading. Aerospace Rse.Lab., WPAFB, Ohio, Report ARL 64-55,
                           1964.

152. Corten, H.T.   Cumulative fatigue damage. Proc.Int.Conf.on Fatigue of Metals, London 1956,
     Dolan, T.J.   pp

153. Ohji, K.   Cumulative damage and effect of mean strain in low-cycle fatigue of a 2024-T351
     Miller, W.R.   aluminum alloy. J.Basic Eng., Trans.ASME, Vol.88 (D), 1966, pp 801-810.
     Marin, J.

154. Topper, T.H.   Effects of mean stress and prestrain on fatigue-damage summation. Symp. Effects
     Sandor, B.Z.   of Environment[a]and Complex Load History on Fatigue Life. Am.Soc.Test.Mats.,
                           STP 462, pp 93-104.

155. Topper, T.H.   Cumulative fatigue damage under cyclic strain control. Aero.Struct.Lab., Report
     Sandor, B.I.   No.NAEC-ASL-1115, 1967.
     Morrow, J,D.

156. Impellizzerri,L.F.   Cumulative damage analysis in structural fatigue. Symp.Effects of Environmental
                           and Complex Load History and Fatigue Life. Am.Soc.Test.Mats, STP 462, 1970,
                           pp 40-68.

157. Martin, J.F.   Computer based simulation of cyclic stress-strain behavior with applications to
     Topper, T.H.   fatigue. Materials Res. and Standards, Vol.11, No.2, 1971, pp 23-28,50.
     Sinclair, G.M.

158. Gassner, E.   Performance fatigue testing with respect to aircraft design. Fatigue in Aircraft
                           Structures, Academic Press, New York 1956, pp 178-206.

159. Gassner, E.   Assessment of the allowable design stresses and the corresponding fatigue life.
     Schütz, W.   ICAF Symp., Munich 1965, Fatigue Design Procedures, ed. by E.Gassner and W.Schütz,
                           Pergamon 1969, pp 291-307.

160. Paris, P.C.   Stress analysis of crack. Symp. Fracture Toughness Testing and its Applications.
     Sih, G.C.   Am.Soc.Test.Mats, STP 381, 1965, pp 30-83.

161. Paris, P.C.   A rational analytic theory of fatigue. The Trend in Engineering, Vol.13, 1961,p.9.
     Comez, M.P.
     Anderson, W.E.

162. Paris, P.C.   The growth of cracks due to variations in load. Doctoc Thesis, Lehigh University
                           1962.

163. Schijve, J.   Significance of fatigue cracks in micro-range and macro-range. Symp.Fatigue Crack
                           Propagation, Am.Soc.Test.Mats, STP 415, 1967, pp 415-457.

164. Figge. I.G.   Fatigue crack propagation in structures with simulated rivet forces. Symp.Fatigue
     Newman, J.C.   Crack Propagation, Am.Soc.Test.Mats, STP 415, 1967, pp 71-93.

165. Paris, P.C.   The fracture mechanics approach to fatigue. Fatigue, an Interdisciplinary Approach,
                           ed.J.J.Burke, N.L.Reed and V.Weiss, Syracuse Un.Press, 1964, p.107.

166. Smith, S.H.   Fatigue crack growth under axial narrow and broad band random loading. Acoustical
                           Fatigue in Aerospace Structures, ed. W.J.Trapp and D.M.Forney, Syracuse Un.Press,
                           1965, p.331.

167. Swanson, S.R.   Crack propagation in Clad 7079-T6 aluminum alloy sheet under constant and random
     Cicci, F.   amplitude fatigue loading. Symp.Fatigue Crack Propagation, Am.Soc.Test.Mats,
     Hoppe, W.   STP 415, 1967, pp 312-360.

168. Schijve, J.   Estimation of fatigue performance of aircraft structures. Symp.Fatigue of Aircraft
                           Structures, STP 338, Am.Soc.Test.Mats, 1962, p.193. Also NLR MP 212.

169. Jacoby, G.   Comparison for fatigue life estimation processes for irregularly varying loads.
                           Proc.3rd Conference on Dimensioning and Strength Calculation, Hungarian Academy
                           of Sciences, Budapest 1968, p.81.

170. Deneff, G.V.   Fatigue prediction study. Flight Dynamics Lab, WADD TR 61-153, 1962.

171. Poe, C.C.   Fatigue crack propagation in stiffened panel. Paper ASTM Symp.Crack Propagation
                           and Damage Tolerance in Aircraft Structures, Toronto, June 1970.

172. Lazzarino, L.   A theoretical and experimental research on the fatigue behavior of reinforced
     Salvetti, A.   sheets. ICAS Paper No.70-35, ICAS-meeting, Rome, Sep.1970.

173. Chilver, A.H.   The estimation of fatigue damage in aircraft wing structures. J.Roy.Aero.Soc.,
                           Vol.58, 1954, p.396.

174. Schijve, J.   The analysis of random-load-time histories with relation to fatigue tests and life
                           calculations. Fatigue of Aircraft Structures. ICAF Symp., Paris 1961, ed.by
                           W.Barrois and E.L.Ripley, Pergamon 1963, p.115. Also NLR MP 201, Amsterdam 1961.
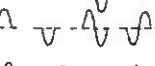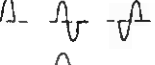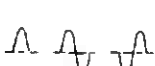
175. Buxbaum, O.   Statistische Zählverfahren als Bindeglied zwischen Beanspruchungsmessungen und Betriebsfestigkeitsversuch. LBF TR No.TB-64, Darmstadt 1966.

176. Van Dijk, G.M.   Statistical load data processing. Paper 6th ICAF Symp., Miami, May 1971. Also NLR MP 71004, Amsterdam 1971.

177. De Jonge, J.B.   The monitoring of fatigue loads. ICAS Congress Rome 1970, Paper No. 70-31. Also NLR MP 70010, Amsterdam 1970.

178. Swanson, S.R.   A review of the current status of random load testing in America. Proc.ICAF-meeting, Stockholm 1969, ed.by G.Wallgren and S.Eggwertz, p.2.3/ .

179. Buxbaum, O.   Extreme value analysis and its application to c.g. vertical accelerations measured on transport airplanes of type C-130. AGARD Report No. 579, 1971.

180. Heywood, R.B.   Designing against fatigue. Chapman and Hall, London 1962.

181.   Data sheets. Fatigue. Roy.Aero.Soc., London.

182. Stone, M.   Structural reliability through detail design and development testing. Proc. Air Force Conf. on Aircraft Structures and Materials. Miami 1969, AFFDL TR 70-144, 1970, p.579. Also Douglas Paper 5683.

183. Jarfall, L.   Optimum design of joints. The stress severity factor concept. Paper 5th ICAF Symp. Melbourne, May 1967.

184. Jarfall, L.   Fatigue cycling of riveted or bolted joints. FFA Report HF-1239, Stockholm 1969.

185. Spencer, M.   The 747 fatigue integrity program. Paper 6th ICAF Symp. on Design of Current Aircraft Systems, Miami, May 1971.

186. Schijve, J.   Crack propagation under variable-amplitude loading. Aircraft Engineering, Vo.34,
     Broek, D.   1962, p.314. Also NLR Report MP 208, Amsterdam 1961.

187. White, D.J.   Narrow band random fatigue testing with Amsler Vibraphore machines. J.Mech.Engrg.
     Lewszuk, J.   Science, Vol.11, 1969, p.598.

188. Laudert, H.   Einige Möglichkeiten der Ermüdungsprüfung bei Random-Beanspruchungen. Fortschritt
     Jacoby, G.   Bericht, VDI-Z, Reihe 5, No.7, April 1969, p.29.
     Nowack, H.
     Weber, H.D.

190. Schütz, L.   Einzelflugversuche an gekerbten Flachstäben aus AlCuMg2 (3.1354.5) mit plastischer
     Lowak, H.   Aufweitung des Kerbgrundes. LBF TM 54/70, Darmstadt 1971.

191. Harpur, N.F.   The value of full-scale fatigue testing. Fatigue Design Procedures, 4th ICAF Symp.
     Troughton, A.J.   Munich 1965, ed. by E.Gassner and W.Schütz, Pergamon 1969, p.343.

192. Morgan, R.C.   Some thoughts on the economics of fatigue. Paper presented at the 5th ICAF Symp. Melbourne, May 1967.

193. Axisa, R.   Economic aspects of fatigue in commercial airlines. Paper presented at the 5th
     Graff, D.   ICAF Symposium, Melbourne, May 1967.

194. Rhomberg, H.   Economic and operational aspects of fatigue figures of a Swiss ground attack-fighter. Paper presented at the 5th ICAF Symposium, Melbourne, May 1967.

195. Schijve, J.   Fatigue of aircraft structures. 4th Von Karman Lecture, Israel J.of Technology, Vol.8, 1970, p.1.

196. Raithby, K.D.   A comparison of predicted and achieved fatigue lives of aircraft structures. Fatigue of Aircraft Structures, 2nd ICAF Symposium, Paris 1961, ed.by W.Barrois and E.L.Ripley, Pergamon 1963, p.249.

197. Lowndes, H.B.   The U.S. Air Force Weapon Systems fatigue certification program. Fatigue Design
     Miller, W.B.   Procedures, 4th ICAF Symposium, Munich 1965, ed.by E.Gassner and W.Schütz, Pergamon 1969, p.139.

198. Hardrath, H.F.   A review of cumulative damage. Paper presented to the AGARD Structures and Materials Panel, Munich, June 1965.

Table 4.1   Investigations on the effect of a preload on fatigue life

Investigation	Material	Specimen	Type of fatigue loading [a]
Forrest (1946, Ref.40)	Al-alloy (2014)	V-notch	Rotating bending, C.A. (preload in tension)
Heyer (1943, Ref.41)	Al Zn Mg alloy Al Cu Mg alloy Cr Mo steel	Lug V-notch	Axial, C.A. with positive mean
Heywood (1955, Refs.42,43)	Al-alloys	Lug Hole notched Channel specimen Wing joints	Axial, C.A. with positive mean
		Meteor tail plane	Bending, C.A. with positive mean
Payne (1955, Ref.44)	2024-alloy	Mustang wing	Bending, C.A. with positive mean
Smith (1958, Ref.45)	7075-alloy	Hole-notched	Axial, C.A. with positive mean
Boissonat (1961, Ref.46)	Al-alloys	Edge-notched Strap joint	Axial, C.A. R = 0.1
	Ti-alloy	Edge-notched Wing fitting	
	Low alloy steel	Tensile bolt	
Nordfin and Halsey (1962, Ref.47)	7075-alloy	Riveted box beam	Bending, C.A. with constant pos.S_{min}
Rosenfeld (1962, Ref.48)	7075-alloy	Wing structure	Bending, program loading wing manoeuvre spectrum
Imig (1967, Ref.49)	Ti-alloy (8-1-1)	Edge-notched	Axial, C.A. R = 0
Kirkby and Edwards (1969, Ref.50)	Al-alloy (2014)	Pinned lug and clamped lug	Axial, random loading with positive mean
Jo Dean Morrow, Wetzel and Topper (1970, Ref.51)	2024-alloy	Hole notched	Axial, C.A. with positive mean

(a)   C.A. = constant-amplitude tests

Table 4.2 Investigations on the effect of periodic-high loads on fatigue life and crack propagation

Investigation	Material	Specimen	Type of high load (a)	Type of fatigue load (b)
Haywood (1955, Ref.42)	Al-alloys	Lug Channel specimen Meteor tailplane		C.A.
	7075-alloy	Channel specimen		
Schijve and Jacobs (1959,1960, Refs.39,58)	2024-alloy 7075-alloy	Riveted lap joint		program loading
Schijve, Broek, De Rijk (1960,1961, Refs.27,59)	2024-alloy	Sheet specimen (c)		C.A.
Boissonat (1961, Ref.46)	Al-alloys	Edge-notched specimen		C.A.
Nordfin and Halsey (1962, Ref.47)	7075-alloy	Riveted box beam		C.A.
Hudson and Hardrath (1963, Ref.60)	2024-alloy	Bar specimen (c)		C.A.
Smith (1966, Ref.61)	Ti-alloy (8-1-1)	Sheet specimen (c)		C.A.
McMillan and Hertzberg (1968, Ref.26)	2024-alloy	Sheet specimen (c)		C.A.
Hudson and Raju (1970, Ref.62)	7075-alloy	Sheet specimen (c)		C.A.
Schijve and De Rijk (1971, Refs.63,64)	2024 and 7075 alloy	Wing structure (c)		flight-simulation loading

(a)   periodic high positive load
      "   " negative "
      "   " load cycle starting with positive part
      "   "   "   "   "   "   "   negative "

(b) C.A. = constant-amplitude loading

(c) crack propagation was studied in these investigations.

Table 4.3 Investigations on the effect of ground-to-air cycles on fatigue life.
(comparative testing with and without CTAC)

Investigation	Material	Specimen	Type of fatigue loading
Gassner and Horstmann (1961, Ref.65)	2024 alloy	Central notch	Program loading
Gassner and Jacoby (1964, Ref.66)	2024 alloy	Central notch	
Naumann (1964, Ref.67)	7075 alloy	Edge notched specimen	
Melcon and McCulloch (1961,1965, Refs.68,69)	7075 alloy	Elliptical hole specimens	
Barrois (1957, Ref.70)	2024 alloy	Riveted lap joint	Simplified flight simulation
Winkworth (1961, Ref.71)	2024 alloy	Dakota wings	
Schijve and De Rijk (1966, Ref.72)	2024 alloy	Sheet specimen, crack propagation	
Gassner and Jacoby (1964,1965, Refs.66,73)	2024 alloy	Central notch	Programmed flight simulation
Mann and Patching (1961, Ref.74)	2024 alloy	Mustang wings	Random flight simulation
Finney and Mann (1963, Ref.75)	4-Al alloys	Round specimens with V-notch	
Melcon and McCulloch (1961,1965, Refs.68,69)	7075 alloy	Elliptical hole specimens	
Naumann (1964, Ref.67)	2024 and 7075 alloy	Edge notched specimen	
Schijve et al. (1965, Ref.76)	7075 alloy	Wing center section	
Schijve, Jacobs, Tromp (1968,1970, Refs.77,78)	2024 and 7075 alloy	Sheet specimen, crack propagation	

(a) Randomized block loading

Table 4.4   Investigations on program testing

Investigation	Material	Specimen	Variables studied					Load spectrum
			Sequence	Size of period	Low S_a cycles	High S_B cycles	Design stress level	
Gessner (1941,Ref.82)	2 Al-alloys	Hole notched specimens	x	x	x		x	gust, mixed
Wallgren (1949,Ref.83)	2024 and 7075 alloys	Hole notched specimen and riveted joints			x		x	gust, manoeuvre
Wallgren and Petrelius (1954,Ref.84)	2024 and 7075 alloys	Lug					x	manoeuvre
Fisher (1958,Ref.85)	AlZnCuMg	Edge notched specimen				x	x	manoeuvre
Fisher (1958,Ref.86)	AlZnCuMg	Edge notched specimen		x	x			gust
Hardrath et al. (1959,Refs.30,31)	2024 and 7075 alloys	Edge notched specimen	x	x			x	gust
Schijve and Jacobs (1959,Refs.39,58)	2024 and 7075 alloys	Riveted lap joint	x	x	x	x		gust
Naumann and Schott (1962,Ref.87)	7075 alloy	Edge notched specimen		x	x	x		manoeuvre (a)
Naumann (1962,Ref.88)	2024 and 7075 alloys	Edge notched specimen			x	x	x	gust, manoeuvre
Rosenfeld(1963,Ref.48)	7075 alloy	Wing, tailplane			x	x		manoeuvre
Nordfin and Halsey (1963,Ref.47)	7075 alloy	Boxbeam			x			manoeuvre
Jsomans (1963,Ref.89)		Bolted joint, greased and dry	x					gust
Corbin and Naumann (1966,Ref.90)	7075 alloy	Edge notched specimen			x	x	x	manoeuvre (a)
Parish (1967/1968, Refs.91,92)	Al alloy	Wing	x					manoeuvre
Dunsby (1968,Ref.93)	2024 alloy	Edge notched specimen			x		x	gust
Lipp and Gessner (1968,Refs.94,95)	Cr steel	Hole notched specimen loaded in bending, $S_m=0$		x			x	gust
Schijve (1970,Refs.96,97)	2024 alloy	Sheet specimen, crack propagation	x	x				gust
Drayan (1970,Ref.98)	7075 alloy	Box beam		x			x	manoeuvre
Impellizzerri (1970,Ref.156)	7075 alloy	Hole notched specimen, including crack propagation				x		manoeuvre

(a) In these investigations randomized block loading was applied.

Table 4.5 Investigations on the shape of the spectral density function for random load fatigue life

Investigation	Material	Specimen	Type of loading
Kowalewski (1959, Ref.102)	2024-T3	Notched, $K_t = 1.8$	Bending, $S_m = 0$
Fuller (1963, Ref.103)	2024-T3	Unnotched	Bending, $S_m = 0$
Naumann (1965, Ref.104)	2024-T3	Edge-notched, $K_t = 4$	Axial , $S_m = 12.2$ kg/mm^2
Smith (1966, Ref. 61)	2024-T3,7075-T6 Ti-8-1-1,Ti-6-4	Sheet, crack propagation	Axial , $S_m = 8.4 - 13.3$ kg/mm^2
Clevenson and Steiner (1967, Ref.105)	2024-T4	Notched, $K_t = 2.2$	Axial , $S_m = 0$
Hillberry (1970, Ref.101)	2024-T3	Mildly notched	Bending, $S_m = 0$

Table 4.6 Investigations on the comparison between the results from program tests and random tests

Investigation	Material	Specimen	Load spectrum	Remarks
Kowalewski (1959,Ref.102)	2024 alloy	Notched, $K_t = 1.8$	Rayleigh distribution	$S_m = 0$, bending
Melcon and McCulloch (1961/63,Refs.68,69)	7075 alloy	Elliptical hole, $K_t = 4$ and 7	Gust and manoeuvre	Tests with and without CTAC
Rosenfeld (1962,Ref.48)	7075 alloy	Wing	Manoeuvre	
Naumann (1964,Ref.67)	7075 alloy	Edge notched specimen, $K_t = 4$	Severe gust spectrum	Tests with and without CTAC
Naumann (1965,Ref.104)	2024 alloy	Edge notched specimen, $K_t = 4$	Severe gust spectrum	Different types of random and program tests
Corbin and Naumann (1966,Ref.90)	7075 alloy	Edge notched specimen, $K_t = 4$	Manoeuvre	3 load spectra
Schijve et al. (1965,Ref.76)	7075 alloy	Wing center section	Severe gust spectrum	Tests with and without CTAC
Schijve and De Rijk (1965,Ref.106)	2024 and 7075 alloys	Sheet specimen (c)	Severe gust spectrum	Tests with and without CTAC, tests indoors and outdoors
Lipp and Caesner (1968,Refs.94,95)	Cr steel	Hole notched specimen	Gust spectrum, $S_m=0$	$S_m = 0$, bending
Jacoby (1970, Refs.107,108)	2024-T3	Elliptical hole specimen, $K_t = 3.1$	Gust spectrum	2 design stress levels
Jacoby (1970,Ref.109)	CoCrNiW alloy Ti6Al 4V alloy 2024-T3	Circumferential notch $K_t = 3.1$ Elliptical hole,$K_t=3.1$	Rayleigh distribution	3 S_m-values
Breyan (1970, Ref.98)	7075 alloy	Riveted box beam	Manoeuvre	2 design stress levels 4 load spectra
Schijve et al. (1970,Refs.96,97)	2024-T3	Sheet specimen (c)	Gust	Different types of random and program loading

(c) crack propagation specimen

Table 4.7   Investigations on flight-simulation testing

Investigation	Material	Specimen	Load spectrum	Variables studied					
				Load sequence	Flight loads		GTAC		Design stress level
					Low-S_e cycles	High-S_a cycles	S_{min}	Taxiing loads	
Naumann (1964,Ref.67)	7075-T6 2024-T3	Edge notched specimen, K_t=4	Severe gust	x	x		x x		
Gessner and Jacoby (1964/65,Refs.66,73)	2024-T4	Elliptical hole specimen K_t = 3.1	gust	x	x	x		x	
Jacoby (1970,Refs.107,108)	2024-T4	same	gust	x					
Branger (1967,1971, Refs.100,111)	7075 bar 2014 plate	Hole notched specimen K_t = 3.6	manoeuvre		x	x		x	x
Branger and Ronay (1968,Ref.112)	CrNi steel	Hole notched specimen K_c = 2.3	manoeuvre						x
Imig and Illg (1969,Ref.80)	Ti-8Al 1Mo1V	Elliptical hole specimen K_t = 4	typical for supersonic aircraft	x			x	x	x
Schijve,Jacobs,Tromp (1968,1969,Refs.77,78)	2024-T3 7075-T6			x	x	x	x	x	
Schijve,Jacobs,Tromp (1969,Ref.113)	2024-T3	Sheet speci- men, crack propagation	gust			x			
Schijve (1971,Ref.64)	2024-T3 7075-T6								x
D.Schütz (1970,Ref.114)	7075-T6	Lug-type specimen	gust						x
Schijve,De Rijk (1971,Refs.63,64)	2024-T3 7075-T6	Wing struc- ture, crack propagation	gust		x	x			

Investigations on the effect of omitting GTAC are mentioned in table 4.3

Table 4.8   Investigations on the superposition of two cyclic loads

Investigation	Material	Specimen	Type of loading	ω_2/ω_1	Variables studied
Loceti (1956,Ref.122)	2024-T3 Steel	Unnotched	Bending	14 7 and 19	S_{a2}/S_{a1}
Nishihara and Jamada (1956,Ref.123)	Carbon steele	Notched	Bending	115-740	S_{a2}
Starkey and Macro (1957,Ref.124)	AlZn alloy SAE 4340 steel	Unnotched	Axial	2	S_{a2}/S_{a1}, phase angle
Gassner and Svenson (1962,Ref.125)	Mild steel	Notched	Bending	30	S_{a2}/S_{a1}, S_{a2} also programmed
Jacoby (1963,Ref.126)	AlMg alloy	Crack propagation	Axial	500	Fractographic observations
Jamada and Kitawage (1969,Ref.127)	7075 alloy 17 ST4	Unnotched	Bending		S_{a2}/S_{a1}
Nowack (1969,Ref.128)	2024-T3	Notched	Axial	2	S_{a2}/S_{a2}, phase angle
Dowling (1971,Ref.129)	2024-T4	Unnotched	Axial	2-600	S_{a2}/S_{a1}, S_{a2} also random

Table 5.1   Three different approaches for calculating fatigue life

•   Incremental damage theories, see table 5.2

•   Similarity approach based on   {   stress
   strain
   stress intensity factor

•   Interpolation methods

Table 5.3   Some test cases for the significance of cumulative damage theories

● Aspects of the physical relevance of a theory
<u>a</u> crack   nucleation and crack growth
<u>b</u> residual stress
<u>c</u> other damage parameters
<u>d</u> simple sequence effects
● Aspects of the practical usefulness of a theory
<u>e</u> 1. prediction of life until visible cracks
2. prediction of macro crack propagation
<u>f</u> complicated sequence effects
<u>g</u> effect of a change of the load spectrum
<u>h</u> effect of a few high-amplitude cycles
<u>i</u> effect of many low-amplitude cycles

STARTING FRDM CONSTANT – AMPLITUDE TEST DATA ?

DAMAGE ACCUMULATIDN SENSITIVE TD SEQUENCE OF LDAD HISTORY ?

INCREMENTAL DAMAGE THEORIES

YES

NO

NO

YES

NO

PALMGREN – MINER $\sum n/N = 1$
- FREUNDENTHAL ANO HALLER
- MARSH
- HAIBACH
- SMITH

READJUSTED S – N CURVES
- HENRY

REDUCING S – N CURVES
- SHANLEY
- VALLUR!
- CDRTEN AND DOLAN

CRACK PROPAGATION BASIS
- OHJI, MILLER AND MARIN

STRAIN – CYCLE BASIS

STRAIN – HISTDRY BASIS
- CREWS AND HARORATH
- JD DEAN MDRRDW ET AL

STRAIN – HISTORY BASIS AND RELAXATIDN OF RESIDUAL STRESS
- IMPELLIZZERRI

BASED ON PRDGRAM TEST DATA
- GASSNER

BASED DN RANDDM LDAD TEST DATA
- KIRKBY AND EDWARDS

TABLE 5.2 SURVEY OF INCREMENTAL DAMAGE THEORIES

Table 6.1 Survey of aircraft fatigue problems (Ref.78)

DESIGN PHASE	Design efforts	. Type of structure, fail-safe characteristics . Joints . Detail design . Materials selection . Surface treatments . Production technique	
		. Airworthiness requirements	

	Estimatione Calculations Testing	. Prediction of fatigue environment
		        mission analysie
		        load statistics
		        required target life	

		. Dynamic response of the structure	

		. Estimation of fatigue properties
		        fatigue lives
		        crack propagation
		        fail-eafe strength
		. Exploratory fatigue tests for
		        design studies
		        eupport of life estimates
			o
			o
			
			o
			o

CONSTRUCTION OF AIRCRAFT PROTOTYPES TEST FLIGHTS		. Load measurements in flight . Proof of satisfactory fatigue propertiae by testing components or full-etructure . Allowances for service environment . Structural modifications . Inspection procedures for use in service	 o o
AIRCRAFT IN SERVICE		. Load measurements in service . Corrections on predicted fatigue properties . Cracks in service, relation to prediction . Structural modifications	o o o

Problems involving aspects of fatigue damage accumulation are indicated by o
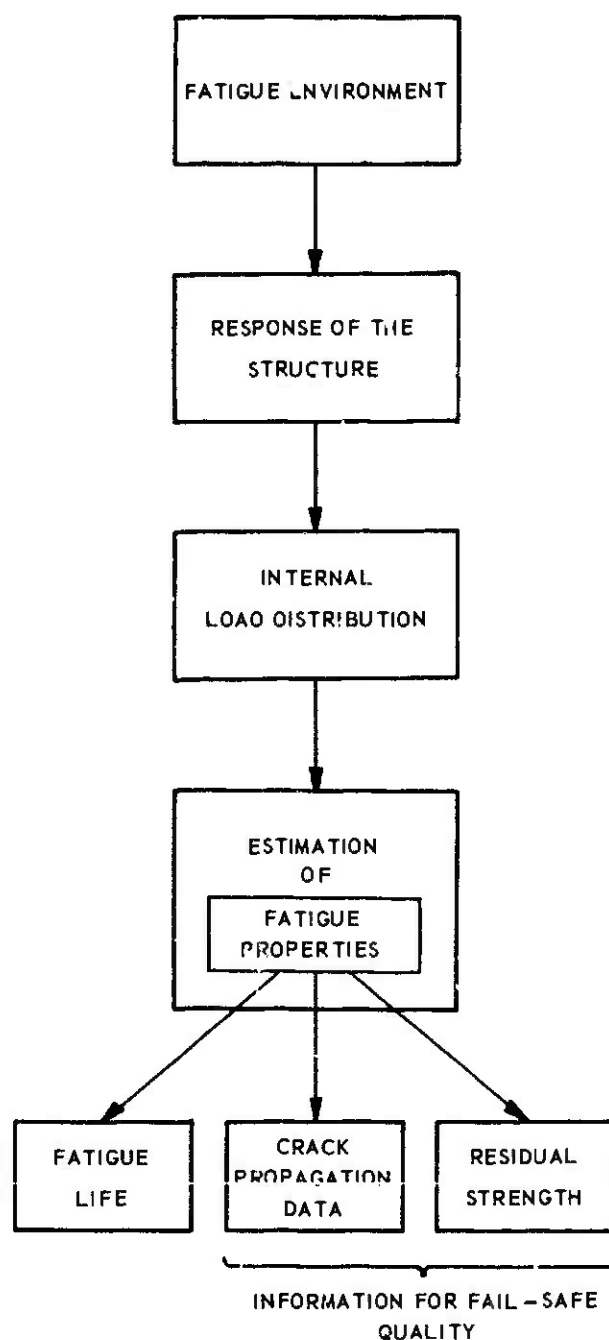
TABLE 6.2 SEVERAL PHASES OF ESTIMATING
FATIGUE PROPERTIES

Table 6.3   Various aspects of the airoraft fatigue environment (Ref.78)

Load-time history	. Mission analysis, flight profiles
	. Fatigue loads
	       gusts
	       manoeuvres
	       GTAC
	       ground loads
	       acoustic loading
	       etc.
	. Statistical description of fatigue loads
	       Counting of peaks, ranges, etc.
	       PSD approach
	       Unstationary character of environment
	       Scatter of environmental conditions
	. Sequence of fatigue loads
	. Loading rate
	       Time-history
	       Wave form
	       Rest periods

Temperature-time history	. Fatigue at low and high temperature . Thermal stresses . Interaction creep-fatigue
Chemical environment	. Corrosion, influence on crack initiation crack propagation . Interaction stress corrosion-fatigue

Table 6.4   Basic elements of fatigue life estimating
procedures in the design stage

a	Estimated service load-time history
b	Structure, component: dimensions and material
c	Available fatigue data
d	Fatigue life calculation theory
e	Additional fatigue tests

Table 6.5 Aspects of available fatigue data for making life estimates

Aspect	Specification of available data
Materiel	. Similar material . Same material
Type of specimen	. Unnotched . Simply notched specimens . Similar structural element . Same component
Type of loading	. Constant-amplitude test data . Data from more complex fatigue load sequences . Loading in service

Table 6.6 Various procedures for making life estimates in the design stage

Starting point	Type of data	Improvement of data by accounting for :	Life calculation
1. Available fatigue life data	S-N data for: 1a. simple specimens 1b. components	Material S_m K_t and size	$\sum \frac{n}{N} = 1$
	Program test data or random load test data for: 1c. simple specimens 1d. components		$\sum \frac{n'}{N'} = 1$ (Sect.5.3.3.)
	1e. Flight-simulation test data		Interpolation between available data (Sect.5.3.5)
2. Service experience from previous design	2a. Stress level giving sufficient crack free life		New design is superior to old design. Result: At least same life
	2b. Crack free life for specific components	Materiel, S_m, K_t, size and load spectrum	Similar life as for old design
3. Testing of new component or structure			

Table 6.7   Procedures for estimating crack propagation
rates in the design stage

Starting point	Type of data
Available crack propagation data	Data from constant-amplitude tests
	Data from flight-simulation tests
Experience from previous design	Data from panel tests of full-scale fatigue tests
Testing of new component or full-scale structure	

Table 7.1   Survey of fatigue specimens

Type of specimen	Remarks
Unnotched specimen	$K_t \sim 1$
Simple notched specimen	Examples: Edge notched specimens, specimens with central notch. Specimens mainly characterized by K_t-value and notch root radius r.
Simple joint specimen	Lap joint, strap joint, either riveted or bolted. Lug type specimens.
Component	Part of a structure, full size. Examples: joint, skin panel with fatigue critical details, brackets, etc.
Full-scale structure	Large part of an aircraft structure. Examples: wing, fuselage, empennage, or large parts of these items, for instance nose section of fuselage, tailplane, etc.

Table 7.2 Survey of different types of fatigue trouble in service (Ref.195)

Type of fatigue trouble	Possible consequence
Insufficient fatigue strength — Safe-life component	Catastrophe
Insufficient fatigue strength — Fail-safe component	Expensive repair
Deficiencies of the detail design	Extra maintenance by repair, modification or replacement
Fatigue cracks in components that were assumed to carry no cyclic load	Extra maintenance by repair, modification or replacement
Fatigue cracks in secondary structure	Extra maintenance by repair, modification or replacement
Fatigue cracks due to incidental service damage	Depends on type of component
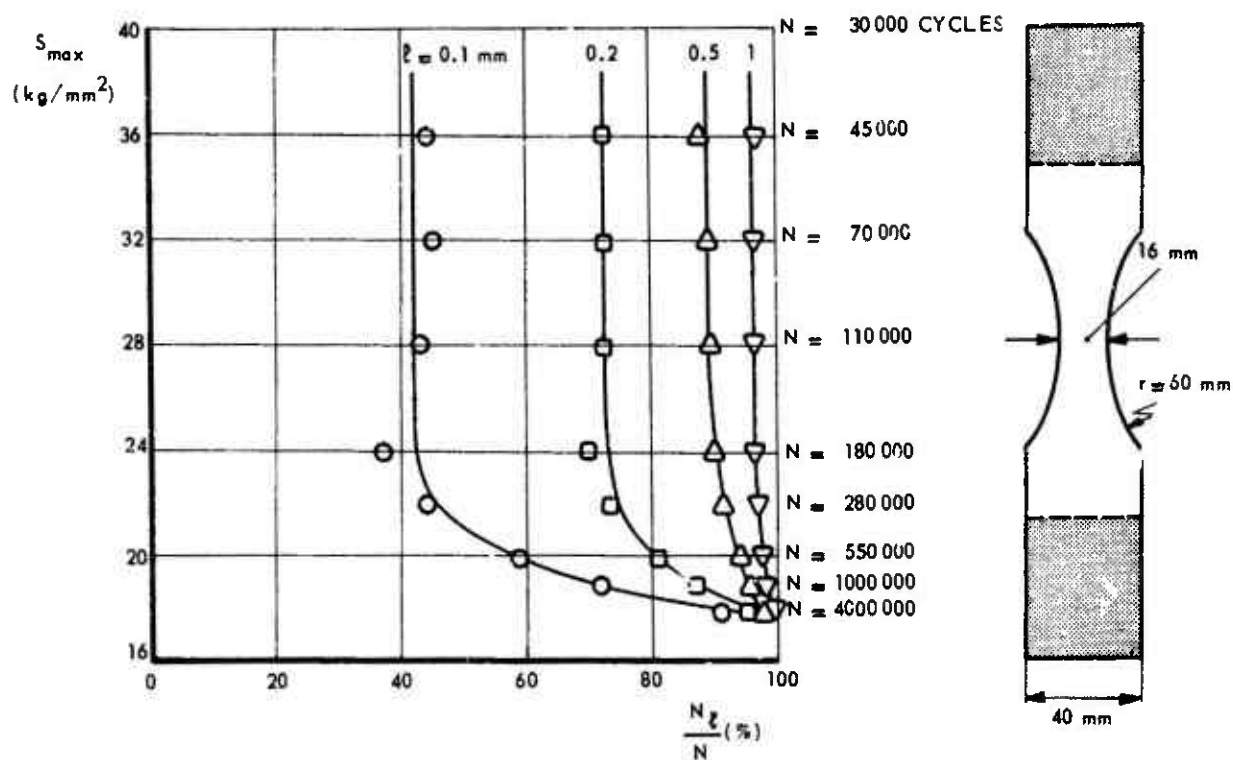
FIG. 2.1 PERCENTAGE OF FATIGUE LIFE COVERED BY CRACK PROPAGATION IN 2024 – T 3
SPECIMENS UNTIL A CRACK LENGTH ℓ HAS BEEN REACHED (REF. 7).
TESTS AT R = 0
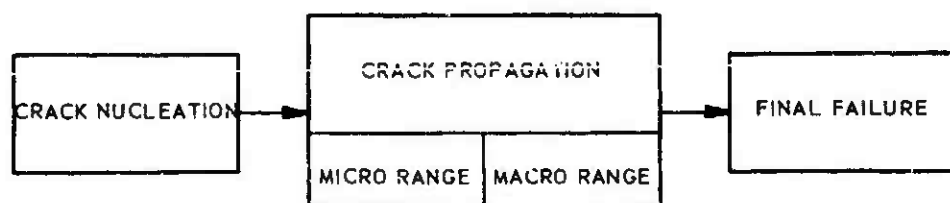
FIG. 2.2 THREE PHASES IN THE FATIGUE LIFE.
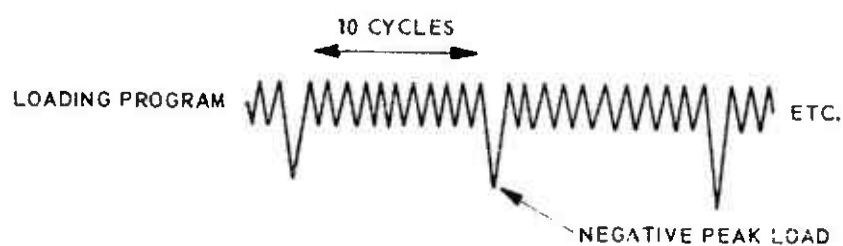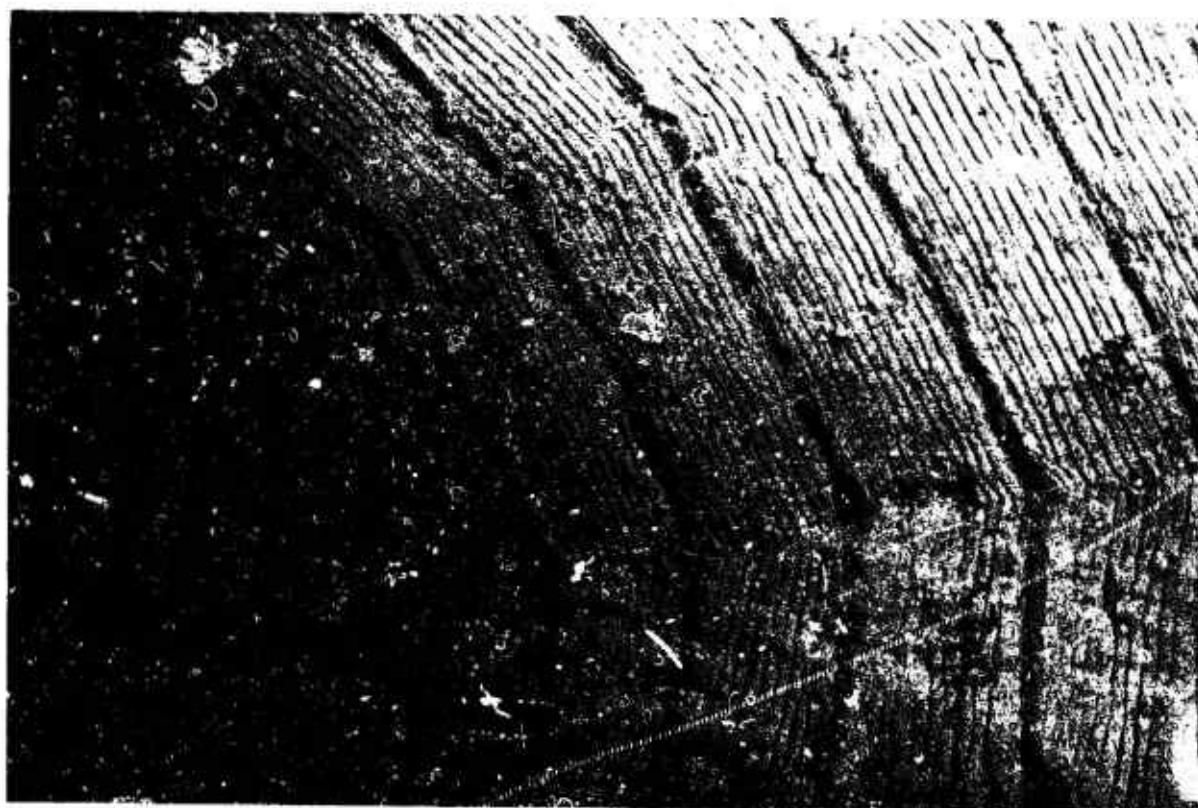
FIG. 2.3 ELECTRON MICROGRAPH FROM A FRACTURE SURFACE OF A FATIGUE CRACK.(REF.8)
PROPAGATION FROM LEFT TO RIGHT. MATERIAL 2024 – T 3 ALCLAD SHEET.
EACH STRIATION CORRESPONDS TO A SINGLE LOAD CYCLE.
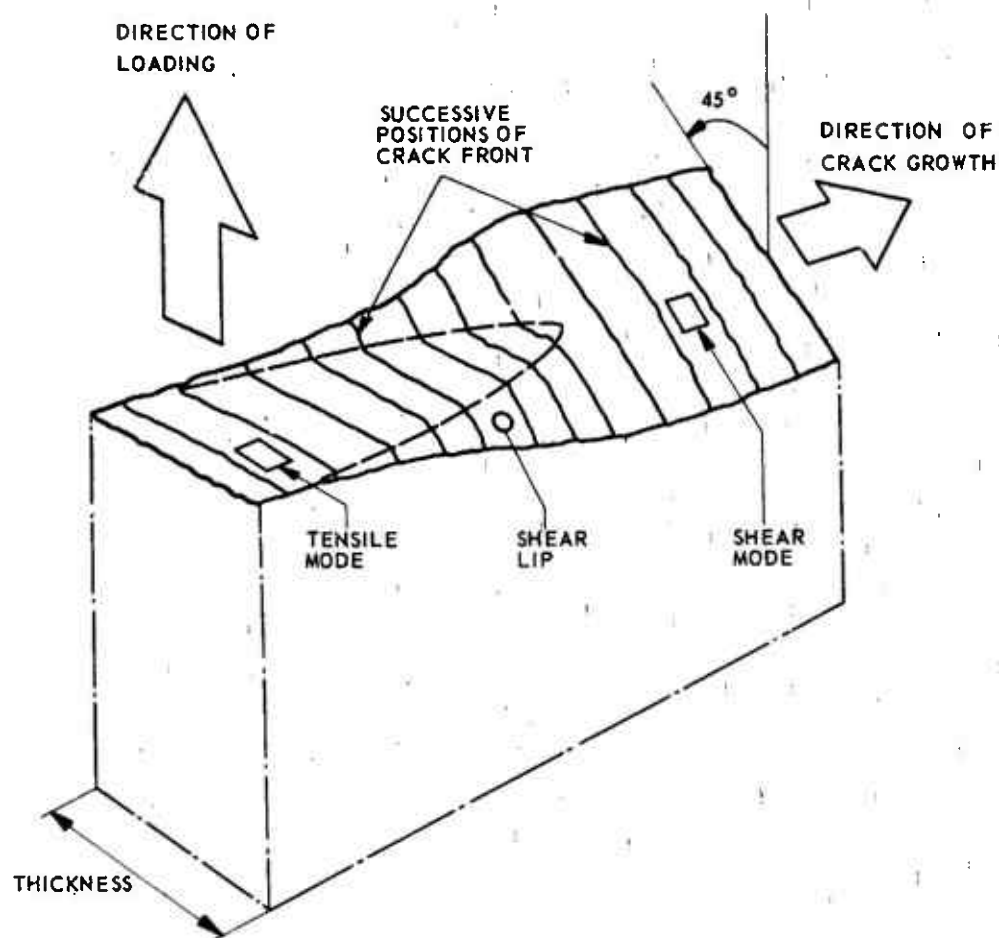
FIG. 2.4 THE SURFACE OF A FATIGUE FRACTURE IN SHEET MATERIAL DURING THE TRANSITION FROM THE TENSILE MODE (90° MODE) TO THE SHEAR MODE (45° MODE), SEE ALSO FIGURE 3.5.

2024 – T 3 SHEET SPECIMEN
WITH FATIGUE CRACK

STRESS S

A
8 mm
B

2 ℓ

160 mm

THICKNESS 2 mm
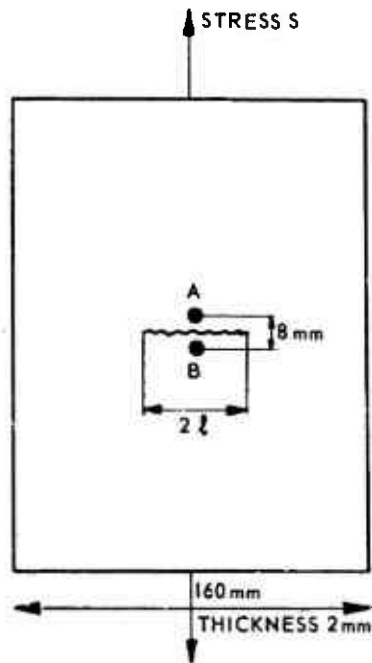
STATIC MEASUREMENT OF CRACK OPENING

S

LINEAR, CRACK FULLY OPEN

STRESS LEVEL S_o

CRACK OPENING
INCREASE OF DISTANCE A B

NON – LINEAR,
CRACK PARTLY CLOSED

TEST RESULTS (CONSTANT – AMPLITUDE FATIGUE TESTS)

FATIGUE
STRESS CYCLE

(kg/mm^2)

18
1   2   3   4
16
14
12
10
8
6
4
2
0

S_o – LEVELS

AT ℓ = 30 mm
20 mm
10 mm
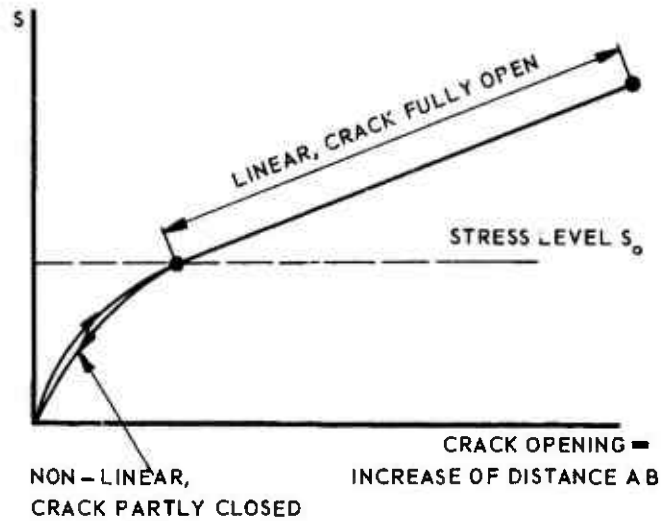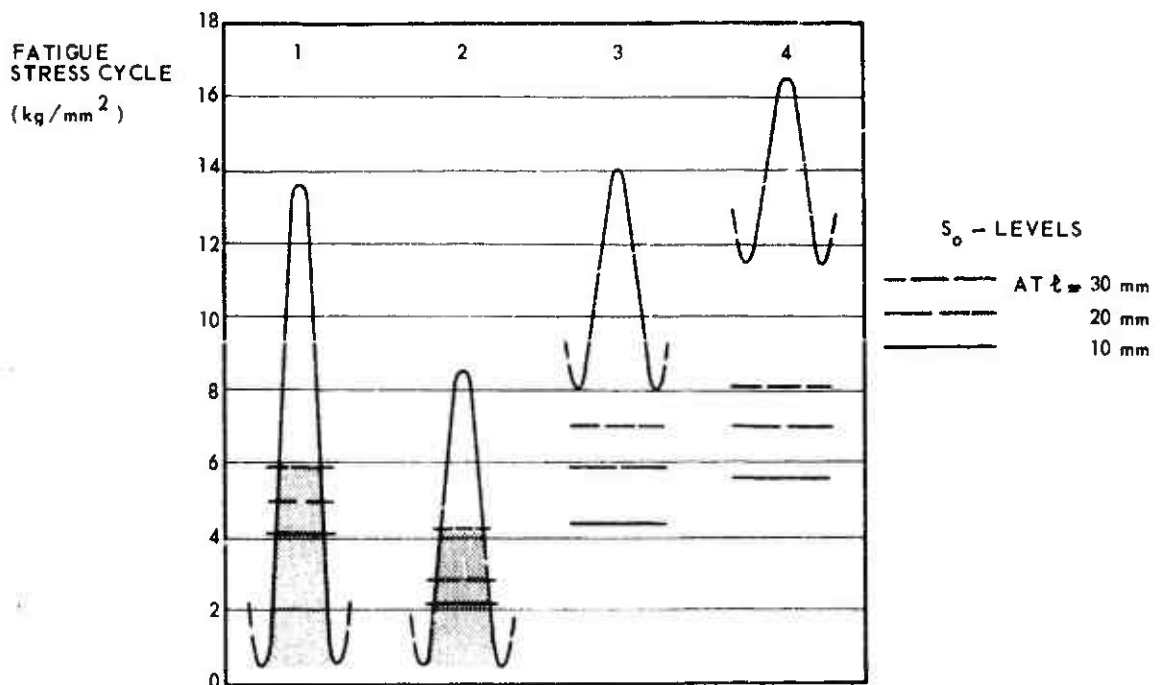
FIG. 3.1 CRACK CLOSURE ACCORDING TO ELBER (REF. 18). RESULTS FROM NLR TESTS
(REF. 20).

CRACK LENGTH ℓ
CRACK LENGTH $\ell + \Delta\ell$

$\Delta\ell$ IN A CERTAIN LOAD CYCLE WILL DEPEND ON :

a. AMOUNT OF CRACKING (CRACK LENGTH ℓ, CRACKED AREA)

b. CRACK FRONT ORIENTATION (TENSILE MODE OR SHEAR MODE) } CRACK GEOMETRY

c. CRACK BLUNTING (SHAPE OF CRACK TIP)

d. CRACK CLOSURE (PLASTIC DEFORMATION IN THE WAKE OF THE CRACK) } CONDITION OF THE MATERIAL AT THE TIP OF THE CRACK

e. CYCLIC STRAIN-HARDENING

f. RESIDUAL STRESSES

} FATIGUE DAMAGE BEING PRESENT

g. INTENSITY OF LOAD CYCLE (ΔS, S_{max})

h. ENVIRONMENT

} EXTERNAL CONDITIONS

$\Delta\ell$ WILL BE DIFFERENT FOR A, B, C, D AND E BECAUSE b, c, d, e and f ARE DEPENDENT ON THE PRE-HISTORY

A CONSTANT S_a

B DECREASE OF S_a

C INCREASE OF S_a

D SINGLE PEAK LOAD

E RANDOM LOAD

PRE-HISTORY

FIG. 3.2 CRACK EXTENSION AS EFFECTED BY THE LOAD HISTORY. INTERACTION MECHANISMS.
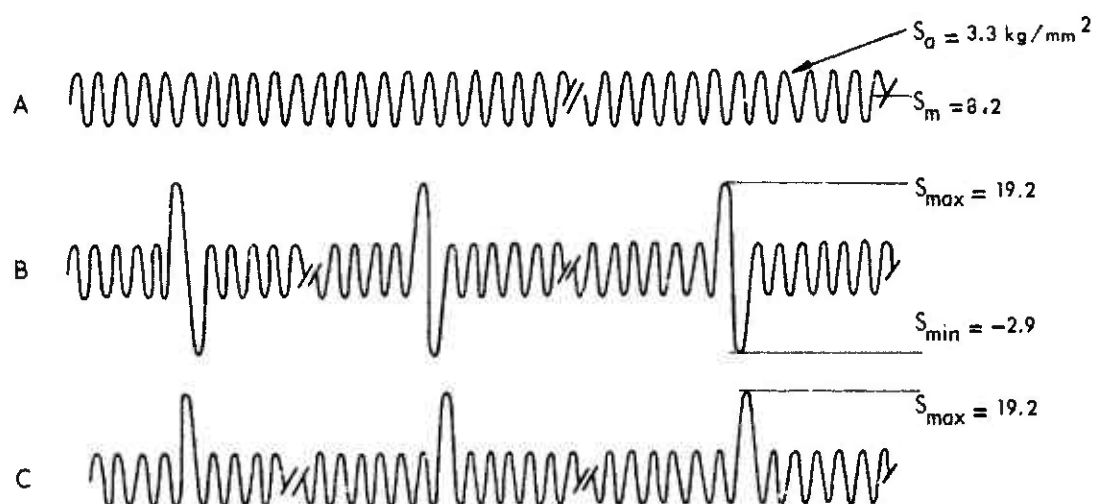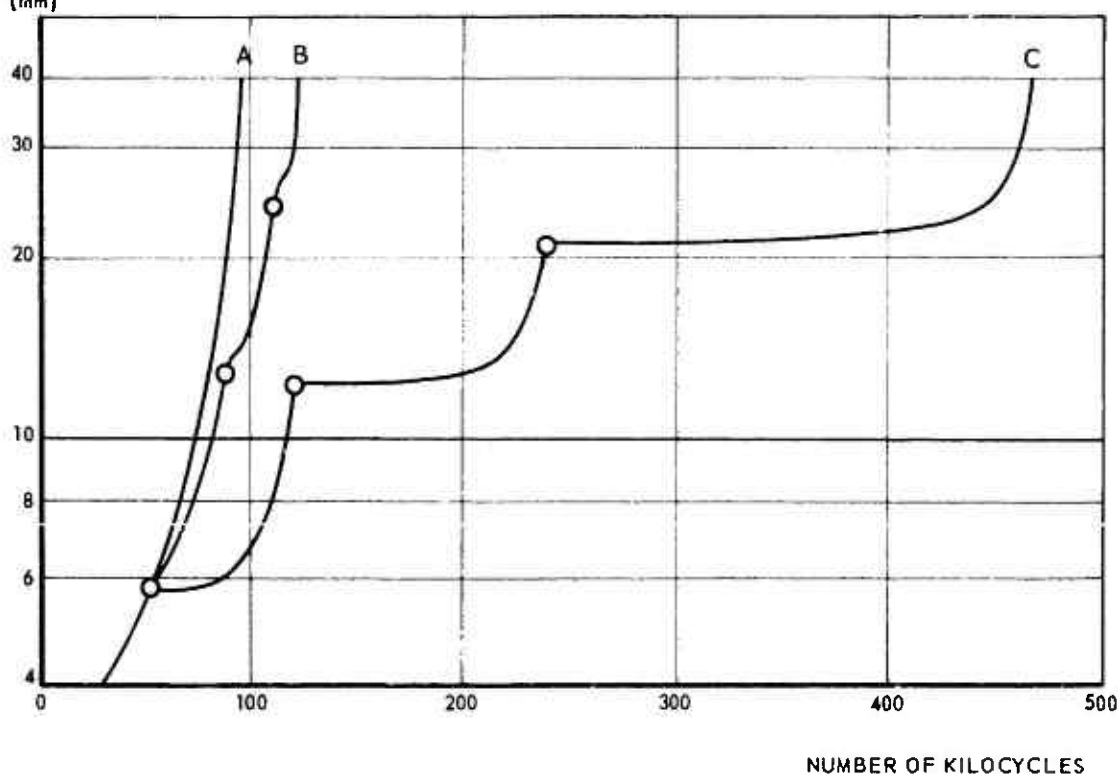
FIG. 3.3 THE DELAYING EFFECT OF PEAK LOADS ON CRACK PROPAGATION IN 2024 – T 3
ALCLAD SHEET SPECIMENS, WIDTH 160 mm, THICKNESS 2 mm (REF. 27).
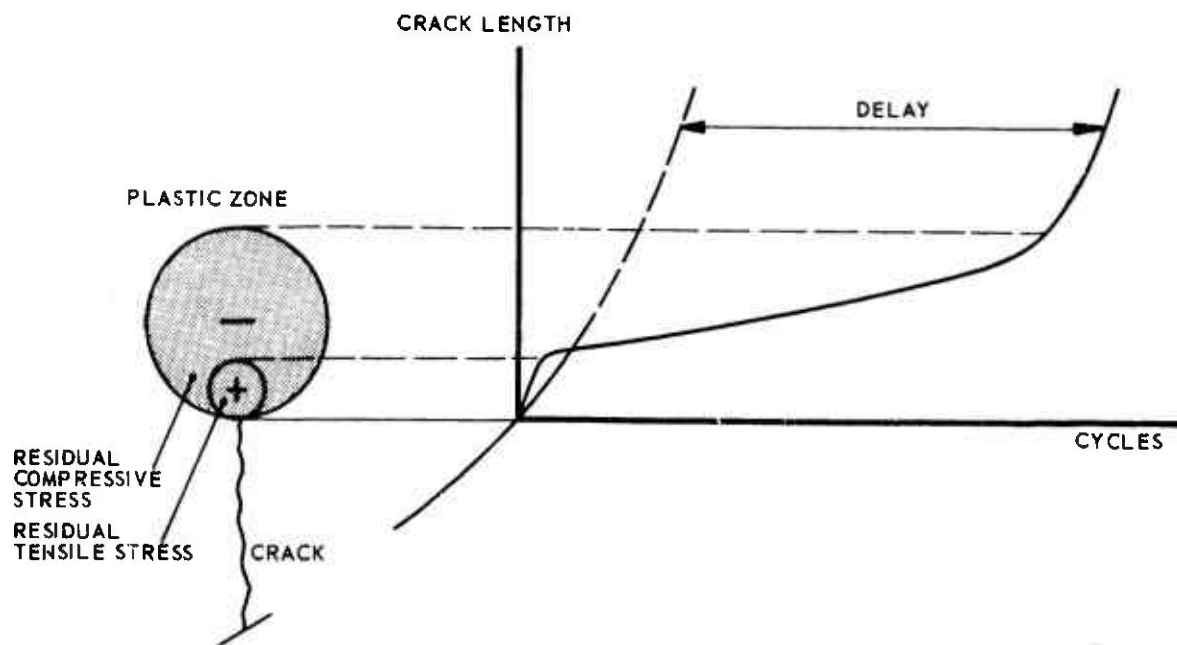
FIG. 3.4 CRACK GROWTh AFTER A PEAK LOAD CYCLE SEQUENCE b IN FIG. 7.

FIG. 3.5a HIGH – AMPLITUDE CYCLES OCCURRING AT 90° CRACK FRONT ORIENTATION
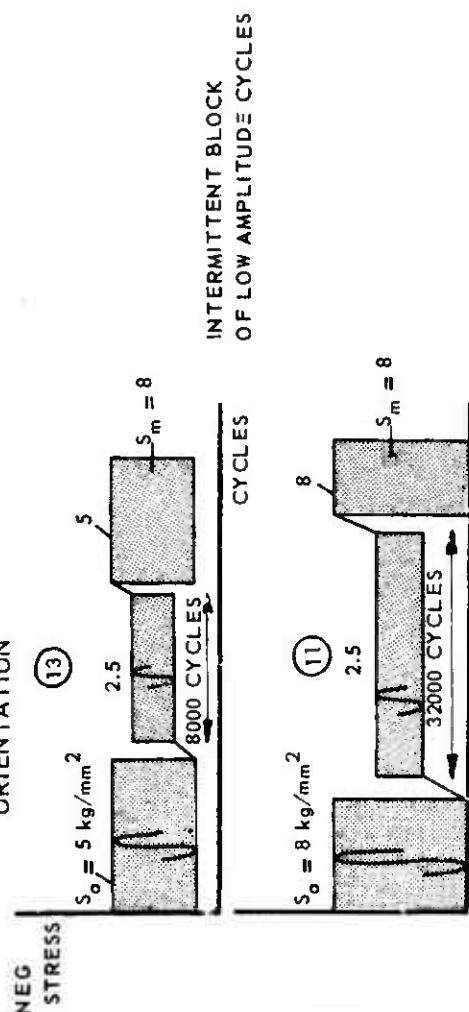
FIG. 3.5b LOW – AMPLITUDE CYCLES OCCURING AT 45° CRACK FRONT ORIENTATION.

SPECIMENS 2024 – T 3 ALCLAD WIDTH 80 mm, THICKNESS 4 mm

ARROWS INDICATE CRACK EXTENSION BY INTERMITTENT CYCLES

FIG. 3.5 INCOMPATIBILITY BETWEEN CRACK FRONT ORIENTATION AND STRESS AMPLITUDE (REF. 22).
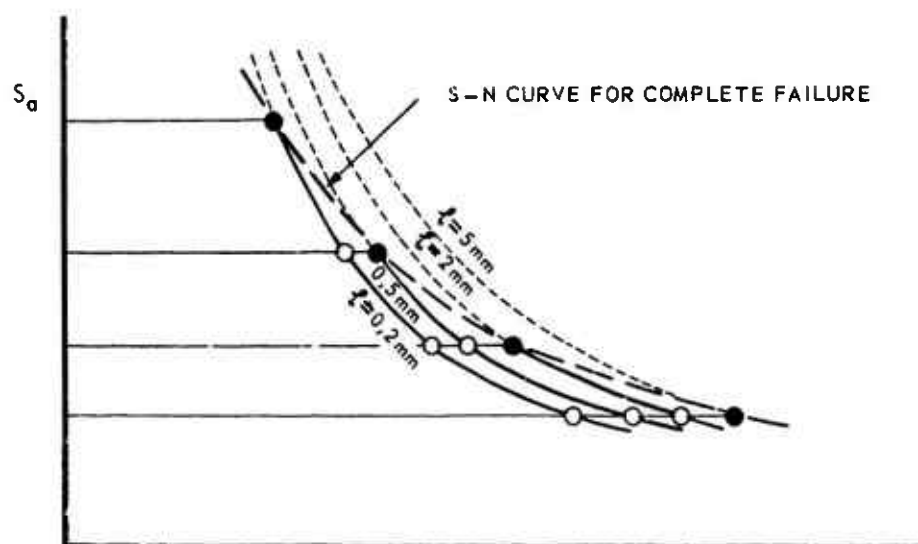
FIG. 3.6 S-N CURVES FOR CONSTANT AMOUNTS OF CRACKING
(ℓ IN MILLIMETERS) AND S – N CURVE FOR COMPLETE FAILURE .
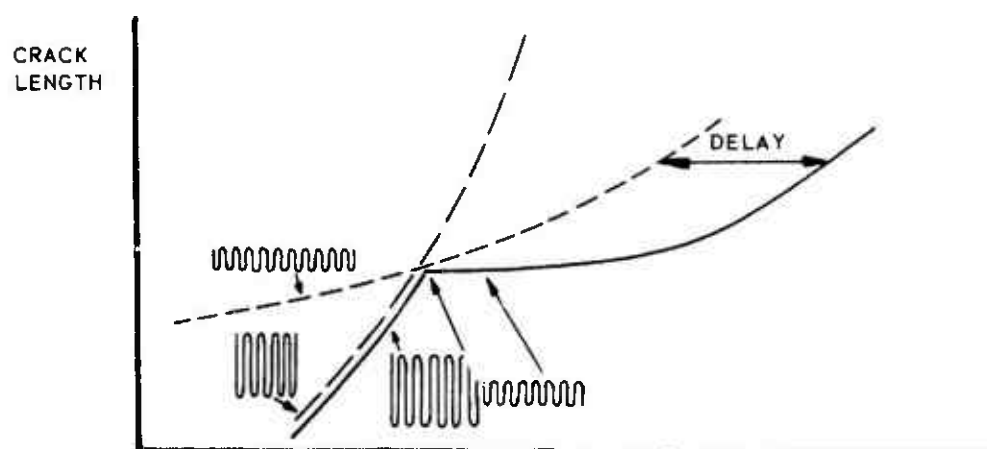
A CRACK GROWTH OELAY IN TWO-STEP TEST.
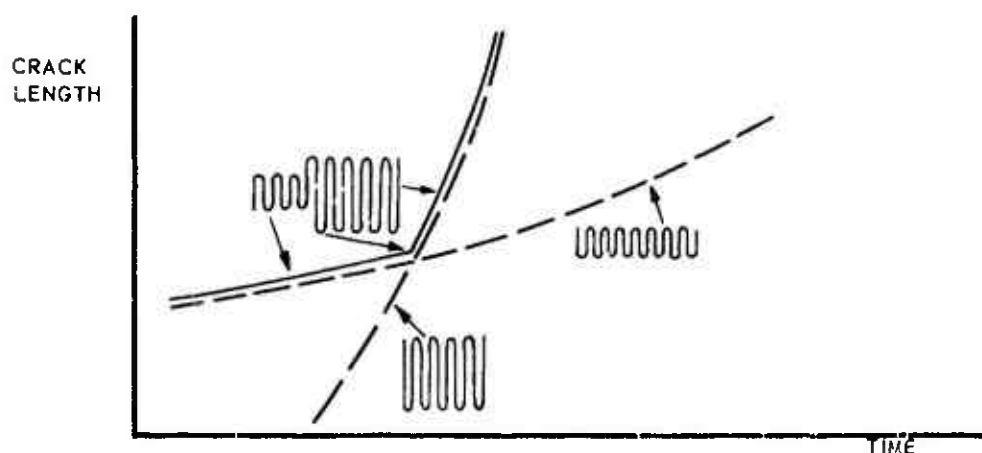
B APPARENT ABSENCE OF INTERACTION EFFECT IN TWO-STEP TEST

FIG.4. 1 MACROCRACK PROPAGATION, INTERACTION EFFECTS IN TWO–
          STEP TESTS.

A 1   TWO – STEP TEST
      WITH HI – SEQUENCE

A 2   TWO – STEP TEST
      WITH LD –HI SEQUENCE

B   INTERVALTEST
      PERIODIC REPETITIDN DF
      LOAD CYCLES

C   SINGLE HIGH PRELDAD

D   PERIDDIC HIGH LOADS
      HIGH LDADS MAY BE EITHER
      UPWARDS DR DDWNWARDS,DR
      BDTH, SEE FIG.3.3

E   SUPERPOSITION OF TWD
      CYCLIC LOADS WITH
      DIFFERENT FREQUENCEES
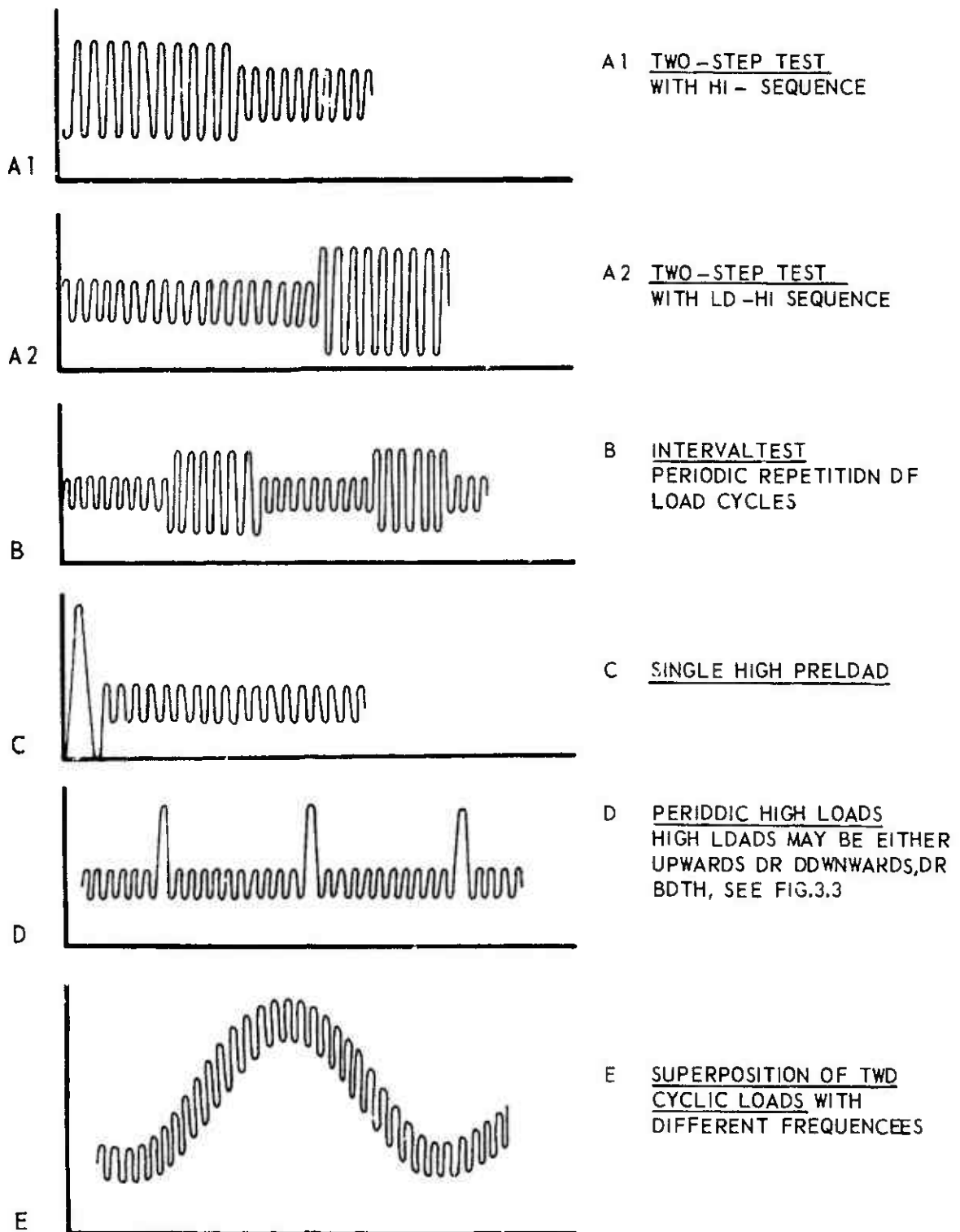
FIG. 4.2 SEVERAL SIMPLE TYPES DF VAVIABLE – AMPLITUDE LOADING.
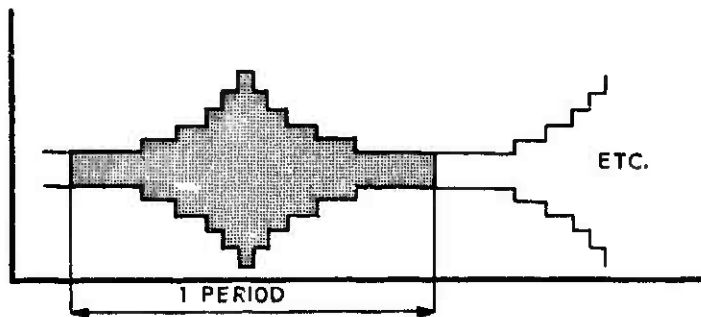
F PROGRAM LOADING WITH
   LO – HI – LO SEQUENCE.
   LO – HI AND HI – LO SEQUENCES
   WERE ALSO ADOPTED, SEE
   FIGURE 4.17
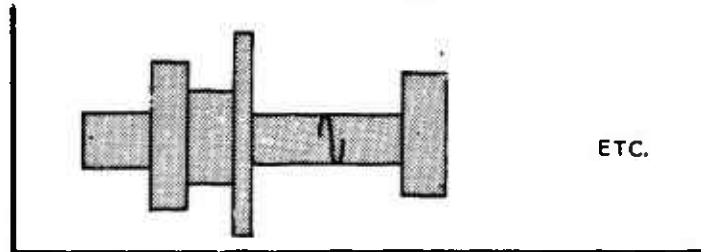
G RANDOMIZED BLOCK LOADING
   SIMILAR TO PROGRAM LOADING,
   HOWEVER, BLOCKS OF CYCLES
   IN RANDOMIZED SEQUENCE
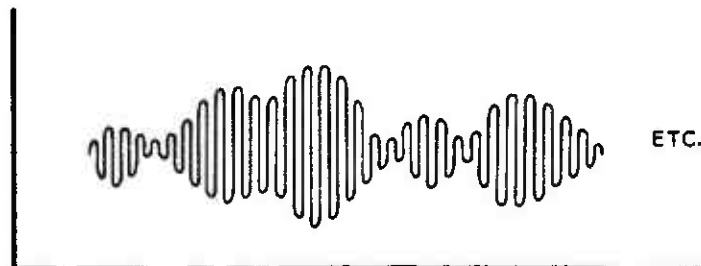
H NARROW – BAND RANDOM LOA-
   DING (SEE FIG 4.20)
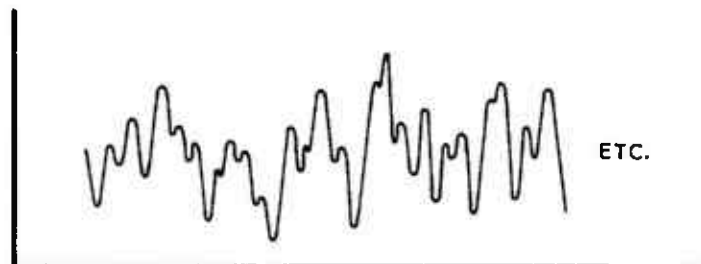
J BROAD – BAND RANDOM LOA-
   DING (SEE FIG 4.20)

K QUASI – RANDOM LOADING
   PSEUDO – RANDOM LOADING
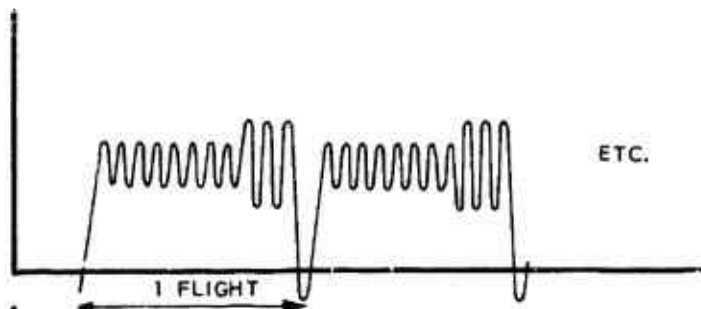
L SIMPLE FLIGHT – SIMULATION
   LOADING ALL FLIGHTS SIMILAR
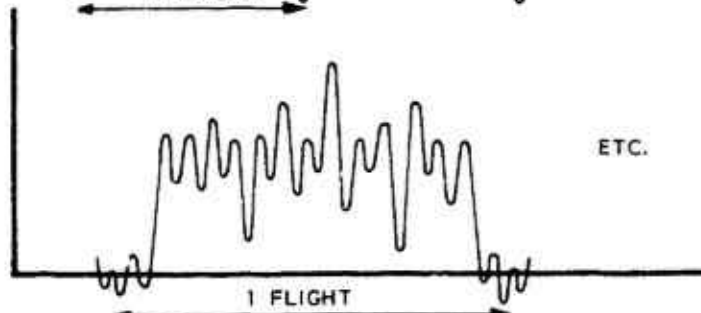
M COMPLEX FLIGHT – SIMULATION
   LOADING
   DIFFERENTS FLIGHTS, SEE FIG.
   7.3

FIG.4.3 SEVERAL TYPES OF COMPLEX FATIGUE LOAD HISTORIES.
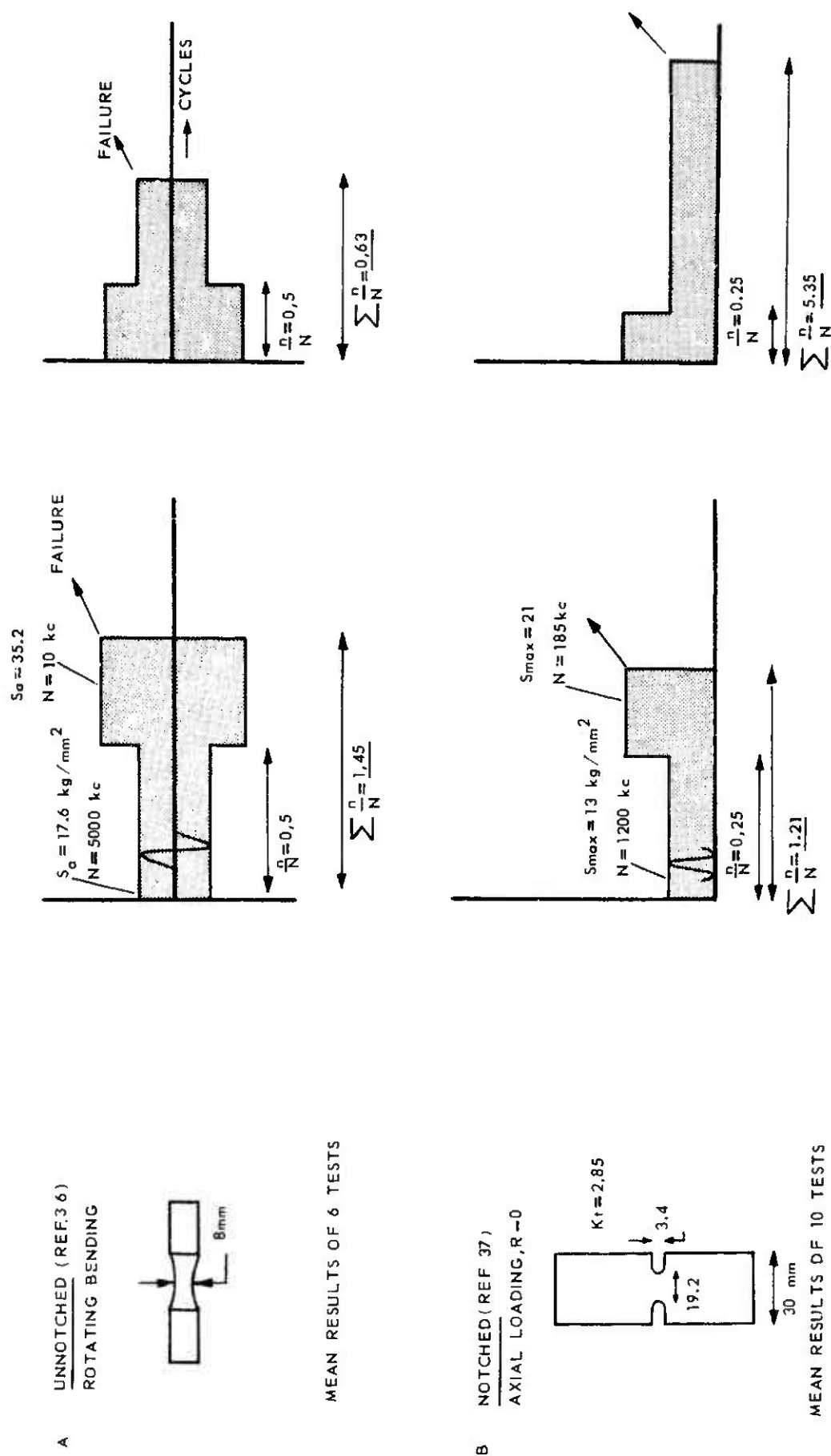
FIG. 4.4 OPPOSITE INTERACTION EFFECTS IN TWO-STEP TESTS ON UNNOTCHED AND NOTCHED AL-ALLOY SPECIMENS.
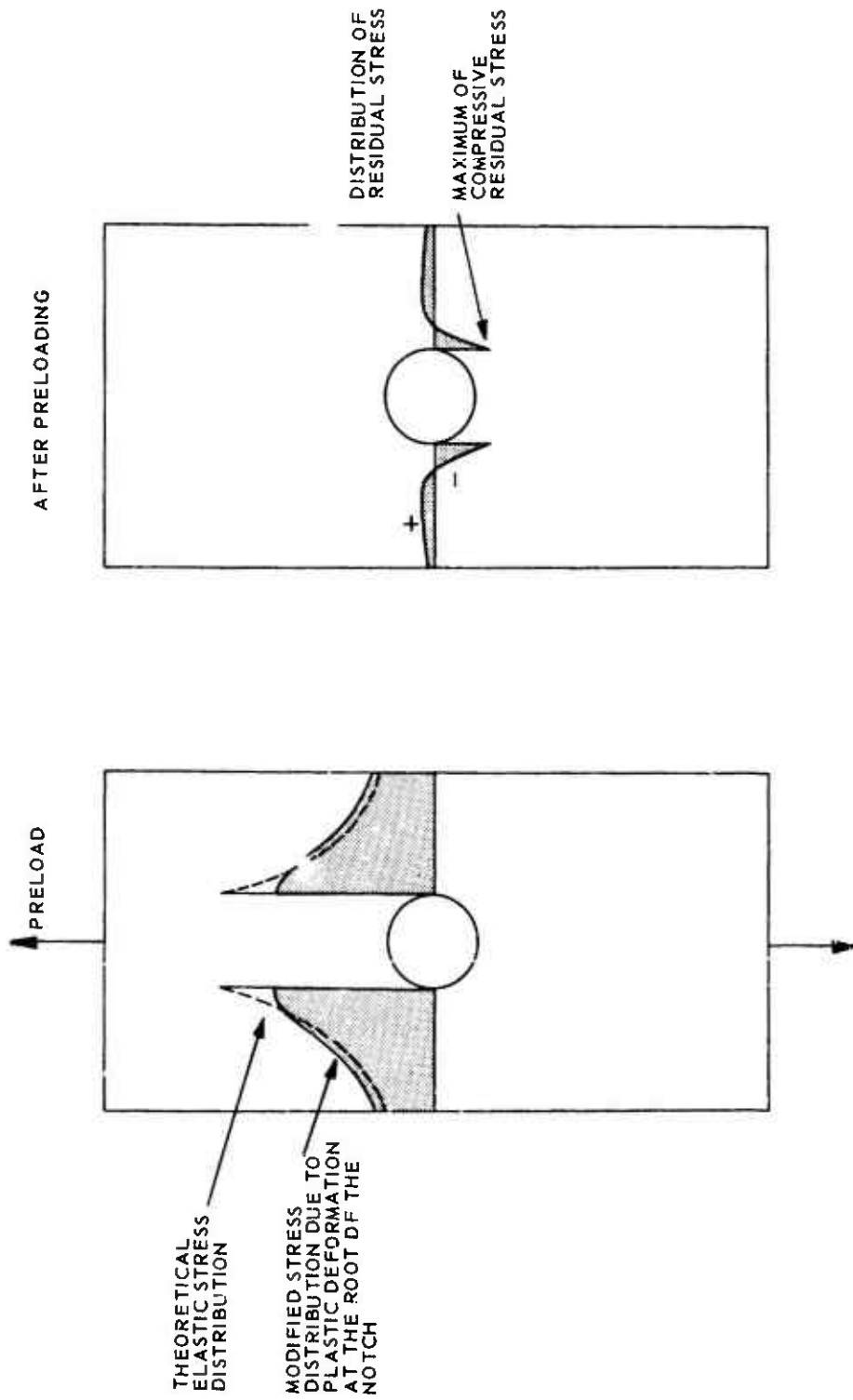
FIG. 4.5 RESIDUAL STRESS INTRODUCED BY PRELOADING IN TENSION. SPECIMEN NOTCHED BY A CENTRAL HOLE

Kt = 3.5   A   CONSTANT – AMPLITUDE TESTS ON TI – ALLOY SPECIMENS (R=0.1)
RESULTS FROM BOISSONAT(REF.46)

Kt = 2.96   B   NARROW – BAND RANDOM LOAD TEST ON AL – ALLOY LUG SPECIMENS
($S_m = 10 \, kg/mm^2$) RESULTS FROM KIRKBY AND EDWARDS (REF.50)
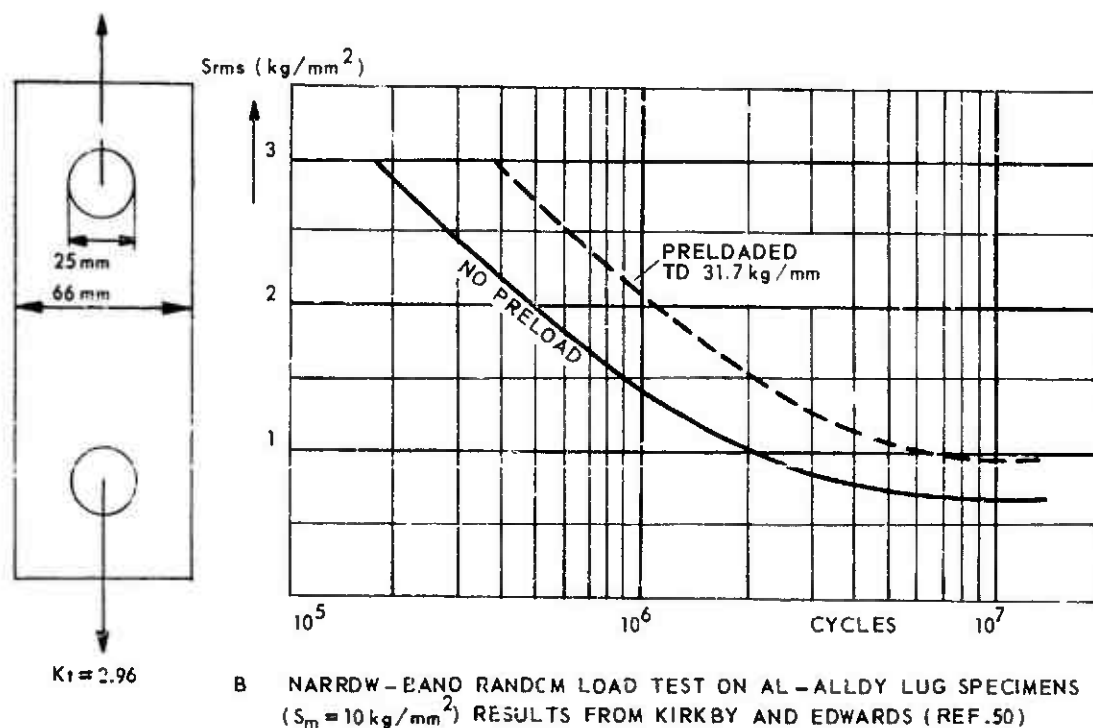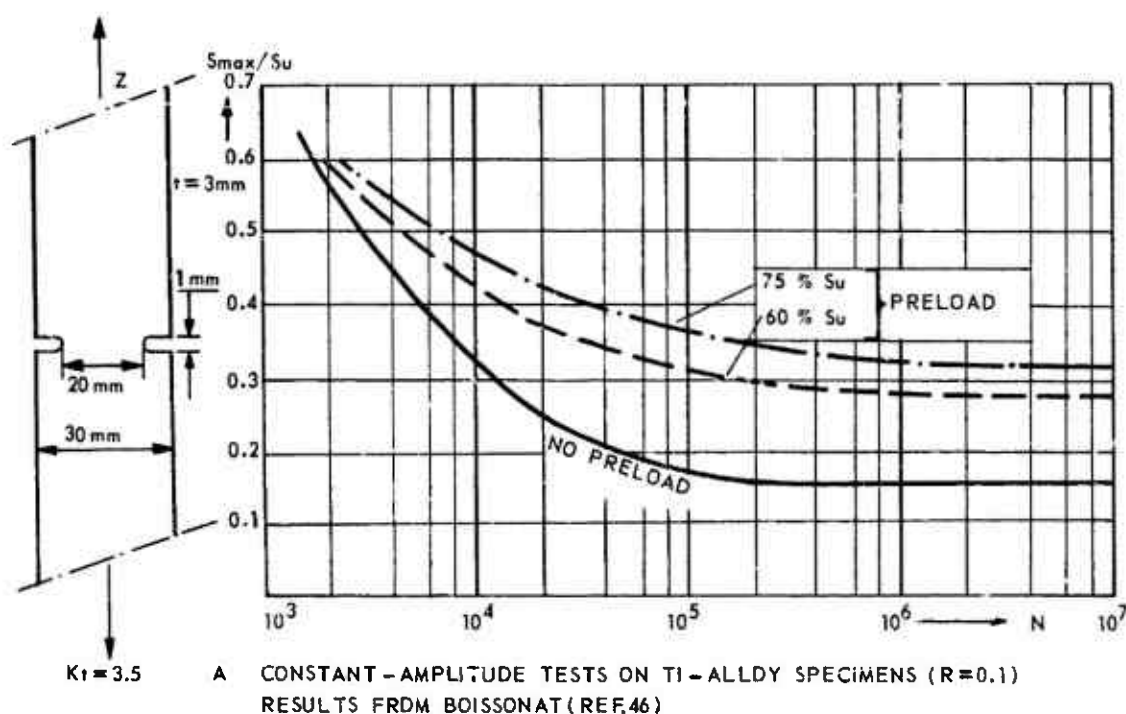
FIG.4.6 THE EFFECT OF A PRELOAD ON FATIGUE CURVES FOR CONSTANT – AMPLITUDE
LOADING AND NARROW – BAND RANDOM LOADING.

3-88
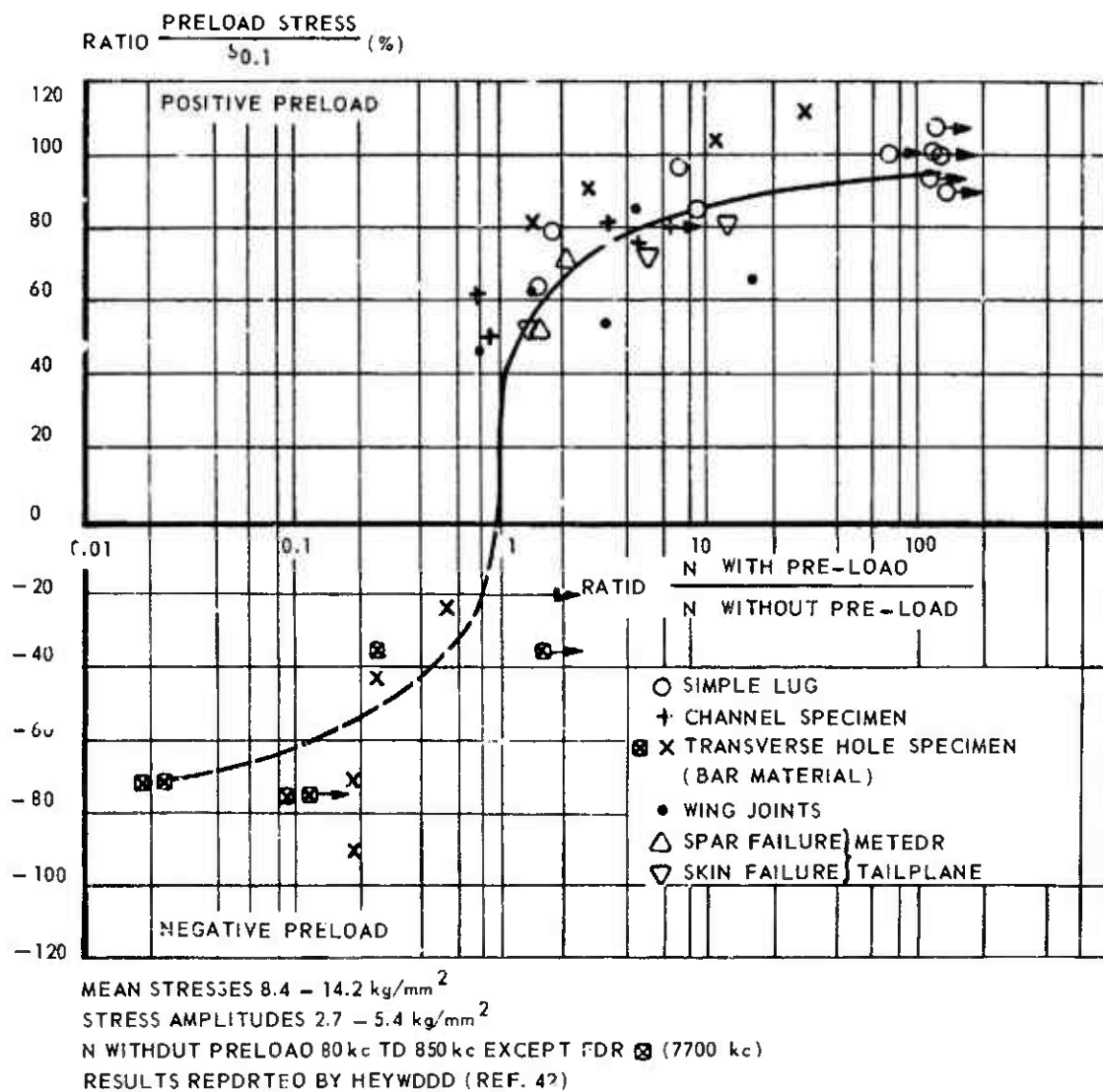
FIG. 4.7 EFFECT OF THE MAGNITUDE OF A PRELOAD ON FATIGUE LIFE UNDER
CONSTANT – AMPLITUDE LOADING.
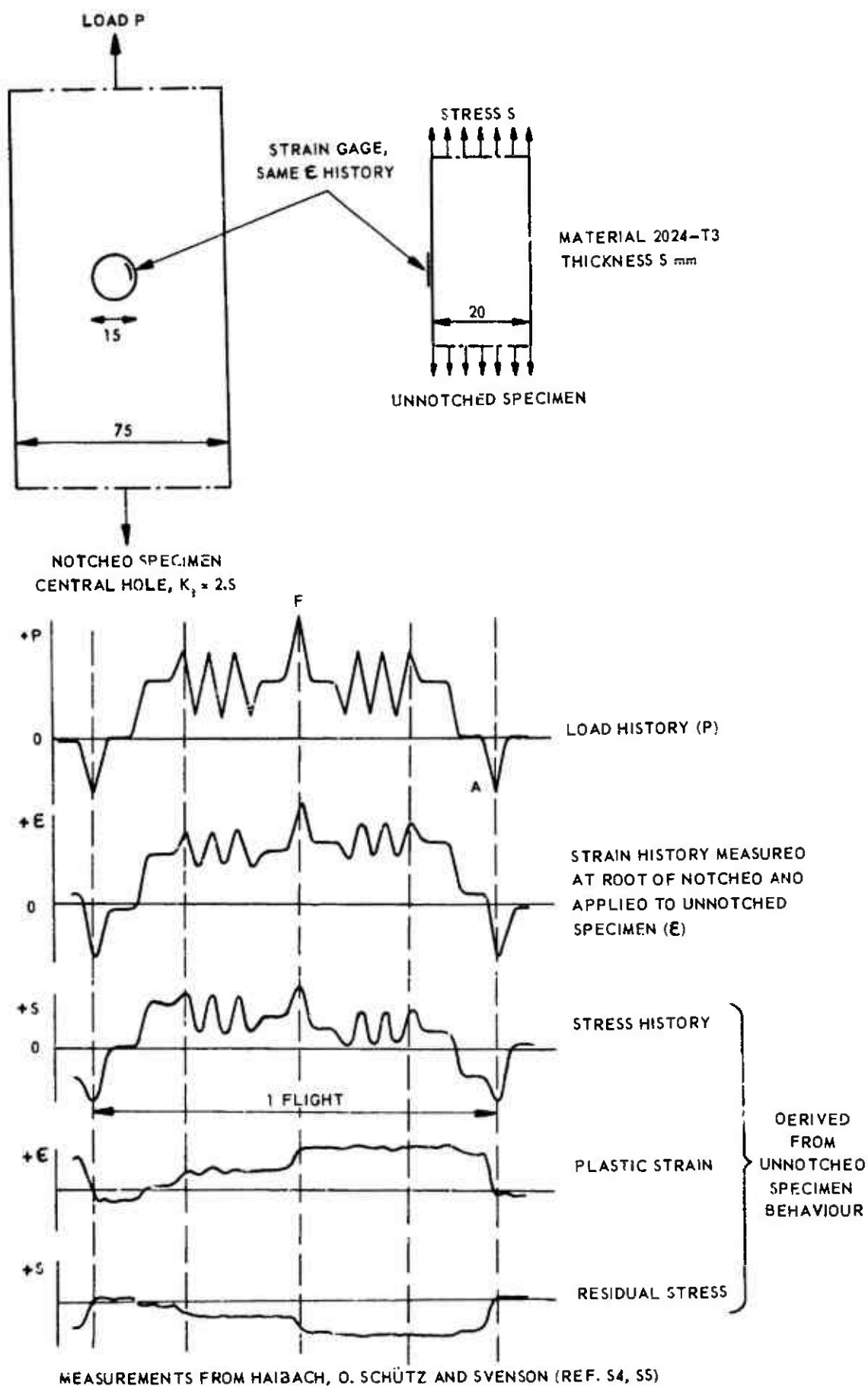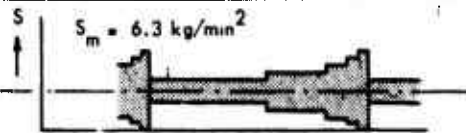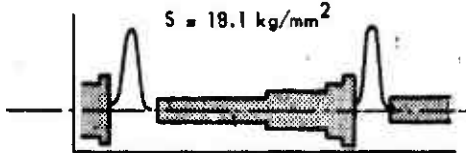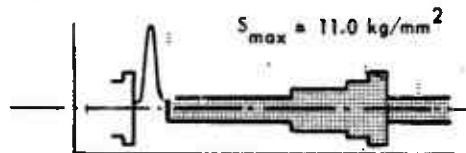
FIG. 4.8 DETERMINATION OF RESIDUAL STRESS AT THE ROOT OF A NOTCH DURING A SIMPLE FLIGHT—SIMULATION LOADING

TEST SERIES	LOADING SEQUENCE	REMARKS	FATIGUE LIFE (PERIODS)
10	$S_m = 6.3$ kg/min^2	PROGRAMMED GUST CYCLES	11
6	$S = 18.1$ kg/mm^2	1 HIGH LOAD PER PERIOD	126
6a		HIGH LOADS OMITTED AFTER 50th PERIOD	58
6b	$S_{max} = 11.0$ kg/mm^2	1 HIGH LOAD PER 2 PERIODS	40
17		SIMILAR TO SERIES 6 BUT GUST CYCLES IN REVERSED ORDER	22

RESULTS FROM REF. 39
FATIGUE LIFE IN PROGRAM PERIODS, 1 PERIOD = 81500 CYCLES
EACH RESULT IS THE MEDIAN OF 7 TESTS.

FIG. 4.9 THE EFFECT OF PERIODIC HIGH LOADS ON THE PROGRAM – FATIGUE LIFE OF 7075 – T6 RIVETED LAP JOINTS.
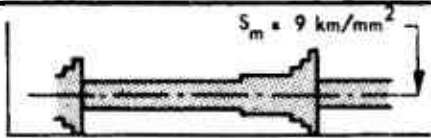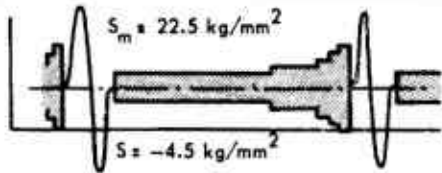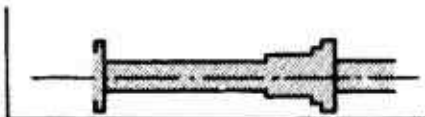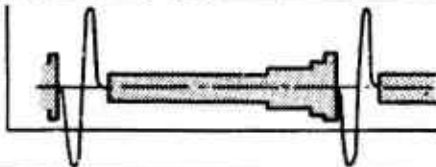
TEST SERIES	LOADING SEQUENCE	REMARKS	FATIGUE LIFE (PERIODS)
21	$S_m = 9$ km/mm²	PROGRAMMED GUST CYCLES (5 ampl.)	31
27	$S_m = 22.5$ kg/mm² $S = -4.5$ kg/mm²	HIGH LOAD CYCLE IN POS.-NEG. SEQUENCE	11
24		PROGRAMMED GUST CYCLES (4 AMPL.)	14
28		HIGH LOAD CYCLE IN NEG.-POS. SEQUENCE	85

FIG. 4.10 THE EFFECT OF THE SEQUENCE OF A PERIODIC HIGH LOAD CYCLE ON THE PROGRAM–FATIGUE LIFE OF 2024–T3 RIVETED LAP JOINTS.
RESULTS FROM REF. 39
FATIGUE LIFE IN PROGRAM PERIODS, 1 PERIOD = 432300 CYCLES
EACH RESULT IS THE MEDIAN OF 7 TESTS

SEQUENCE a   SEQUENCE b (HIGHER GUST AT
                                                        END OF FLIGHT)

STRESS
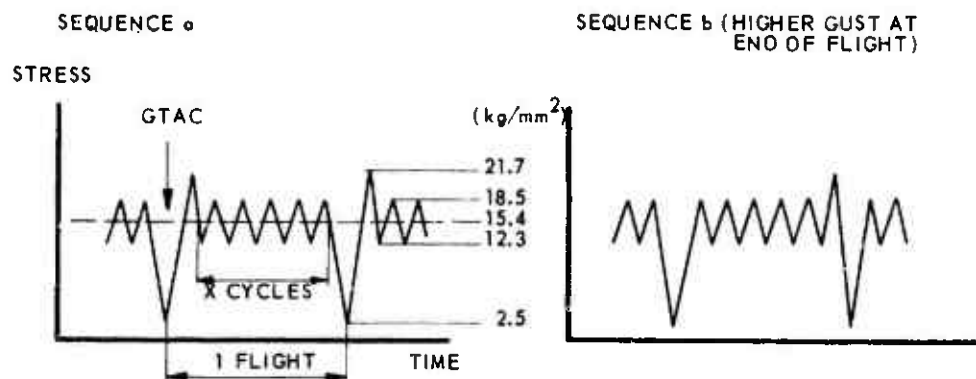
SPECIMEN : RIVETEO LAP JOINT, 2 ROWS OF 5 RIVETS, 2024 – T3 MATERIAL

CYCLES PER FLIGHT (X)		5	10	49	99	999
LIFE	CYCLES a	19740	30380	S8400	S98S0	12S800
	CYCLES b	22400	28350	S1500	55431	84600
	FLIGHTS a	3290	2762	1168	598	126
	FLIGHTS b	3733	2577	1010	SS4	85
$\sum n / N$	a	0.53	0.51	0.44	0.37	0.63
	b	0.60	0.48	0.38	0.34	0.42

ALL OATA ARE THE MEAN OF THREE TESTS
FOR GUSTS ONLY N = 20S300 CYCLES. FOR GTAC ONLY (S_{max} = 21.7 ANO S_{min} = 2.S kg/mm^2)
N = 7360 CYCLES
RESULTS REPORTEO BY BARROIS (REF. 70)

FIG. 4.11 THE EFFECT OF GROUND–TO–AIR CYCLES ON THE FATIGUE LIFE IN A
SIMPLIFIED FLIGHT SIMULATION TEST.

MATERIAL	LOAD SPECTRUM	S_{min} IN GTAC (kg/mm^2)	LIFE (FLIGHTS)
7075 – T6	SEVERE GUST SPECTRUM	0	2699
		–7.0	1334
Ti–8Al–IMo–IV	FAIRLY SEVERE SPECTRUM	0	>52000
	REPRESENTATIVE OF A SUPERSONIC	–10.S	16600
	TRANSPORT. TESTS AT ROOM TEMPERA - TURE	–21.1	8500

707S – T6 SHEET SPECIMENS, TWO EOGE NOTCHES, K_t = 4
Ti–8Al–IMo–IV, Ti ALLOY SHEET SPECIMENS, QUASI ELLIPTICAL HOLE, K_t = 4
ALL DATA ARE THE MEAN OF 5 – 7 TESTS
RESL ⁀S REPORTEO BY NAUMANN (REF. 67) ANO BY IMIG ANO ILLG (REF. 80).

FIG. 4.12 THE EFFECT OF THE MINIMUM STRESS OF THE GROUND–TO–AIR CYCLE
ON THE FATIGUE LIFE IN RANDOM FLIGHT SIMULATION TESTS.

MATERIAL	CRACK PROPAGATION LIFE (FLIGHTS)		RATIO
	WITHOUT GTAC	WITH GTAC	
7075–T6	7518	5062	1.5
2024–T3	20869	11781	1.8

SHEET SPECIMENS WITH A CENTRAL CRACK, SPECIMEN WIDTH 160 mm.
CRACK LIFE COVERS PROPAGATION FROM $2\ell \approx 20$ mm TO COMPLETE FAILURE.
FLIGHT SIMULATION LOADING WITH GUST SPECTRUM, $S_m = 7.0$ kg/mm^2, S_{min} IN GTAC $= -3.4$ kg/mm^2
ALL DATA ARE MEAN RESULTS OF 4 TESTS.
RESULTS REPORTED BY SCHIJVE, JACOBS AND TROMP (REFS. 77, 78)

FIG. 4.13   EFFECT OF THE GTAC ON CRACK PROPAGATION LIFE UNDER FLIGHT
SIMULATION LOADING.
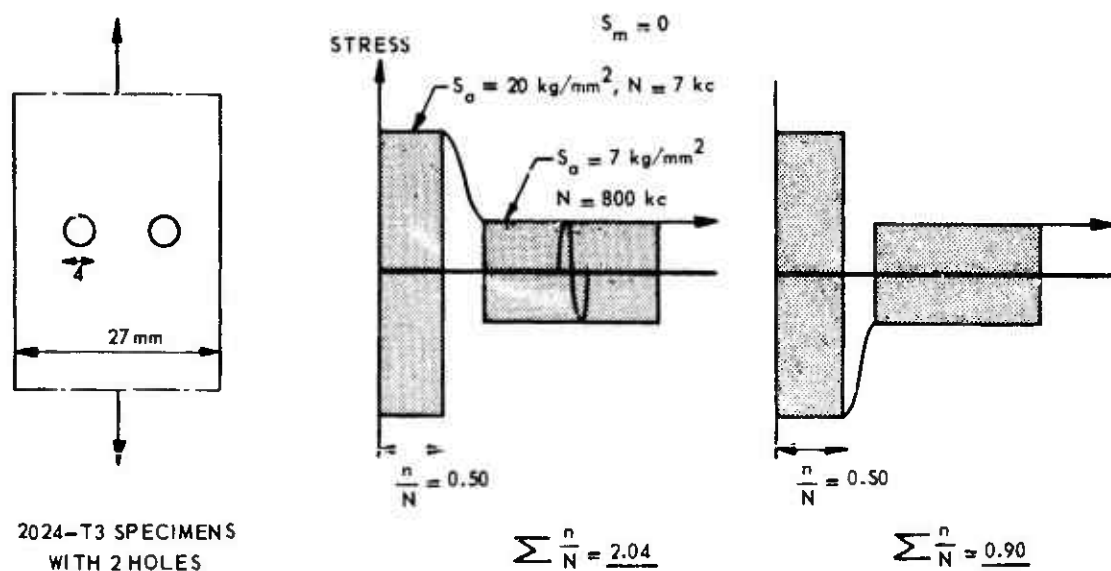
RESULTS REPORTED BY WÅLLGREN (REF. 81), MEAN VALUES OF 9 TESTS

FIG. 4.14   TWO–STEP TESTS WITH DIFFERENT WAYS FOR CHANGING THE AMPLITUDE

CRACK PROPAGATION TESTS ON 2024 – T 3 ALCLAD SHEET SPECIMENS (WIDTH 160 mm, t = 2 mm)
RESULTS FROM REFS. 96, 97 MEAN VALUES OF 2 – 4 TESTS.
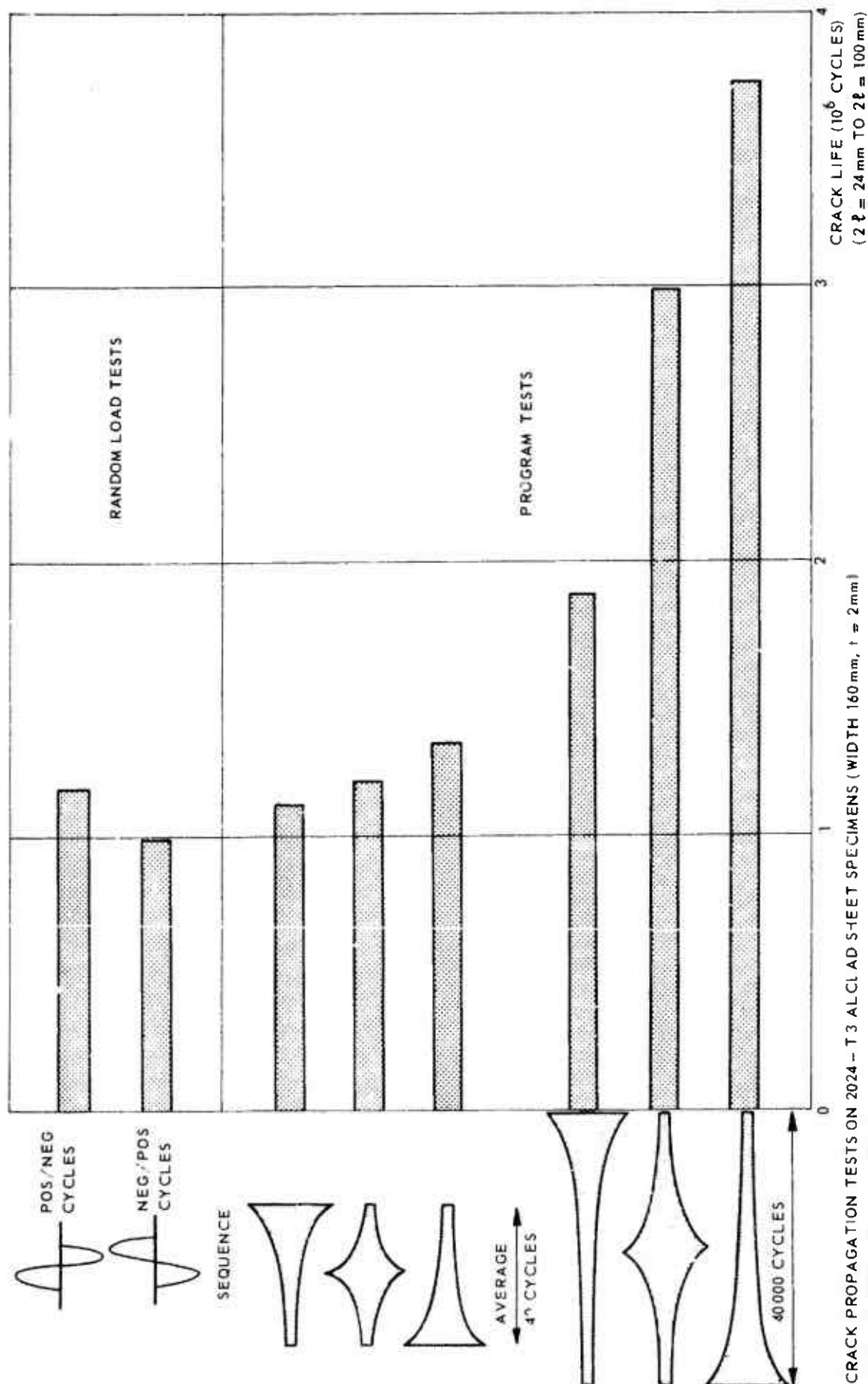
FIG. 4.16 EFFECTS OF LOAD SEQUENCE AND SIZE OF PERIOD ON PROGRAM FATIGUE LIFE. COMPARISON WITH RANDOM LOAD TEST RESULTS.
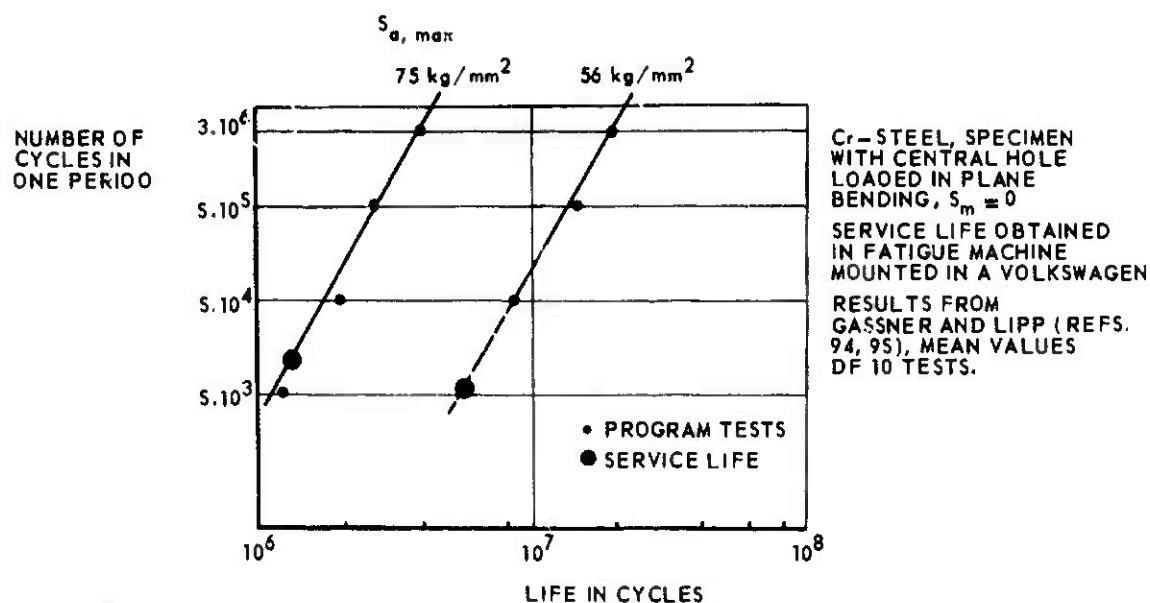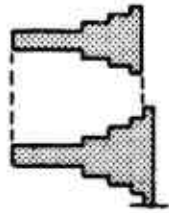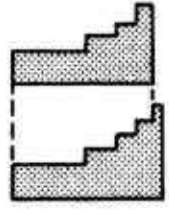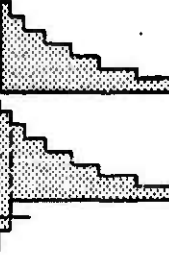
FIG. 4.15 EFFECT OF SIZE OF PERIOD ON PROGRAM FATIGUE LIFE AND COMPARISON
WITH RANDOM LOAD FATIGUE LIFE
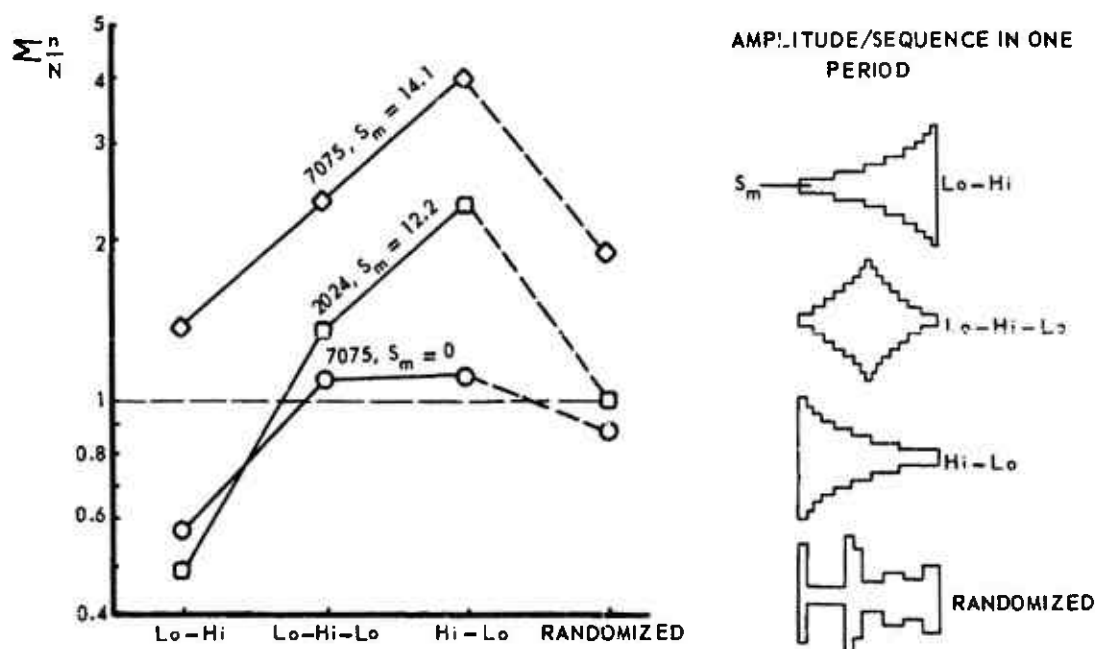
TESTS ON EDGE NOTCHED SPECIMENS, $K_t = 4$, S_m IN kg/mm^2 RESULTS REPORTED BY HARDRATH ET
AL (REFS. 30,31), MEAN VALUES OF 3 – 4 TESTS.

FIG. 4.17 THE EFFECT OF THE AMPLITUDE SEQUENCE ON THE FATIGUE LIFE IN PROGRAM
TESTS.

SPECIMEN SPECTRUM	S_a – SEQUENCE IN DNE PERIOD	LIFE		LIFE RATID		EFFECT DF ADDING
		CYCLES	$\Sigma n/N$	CYCLES/CYCLES	Σ/Σ	HIGH S_a – CYCLES
RIVETED JDINT 2024–T3		6 130 000	1.31			
GUST SPECTRUM (REF. 39)		13 060 000	2.90	2.14	2.21	INCREASED LIFE
TAIL PLANE 707S–T6		44 000	3.0			
MANEUVER SPECTRUM (REF. 48)		91 800	6.S	2.08	2.17	INCREASED LIFE
EDGE NDTCHED SPECIMEN		41 S20	2.16			
707S–T6 MANEUVER SPECTRUM (REF. 87)		17 730	1.31	0.43	0.61	REDUCED LIFE

OATA ARE MEAN VALUES OF 7,7, 3, 1, 7 AND 6 TESTS RESPECTIVELY.

FIG. 4.18 DIFFERENT EFFECTS OF HIGH–AMPLITUDE CYCLES IN PROGRAM TESTS.

RIVETED JOINT	S_m (kg/mm^2)	S_a –VALUES BELDW FATIGUE LIMIT	LIFE		RATID	
			PERIDDS	CYCLES(KC)	PERIOD/PERIOO	CYCLE/CYCLE
2024–T3 DOUBLE LAP JOINT	3.5	3	1S	166 000	1.1	160
		DMITTED	16	1 040		
7075–T6 SINGLE STRAP JCINT	9.3	1	98	3 080	1.3	3.3
		OMITTED	129	900		
	4.7	2	20	107 000	1.7	16
		OMITTED	34	6 S00		

RESULTS REPDRTEO BY WALLGREN (REF. 83). ALL DATA ARE MEAN VALUES DF 2–4 TESTS.

FIG. 4.19 THE EFFECT OF OMITTING LOW–AMPLITUDE CYCLES FROM A PROGRAM TEST ON FATIGUE LIFE AND TESTING TIME.
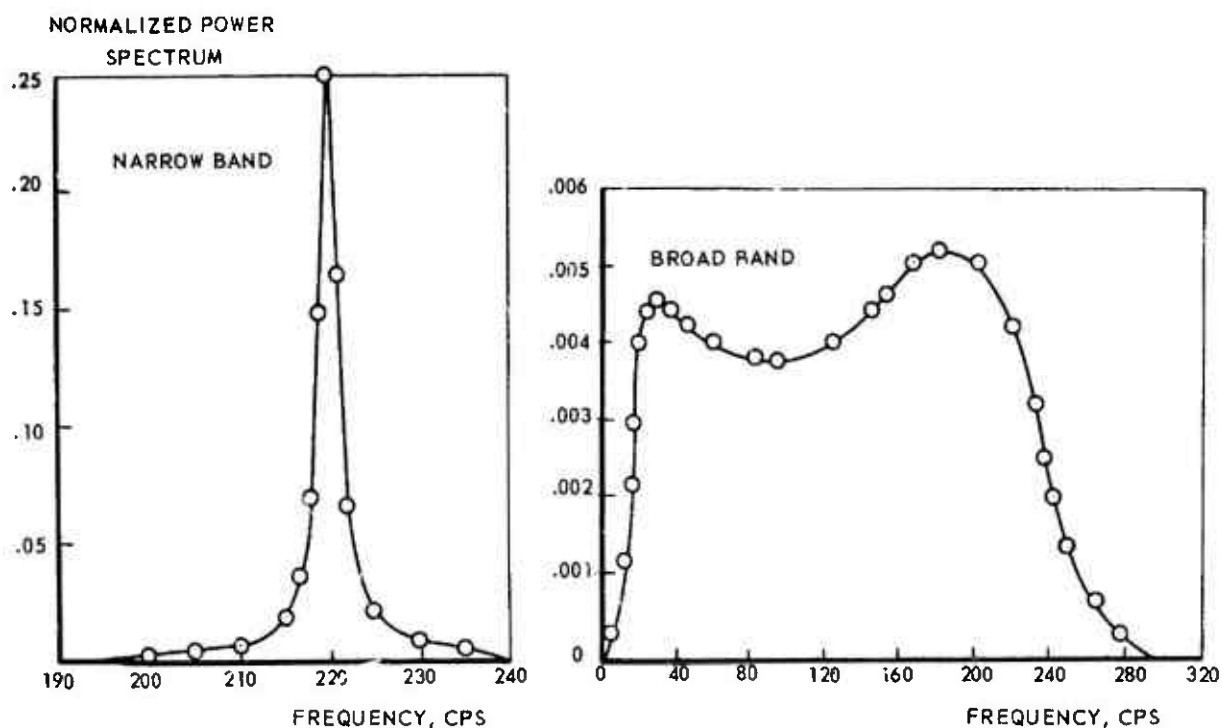
a. POWER SPECTRA NORMALIZED TO GIVE UNIT AREA UNDER THE CURVE.
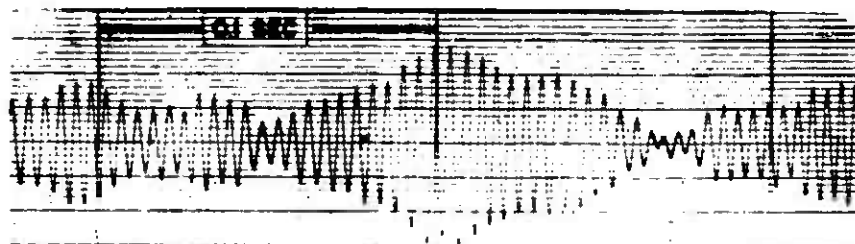
NARROW BAND
IRREGULARITY FACTOR ~ 1
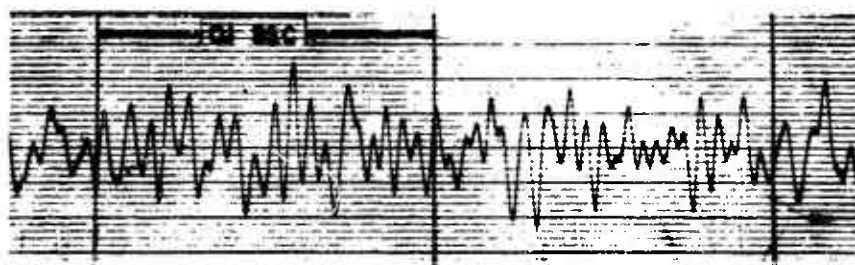
BROAD BAND
IRREGULARITY FACTOR 0.79

b. STRESS-TIME HISTORY FOR NARROW-BAND AND BROAD-BAND LOADING.

FIG. 4.20 ILLUSTRATION OF THE EFFECT OF THE POWER SPECTRAL DENSITY FUNCTION ON THE LOAD-TIME HISTORY (REF. 101)

SEQUENCE	EXAMPLE OF SEQUENCE	RANDOM LOAD TESTS		FLIGHT – SIMULATION TESTS	
		FATIGUE LIFE (CYCLES)	RATIO	FATIGUE LIFE (FLIGHTS)	RATIO
RANDOMIZED BLOCK (PROGRAM TEST)	SEE FIG. 4.17	617 000	1.56		
RANDOM SEQUENCE OF COMPLETE CYCLES		395 500	1	1 334	1
RANDOM SEQUENCE OF HALF CYCLES, ALTERNATELY POS. AND NEG.		504 700	1.28	1 515	1.14
RANDOM SEQUENCE OF HALF CYCLES NO RESTRICTION ON SEQUENCE OF POS. AND NEG.		598 300	1.51	1 588	1.19

TESTS ON EDGE NOTCHED 7075 – T 6 SPECIMENS ($K_t = 4$). GUST SPECTRUM
RESULTS REPORTED BY NAUMANN (REF. 67), MEAN VALUES OF 6 TESTS

FIG. 4.21   THE EFFECT OF THE CYCLE SEQUENCE IN RANDOM LOADING AND FLIGHT–SIMULATION LOADING.
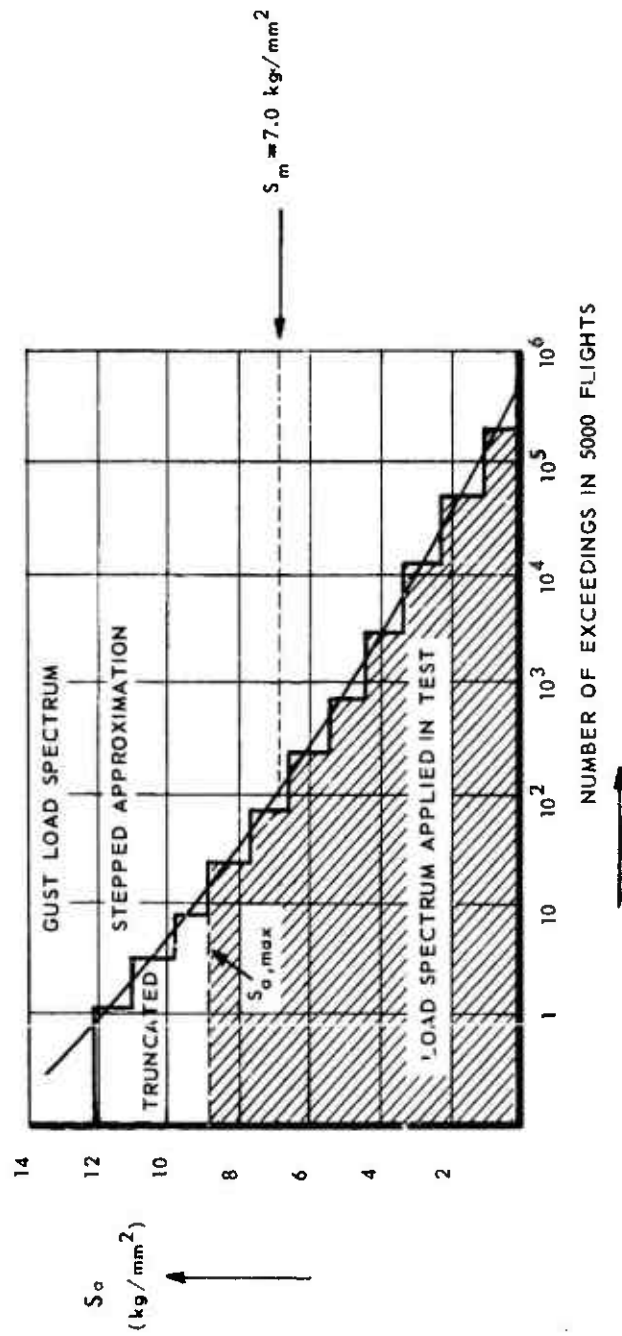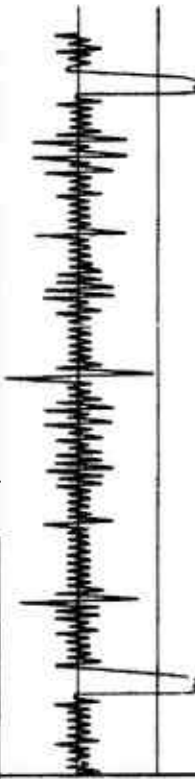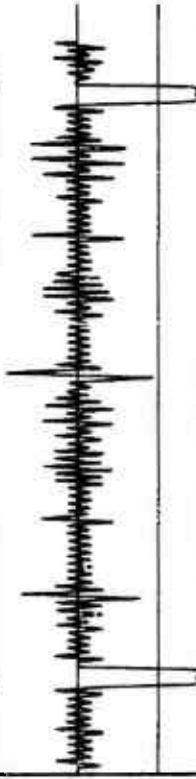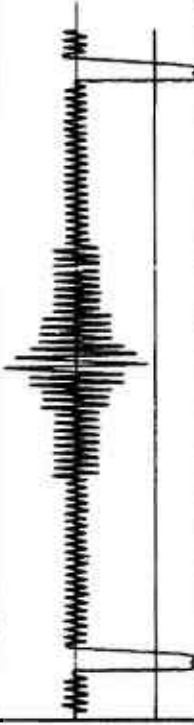
FIG.4.22 LOAD SPECTRUM APPLIED IN NLR-TESTS ON CRACK PROPAGATION UNDER RANDOM FLIGHT – SIMULATION LOADING (REFS 77,78)

LOAD SEQUENCE (FLIGHT No. 19, TYPE F)	REMARKS	CRACK PROPAGATION LIFE (o)			
		FLIGHT		RATIO	
		2024—T3	7075—T6	2024—T3/7075—T6	2024—T3/7075—T6
B		11781	5062	1	1
C	GUST CYCLES IN REVERSED SEQUENCE	11184	4851	0.95	0.96
H	PROGRAMMED SEQUENCE OF GUST CYCLES	11365	5061	0.96	1.00

(o) THE CRACK LIFE COVERS PROPAGATION FROM $2\ell = 20\,mm$ TO COMPLETE FAILURE OF THE SHEET SPECIMEN, WIDTH 160 mm. ALL DATA ARE MEAN VALUES OF 4 OR 6 TESTS.
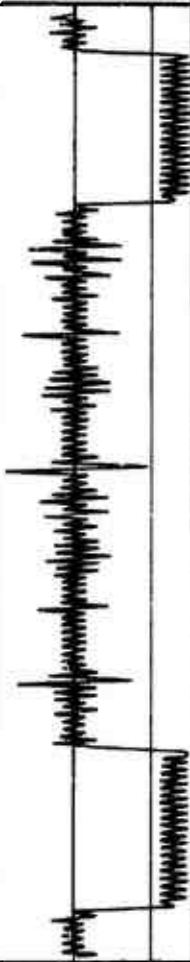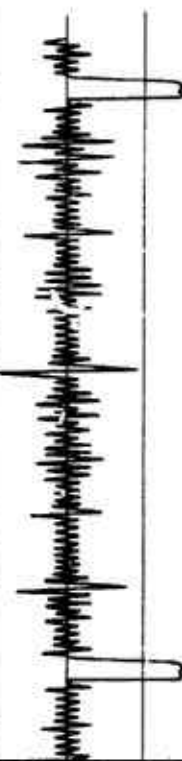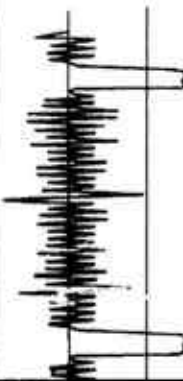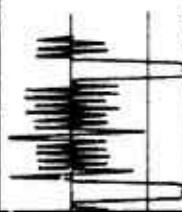
FIG. 4.23 THE EFFECT OF THE CYCLE SEQUENCE IN FLIGHT–SIMULATION TESTS. CRACK PROPAGATION TESTS ON SHEET MATERIAL. (REFS. 77, 78)

INVESTIGATION (a)	PERCENTAGE INCREASE OF LIFE IN FLIGHTS CAUSED BY	
	OMITTING LOW-AMPLITUDE CYCLES	OMITTING TAXIING LOADS (b)
NAUMANN (1964, REF. 67)	6 % AND 17 %	
GRASSNER AND JACOBY (1964, 1965, REF. 66, 73)	150 %	0
BRANGER (1967, REF. 110)	− 14 %	− 23 %
IMIG AND ILLG (1969, REF. 80)		2 % TO 12 %
NLR (SEE FIG. 4.25)	18 % TO 93 %	− 8 % AND + 16 %
SCHIJVE AND DE RIJK (1971, REF. 43)	0 − 50 %	

(a) FOR MORE INFORMATION SEE TABLE 4.7

(b) S_{min} IN THE GTAC HAD THE SAME VALUE WITH AND WITHOUT TAXIING LOADS

FIG. 4,24 THE EFFECT OF OMITTING LOW−AMPLITUDE CYCLES FROM FLIGHT − SIMULATION TESTS.

	LOAD SEQUENCE (FLIGHT NO. 19, TYPE F)	REMARKS	CRACK PROPAGATION LIFE (a)			
			FLIGHTS		RATIO	
			2024–T3	7075–T6	2024–T3/7075–T6	7075–T6
A		RANDOM FLIGHT SIMULATION	10 876	5 889	0.92	1.16
B		TAXIING LOADS OMITTED	11 781	5 062	1	1
C		SMALL GUST CYCLES OMITTED ($S_a = 1.1\ kg/mm^2$)	13 924	7 006	1.18	1.38
E		MORE SMALL GUST CYCLES OMITTED $S_a = 1.1$ AND $2.2\ kg/mm^2$	20 759	9 779	1.76	1.93
F		ONE GUST LOAD PER FLIGHT ONLY (THE LARGEST ONE)	36 583	14 556	3.11	2.89

(a) THE CRACK LIFE COVERS PROPAGATION FROM $2\ell = 2\ mm$ TO COMPLETE FAILURE OF THE SHEET SPECIMEN, WIDTH 160 mm
ALL DATA ARE MEAN VALUES OF 4 OR 6 TESTS.

FIG. 4.25 THE EFFECT OF OMITTING LOW–AMPLITUDE GUST CYCLES AND TAXIING LOADS IN FLIGHT–SIMULATION TESTS.
CRACK PROPAGATION TESTS ON SHEET MATERIAL (REFS. 77, 78)
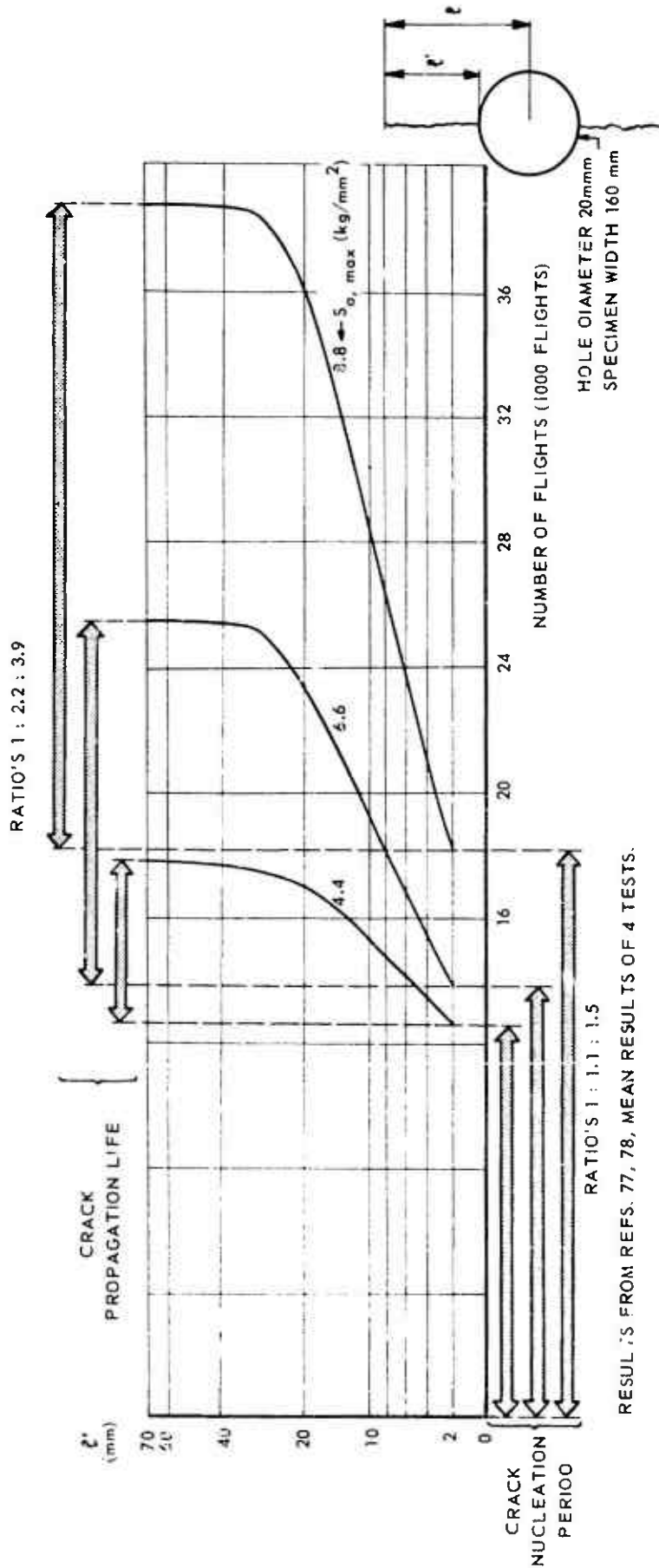
FIG. 4.26 EFFECT OF TRUNCATION LEVEL ($S_{a, max}$) ON THE CRACK NUCLEATION PERIOD (TO $\ell' = 2$ mm) AND THE CRACK PROPAGATION LIFE. RANDOM FLIGHT-SIMULATION TESTS ON 2024-T3 ALCLAD SHEET SPECIMENS WITH A CENTRAL HOLE.

	TAXIING LOADS	GUST SEQUENSE IN EACH FLIGHT
△ ▲	NO	RANDOM
□ ■	NO	PROGRAMMED
○ ●	YES	RANDOM

$S_{a,max}$
(kg/mm^2)

CRACK PROPAGATION LIFE (FLIGHTS)
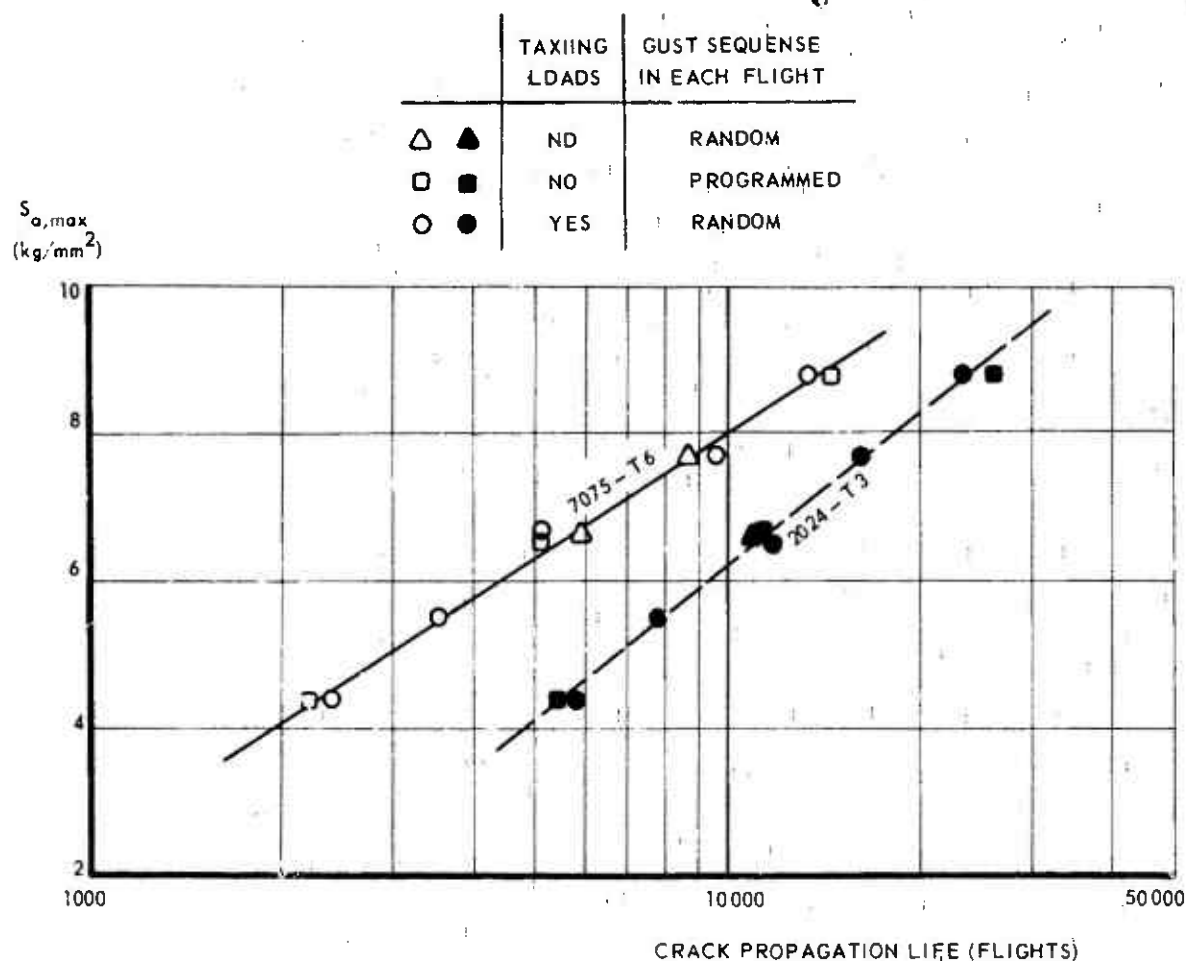
ALL DATA POINTS ARE MEAN VALUES OF 4–6 TESTS. THE CRACK LIFE COVERS PROPAGATION FROM $2\ell = 20$ mm TO COMPLETE FAILURE; SPECIMEN WIDTH 160 mm.

FIG. 4.27   THE EFFECT OF TRUNCATING THE GUST LOAD SPECTRUM ON THE CRACK PROPAGATION LIFE IN FLIGHT–SIMULATION TESTS (REFS. 77, 78)
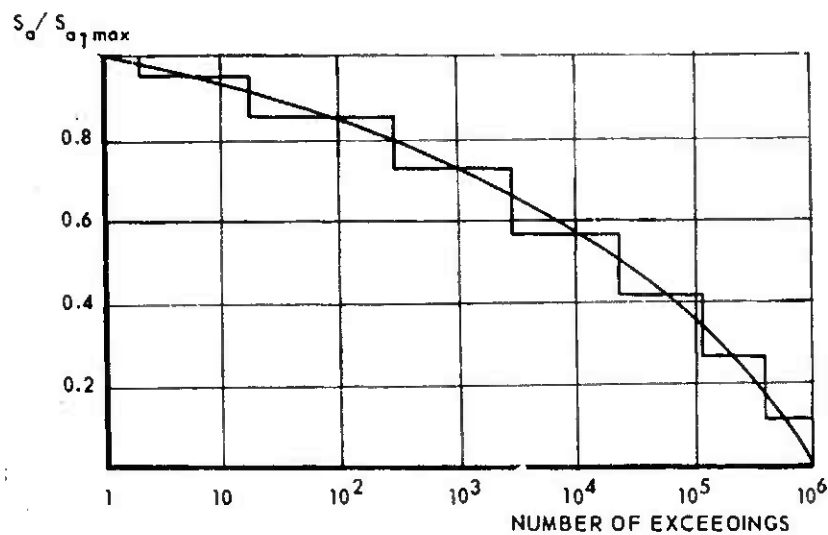
LOG BINOMIAL DISTRIBUTION

STEPPEO APPROXIMATION	
$S_a / S_{a, max}$	NUMBER OF EXCEEOINGS
1	2
0.95	18
0.85	298
0.725	3018
0.575	23000
0.425	115000
0.275	395000
0.125	1000000

a. STANDARDIZED LOAD SPECTRUM
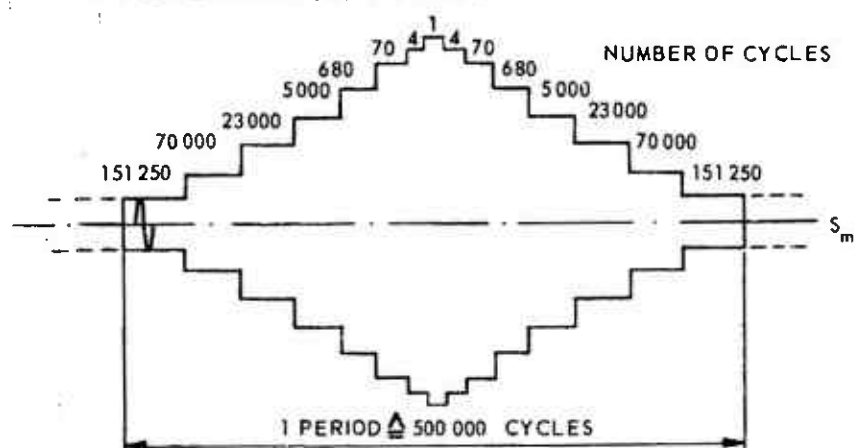
b. LOAO SEQUENCE IN PROGRAM TEST AHO NUMBERS OF CYCLES IN ONE PERIOO
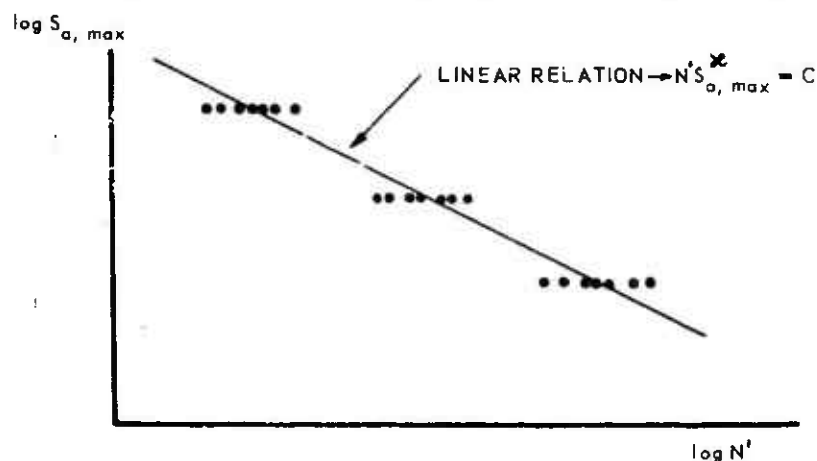
c. ENOURANCE CURVE, RESULTS FROM TESTS WITH OIFFERENT $S_{a, max}$ VALUES, BUT SAME $S_{a, max} / S_m$ RATIO.

FIG. 4.28 ENDURANCE CURVE OBTAINED IN STANDARDIZED PROGRAM TEST ACCORDING TO GASSNER
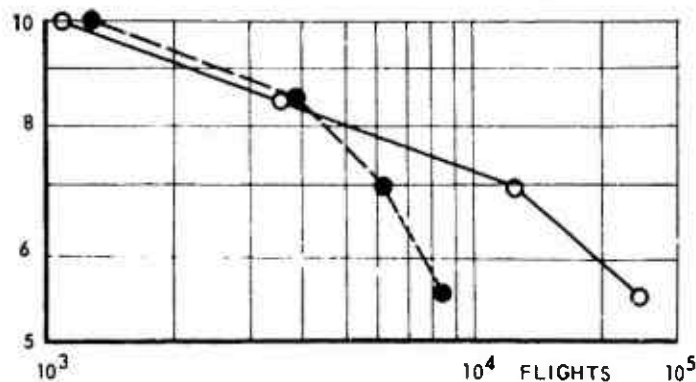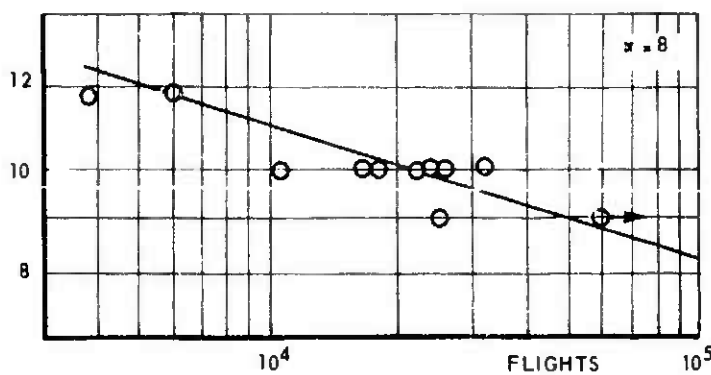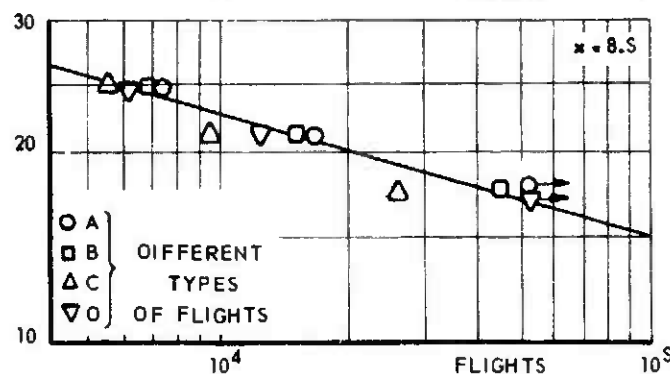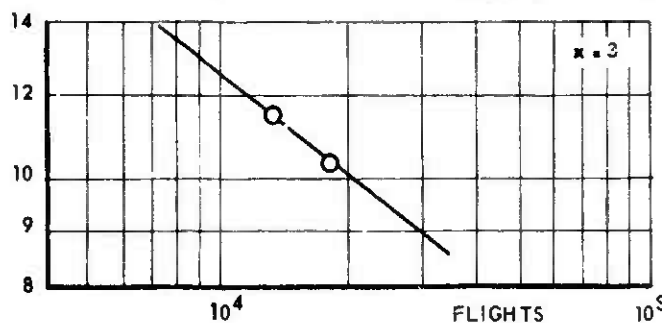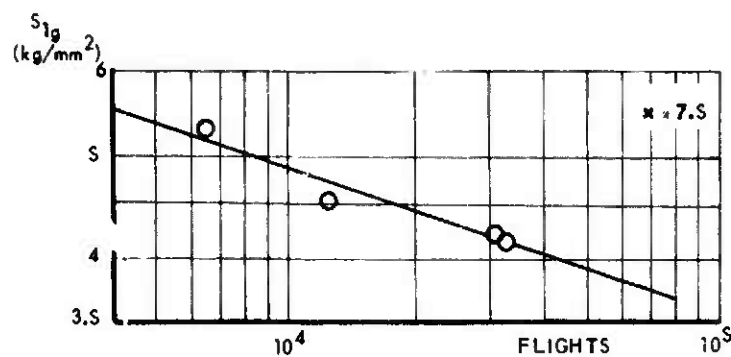
FIG. 4.29 THE EFFECT OF THE DESIGN STRESS LEVEL ON FATIGUE LIFE UNDER FLIGHT-SIMULATION LOADING. S_{1g} = CHARACTERISTIC 1g-STRESS LEVEL IN FLIGHT.
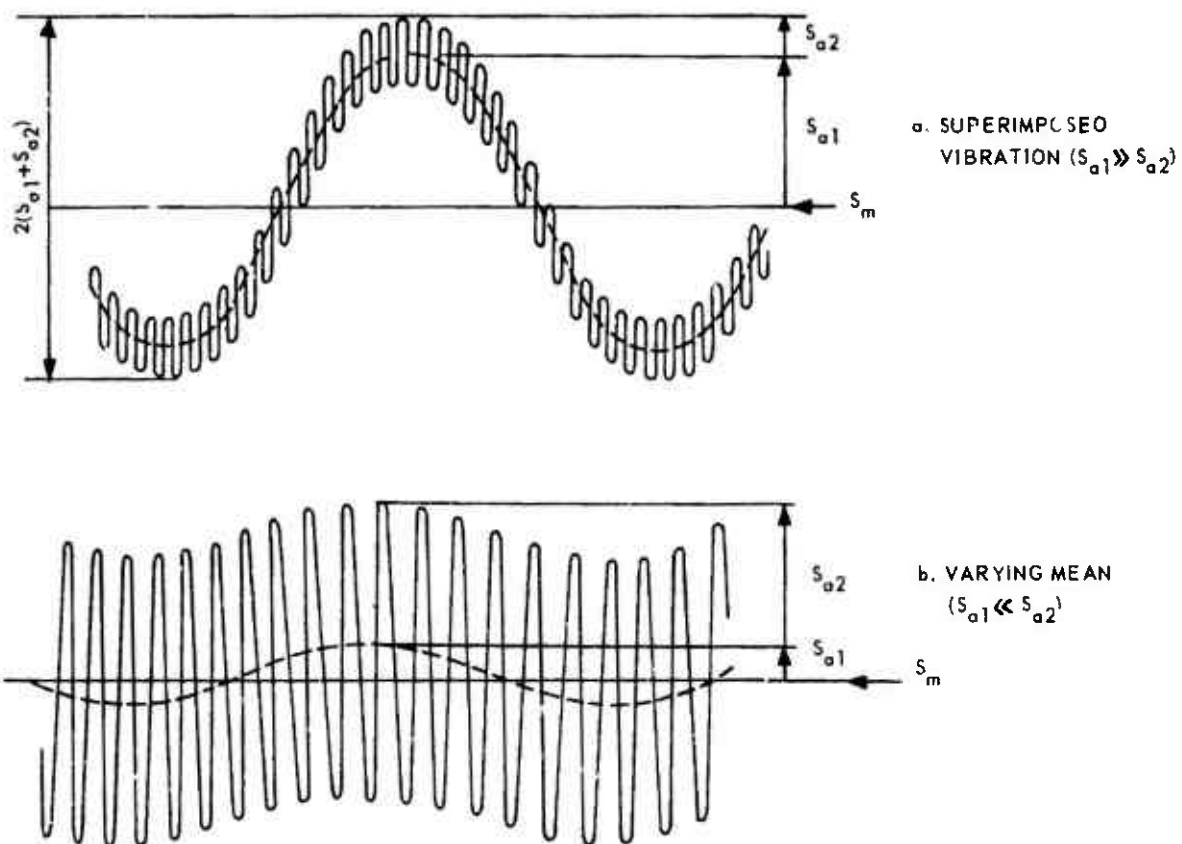
FIG. 4.30   TWO TYPES OF SUPERIMPOSED CYCLIC LOADS.
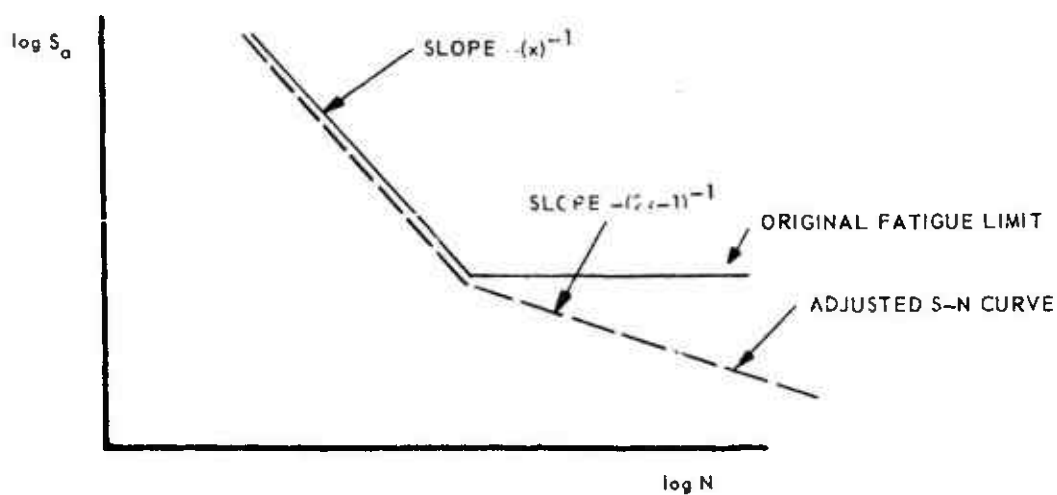
FIG. 5.1   ADJUSTED S–N CURVE FOR LIFE CALCULATIONS ACCORDING TO HAIBACH (REF.148)
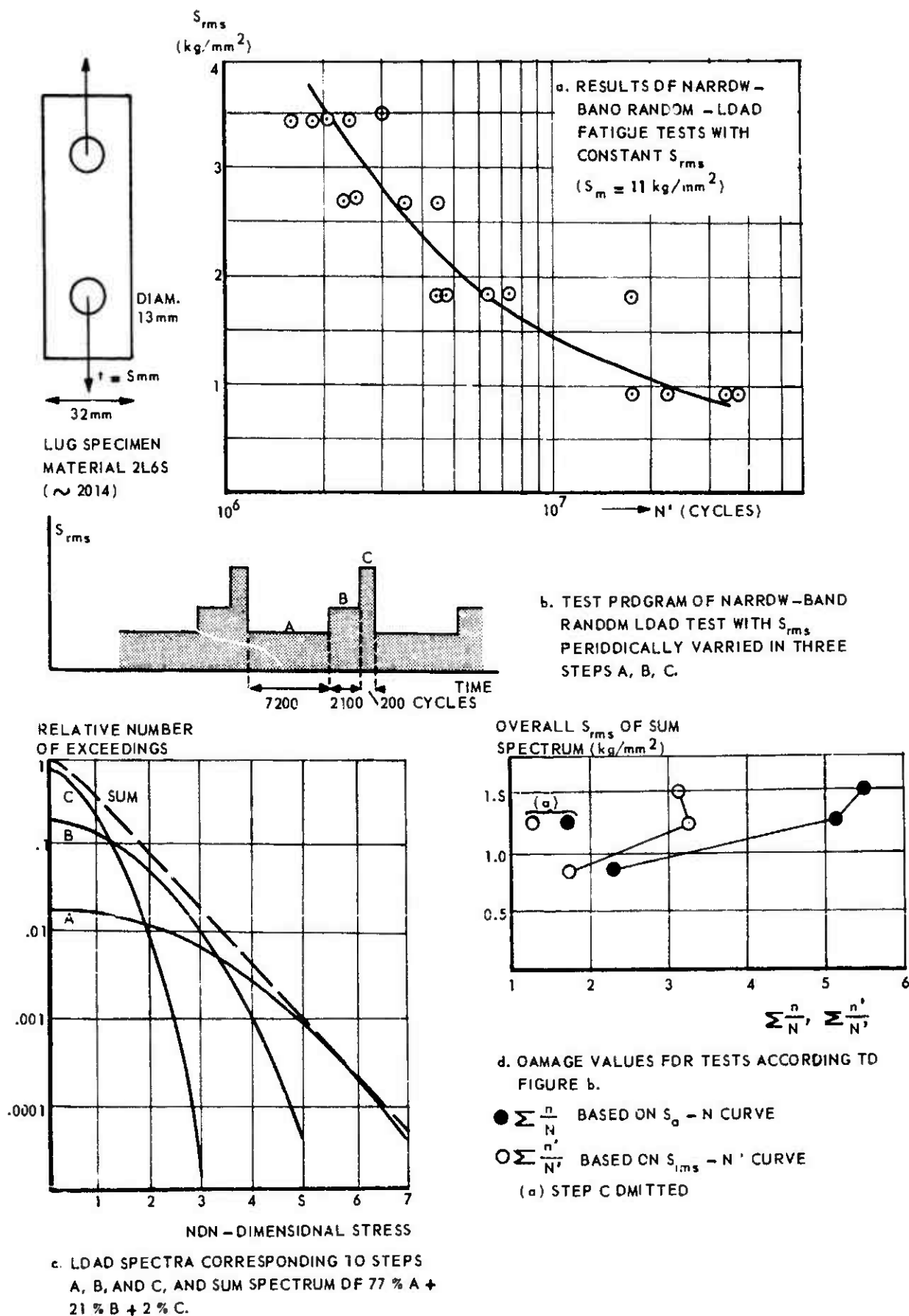
FIG. 5.2 NARROW-BAND RANDOM LOAD TESTS WITH CONSTANT S_{rms} AND PROGRAMMED S_{rms}. RESULTS FROM KIRKBY AND EDWARDS (REF. 99).
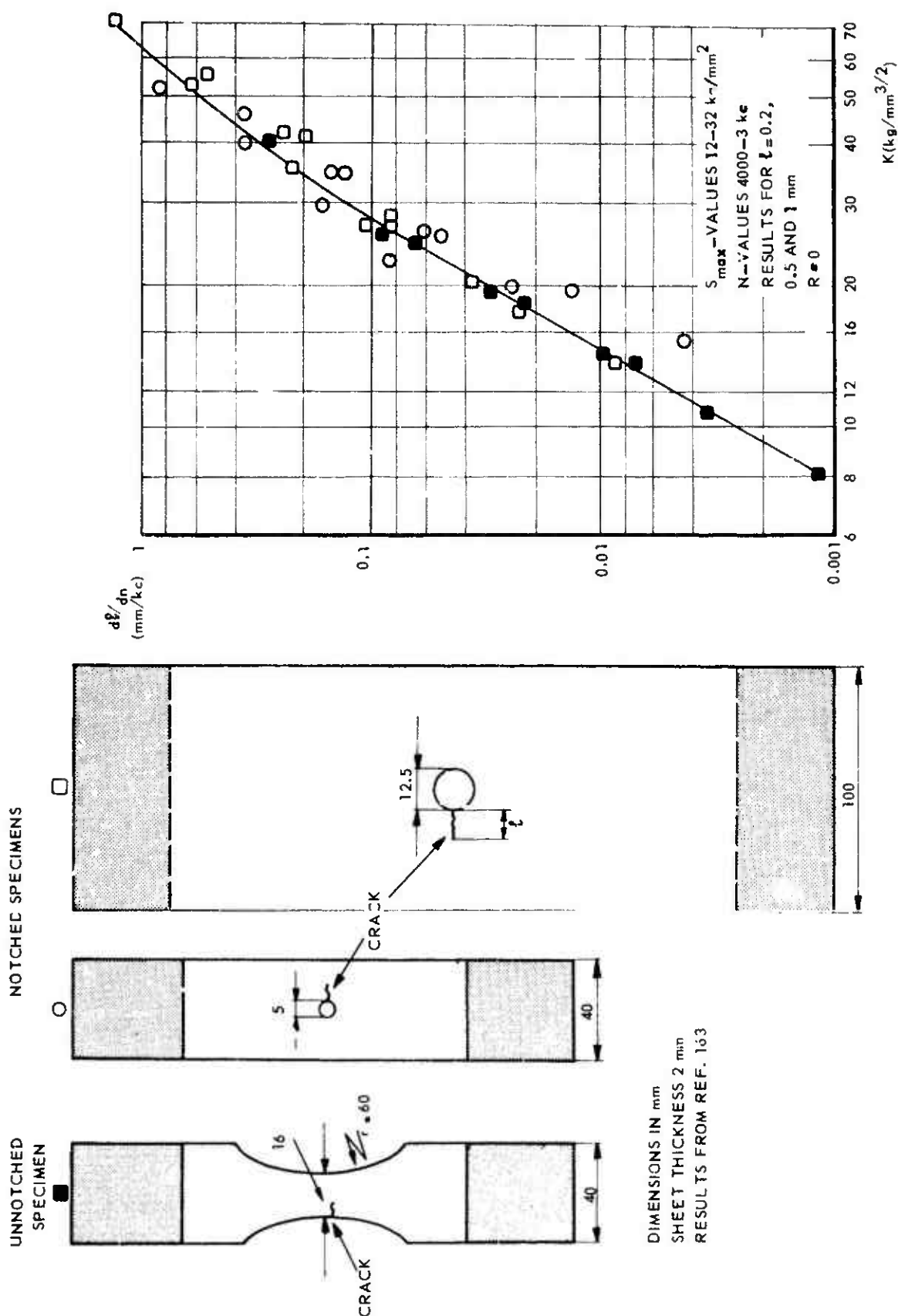
FIG. 5.3   THE CRACK RATE AS A FUNCTION OF THE STRESS INTENSITY FACTOR FOR SMALL CRACKS (0.2 – 1.0 mm)

ℓ (mm)

P = 900 kg

S = 3.9 kg/mm^{-2}

KILOCYCLES
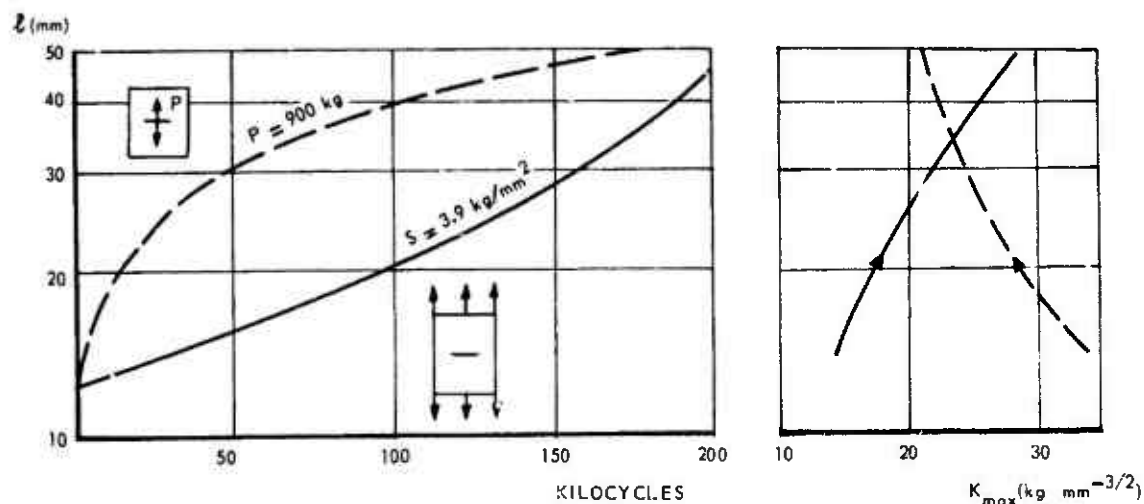
a. EXAMPLES OF DIFFERENT CRACK PROPAGATION CURVES

b. CORRESPONDING K-VALUES

K_{max} (kg mm$^{-3/2}$)

$\frac{d\ell}{dn}$, $\frac{\mu m}{CYCLE}$

K_{max}, lbf · in$^{-3/2}$

K_{max}, MN · m$^{-3/2}$

$\frac{d\ell}{dn}$ $\frac{\mu in.}{CYCLE}$

c. CRACK RATES AS A FUNCTION OF K_{max}

UNIFORMLY LOADED PANEL

$2\ell_i = 0.2$ in.
(9.5 cm)

$2b = 12$ in.
(30 cm)

$2h = 36$ in.
(91 cm)

WEDGE–FORCE PANEL

$2\ell_i = 0.5$ in.
(1.3 cm)

$2b = 12$ in.
(30 cm)

$2h = 5, 8, 12, 17, 25$ in.
(13, 20, 30, 43, 64 cm)

d. DIMENSIONS OF 7075–T6 SHEET SPECIMENS
t = 0.09 in, ℓ_i = INITIAL CRACK LENGTH
TESTS AT R = 0.05
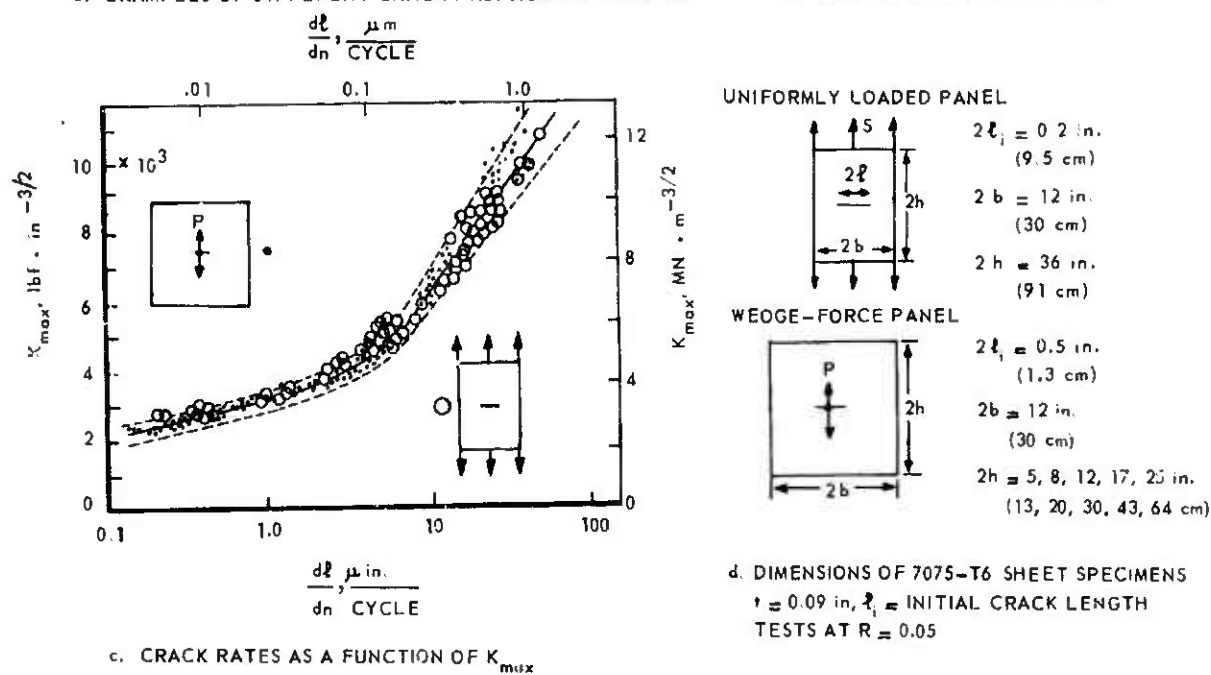
FIG. 5.4 A COMPARISON BETWEEN THE CRACK RATES IN UNIFORMLY LOADED AND
WEDGE – FORCE LOADED SPECIMENS
RESULTS FROM FIGGE AND NEWMAN (REF. 164).
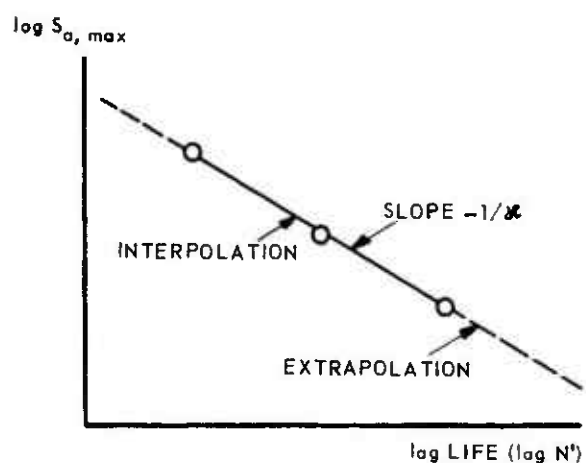
FIG. 5.5 a
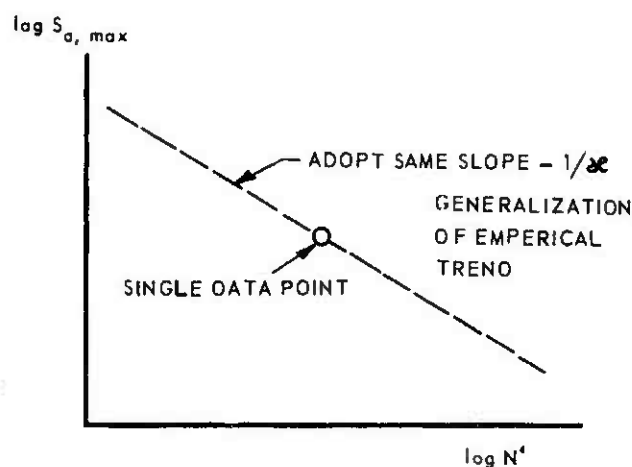
FIG. 5.5. b

EFFECT OF DESIGN STRESS LEVEL IN PROGRAM FATIGUE TESTS
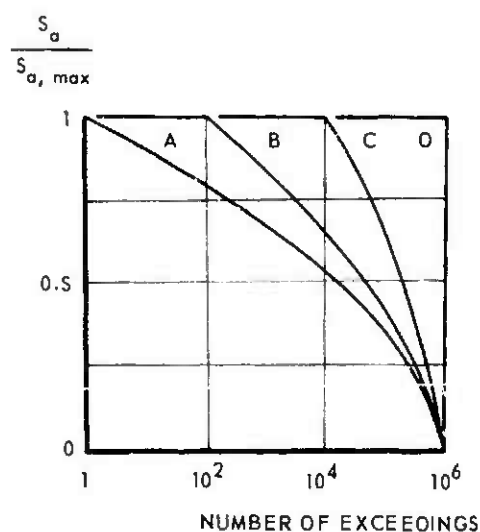
FIG. 5.5 c
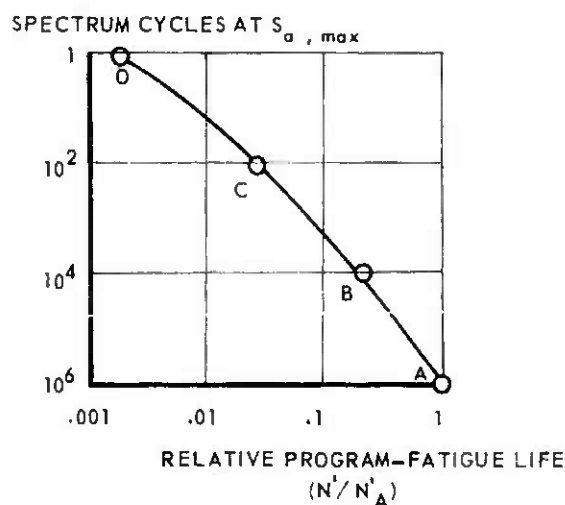
FIG. 5.5 d

EFFECT OF LOAD SPECTRUM SHAPE (A—O) ON PROGRAM FATIGUE LIFE

FIG. 5.5 SOME CONCEPTS OF GASSNER AND CO—WORKERS FOR EMPLOYING PROGRAM FATIGUE
TEST DATA.
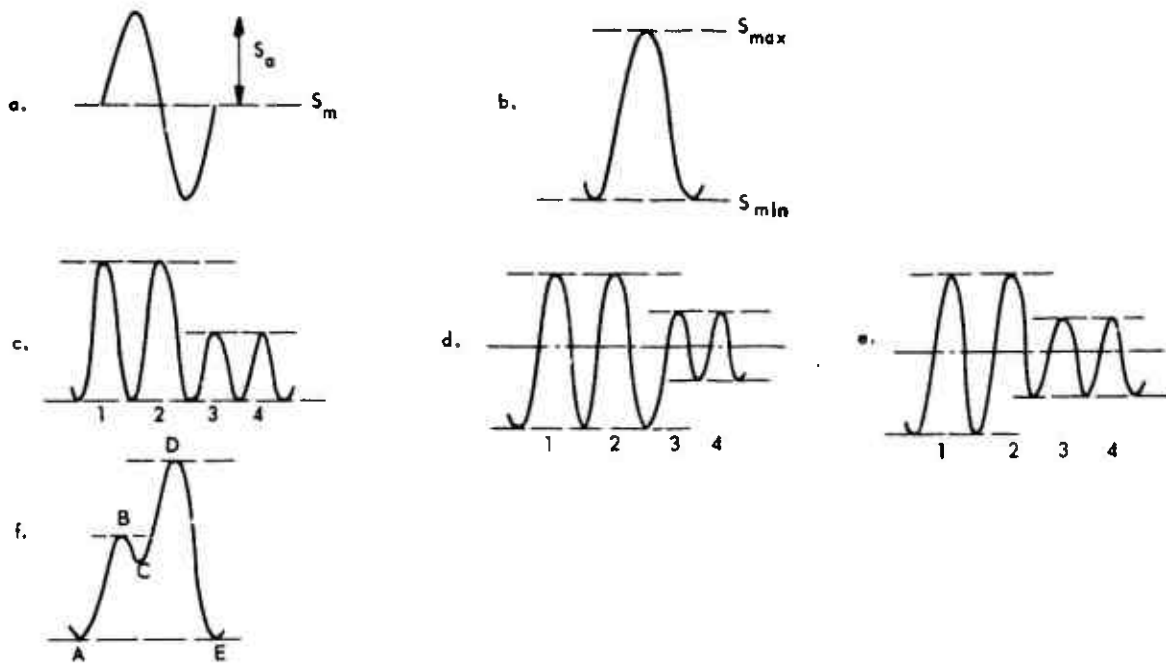
FIG. 6.1 EXAMPLES OF SIMPLE LOAD VARIATIONS REGARDING THE DEFINITION OF
LOAD CYCLES
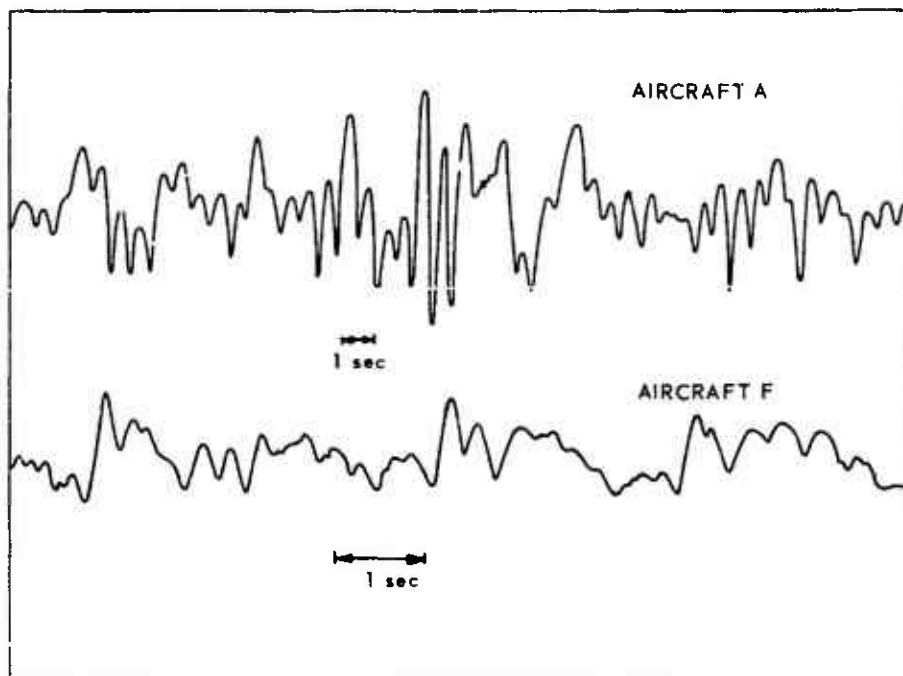
FIG. 6.2 STRAIN GAGE RECORDS OF THE WING BENDING MOMENT OF 2 AIRCRAFT FLYING
IN TURBULENT AIR (REF. 174)
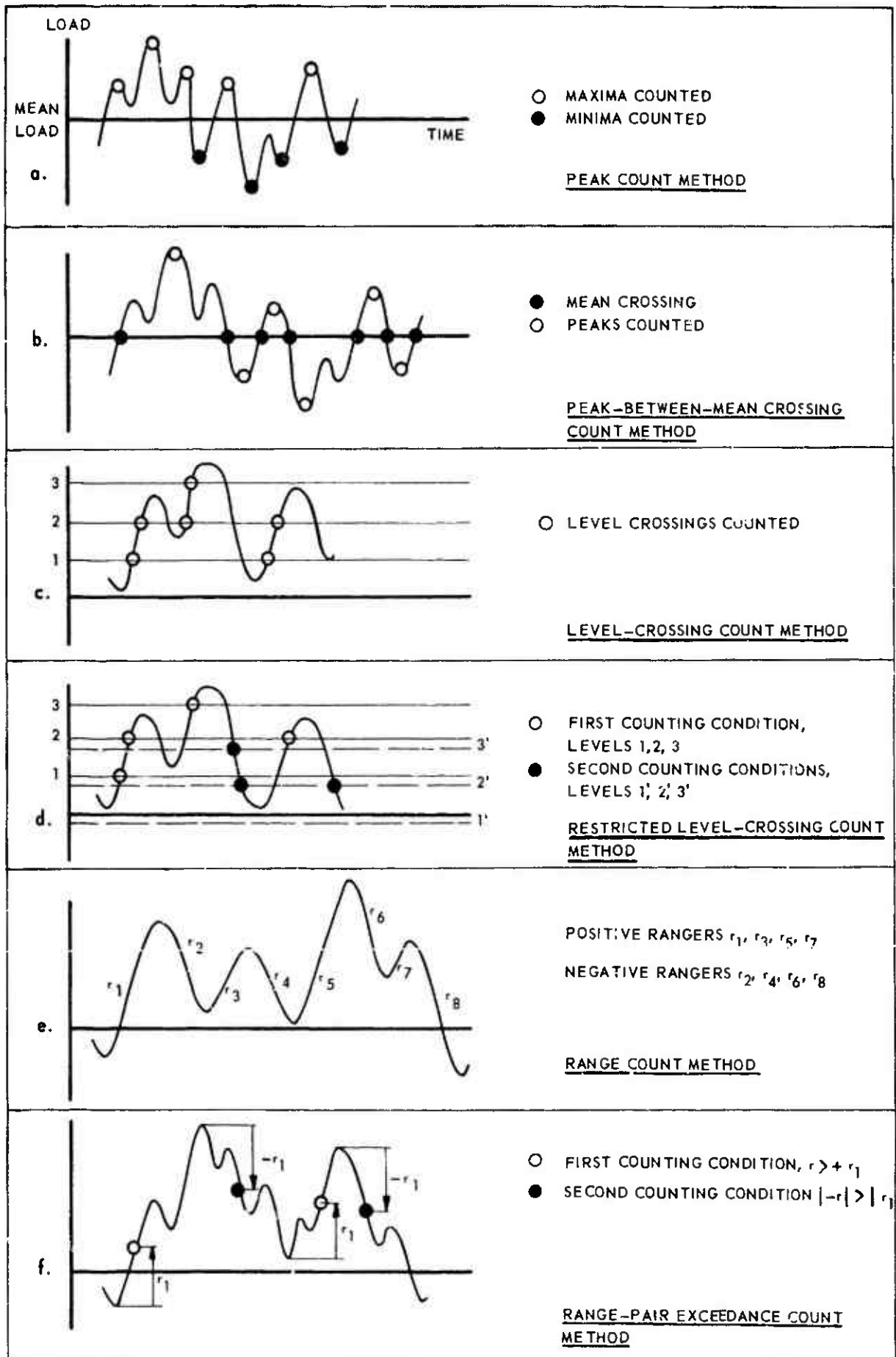
FIG. 6.3 SEVERAL COUNTING METHODS FOR A STATISTICAL DESCRIPTION OF A LOAD—TIME HISTORY. NAMES OF METHODS AFTER VAN DIJK (REF. 176)

GUST VELOCITY

GUST SPECTRUM

0

NUMBER OF EXCEEDANCE
(log SCALE)

NEGATIVE GUSTS, SYMMETRIC TO
POSITIVE PART OF SPECTRUM

LOAD FACTOR
INCREMENT

MANEUVER SPECTRUM

0

NUMBER OF EXCEEDANCE
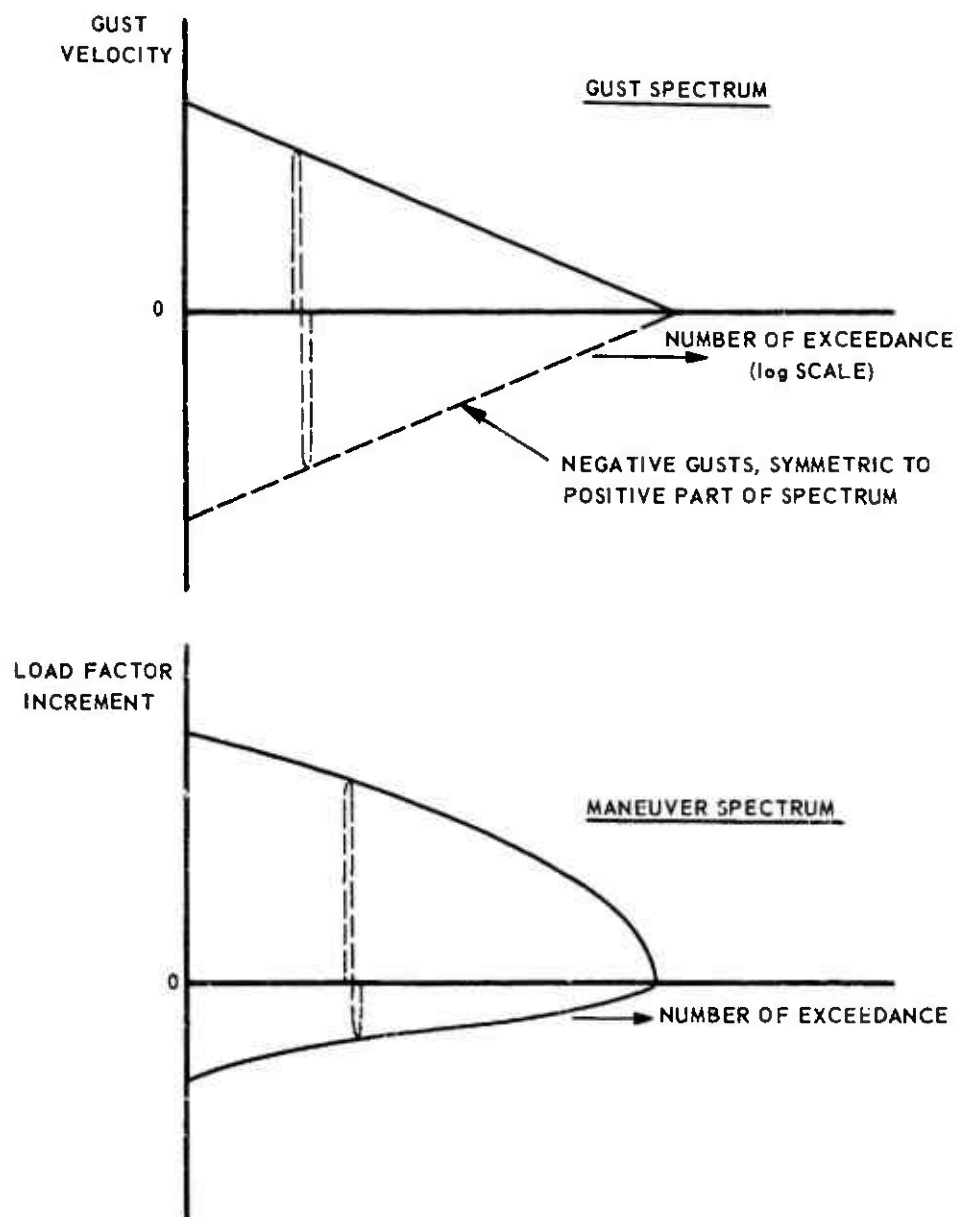
FIG. 6.4 DIFFERENCES BETWEEN GUST AND MANEUVER SPECTRA
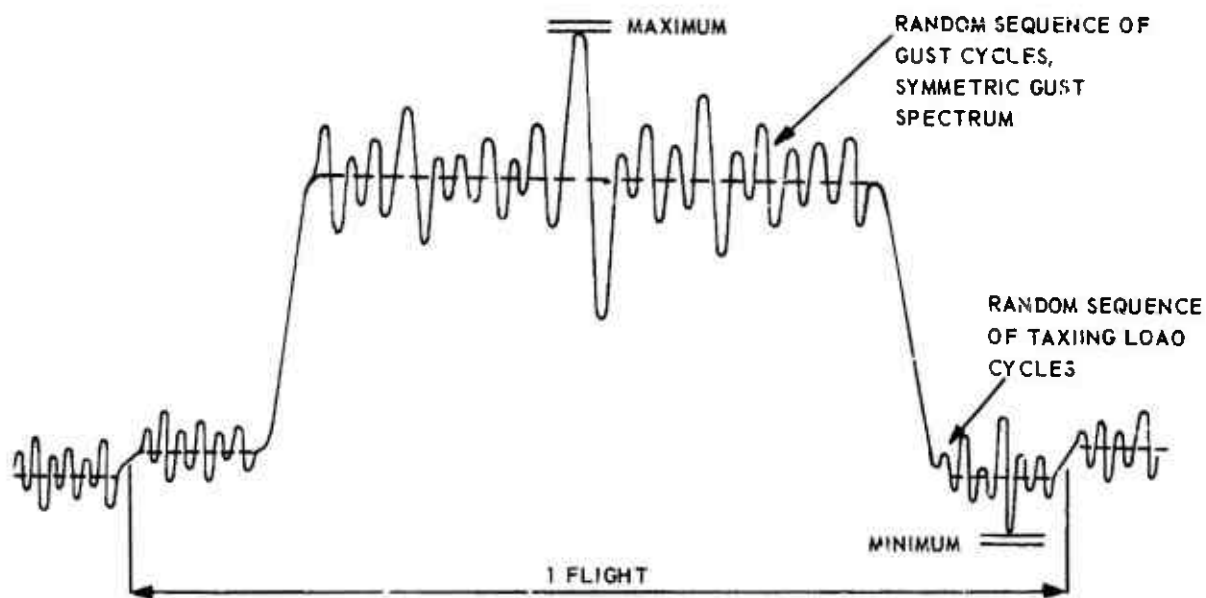
a. TRANSPORT AIRCRAFT.
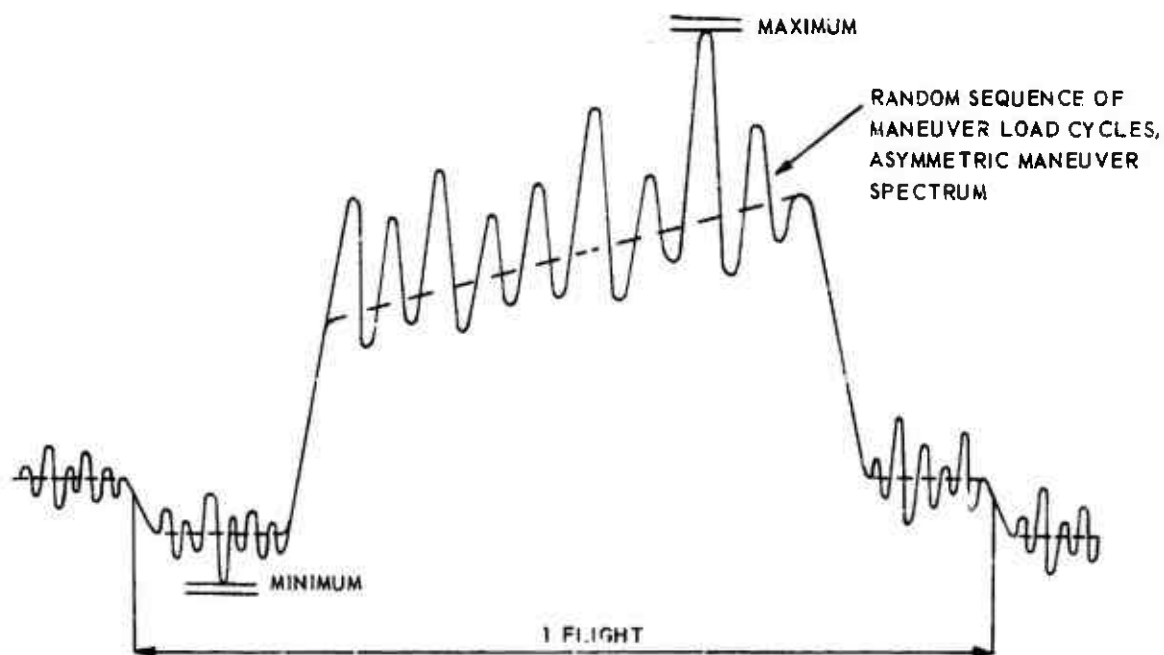
b. FIGHTER AIRCRAFT.

FIG. 6.5 TWO SIMPLIFIED EXAMPLES OF ESTIMATED FLIGHT-LOAD PROFILES FOR THE AIRCRAFT WING ROOT STRUCTURE.
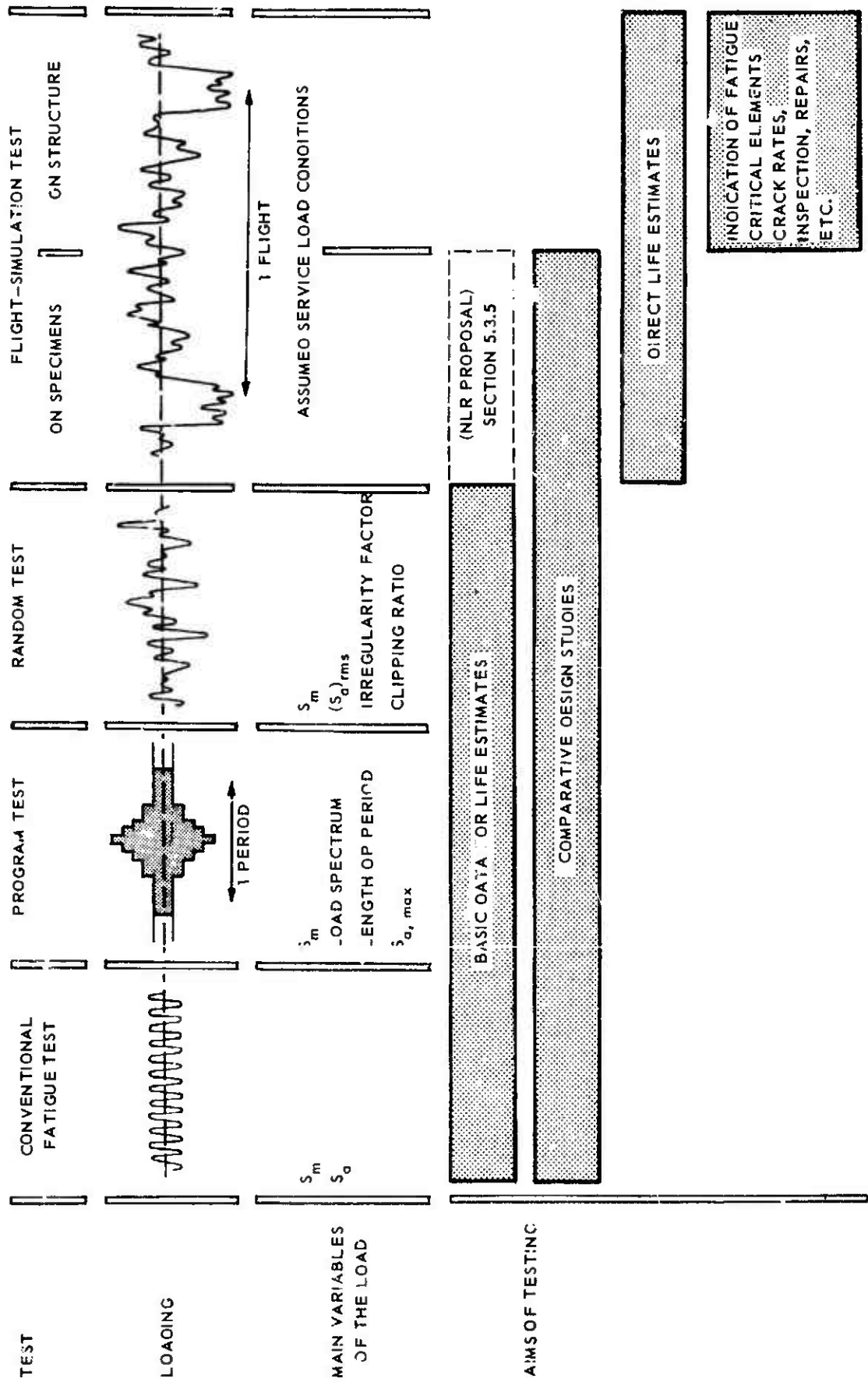
FIG. 7.1 SOME FATIGUE TEST LOAD SEQUENCES, MAIN VARIABLES AND TESTING PURPOSES.
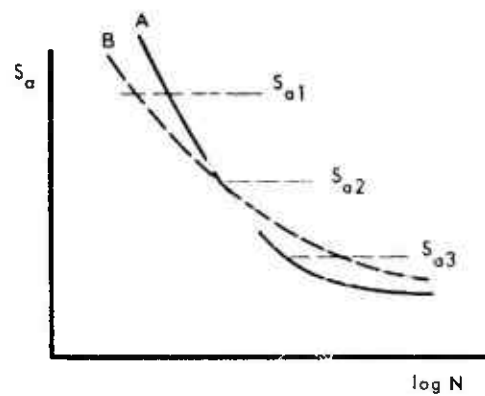
FIG. 7.2 TWO INTERSECTING S–N CURVES
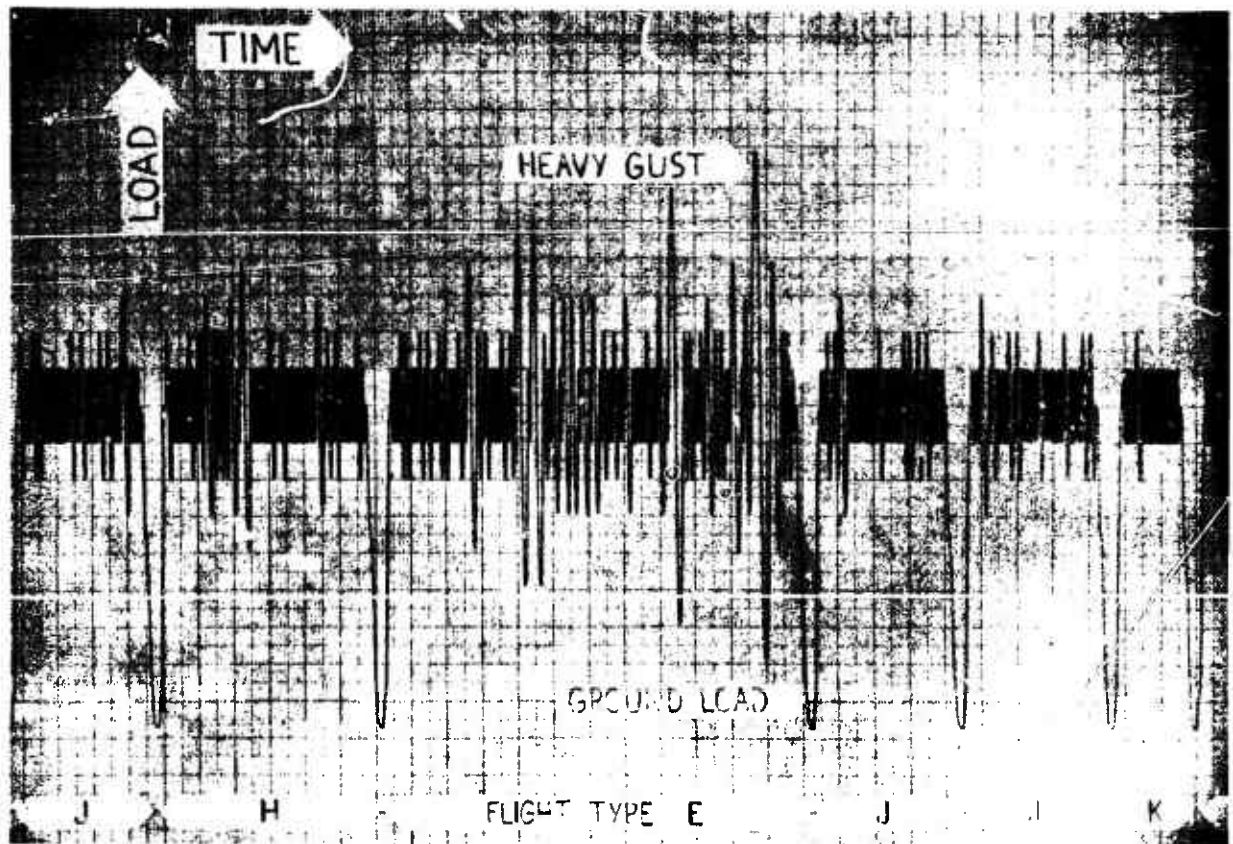
FIG. 7.3 SAMPLE OF A LOAD RECORD, ILLUSTRATING THE LOAD SEQUENCE APPLIED IN THE F-28 WING FATIGUE TEST. TEN DIFFERENT TYPES OF WEATHER CONDITION ARE SIMULATED, FLIGHT TYPE E CORRESPONDS TO FAIRLY SEVERE STORM WHILE FLIGHT TYPE K IS FLOWN IN GOOD WEATHER (REF. 96)
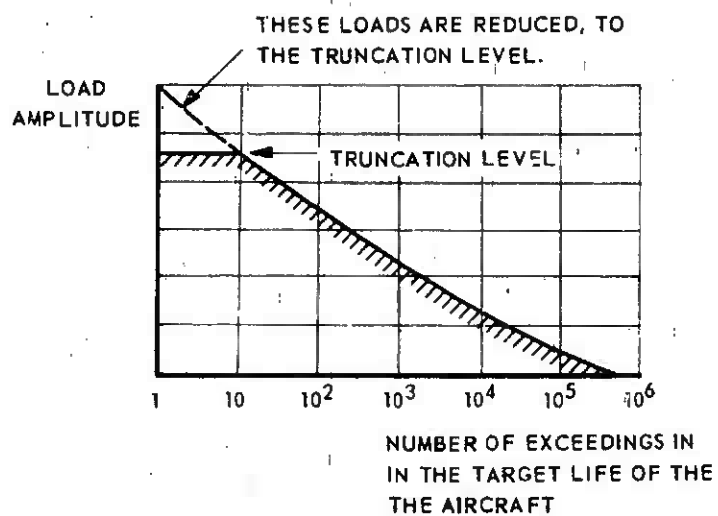
FIG. 7.4 EXAMPLE OF TRUNCATING THE INFREQUENTLY
OCCURRING HIGH AMPLITUDES OF A LOAD SPECTRUM.
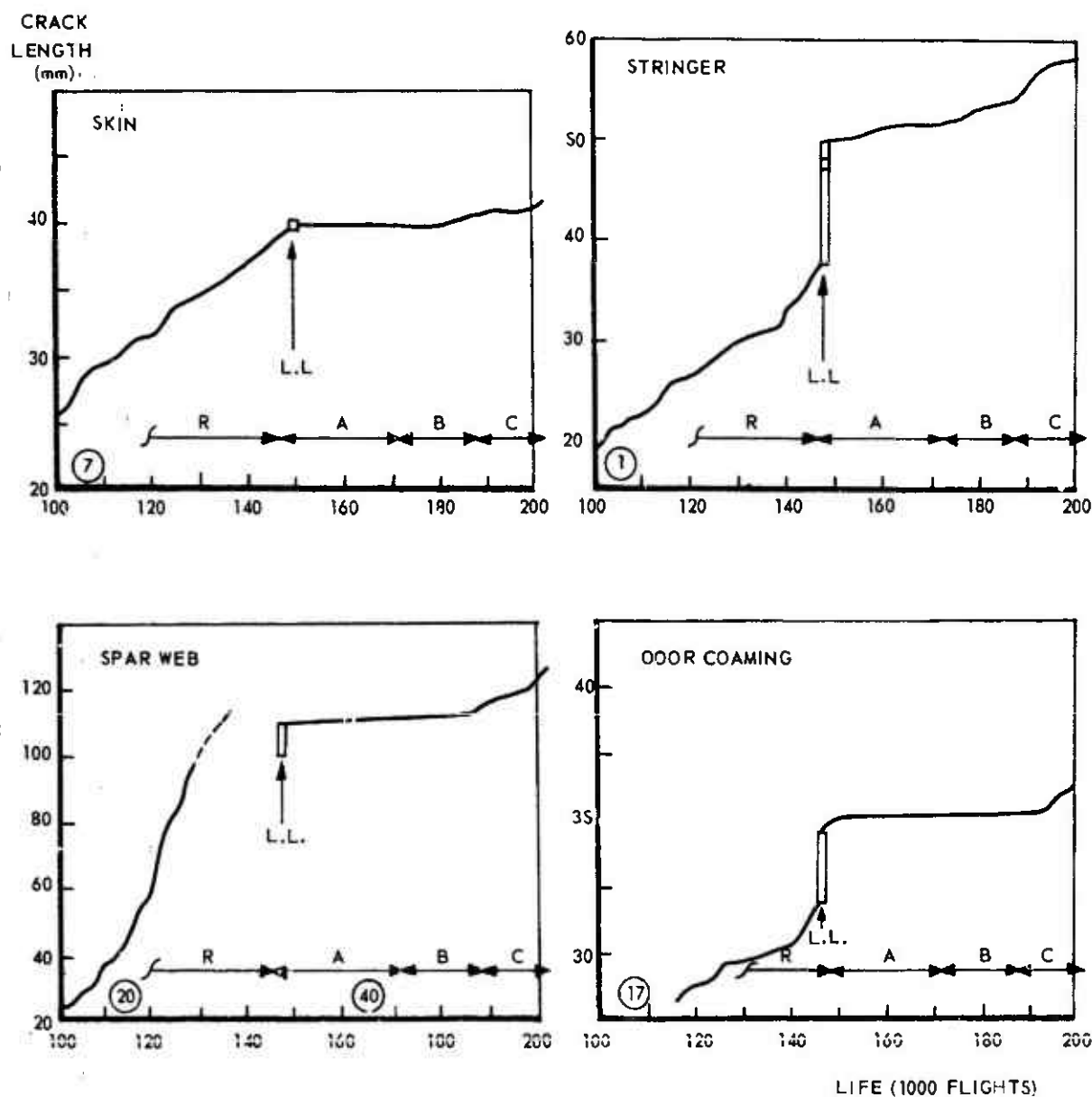
R : : CERTIFICATION TESTS
LL : : CRACK EXTENSION DUE TO LIMIT LOAD APPLICATION AT END OF CERTIFICATION TESTS
A, B, C : PERIODS OF SUBSEQUENT RESEARCH PROGRAM
A   : LOW—AMPLITUDE GUST CYCLES OMITTED
B   : LOWER TRUNCATION LEVEL
C   : LOAD LEVELS INCREASED 25 PERCENT

FIG.7.5   THE EFFECT OF LIMIT LOAD APPLICATION ON CRACK PROPAGATION.
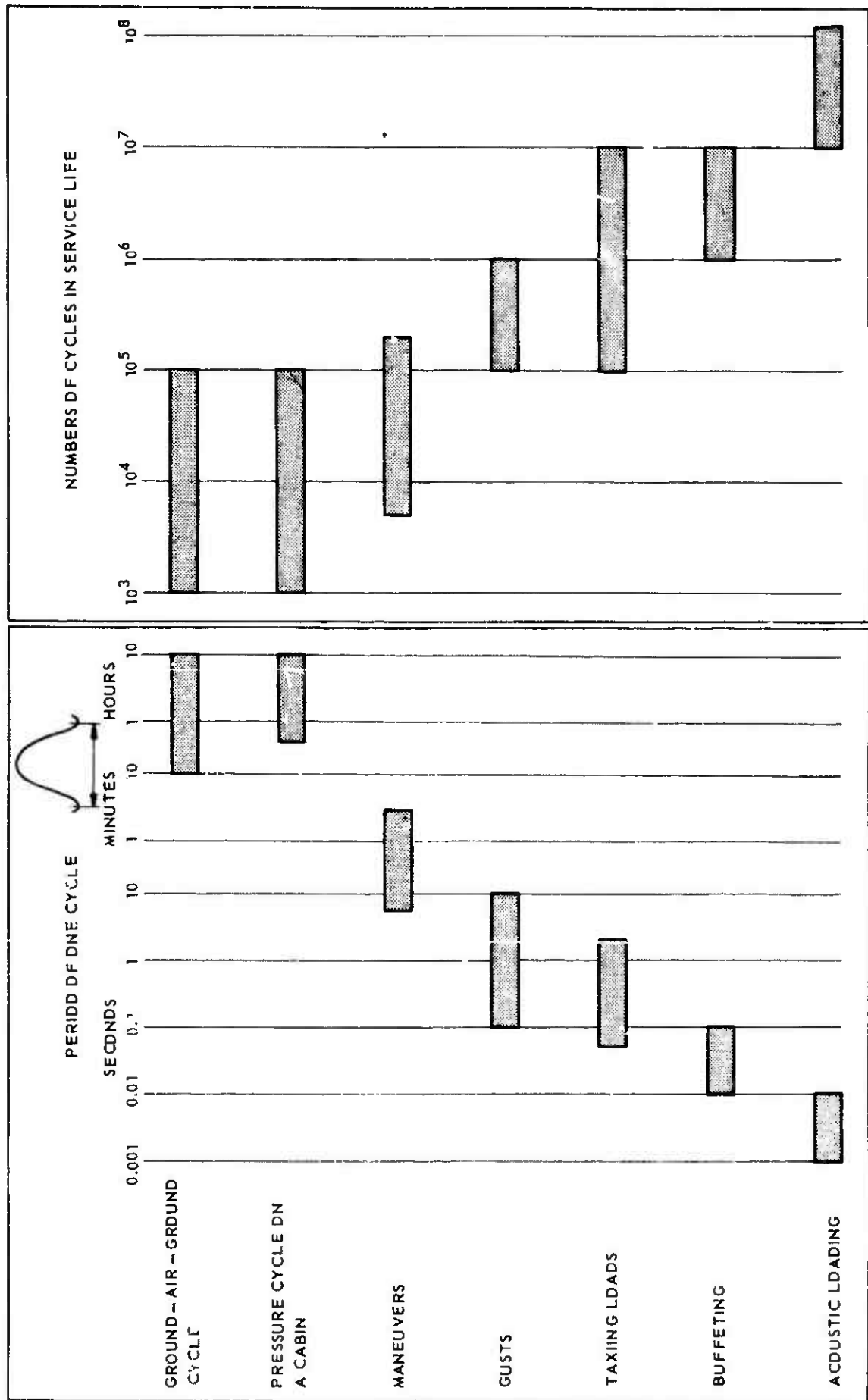
FIG. 7.6 PERIODS AND NUMBERS OF SEVERAL TYPES OF AIRCRAFT FATIGUE LOADS (REF. 195). ORDERS OF MAGNITUDE.

EFFECTS OF TEST FREQUENCY ON FATIGUE CRACK PROPAGATION UNDER FLIGHT-SIMULATION LOADING

J. Schijve

National Aerospace Laboratory NLR, Sloterweg 145, Amsterdam, The Netherlands

SUMMARY

In a recent test program, fatigue crack propagation in
2024-T3 and 7075-T6 sheet material was studied at three
test frequencies, viz. 10, 1 and 0.1 cycles per second.
The flight-simulation loading was based on a gust spectrum.
The design stress level was adopted as a second variable
of the investigation. Differences between the crack propa-
gation rates at the three test frequencies were small and
unsystematic. The propagation was much slower than predict-
ed from constant-amplitude test data. Moreover, the macro-
cracking behaviour appeared to be different. In the dis-
cussion attention is paid to interaction with environmental
effects and to implications for practical problems of
aircraft fatigue.

LIST OF SYMBOLS

GTAC	ground-to-air cycle
K	stress intensity factor
KI_{scc}	threshold K value for stress corrosion cracking
ℓ	half crack length, see figure 1
$d\ell/dn$	crack propagation rate
N	life
$N_{30} - N_{12}$	crack propagation life covered by crack growth from ℓ = 12 mm to ℓ = 30 mm
S_a	stress amplitude
$S_{a,max}$	maximum stress amplitude, applied in flight-simulation test (truncation level)
S_m	mean stress in constant-amplitude test, or (particularly in this paper) mean stress in flight during flight-simulation test

UNITS

cps	cycles per second
stress	1 kg/mm^2 = 1.422 ksi $\approx$ 9.81 kN/m^2
crack length	1 mm = 0.0394 inch, 1 inch = 25.4 mm
crack propagation rate	1 μ/fl = 1 micron per flight = 0.001 mm per flight

1   INTRODUCTION

A comparison between fatigue in an aircraft structure in service and fatigue in a laboratory specimen
reveals significant differences. The more important ones are to be related to:

a   Load sequences

b   Test article

c   Loading rates

d   Environment

A survey of the effect of the load sequence on fatigue life and crack propagation was recently given in
reference 1. It turned out that there was no unique relation between fatigue under different load

sequences. As an example, the fatigue lives and the crack propagation curves obtained in a program test with a long period and in a random load test with the same peak load distribution function could be considerably different. Even the cracking mechanism could be different (Ref.2). The apparently trivial conclusion is that quantitatively realistic information on fatigue properties should be drawn from tests with realistic load sequences. For many parts of an aircraft structure this implies a mixture of stochastic loads and deterministic loads, that means a flight-simulation test. Fortunately, the present time fatigue machines are capable of applying complex load-time histories.

With respect to the test article, it is now generally recognized that a test on a full-scale component or structure will give more relevant information than a test on a simple specimen. As a consequence, it is fairly common to carry out a flight-simulation test on a full-scale structure (Ref.3). Unfortunately, it is impracticable to carry out a flight-simulation test at the loading rates occurring in service, in view of unacceptably long testing times.

In order to explore the effect of the loading rate, flight-simulation tests were carried out on aluminium alloy sheet specimens at three different load frequencies. Crack propagation was investigated only. This aspect is a significant one for establishing safe inspection periods for service use as part of the fail-safe concept. If the load frequency is decreased, the time available for environmentally assisted crack growth increases. In principle a frequency effect may always be related to an environmental effect. The present paper summarizes the results of the test program, including a brief discussion of several aspects involved. Fully detailed results were presented in an NLR report (Ref.4).

2 TEST PROGRAM

2.1 The variables

Crack propagation in sheet specimens (Fig.1) was studied under flight-simulation loading (Fig.2). The variables adopted are shown in the table below.

Materials	Frequencies (cycles per second)	Design stress levels as characterized by the mean stress in flight	
		kg/mm^2	ksi
2024-T3 Alclad	10	10	14.2
7075-T6 Clad	1	8.5	12.1
	0.1	7.0	10.0
		6.5	7.8
		4.0	5.7

2.2 The fatigue loads in the flight simulation tests

The design stress level is characterized by the mean stress in flight (S_m) and the values adopted cover a wide range. The amplitudes of the various gust cycles are all proportional to S_m as illustrated by the gust load spectrum in figure 3. This spectrum applies to all test series with different S_m values. For empirical reasons, the gust load spectrum was approximated by a stepped function, see figure 3. The truncation level (Ref.5) was chosen to be $S_{a,max} = 1.1\ S_m$, that means that all higher amplitudes were reduced to this level. A higher truncation level might have led to unrealistically slow crack propagation (Ref.5), but it should be said that the present choice to some extent was arbitrarily made.

Taxiing loads were not applied since a previous investigation had shown (Ref.5) that these loads do not contribute to crack growth if they occur in compression. However, since taxiing loads increase the stress range of the ground-to-air cycle (GTAC), the minimum stress during the GTAC was chosen at a relatively more severe level than would apparently be required from a static point of view. The minimum stress in all GTAC was - 0.435 S_m.

The load spectrum was distributed over ten different flights (A-K), each characterized by its own spectrum varying from "good weather" to "storm" conditions. The procedure for doing so was previously adopted in reference 5 and is described there in more detail. The aim was to have a more or less similar shape of the load spectrum for all types of weather conditions. The severity, however, was different for each type of weather. Quantitative data on the load spectra are given in table 1.

The sequence of the flights (types A-K) was selected at random by a computer, with the exception of the most severe flights. As these flights may have a predominant effect on crack growth, they were uniformly distributed over the total sequence of flights in order to avoid that the severe flights had a chance to cluster together.

A sample of the load history applied in the tests is shown in figure 2. In each flight gust loads are applied in a random sequence. Each up gust is followed by a down gust and vice versa. However, the amplitudes of successive up and down gusts are not necessarily equal. A computer has randomly selected half cycles from the required load spectrum (random half cycles "restrained", after Naumann) (Ref.6). All flights of the same type have the same load spectrum, but in general they will have a different gust load sequence. After 5000 flights being applied, the same block of flights was repeated periodically. In view of the random sequence of the flights and the gust loads in each flight, the repetition of such a large block of flights is thought to be irrelevant with respect to the random character of the load time history.

2.3 Experimental details

The aluminium alloys adopted are representing the two most widely used sheet materials in present day aircraft. The specimens were cut from sheets with a nominal thickness of 2 mm. The static properties (rolling direction) are given below.

Material	$S_{0.2}$		S_u		Elongation (%)
	(kg/mm^2)	(ksi)	(kg/mm^2)	(ksi)	(50 mm gage length)
2024-T3 Alclad	35.6	50.6	47.3	67.3	13
7075-T6 Clad	50.2	71.4	56.4	80.2	14

The dimensions of the specimens are shown in figure 1. Each specimen was provided with a central crack starter and a number of line markings for recording of the crack growth. Originally, the specimens were pre-cracked under constant-amplitude loading ($S_m \pm S_a = 5 \pm 5$ kg/mm^2) from $\ell = 1.5$ mm to $\ell = 10$ mm. Later on the specimens were provided with longer saw cuts, corresponding to $\ell = 8$ mm and flight-simulation loading started without fatigue pre-cracking.
All tests were carried out in an MTS fatigue machine with a maximum capacity of 25 tons. The electro-hydraulic closed loop system for controlling the fatigue load is fed by a special device, called PACE (Programmed Amplitude GEnerator) developed at NLR. The sequence of amplitudes and the GIAC are represented by a series of digital code numbers on a magnetic tape containing sufficient information for 60000 flights. In all flight-simulation tests two specimens were tested in series, which almost halved the testing time. Scatter between similar tests was low as is usual for crack propagation. In some tests the fully cracked specimen was replaced by a dummy specimen for completing the test on the second one.
In order to prevent buckling of the specimens two felt covered aluminium alloy plates were used as anti-buckling guides, as described in reference 5. The plates were provided with windows for observing the crack growth (Fig.4). The specimens were provided with fine line markings. If the tip of a crack reached such a line the corresponding number of flights was recorded. In the majority of the tests these numbers were used for the evaluation of the crack propagation data.
Tests carried out at a low stress level or at a low frequency consumed much testing time. These tests were run overnight or during the weekend without supervision. Crack growth observations were made by two Nikon cameras with telelenses. Pictures of the cracks were automatically taken during the more severe flights at the moment that the specimens were at maximum load ($S_m + S_{a,max}$), see figure 4.
A third method, adopted for some special cases, is based on determining the positions of growth bands on the fracture surface (Sec.3).

The tests were carried out in the laboratory without any special means to control the temperature and the humidity. These two quantities, however, were constantly recorded. It turned out that the mean temperature usually was in the range of 22 to 25° C, while the mean value of the humidity was 40 to 45 percent.

2.4 Constant-amplitude tests

In addition to the flight-simulation tests a small number of constant-amplitude tests was carried out. The results of these tests were used for damage calculations, for checking the validity of the stress intensity factor conception and for comparing fracture surfaces with those obtained in the flight-simulation tests.

3 TEST RESULTS

Detailed results of 70 flight-simulation tests and 27 constant-amplitude tests are presented in reference 4. Here only a summary will be given. In figure 5 the crack propagation rate in microns per flight is plotted as a function of the crack length. This has been done for $S_m = 10$ and $S_m = 8.5$ kg/mm^2. The results for the three frequencies applied (10, 1 and 0.1 cps) are quite erratically distributed in a narrow scatter band, without noticeably systematical trends. The same can be observed in table 2, where the crack propagation lives covering two crack growth intervals (l from 12 mm to 20 mm and l from 20 mm to 30 mm) are compared. The life ratios are fairly close to 1, and do not show a systematic trend.

For $S_m = 7.0$ and 5.5 kg/mm^2 a test at 0.1 cycles per second would have required about 1800 and 4500 hours for the 2024-T3 alloy and about 900 and 1800 hours for the 7075-T6 alloy. This was considered to be prohibitive and it was decided to determine only smaller parts of the crack propagation curves for these conditions. In a test at 10 cps a period of 595 flights was carried out at 1 cps, followed by a similar period at 0.1 cps, after which the test was completed at 10 cps. The crack extension during the two lower-frequency periods was deduced from fractographic observations. The most severe flights with the maximum amplitude ($S_{a,max}$ = truncation level) were applied at regular intervals, see section 2.2, that means after each 119 flights. These severe flights produced a dark band on the fracture surfaces as shown by the pictures in figure 6. By measuring the spacing between the bands, crack rates were derived from such pictures.

The results were plotted in figure 7 with the data from the visual crack growth observations as a standard for comparison. The accuracy of the fractographic observations is sometimes limited due to ill-defined growth bands. Nevertheless, it appears to be justified that the data in figure 7 do not indicate any frequency effect at all. For $S_m = 4.0$ kg/mm^2 tests were carried out at 10 cps only.

The effect of the design stress level is not a subject of this paper and therefore a few comments will be made only. Figure 5 already illustrates a significant effect of the stress level. Crack propagation lives obtained at 10 cps at all five stress levels employed are given in figure 8. This figure shows that the effect is different for the two alloys.

It was hoped that the crack rates for different stress levels could be correlated by the stress intensity factor which for the flight-simulation tests may be written as $K = C \, S_m \sqrt{\pi l}$. Unfortunately, coinciding $dl/dn - K$ curves for the five stress levels were not obtained, on the contrary, the curves were significantly different. For the constant-amplitude tests, however, the relation $dl/dn = f_R (\Delta K)$ was clearly confirmed once again. The different behaviour for the two types of tests is further analysed in reference 4.

4 DISCUSSION

4.1 The frequency effect

The results shown in figures 5 and 7 and table 2 indicate small and unsystematic differences between the results for the three frequencies. Two questions should be asked now:

a Is the absence of a frequency effect in the flight-simulation tests a logical result?

b What are the consequences of the present findings?

Investigations on the frequency effect as reported in the literature (surveys in references 7,8) were almost exclusively constant-amplitude tests. An exception are flight-simulation tests performed by

Branger (Ref.9) on light-alloy specimens notched by two holes. He found a slightly lower life at 1.6 cps as compared to 2.9 cps. Surprisingly enough he found a reversed frequency effect in another test series with frequencies of 3.5, 0.7 and 0.09 cps respectively. The longer life was obtained at the lower frequency. Trends of investigations with constant-amplitude loading will be summarized below. A frequency effect may be caused by environmental effects or by time dependent mechanisms in the material itself. Moreover, co-operation of different mechanisms appears to be possible. Considering first the material itself, time dependent mechanisms could be associated with activities of dislocations, changing precipitated zones and interactions of both. Such mechanisms should be promoted by higher temperatures and should be active in creep as well. However, the present alloys at room temperature appear to be well below the creep range. If a time dependent mechanism in the material itself would be active it should be so especially at high stress levels. Data from constant-amplitude tests at room temperature revealed a small frequency effect only, whereas the effect was somewhat larger at elevated temperature (see the survey given by Barrois in reference 8). In the present investigation there is no tendency for longer crack propagation in the tests with the highest stress level ($S_m = 10 \ kg/mm^2$) and the lowest frequency (0.1 cps).

The environmental effect on crack propagation in aluminium alloys was studied in several investigations (Refs 10-20). Environments employed may be divided in four groups:

1. Aqueous NaCl solutions
2. Distilled water
   Humid gaseous environments (air, oxygen, inert gas)
3. Dry gaseous environments
4. Vacuum.

Maximum crack rates were found in the first and minimum crack rates in the last group. Three different types of mechanisms may be indicated, which could affect fatigue crack growth.

a. Corrosion fatigue
b. Stress corrosion
c. Rewelding of the crack surfaces (vacuum).

Whereas the latter one will delay crack growth, the former two mechanisms are deleterious. In a particular case it may be difficult to separate the activities of corrosion fatigue and stress corrosion. The corrosion fatigue is understood to be a resolving of the material from the anodic crack tip material, which requires an aqueous solution. This will occur at any stress level and it will be time dependent. In general terms the contribution of stress corrosion to crack growth is supposed to be a lowering of the strength of metallic bonds. Hence it should be dependent on the stress intensity at the tip of the crack. If the intensity is below $K_{I_{scc}}$, crack growth will not be assisted by stress corrosion. If $K > K_{I_{scc}}$, accelerated crack growth should be expected at lower frequencies. For Al-alloy sheet material $K_{I_{scc}}$ will be large enough to avoid a contribution of stress corrosion. However, for forgings of Al-alloys if loaded in the unfavourable short-transverse direction a contribution will be possible and it might even predominate fatigue.

A frequency effect should also be expected if it requires some time for the environment to reach the tip of the growing crack (Ref.21), or if diffusion is involved. In this respect the predominating effect of water vapour in gaseous environments is relevant, as shown by the work of Hartman et al. (Refs 10-12) and Bradshaw and Wheeler (Refs 13-15). It should be said that the mechanism of the water vapour effect is not yet fully understood. It might even be labelled as corrosion fatigue. Nevertheless, crack rates in dry air were found to be much lower than those in humid air. The effect of the water vapour contents of the air on crack propagation was frequency dependent, indicating some time dependent mechanism to be active. For the present investigation it may be deduced from references 11, 12 and 14 that the conditions (room temperature, 40-45 percent relative humidity, frequency range 0.1-10 cps) are beyond the range where an important frequency effect should be expected. That means that there is sufficient water vapour available and also sufficient time, even at 10 cps, for an almost maximum harmful effect of the water vapour. Consequently, the constant-amplitude test data predict a small effect only, if any at all. This is in agreement with the results of the flight-simulation tests.

There were some reasons why it was desirable to check empirically the frequency effect under flight-simulation loading.

(1) The accumulation of fatigue damage under such a complex load hietory may be different from what it ie under constant-amplitude loading. Actually it is different as will be diecuseed later.

(2) A previous investigation (Ref.22) on sheet specimens of the same alloys loaded by a very severe flight-simulation loading indicated an environmental effect for the 7075 alloy. Comparative teets were carried out indoore and outdoors. Crack ratss wsrs practically the same for the 2024 alloy, but those obtained outdoors for the 7075 alloy were about 1.5-2 times faster than the indoors rssulte. The outdoors specimene were subjectad to rain and dew.

(3) The arsessmsnt of eafe inspection periods for an aircraft in eervice requires that safety factore are applied to crack propagation data obtained in laboratory teste or in a full-scale fatigue teet. A maaning-ful celection of such factors cannot be made without some direct empirical evidence.

Orders of magnitude of the duration of a single load cycle and the correeponding frequencies are given in figure 9. Frequencies employed in the present investigation are conforming to guets, short-duration manoeuvres and taxiing loade. For these types of loads the prssent investigation euggests that a frequency effect in a gaseous environment may be expscted to be emall and safety factore ehould mainly serve for covering scatter in material propsrties and aircraft load epsctra.

For a fuselage, the preesurisation may be the prsdominating load cycle. This cycle has a very long psriod while the variabiiity of the load amplitude is much smallsr than for a wing structure. In this cass some more empirical evidence seems desirable. Unfortunately testing times for relevant frequenciee are extremely long.

The problem ie much more difficult for an aqueous environment. The empirical evidence, available from constant-amplitude teata only, indicatee that crack rates in diatilled water and in humid air are quite similar, whereas crack growth in salt water is generally faeter. The problem ie to find out whether salt water could be present in fatigue cracks in an aircraft in eervics. Moreover, it ehould be there for a long time in order to affect the crack propagation. Although it is known that severe corroeion may occur in aircraft flying in a marine environmant (Refa 18,23), this does not imply that salt water will generally ba preeent in fatigue cracke, especially if the aircraft is not flying in a marine environment, such as a civil transport. Neverthelese, it appears worthwhile to perform some flight-eimulation tests in order to check what the magnitude of the effect of a ealt water environment cn crack propagation may be for this type of loading. Such a test aeries should include low frequencies.

4.2 Damage accumulation

It is well recognized by now that the Palmgren-Miner rule will not produce accurate life estimates. This ie largely a consequence of interaction effects aesociated with load cycles of different magnitudes, as explained once again in a recent survey (Ref.1). Neverthelese, a calculation of n/N may give a qualita-tive indication of the presenre of such interaction effects. The results of damage calculations baeed on the crack propagation life are given in table 3 for $S_m = 3.5$ and 5.5 kg/mm^2. Constant-amplitude data were determined for theee S_m-valuee only. The ground-to-air cycle for each flight wae aesumed to be a cycle between S_{min} of the CTAC and $S_{max} = S_m + S_{a,max}$ pertaining to that flight. In table 3 the damage increments of the gust cycles and the CTAC are given separately. The total damage values n/N are far in excess of 1, which indicates that the damage accumulation was much elower than predicted by the Palmgren-Miner rule. Crack propagation ratee were aleo calculated, employing the formula:

$$\left(\frac{d\ell}{dn}\right)_{FST,\ell=\ell_j} = \frac{\sum^i n_i \left(\frac{d\ell}{dn}\right)_{CA,\ell=\ell_j}}{\sum^i n_i}$$

In this equation FST and CA refer to flight-eimulation teet and constant-amplitude test respectively. The calculations were made for eeveral valuee of the crack length $\ell = \ell_j$. The number of individual cycles of each magnitude (n_i) was drawn from table 1. The equation implies that the Palmgren-Miner rule is applied to the fatigue life increment required for a small crack growth increment $\Delta\ell$. In agreement with table 3 it wae found that the actual crack rates were 2-15 timee lower than predicted, depending on ℓ_j and S_m. The low crack rates should per definition be attributed to interaction mechaniems. In reference 1 eeveral

mechanisms were mentioned, namely residual stress, cyclic strain-hardening, crack blunting, crack closure and mismatch of crack front orientation. It is difficult to indicate the mechanisms that were most active. It is thought that residual stresses due to the higher-amplitude cycles certainly have delayed crack growth during the lower-amplitude cycles. The preference for the plane-strain situation, as discussed hereafter, is pointing to lower amounts of plastic deformation. This could be a consequence of cyclic strain hardening by the higher-amplitude cycles, while crack closure could also be responsible. The latter mechanism might be associated with the dark growth bends in the 2024 specimens. The mismatch of crack front orientation should also have some significance, anyhow for the larger amplitude cycles. It might even be essential for the dark growth bands in the 7075 specimens.

A second important difference between damage accumulation in flight-simulation tests and constant-amplitude tests was offered by macro-fractographical observations. These observations indicated that the fatigue crack in the flight-simulation test is propagating in the 90°-mode to a much larger crack length than expected on the basis of corresponding constant-amplitude tests. In other words flight-simulation loading appears to emphasize plane-strain conditions. Consequently one hardly can expect that the damage accumulation in a flight-simulation test can be simply derived from the results of constant-amplitude tests.

The conclusion to be drawn from the above arguments is that empirical trends as observed in constant-amplitude tests, need not necessarily be valid for flight-simulation tests. Actually for that reason the frequency effect was studied under flight-simulation loading. In this respect reference may be made once again to the different types of growth bands exhibited by the two alloys (Fig.6). Another difference observed in constant-amplitude tests on a micro scale (Ref.24) is the tendency to brittle striations which may occur in the 7075 alloy whereas ductile striations are predominant in the 2024 alloy. Brittle striations are frequently associated with a larger environmental effect (Refs 19,20). Fortunately this effect did not emerge from the present flight-simulation tests. However, it is somewhat disturbing that it might be present in more aggressive environments (Ref.18). Consequently, the need for flight-simulation tests in more aggressive environments may be repeated here.

5 CONCLUSIONS

Fatigue crack propagation was studied in random flight-simulation tests on 2024-T3 Alclad and 7075-T6 Clad specimens. The main variables were the load frequency (10, 1 and 0.1 cps) and the design stress level. The design stress level was characterized by the mean stress in flight, for which five values were adopted (10.0, 8.5, 7.0, 5.5 and 4.0 kg/mm^2). The ratios between the amplitudes of the gust cycles, the GTAC and the mean stress in flight were the same in all tests. A small number of constant-amplitude tests was carried out for supporting the flight-simulation test results. The results and the discussion are summarized below.

1. Differences between the crack propagation rates at the three test frequencies (10, 1 and 0.1 cps) were small and unsystematic. From a discussion on the effects of frequency and environment it was concluded that safety factors on inspection periods in service should be applied mainly to cover scatter in material properties and aircraft load spectra. This conclusion only holds if the environment of the aircraft is not particularly aggressive. If a more aggressive environment, for instance salt water, is continuously present in the crack, faster crack rates may occur and the loading rate may become important. This should be verified by tests.

2. The damage accumulation in the flight-simulation tests could not be predicted from the data obtained in constant-amplitude tests. The values of $\sum n/N$ varied from 4 to 8. Moreover, the cracking behaviour was different for the two types of testing. Flight-simulation loading is emphasizing plane-strain conditions at the tip of the crack. As a consequence trends observed in constant-amplitude tests need not be valid for flight-simulation loading. This should be checked empirically.

REFERENCES

1. Schijve, J.   The accumulation of fatigue damage in aircraft materials and structures. AGARDograph 157, 1972.

2. Schijve, J.   The effect of load sequence on fatigue crack propagation under random loading and program loading. NLR TR 71014, Amsterdam, 1971.

3.   Sixth ICAF Symposium, Miami, May 1971. To be issued as an NASA document.

4. Schijve, J.   Jacobs, F.A.   Tromp, P.J.   Fatigue crack growth in aluminium alloy sheet material under flight-simulation loading. Effects of design stress level and loading frequency. NLR TR 72018, Amsterdam, 1972.

5. Schijve, J.   Cumulative damage problems in aircraft structures and materials. The 2nd F.J. Plantema Memorial Lecture, ICAF Conference, Stockholm, 1969. The Aeronautical Journal, 1970, Vol.74, 517-532. Also NLR MP 69005, Amsterdam,1969.

6. Naumann, E.C.   Evaluation of the influence of load randomization and of ground-to-air cycles on fatigue life. NASA TN D-1584, 1964.

7. Van Leeuwen, H.P.   Predicting material behaviour under load, time and temperature conditions. AGARD Report 513, 1965.

8. Barrois, W.C.   Manual on fatigue of structures. Fundamental and physical aspects. AGARD-MAN-8-70, 1970.

9. Branger, J.   The influence of modifications of a fatigue history loading program. Paper 6th ICAF Symposium, Miami, May 1971. To be issued as an NASA document.

10. Hartman, A.   On the effect of oxygen and water vapour on the propagation of fatigue cracks in 2024-T3 Alclad sheet. Int. J. of Fract. Mech., 1965, Vol.1, 167-188.

11. Hartman, A.   Jacobs, F.A.   Nederveen, A.   De Rijk, P.   Some tests on the effect of the environment on the propagation of fatigue cracks in aluminium alloys. NLR Report M.2182, Amsterdam, 1967.

12. Hartman, A.   Schijve, J.   The effects of environment and load frequency on the crack propagation law for macro fatigue crack growth in aluminium alloys. Eng. Fract. Mech., 1970, Vol.1, 615-631.

13. Bradshaw, F.J.   Wheeler, C.   The effect of environment on fatigue crack growth in aluminium and some aluminium alloys. Appl. Mats. Res., 1966, Vol.5, 112-120.

14. Bradshaw, F.J.   Wheeler, C.   The influence of gaseous environment and fatigue frequency on the growth of fatigue cracks in some aluminium alloys. Int. J. of Fract. Mech., 1969, Vol.5, 255-268.

15. Bradshaw, F.J.   Gunn, N.J.F.   Wheeler, C.   An experiment on the effect of fatigue wave form on crack propagation in an aluminium alloy. RAE Tech. Memo. Met. 93, July, 1970.

16. Figge, I.E.   Hudson, C.M.   Crack propagation, delayed fracture and residual static strength of titanium, aluminium, and stainless steel alloys in aqueous environments. NASA TN D-3825, 1967.

17. Smith, S.H. Fatigue crack propagation and freoture toughness characteristics of 7079
    Porter, T.R. aluminum alloy sheets and plates in three aged conditions. NASA CR-996, 1968.
    Sump, W.D.

18. Gruff, J.J. Effects of corrosive environments on fatigue life of aluminum alloys under
    Hutcheson, J.G. maneuver spectrum loading. Proc. Conference on Fatigue and Fracture of Aircraft
                 Structures and Materials, AFFDL Tech. Rep. 70-144, 1970, 521-537.

19. Feeney, J.A. Environmental fatigue crack propagation of aluminum alloys at low stress intensity
    McMillan, J.C. levels. Metallurgical Trans., 1970, Vol.1, 1741-1757.
    Wei, R.P.

20. Speidel, M.O. Corrosion-fatigue and stress-corrosion crack growth in high-strength aluminium
    Blackburn, M.J. alloys, magnesium alloys and titanium alloys, exposed to aqueous solutions.
    Beck, T.R. Paper at Int. Conf. on Corrosion Fatigue, University of Connecticut, June 1971.
    Feeney, J.A.

21. Bradehaw, F.J. The effect of gaseous environment on fatigue crack propagation. Scripta Metallurgica,
                 1967, Vol.1, 41-43.

22. Schijve, J. The crack propagation in two aluminium alloys in an indoors and an ourdoors
    De Rijk, P. environment under random and programmed load sequences.
                 NLR TR M.2156, Amsterdam, 1965.

23. Shaffer, I.S. Corrosion and fatigue studies of extruded 7075-T6 spar caps.
    Sebastion, J.C. J. of Materials, 1968, Vol.3, 400-424.
    Rosenfeld, M.S.
    Ketchan, S.J.

24. Ryder, D.A. The elements of fractography. AGARDograph No. 155, 1971.

Table 1   Gust load occurrences in the 10 different types of flights

Flight type	Number of flights in 5000 flights	Numbers of gust cycles with amplitude S_a/S_m											Total number of cycles per flight
		1.729	1.571	1.414	1.257	1.100	0.943	0.786	0.629	0.471	0.314	0.157	
A	1	1	0	1	1	2	3	5	9	15	27	43	107
B	2		1	1	1	1	2	4	8	14	26	43	101
C	2			1	1	1	2	3	7	12	25	43	95
D	10				1	1	1	3	5	11	24	43	89
E	27					1	1	2	3	9	22	43	81
F	91						1	1	3	7	18	43	73
G	301							1	2	4	15	42	64
H	858								1	3	11	38	53
J	3165									1	7	23	36
K	543										1	19	20
Total number of cycles in all flights		1	2	5	15	43	139	495	1903	3000	39252	149902	Average per flight 40
Number of exceedings, see figure 3		1	3	8	23	66	205	700	2603	10603	49855	199757	

Table 2 The effect of frequency on the crack propagation life for two crack growth intervals ($\ell = 12 \rightarrow 20$ mm and $\ell = 20 \rightarrow 30$ mm)

Material	σ_m (kg/mm²)	Frequency (cps)	Mean life (flights)		Life ratios	
			$N_{20} - N_{12}$	$N_{30} - N_{20}$	$N_{20} - N_{12}$	$N_{30} - N_{20}$
2024	10	10	364	294	1	1
		1	934	319	1.08	1.09
		0.1	856	377	0.99	1.23
	8.5	10	2489	1242	1	1
		1	2645	1200	1.06	0.97
		0.1	-	1179	-	0.95
7075	10	10	1108	393	1	1
		1	921	343	0.83	0.87
		0.1	1206	548	1.09	1.39
	8.5	10	2035	1561	1	1
		1	2206	1566	1.08	1.00
		0.1	-	1274	-	0.82

Table 3 Damage values for crack propagation lives in the flight-simulation tests

The crack propagation life N in this table is covering crack growth from $\ell = 12$ mm to $\ell = 30$ mm ($N = N_{30} - N_{12}$)

Material	σ_m (kg/mm²)	Damage increments		$\sum n_i/N$
		Gust cycles	GTAC	
2024	8.5	2.2	1.8	4.0
	5.5	3.0	1.5	4.5
7075	8.5	6.0	2.3	8.3
	5.5	4.4	0.6	5.0

SHEET THICKNESS 2 mm

MATERIAL : 2024 — T3 ALCLAD AND

7075 — T6 CLAD
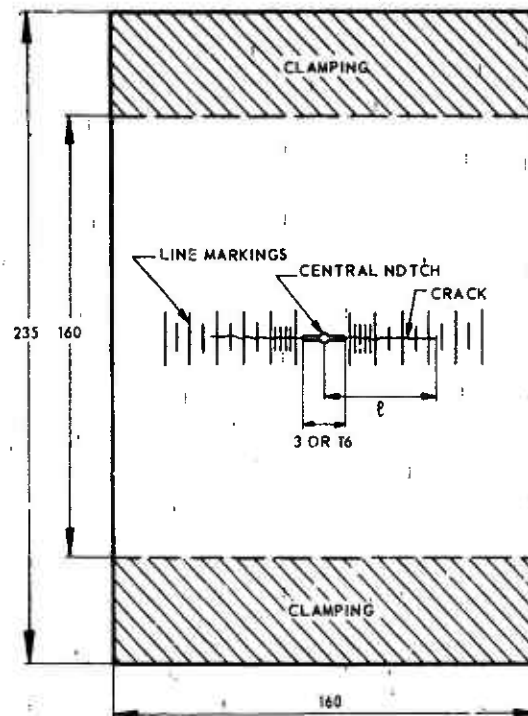
DIMENSIONS IN mm (1mm = 0.04'')

Figure 1   Dimensions of the specimens
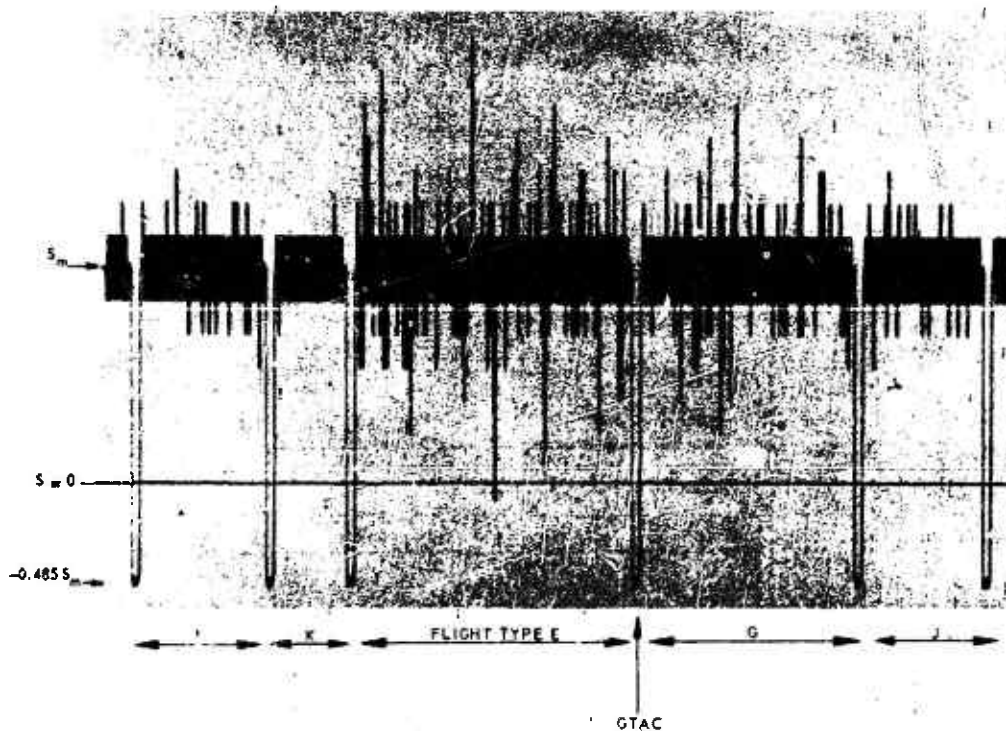
Figure 2   Sample of the flight-simulation loading with different types of
flights, illustrating the random sequence of the gust loads
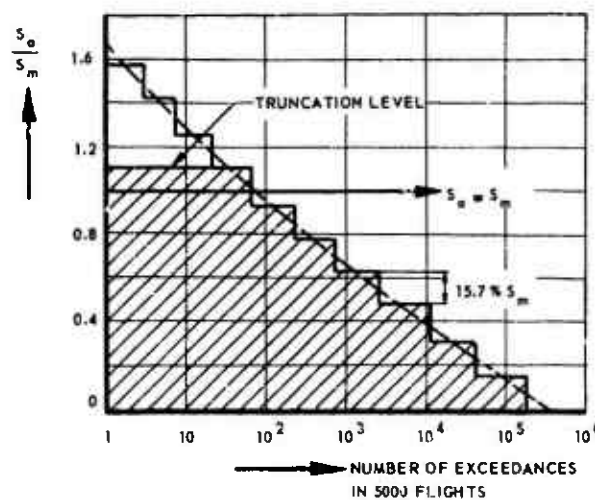
Figure 3 Stepped approximation of the gust load spectrum

Figure 4 Picture taken with the Nikon camera for crack growth recording overnight. Flight counter at right. (Magnification 0.8 x)
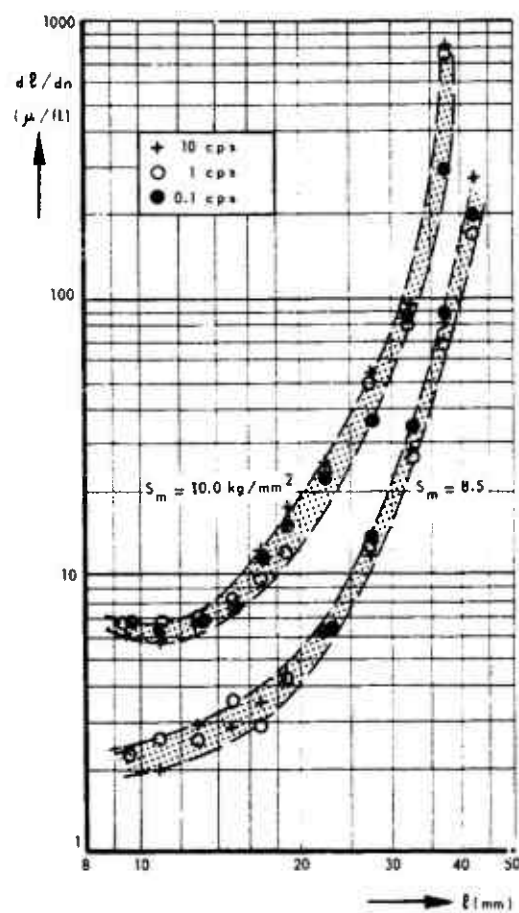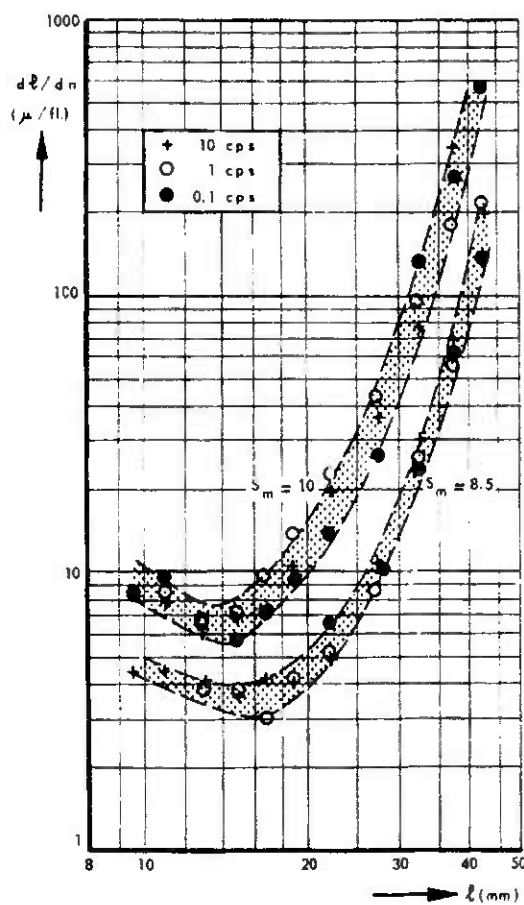
Figure 5 The effect of the loading frequency on the crack propagation rate
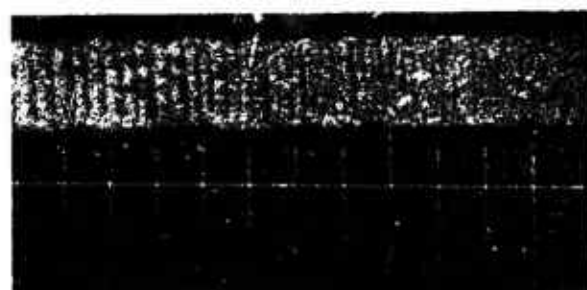
SPECIMEN C 3, 2024 – T 3
ℓ = 18 mm TO ℓ = 30 mm

SPECIMEN D 3, 7075 – T 6,
ℓ = 18 mm TO ℓ = 30 mm

Figure 6 Macro growth bands caused by the most severe flights.
Crack growth from right to left. (Magnification 7 x)
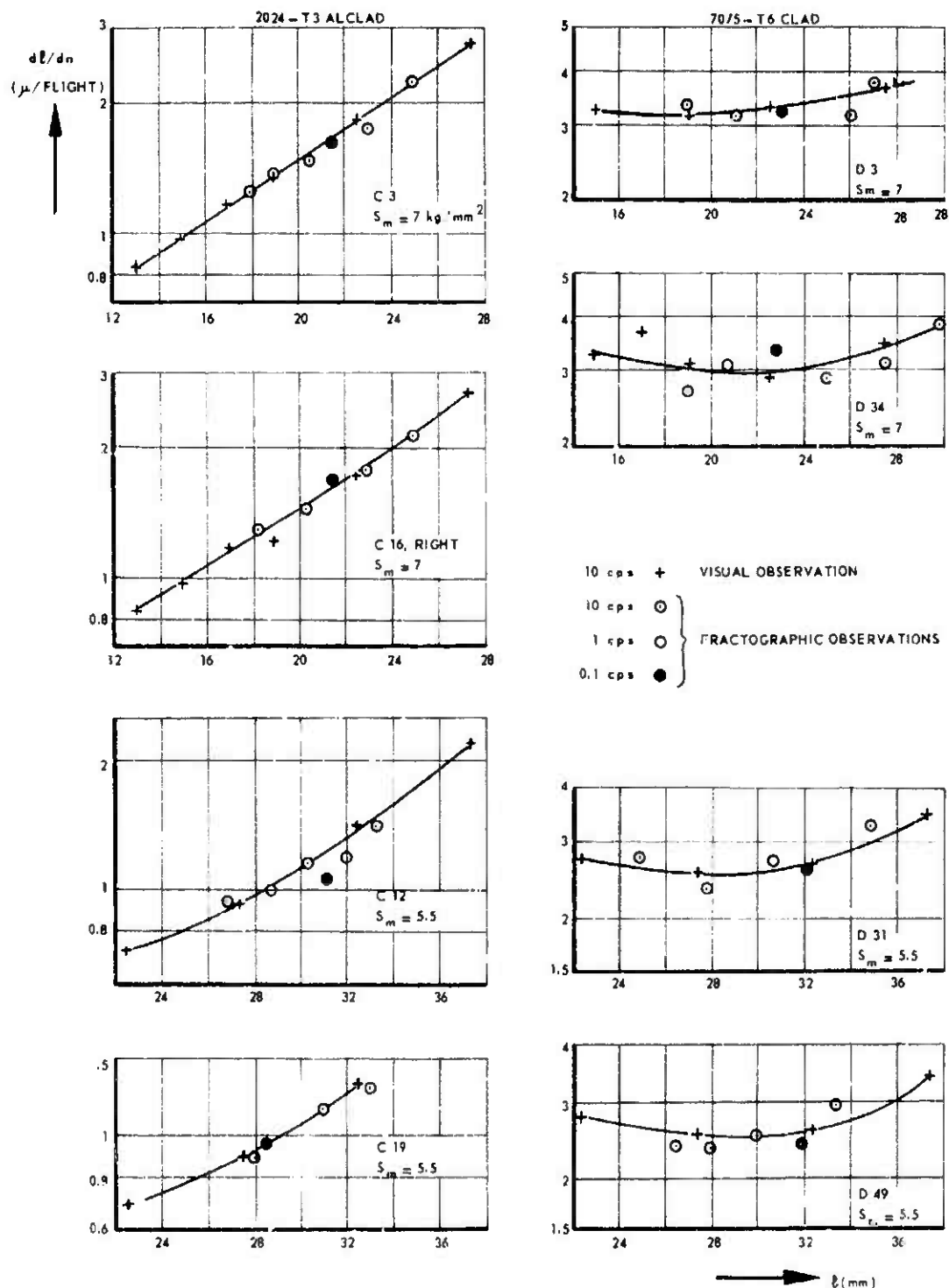
Figure 7 Comparison between crack rates derived from visual and
fractographic observations. Effect of frequency
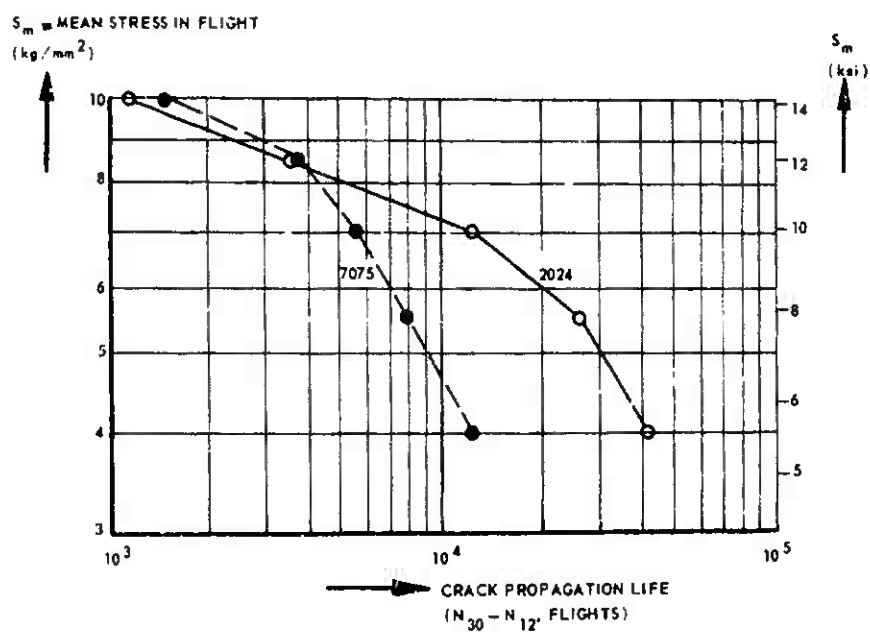
Figure 8 The effect of stress level on the crack propagation life
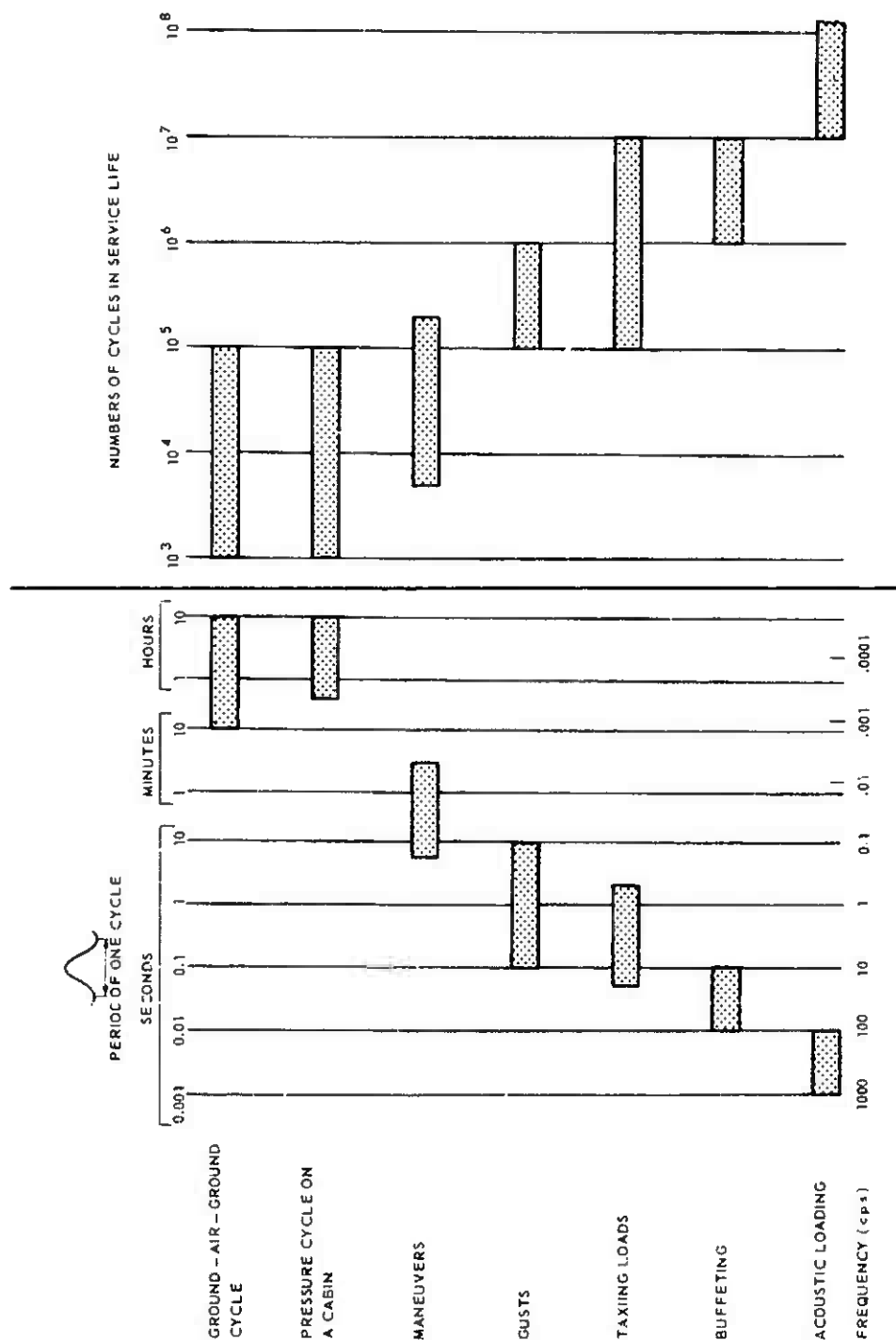
Figure 9 Periods, frequencies and numbers of several types of aircraft
fatigue loads (Ref.1). Orders of magnitude

CORRELATION BETWEEN LABORATORY TESTS ANO SERVICE EXPERIENCE

W. B. MILLER
Technical Director
Directorate of Airframe Subsystems Engineering
Aeronautical Systems Oivision
U. S. Air Force Systems Command
Wright-Patterson Air Force Base, Ohio 45433

HOLLAND B. LOWNOES
Assistant for Experimental Simulation
Structures Oivision
Air Force Flight Oynamics Laboratory
U. S. Air Force Systems Command
Wright-Patterson Air Force Base, Ohio 45433

SUMMARY

Oirect comparisons are made between full scale fatigue test failures and actual service failures for several military aircraft. The correlations are discussed in relation to the basic fatigue test procedures ꞏnd spectra used. Some methods used to force correlation where apparent correlation is lacking are discussed. The paper concludes with a historical summary of the improvements in fatigue testing evolved over the past 25 years.

LIST OF ABBREVIATIONS

VGH – Velocity, load factor, altitude
KIAS – Knots, indicated air speed
GAG – Ground air ground cycle
ASD – U. S. Air Force Aeronautical Systems Division
TAC – U. S. Air Force Tactical Air Command
SS – Stabilator station
WS – Wing station
FS – Fuselage station

I. INTRODUCTION

Since 1958 when a number of serious fatigue problems in military airplanes confronted the military services in the United States, the Air Force and the Navy have been working toward programs to identify and cope with potential service fatigue problems. The very large costs of these programs drive us toward a continual assessment of the level of success we have had in implementing the procedures evolving from these programs.

The U. S. Air Force continues to be perplexed by the problem of correlation of critical full scale fatigue test results from our aircraft systems and their actual fatigue damage experience once they are in operational service.

We have continued to try to develop as extensive a data base as possible to assist in our understanding of this problem. References 1 and 2 present previous data and analysis we have assembled. We will make frequent reference to these two papers as this presentation is developed.

Again, as was stated in Reference 2, it is strongly felt that in considering the information of this nature it should be kept in mind that, while each of the structural certification programs studied were conducted in essentially the same manner - around the same general criteria requirements, they each varied to some degree from each other due to particular circumstances of that specific aircraft program. In other words, the results from these programs cannot be compared to each other in the same sense - and with the same accuracy - as test results from identical specimens tested and evaluated to the same identical criteria and with identical test methods. However, it is felt that general trends established from comparing these results are valid trends. The understanding of these limitations cannot be over-emphasized. In fact, perhaps the technical community has erred in the way we have "expressed our concern" over this test-to-service correlation - or lack of correlation - problem.

II. WHAT IS THE PROBLEM?

The major problem encountered as stated in Reference 2 by Lowndes has been the lack of correlation between our predicted time to failure based upon the fatigue analysis and full scale test program as compared to the actual time to failure in the fleet operation. Unfortunately, this continues to be the same problem. In Reference 1, Miller and Lowndes attempted to add some data to that previously presented by Raithby in an effort to shed more light on the scatter in the data correlation. In Reference 2, Lowndes looked at some ways of forcing correlation and the thesis advanced appears to offer some hope that correlation can be improved if a good data base on usage can be obtained.

In trying to cope with the scatter encountered in fatigue life prediction, two theses have been proposed in the U. S. In one case, loads are applied representing the high side of the loads scatter band and test results divided by a factor of two. In the other case, loads are applied representing average conditions and the test results divided by a factor of four. While these approaches are used to establish the initial life estimates, a true correlation of test life to service life is ultimately dependent on validation of the actual usage.

III. DISCUSSION

Medium Transport A

For transport type aircraft, the best correlation study information is still that presented in Reference 2 for the airplane referred to as "Medium Transport A". This transport was tested to a spectrum representing taxi, ground-air-ground and gust loads. Within each type of loading, 3 different mean loads were employed and 2 to 3 different load levels about each mean. The loads were applied in 1000 hour blocks of 16021 individual load cycles using a negative-low-high-low-negative truncation. As is pointed out in Reference 2, service aircraft exhibited a wide spread in time of occurrence of failure. In this case, a good multi-channel service loads data recording program coupled with aircraft usage data forms enabled us to obtain much better correlation and to do tail number tracking. The recorded data were consolidated into 9 mission profiles. Correlation was attempted using a sample of 42 aircraft. The first correlation using these data assumed all 42 aircraft flew the same mission mix. The test-to-service correlation is shown by the upper curves in Figure 1. A second correlation, using the individual aircraft service records plus the recorded loads data, on a tail number basis, was attempted and this correlation is shown by the lower curve in Figure 1.

Fighter Bomber A

This aircraft is referred to as "Fighter Bomber A" in Reference 2. Since the full scale wing fatigue test was conducted late in its service life, the spectrum was developed from a limited amount of service load data measured during squadron training correlated with actual load data from a structural loads measurement flight vehicle. The test spectrum was a random load flight by flight spectrum including positive and negative flight loads plus landing gear loads. Thirty load levels were applied each flight, a load equal to 121.5% limit load was applied each 10th flight, and a load equal to 137.5% limit load was applied each 100th flight. In this case, a good correlation was obtained using a factor of 2 as shown in Figure 2. In pursuing this correlation further, one can review the test load exceedance data used in this test and its correlation with flight loads exceedance data as presented in Figure 10. In this case, it can be seen that the original estimated usage (the test spectra) was not very different from the measured fleet usage - particularly the actual operational usage to which a large percentage of the fleet had been subjected. The fact that this test program was conducted late in the airplane's life as a re-evaluation/life extension program undoubtedly provided us with better visibility as to how we were flying the aircraft than would normally be the case for a new aircraft just being introduced into the inventory. However, in this instance the test spectrum was still more severe than any of the measured operational usage, a fact which to some extent

Influences the fact that our test-to-service scatter was only in the neighborhood of 2 - quite consistently so for all four critical areas. The fact that this is the only example which utilized a flight-by-flight approach - introducing landing loads alternately with the wing loads, and also utilized a random application of the flight loads - may also be an influencing effect on the small scatter factor.

Fighter Bomber B

As explained in Reference 2, the full scale test was started early, before a significant number of these aircraft were in service and before any measured service loads were available. The early tests were made using a block spectrum; each block representing 200 hours and consisting of 1000 load cycles. After a very early failure, the structure was revised and the test spectrum revised to reflect 400 hours of recorded VGH data - both training and operational readiness flying. Figure 3 presents a summary of predicted life from the test, calculated life using data from training operations, and calculated life using data from actual service. It may be seen that the calculated life at all of the critical areas decreased. However, at the fuselage station 442 - main wing attach frame this reduction is quite small - approximately 15%; whereas the remainder of the areas showed life reductions of approximately 40 to 60%.

In reviewing why this one area showed only a small reduction in life for apparently a significantly more severe operational environment one must look beyond the generalized maneuver exceedance data from the VGH records and review the additional aspects of gross weight and stores configuration. It was determined that this main wing frame at fuselage station 442 - which is influenced primarily by wing root bending moment - was experiencing the approximate same wing bending moment from higher load factor operational maneuver experience as that determined from the peace time usage because the operational missions were being flown over the target with full inboard wing tanks - which had been empty in simulated operational exercises.

Two fuselage failures in this airplane provide us with an example of the need to faithfully duplicate the production structure in the test article. The full scale fatigue test was performed on a specimen in which a cutout in the fuselage station 350 cover splice on the top centerline was rectangular in shape. In production, it was changed to a trapezoidal shape. At the time, the change was reviewed as an engineering deviation, but was not considered a fatigue critical item. After about 500 flight hours, one of these aircraft crashed in May 1964 as a result of the failure of F.S. 350 at the top centerline. Another crashed in June 1965 for the same reason. Subsequent to the first failure, a tensile test and a fatigue test of the fuselage components in the production configuration were conducted. The fatigue test confirmed the mode and location of the failure. What was determined to be a "non-fatigue critical item", was thus shown to be critical in fleet use. The test article must be representative of the production (fleet) configuration. Fatigue testing and analysis focus attention on structural details because that is where the service problems will be found. Since the emphasis is on details, it is essential that the test article and analyses reflect those details. If this is not accomplished, the test results (as this example shows) will not correlate with service experience.

Fighter Bomber C

The test spectrum for the first 6000 test hours represented one maneuvering flight condition (40,000 lbs gross weight at 1.14 Mach at 25,000 ft altitude, positive loads only, clean wing aircraft). This altitude/airspeed represented the maximum load condition for any given maneuver. No negative loads, external store loads, gust loads, or ground-air-ground (take-off, landing etc) loads were included in the test spectrum. Testing beyond 6000 test hours was performed to a modified spectrum in which all loads below 65 percent of design limit load were eliminated in order to reduce the testing time required. See Figure 4 for a representation of the test spectrum. Loads were applied in blocks representing 100 hours per block.

From December 1968 to December 1970 approximately 5640 valid flight hours of VGH (velocity, load factor, altitude) data were recorded on operational aircraft. The mission distribution is as follows:

a.	Recon	15.5 percent
b.	Test	0.6 percent
c.	Instruments	9.9 percent
d.	Air Intercept	3.7 percent
e.	Air to Ground	70.3 percent

The average airspeed flown during the maneuver phase of the air-to-ground mission is 367 KIAS while the average altitude is 10,800 ft. significantly different from the condition simulated in test. Figure 4 shows the full usage spectrum (positive and negative loads) for the air-to-ground mission. The load spectrum curves are corrected to a mission average gross weight of 45,800 lbs. This high average gross weight is indicative of the heavy external store loads carried during this operational mission (empty weight approximately 29,000 lbs; maximum take off gross weight 58,000 lbs).

During calendar year 1965, 2956 flight hours of VGH data were recorded on this type aircraft at two bases. The mission distribution is as follows:

a.	Special Weapons Delivery	8.3 percent
b.	Conventional Weapons Delivery	32.7 percent
c.	Air Intercept	13.7 percent
d.	Air Tactics	27.7 percent
e.	Instruments and Navigation	15.2 percent
f.	Test	2.4 percent

The load spectrum curve for mission B (only the positive load portion is available) corrected for a gross weight of 40,300 lbs is shown on Figure 4. Comparison of the operational data with the earlier TAC data demonstrates the significant changes in mission distribution and flight loads.

Eight special mission aircraft began operation in July 1969. Each aircraft is equipped with a VGH recorder and a substantial amount of flight loads data has been gathered on these aircraft. Figure 4 shows the usage spectrum (positive and negative portions) for the one most severely used special mission aircraft. Its usage is much more severe than any other usage spectrum including spectrum "A" of Specification MIL-A-8866. The other special aircraft usage is about as severe as MIL-A-8866. The MIL-A-8866 spectrum and th special mission spectrum for other than the severely used one have not been shown on Figure 4 in order to prevent confusion.

To date there have been three major structural components that have failed in-service where the failure has been attributed to metal fatigue. Each will be discussed separately:

    4. Stabilator:

The Fighter Bomber "C" fleet has experienced three in-flight failures of the stabilator where the outer portion of the stabilator separated at the SS 51.85 splice rib (see Figure 5). The crack begins at the aft edge of the aluminum skin and progresses forward along SS 51.85. The crack cannot be detected visually due to its being hidden by the overlap of the inner skin. The crack progresses forward at least halfway then turns outboard towards the forward edge of the skin. Total crack length is 15 inches to 18 inches. In each case, the aircraft was recovered safely. The cause of failure in the first two cases could not be positively determined since the crack was present for a period of time before complete failure occurred. Evidence of fatigue was destroyed by the fractured surfaces rubbing against each other. In addition, about fifteen stabilators have sustained upper skin failures without the outer portion of the stabilator being lost. Flying hours on the stabilator at the time of failure range from 500 to 1540. Without exception, those failures that could be positively diagnosed as fatigue started at or near the aft edge of the upper outboard torque box skin. Some failures were accelerated by the presence of tool marks in the skin as a result of the machining operation. The manufacturer's current recommendation is to remove and replace the upper aluminum skin with a titanium skin. Since no previous fatigue testing has been accomplished on the stabilator, no realistic service life estimates exist for it. As a matter of interest, the high time aircraft has accumulated over 3,400 flight hours, far in excess of the figure at which any failures have occurred.

    B. Outer Wing:

The outer wing was fatigue tested as part of the full scale airframe cyclic test program. Design and fabrication deficiencies caused knife edge fastener holes in the lower torque box skin resulting in a fatigue sensitive member (See Figure 6 for the general location of the cracks). On 16 December 1969, one aircraft experienced a failure of the left outer wing. The location of the failure is shown in Figure 7(A). On 26 February 1970, a second aircraft experienced a failure of the left outer wing (See Figure 7(C) for crack location). On 10 March 1970, a third aircraft sustained a failure and loss of the right outer wing. This failure is also shown in Figure 7(E). Two typical cases of skin cracking that did not result in complete failure are also shown in Figure 7(B) and (D) The flight hours on each aircraft, respectively, were 1,700 hours, 1,259 hours, and 464 hours. The fatigue tests demonstrated the outboard lower wing skin to be fatigue sensitive. However, during the test programs repair straps were installed as soon as cracks were observed. For this reason, little is known about the crack propagation rate and residual life of the part once a crack begins. Assuming complete failure of the part at the time of crack discovery a very limited correlation is possible. The cracks began, on the average, at 20 spectrum test blocks (2000 hours). The baseline life is related to the 27 spectrum test block failure of the lower skin of the center wing section. VGH data gathered in 1965 in TAC indicate a service life of 4,800 hours (including a scatter factor - 4.0). VGH data gathered in operational aircraft during 1969 resulted in service life estimates of 1,740 hours (with the same scatter factor). Ratioing these figures by 20/27 gives life estimates for the outer wing of 3,560 hours for operational training and 1,290 hours for actual operation. From this we conclude that, while the second aircraft failure correlates rather well with test data, the other two failures were each highly premature. The poor correlation is further demonstrated by the fact that some of these aircraft had accrued over 2,200 operational hours with no sign of failure. In order to prevent additional failures of this type all outer wings have been reinforced as shown in Figure 8.

    C. Fuselage Station 303.62 Bulkhead:

This bulkhead (Figure 9) provides the means for tying the fuselage to the wing at the main spar. A sheet metal seal is attached to the bulkhead by a series of 5/32 inch rivets. The lower most fastener hole has been demonstrated in cyclic test to be fatigue sensitive. In June 1970, one of the special mission aircraft experienced a crack through the critical fastener hole. This aircraft had accumulated 501.1 hours prior to modification and had flown 320.3 hours in the special mission squadron.

it had been used in the most damaging special mission role and had been subjected to the severe special mission flight profile shown in Figure 4. Following the grounding of this aircraft for repair, another aircraft was moved into that role. By the close of 1970, this second aircraft had accumulated 446.7 previous general usage hours, 178.8 hours of normal special mission usage and 280.0 hours of most severe usage. During the January 1971 maintenance inspection of these special mission aircraft, all were inspected at the FS 303.62 bulkhead. An eddy current inspection revealed that the two severely used aircraft were cracked in exactly the same manner, although one was not as extensively damaged. As previously mentioned, the fatigue tests demonstrated the fatigue sensitivity of this bulkhead. On one test article a failure occurred at 52 spectrum test blocks (5200 hours). A second test article failed at 73 spectrum test blocks (7300 hours). As a conservative measure the manufacturer's analysis 's presently related to the 52 spectrum test block failure. Some very brief element tests were also conducted to develop factors for analytical adjustments to the basic fatigue analysis to account for the negative loads experienced and not simulated in test. During the early part of 1970, one of these aircraft had had a faulty VGH recorder and, as a result, only a limited amount of VGH data was gathered. At the time of crack discovery, the n/N fatigue damage was estimated at .91. By applying all factors to the analysis of the second airplane, a fatigue damage level of .227 was computed in the bulkhead. When these aircraft came in for inspection in December 1971, all FS 303.62 bulkheads were modified in order to reduce the fatigue sensitivity of that member. All fleet aircraft will receive rework of the bulkhead. This after-the-fact analysis indicates that, applying a scatter factor of 4 to these damage calculations, one could have expected failure.

While the airframe has received substantial cyclic testing and possibly all major fatigue sensitive areas have been identified, it is evident that the testing to date and the present analysis are not adequate to accurately predict service life of the aircraft. A large contributing factor could be the lack of negative load cycles in the test spectrum used. This statement is substantiated by work done at the US Naval Air Engineering Center at Philadelphia, Pa. In their report NAEC-ASL-1107 (AO 816653), 3 April 1967 (Reference 3), the effects of including negative loading in the flight spectrum for a typical fighter wing are evaluated. The report shows that including negative loads in the test spectrum has a very significant effect on the life of the test article (reduction in life by a factor of about six). Additional information supporting this position may be found in Reference 4, ASO-TR-61-434, dated March 1962, "An Engineering Evaluation of Methods for the Prediction of Fatigue Life in Airframe Structures". This document cites the necessity of testing a representative airframe to a representative spectrum if the results are to be meaningful in helping to predict airframe service life.

Fatigue Test Techniques

In reviewing the correlation of test-to-service fatigue failures, it is appropriate to also review the full scale fatigue test techniques that have developed along with the other aspects of the total service life evaluation program.

A brief historical look at the USAF fatigue evaluation program reveals the following trend milestones.

a. The first full scale wing fatigue test conducted by the USAF was on an AT-60 air-craft in 1947. It employed a single load level test technique, automatically cycling from 1G to limit load for one wing primary bending condition. The prime purpose of this test was to develop the concept and test techniques. It never played a significant part in the fatigue evaluation of this aircraft in that the aircraft did not experience service fatigue problems of any consequence.

b. The first USAF full scale wing fatigue test program conducted to resolve service incurred fatigue failures was conducted on the F-84D aircraft in 1948. Again, a single load level cycling technique was utilized automatically cycling from 1G to limit load for one wing primary bending condition. This test was successful in duplicating all of the service incurred failures, and suitable reinforcements were developed to preclude further service problems. In this instance a rather simple relationship was established, relating test cycles to actual service hours and projections of failure made upon this basis.

c. Utilizing these same techniques and the same test cycle service hour relationship, all of the remainder of this series of aircraft (F-84E, G, and F series) were fatigue tested to (1) preclude service failures, and (2) project a service life. These programs were successful even though crude by today's standards.

d. In addition, these single load level techniques were utilized in fatigue test programs for the F-86, F-89, and F-101 aircraft either to predict fatigue life or to develop corrective measures for in-service failures.

e. In 1958, the three simultaneous full scale fatigue tests of B-47 aircraft represented the USAF's first series of full scale tests utilizing a "spectrum" type test loading. In this case, an average or "typical" mission was developed, each aircraft in the fleet was assumed to fly this "average" mission, and the test loads developed as a representative blocked spectrum of various load exceedances, two gust levels, and GAG. Test loads were "layered" or applied in sequences of repeated layers representing some percentage of the total service life being simulated. These tests, closely followed by similar tests on the B-52 series aircraft ushered in the first formal USAF requirements for specific service life in its aircraft, and a suitable structural integrity program of analysis, test, and service loads monitoring to assure expected service life (Reference 1).

f. From this foundation, and the requirement as discussed in Reference 1, along with the requirements of US military specifications series MIL-A-8860, dated May 1960, the majority of recent Air Force aircraft have been evaluated (full scale fatigue test wise) on the basis of blocked spectrum load tests, including appropriate negative and positive loads, utilizing typical mission

spectra made up from "historical" load exceedance data. It is from this basis that most of our correlation of test-to-service has to be made.

g.   In the mid 1960's, it became more apparent that the capability of a wide variety of mission usage in the higher performance military aircraft could result in significant variations in experimental life determinations, depending upon the selection of mission mix used in the evaluation. Reference 2 in discussing the transport "A" example makes this extremely clear. In addition to the efforts to establish our historical load exceedance data on a mission segment basis, improvement in full scale test techniques, primarily in the ready availability of off-the-shelf equipments for extensive variability in load programming has led the USAF to now require that our full scale fatigue tests be conducted on a flight-by-flight basis, utilizing a "best estimate" usage built from estimated fleet operation in the various mission segment profiles. (Reference USAF Specification MIL-A-008866 (USAF), dated 31 March 1971).

With the exception of the examples discussed in Reference 2, the USAF is just now completing some aircraft test programs utilizing these newer procedures and we yet do not have the service experience to gather any service data. Perhaps these latter tests will exhibit a "better" test-to-service correlation.

In reviewing this historical sequence, and considering our past successes and failures, the authors feel some test trends are being established. These are as follows:

a.   The capability exists, with currently available test techniques and equipments, to very accurately simulate in full scale test the loads representation of the selected aircraft usage (i.e., flight-by-flight, random loads, including proper sequence of pertinent damage segments such as GAG).

b.   There will always be economic problems to contend with in terms of test cost and duration, and in making the trades associated with these economics one should roughly consider aircraft as falling into two general classes: (1) those maneuver critical such as fighter and attack, and (2) those gust critical or GAG critical such as the large bomber and cargo aircraft. Perhaps more leeway can be taken in extensive test load complexity on the fighter type aircraft, but here again the most "sensitive" features must remain.

c.   The secret of success, in our opinion, is the validity of the input usage load history -- particularly, how will it reflect the significant variation in specific mission segment usage for the particular aircraft in question?

d.   Because of the ready availability of the advanced test techniques mentioned above, maximum advantage should be taken of these techniques and equipment. There is enough evidence, both in our own USAF experience and associated R&D programs, along with substantial similar information from the many NATO nations, that one can encounter significant undesirable effects of test simplification and load truncation. While these effects can, in some instances, be accounted for there are always "nagging unknowns" and some loss of credibility in the results. We do not feel that there is the general justification now for these short cuts.

IV.   CONCLUSIONS

1.   The new data on Fighter Bomber C is added statistical information toward the continuing attempts to study the problem of correlation of test results to service experience. The data does not appear, in itself, to provide anything new. It exhibits the same highly inconsistent initial correlation, yet in certain instances where actual usage data were available, reasonable correlation could be obtained.

2.   The authors are convinced that the lack of ability to initially forecast the aircraft usage can prevent good correlation between initial fatigue test results and eventual service life. For this reason, the fatigue test must serve as a damage index and the eventual life predictions must be based on a good knowledge of actual fleet operation.

3.   The accuracy of correlations can be improved by assuring that tests are made to realistic spectra, on a representative specimen, using the best test techniques available (flight-by-flight loading using random load spectra).

4.   Early acquisition of measured operational usage data is necessary to provide the basis for early fleet life prediction to minimize operational fleet problems.

REFERENCES

1.   "The U. S. Air Force Weapon Systems Fatigue Certification Program" - H. B. Lowndes, Jr. and W. B. Miller - ICAF - Munich, Germany - June 1965.

2.   "Correlation Between Full Scale Fatigue Test and Service Experience" - H. B. Lowndes, Jr. - 11th ICAF Meeting - Stockholm, Sweden - May 1969 - ICAF Document No. 499.

3.   "The Effect of Including Negative Loading in the Flight Spectrum for a Typical Fighter Wing" - L. Berman, U. S. Naval Air Engineering Center - Report No. NAEC-ASL-1107, dated 3 April 1967.

4.   "An Engineering Evaluation of Methods for the Prediction of Fatigue Life in Airframe Structures" - ASD-TR-61-434, dated March 1962.

ACKNOWLEDGEMENT

MEDIUM TRANSPORT "A"

COMPARISON OF PREDICTED AND ACTUAL TIME AT
FATIGUE CRACK INITIATION

PREDICTED FLT. HRS. /ACTUAL FLT. HRS.
(PREDICTED FLEET USAGE)

PREDICTED FLT. HRS. /ACTUAL FLT. HRS.
(ACTUAL INDIVIDUAL AIRCRAFT USAGE)

PERCENTAGE OF AIRCRAFT
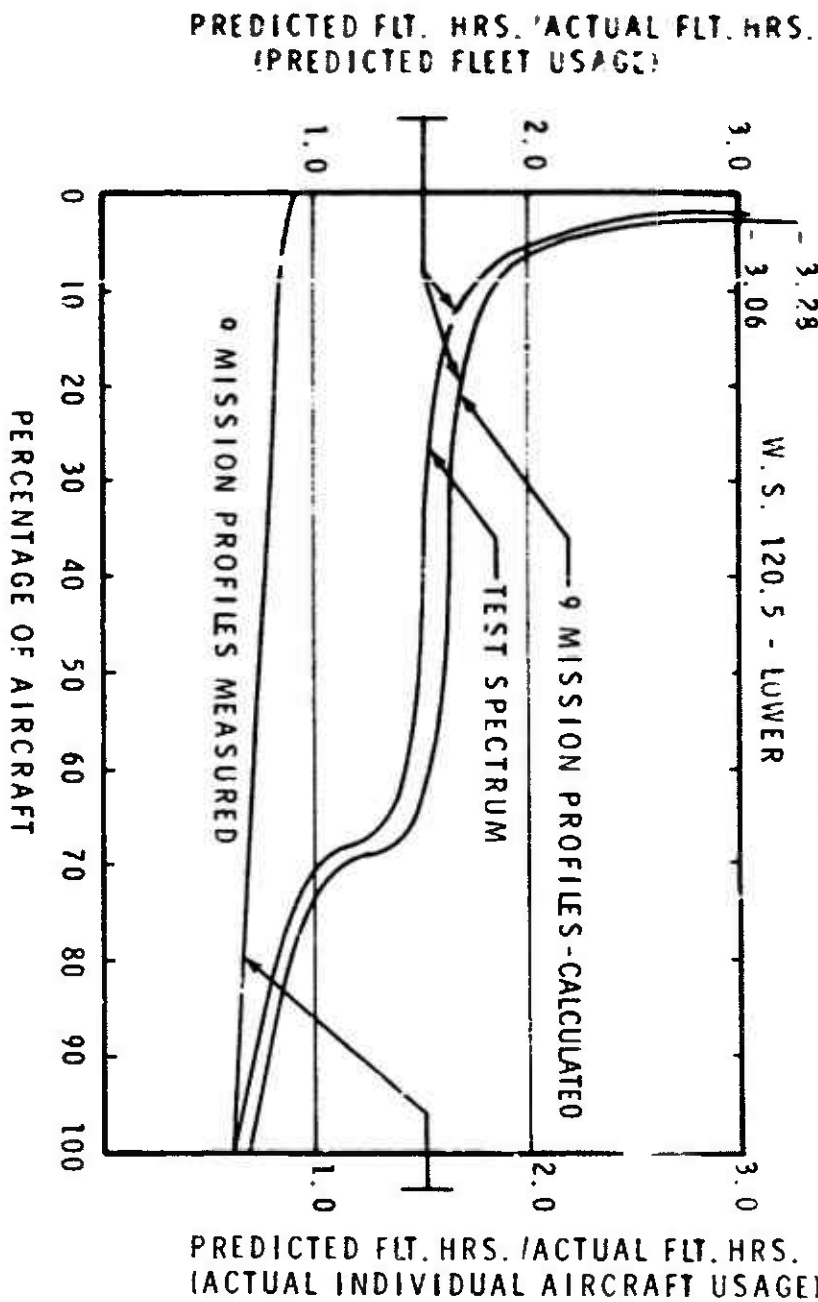
FIGURE 1

FIGHTER BOMBER "A"
WING FATIGUE FAILURE DATA

FAILURE LOCATION	LIFE IN HOURS			NUMBER OF INCIDENTS
	CALCULATED	TEST	SERVICE	
FORWARD FILLET RADIUS LOWER SKIN	4,460	5,508	2,530 AVG	5
FORWARD FILLET RADIUS UPPER SKIN	12,670	5,508	2,300 AVG	35
WING CENTER SECTION LOWER SKIN	2,600	6,192	3,050 AVG 2,890 (1)	27
WING CANTEO STA. 102 LOWER SKIN	1,120	2,860	2,140 (1)	7 (2)

(1) ONE CATASTROPHIC FAILURE AT THIS NUMBER OF HOURS

(2) NO ACCURATE RECORDS KEPT OF CRACKS FOUND DURING FLEET
MODIFCATION OF THIS AREA. THIS NUMBER REPRESENTS KNOWN FAILURES
ONLY.

FIGURE 2

FIGHTER BOMBER "B"
FAILURE SUMMARY

CRITICAL AREAS	LIFE BASED ON TEST (UNFACTORED)	REVISED LIFE BASED ON V-G-H DATA ②	REVISED LIFE BASED ON COMBAT V-G-H DATA ③
FUSELAGE STA. 350 SKIN SPLICE-TANK AREA	5680	10400	6200
FUSELAGE STA. 428 ACCESS CUT-OUT-TANK-DOUBLER	5680	15200	9280
FUSELAGE STA. 500 ACCESS CUT-OUT-TANK-COVER SKIN	5680 ①	56800	23160
FUSELAGE STA. 442 MAIN WING ATTACH. FRAME	4640 ①	29200	24520
WING-SPLICE REAR SPAR-STA. 96.7	5680	21400	8360

FIGURE 3

NOTES: ① THESE TWO ITEMS ACTUAL FAILURE-REMAINDER CALC.
② CALC. LIFE BASED ON 4000 HRS OF TNG/TAC SIMULATION.
③ CALC. LIFE BASED ON 3400 HRS OF OPERATIONAL V-G-H DATA.

FIGHTER BOMBER "C"
LOAD SPECTRA
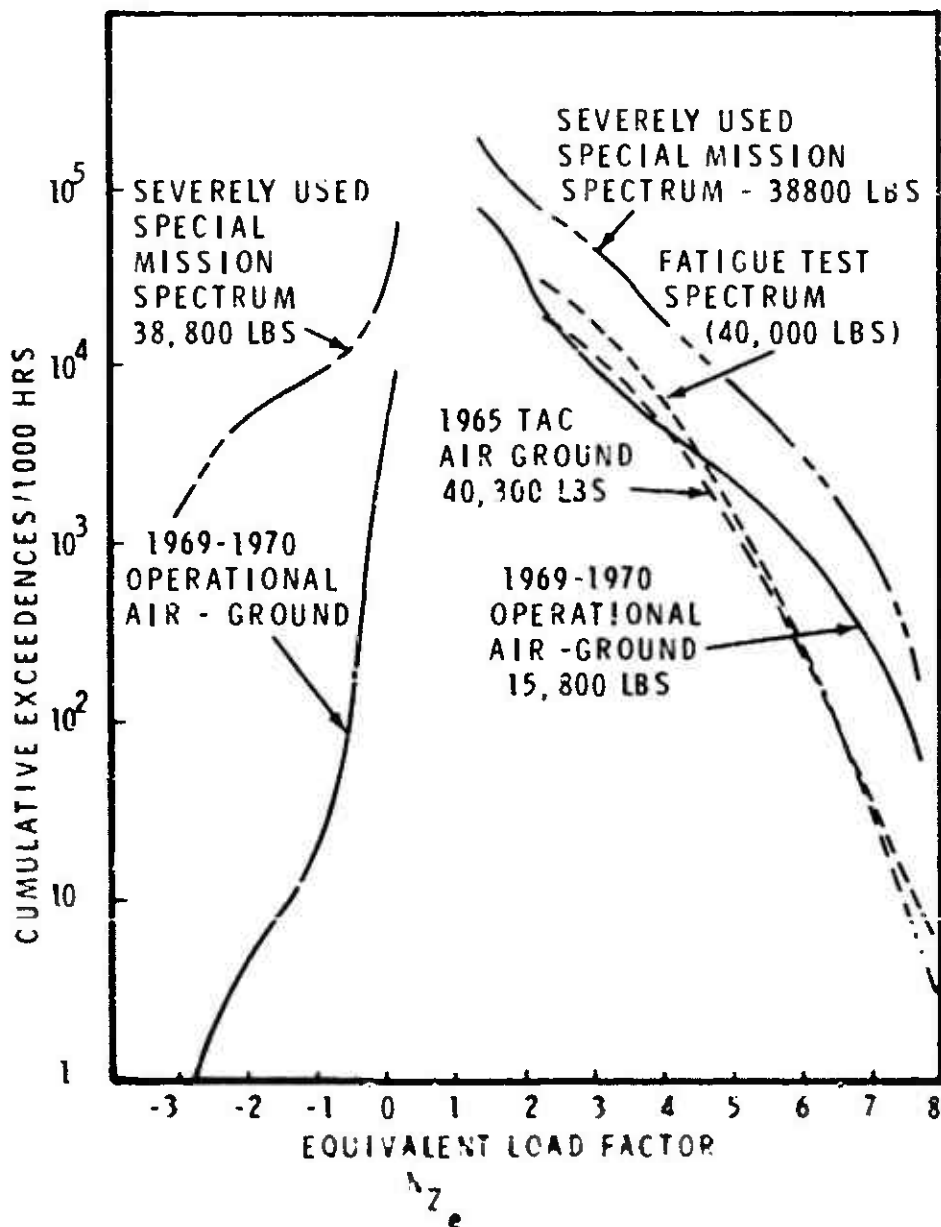
TYPICAL LOCATIONS OF UPPER
OUTBOARD STABILATOR SKIN CRACKS
UPPER SURFACE
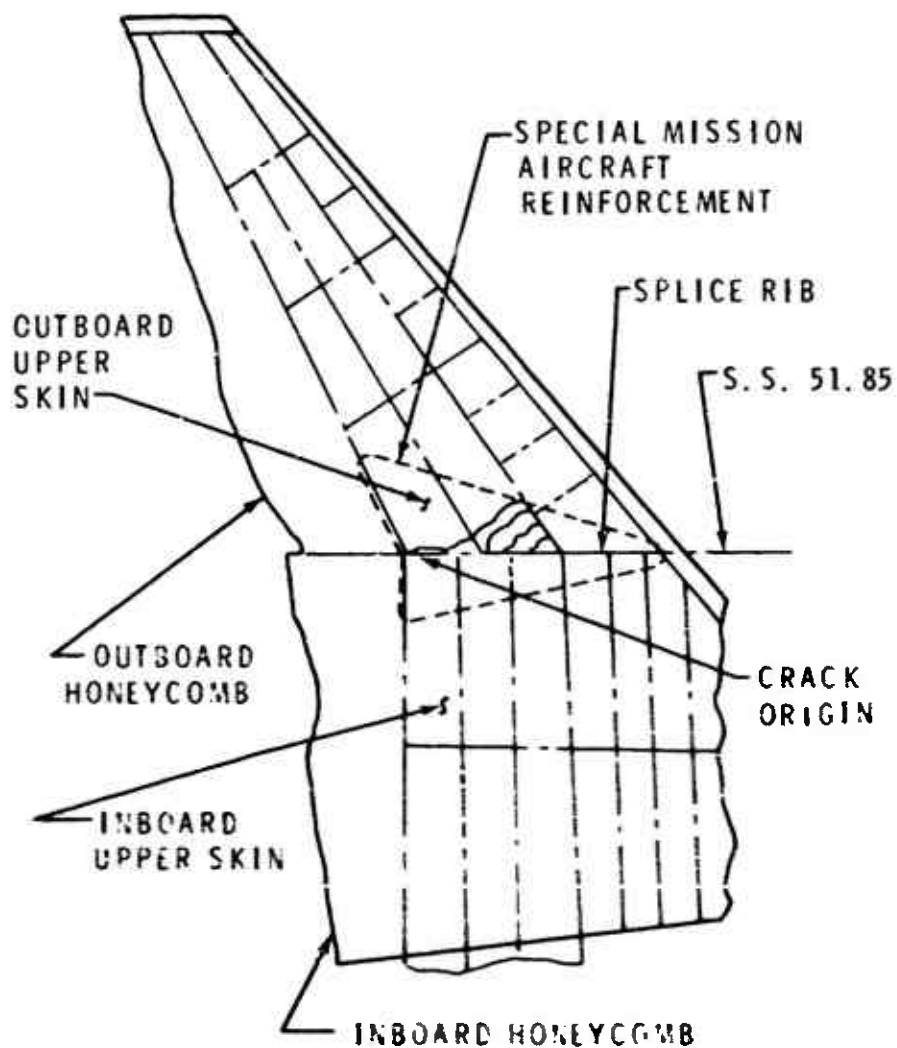
FIGURE 5

LOWER SURFACE OUTER WING CRACKS

AREA WHERE
CRACKS OCCUR
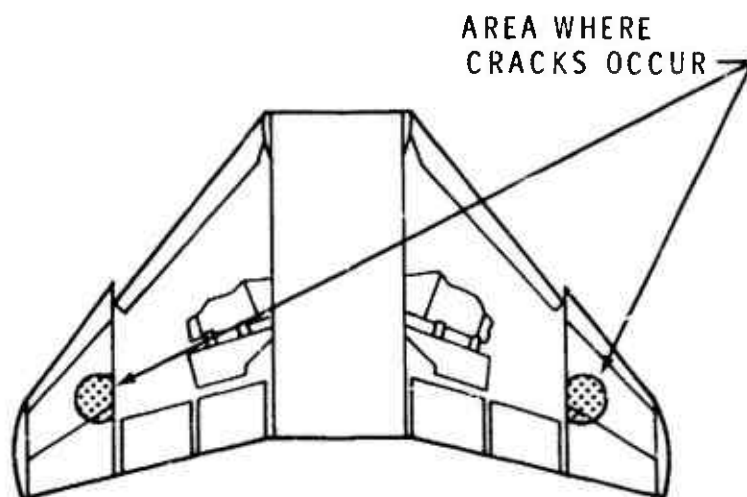
FIGURE 6

TYPICAL SERVICE CRACKS

CRACK FIRST STARTS
HERE IN DOOR

MAIN
RIB

B D

INBD

FWD

E

A&C

59. 968% REAR SPAR PLANE
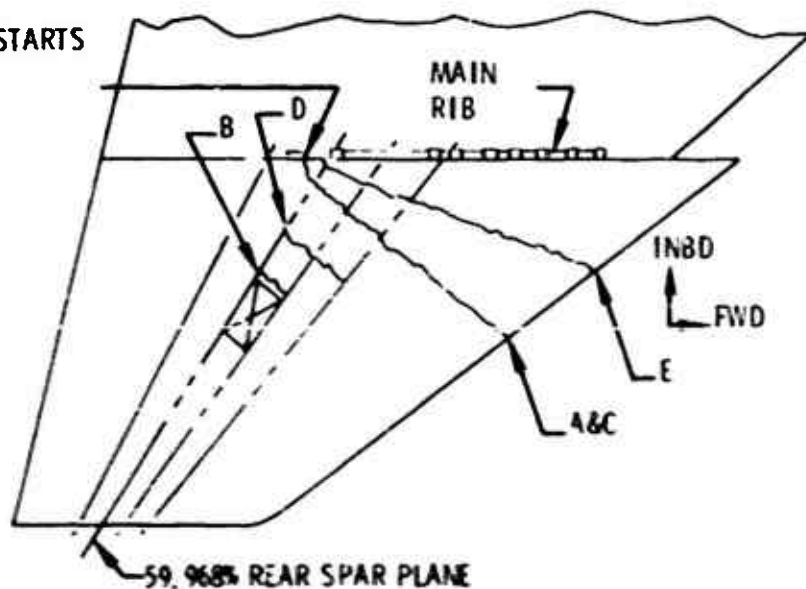
A. WING BROKE OFF
B. CRACK
C. WING BROKE OFF
D. CRACK
E. WING BROKE OFF

NOTE ALL AIRCRAFT RECOVERED SAFELY

ACTION TAKEN

ADD STRAP
.125 7075 T651

ADD STRAP
.125 7075 T651

MAIN RIB

FWD

INBD

5/16 CAP SCREWS
6 PLACES

REAR SPAR

59. 968% REAR SPAR

VIEW LOOKING UP L.H. WING

FIELD RETROFIT ADDITION OF
EXTERNAL STRAPS ON OUTER
PANEL LOWER SKIN AT 59. 9% SPAR

PRODUCTION RETROFIT-SAME AS
FIELD RETROFIT

FIGURE 8

I.S. 303 BULKHEAD CRACKS

PROBLEM:

CRACK INDICATION AT 73 SPECTRUM BLOCKS
FAILURE AT 52 SPECTRUM BLOCKS

MODIFICATION:

(a) ON 7075-T73 BULKHEADS: INSTALL INTERFERENCE
FIT FASTENERS.   INSTALL BELLMOUTH STUD FITTING.

(b) ON 7075-T6 BULKHEAD: REAM FASTENERS 1/32 IN.
OVERSIZE AND INSTALL BELLMOUTH STUD FITTING.

AREA OF INTERFERENCE
FIT FASTENERS OR REWORK

5/32 DIA.
RIVET

FAILURE AREA

FRACTURE
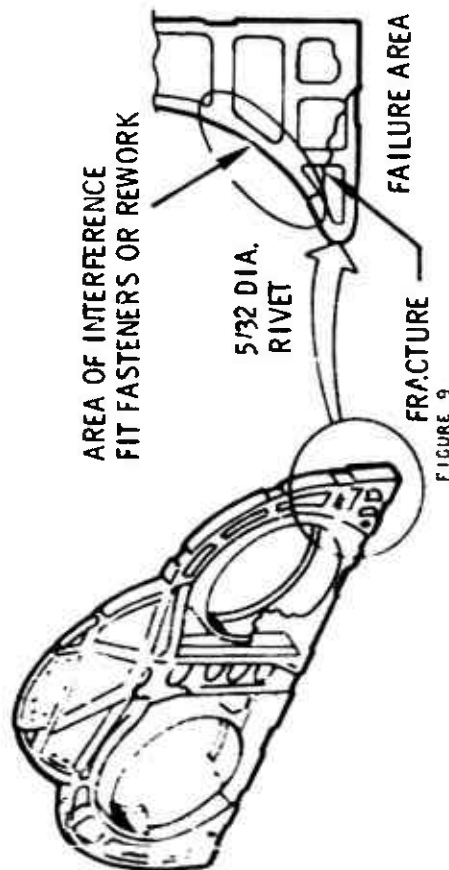
FIGURE 9

FIGHTER BOMBER "A"
LOAD SPECTRA

FIGURE 1
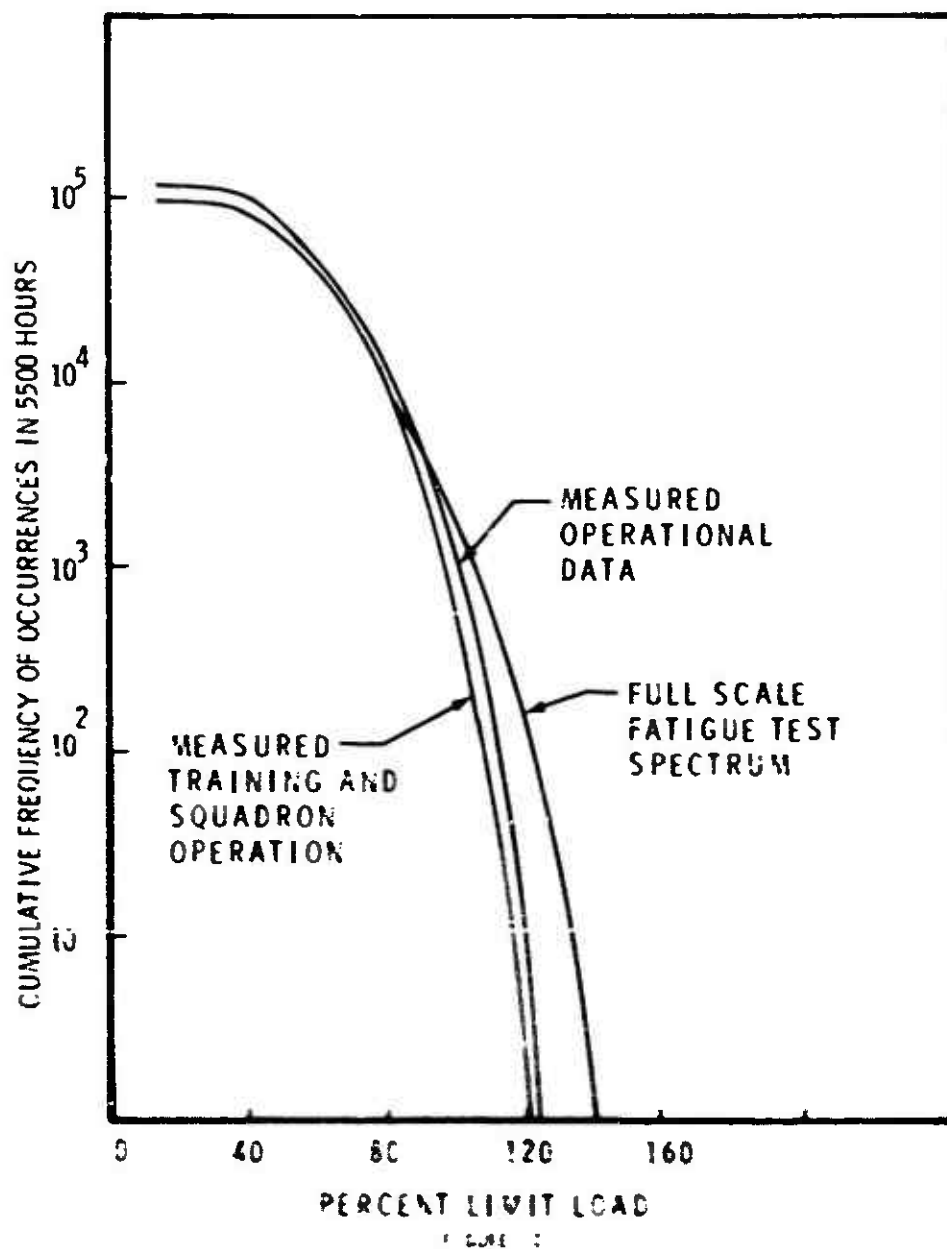
ON RESIDUAL STRESSES DURING RANDOM LOAD FATIGUE

By

FIND ROTVEL

The Technical University
of Denmark
Dept. of Solid Mechanics
Building 404
Lyngby, Denmark

ABSTRACT. The effect of some techniques used to increase the fatigue strength is due to the favourable residual stresses that are created in locations with high fatigue stresses. The purpose of the present paper is to discuss the significance of these techniques when the loads vary randomly. Data are presented from random fatigue tests on normalized carbon steel with 0.7 % carbon. In notched specimens a preload beyond the yield stress induced residual stresses around the notch. The residual stresses were measured with an X-ray measuring technique at intervals during the fatigue loading. Results from broad-band and narrow-band stochastic loading tests are compared with constant-amplitude sinusoidal tests.

LIST OF SYMBOLS

C	Clipping ratio
e	Nominal strain
F_{ty}	Yield stress (0.2%)
K_t	Elastic stress concentration factor based on net area
$K^\varepsilon = \varepsilon/e$	Plastic strain concentration factor
$K^\varepsilon = \sigma/s$	Plastic stress concentration factor
$m(x)$	Mean value of x
m as subscript	Mean value
n	Number of maxima
rms as subscript	Root-mean-square value
s	Nominal stress
$s(x)$	Standard deviation of x
ε	Strain in notch
ε_p	Plastic strain
σ	Stress in notch
σ_R	Residual stress
σ_{R0}	Residual stress before fatigue loading

Compressive residual stresses have often been shown to increase fatigue strength. To make practical use of this several technological processes (e.g. cold rolling, shot peening, grit blast, stretching of notched details) have been developed, that induce favorable residual stresses in areas with high fatigue stresses. The processes mentioned have in common that residual stresses are created by locally loading the material over the yield stress. Generally the processes can only be used in the high cycle (low stress) range, where the width of hysteresis loops is small. In the low-cycle range the large plastic strains quickly relax the residual stresses.

Local yielding may affect the fatigue strength in two ways:

1) Compressive residual stresses are created, which increases the fatigue strength in the same way as mean loading stresses.
2) The plastic deformation may strain harden the material, which also may increase the fatigue strength.

Of primary importance for the application of these methods is the stability of the residual stresses. The stability depends on many factors the most important of which are: The static and dynamic stress-strain curves, stress gradients for loading stress and residual stress, mean value and amplitude of loading stress, tri-axiality of loading stress and residual stress. The effect of and the problems related to the application of local yield methods of increasing fatigue strength have been investigated by many authors, e.g. ESQUIVEL and EVANS [1], MINER [2], NELSON et al. [3], MATTSON and ROBERTS [4]. All these authors used sinusoidal loading.

Stochastic loadings are expected to be more dangerous to the stability of induced residual stresses, because one single high or low peak may drastically change the residual stress distribution. Tests reported by IMPELLIZERI [5] and KIRKBY and EDWARDS [6] demonstrated how omission of high positive peaks in variable amplitude loadings resulted in lower life. The results were explained by assuming the high peaks to maintain the residual stress at a high level. Omission of the high peaks should result in fading of residual stresses. Stochastic loadings were therefore included in the present tests.

To obtain a well defined residual stress distribution notched specimens were preloaded axially beyond the yield stress.

TESTING APPARATUS

All fatigue tests were carried out on a MTS closed-loop testing machine with 170 kN load capacity.

The stochastic command signal for the testing machine was taken from a pseudo-random noise generator through a set of parallel 1/3 octave filters made according to IEC 225 standard. The signal from the noise generator varied in apparently stochastic, but in reality pre-programmed manner. After a certain period of time the same signal was repeated.

The length of the period could be varied by changing the frequency in an external signal generator. The noise generator signal was approximately gaussian distributed, and its PSD-shape (power spectrum density distribution) was flat down to DC. The upper cut-off frequency (3 dB) was 270 Hz.

The 1/3 octave filters shaped the noise generator PSD-distribution to the two shapes used for the loadings in the tests: narrow-band and broad-band. Some data for these PSD-shapes are collected in table I.

TABLE I. Data for stochastic command signals.

	Narrow-band	Broad-band
Frequency of maxima	25	46
Frequency of zero-crossings	25	38
Lower cut-off frequency	22.3	4.5
Upper cut-off frequency	28.1	56.1
Clipping ratio $C \begin{cases} U_{max}/U_{rms} \\ U_{min}/U_{rms} \end{cases}$	4.3 4.3	4.5 4.0
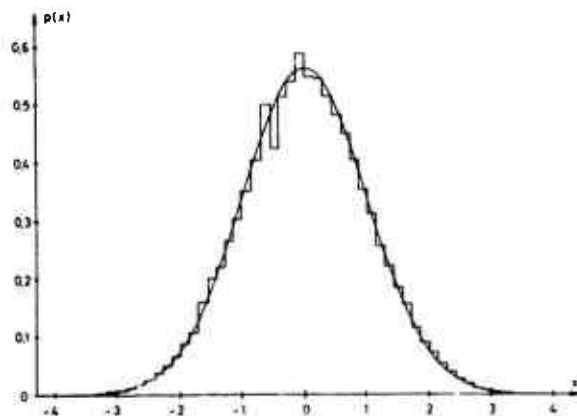
Fig. 1. Probability density distribution of broad-band command signal normalized to give unit area under curve.
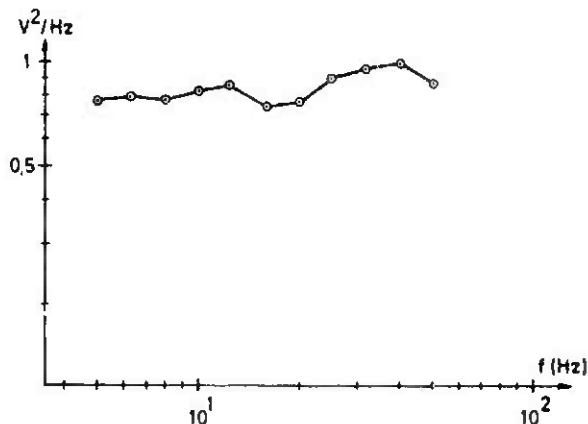
Fig. 2 Power spectrum density distribution for broad-band loading measured through 1/3 octave filters. Normalized at maximum. Outside the shown frequency range the power spectrum was less than 10^{-4}.

a) Narrow-band |— 1 second —| b) Broad-band
Fig. 3. Examples of waveforms for narrow-band and broad-band command signals.

When investigating random load fatigue material properties, programmed loading is an advantage, firstly, because the spread in the test results only is due to a spread in material properties, and, secondly, because a loading may be reproduced at a later time. Also it is possible to stop the fatigue loading in a certain place in the signal pattern to do some investigations on the material, and later on continue the fatigue loading from the same place in the pattern.

Rms-values of load was measured on a true rms-voltmeter with DC-output using a time constant of approximately 300 seconds. Measuring time was 20 to 30 minutes.

X-RAY MEASUREMENT OF RESIDUAL STRESS

Residual stresses were measured by an X-ray method, because this is a non-destructive and absolute measurement of elastic strains from which, assuming Hookes law to be valid on the microscopic level, the elastic stresses may be computed. As the method of X-ray stress measurement is well treated in the litterature (e.g. [7], [8], [9], [10]) only a short introduction will be given here.

A set of crystal lattice planes reflects X-rays only if the Bragg equation

$$n \cdot \lambda = 2 \cdot d \cdot \sin \theta \tag{1}$$

is fulfilled. In eq. (1) n is an integer, λ is the wavelength of the X-rays, d is the distance between lattice planes and θ is the reflection angle (see fig. 4).
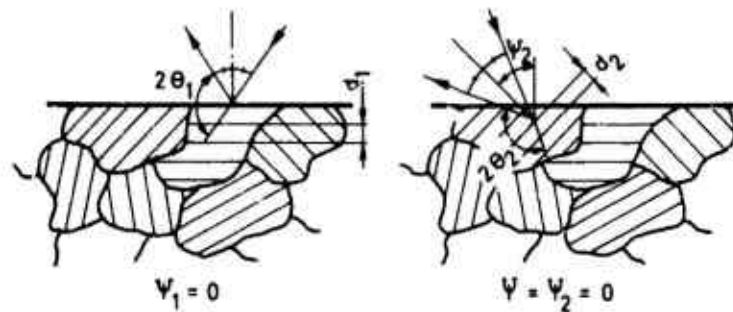
Fig. 4. Reflection of X-rays from polycrystalline material at two angles of incidence ψ. Differently oriented crystals contributes to the reflected intensity at different ψ-values.

A state of stress changes the value of d in different directions ψ in the material, and this again changes the angle of reflection as seen from eq. (1). The stress parallel to the surface and in the plane of the paper on fig. 4 can be computed by

$$\sigma = \frac{2}{s_2(\sin^2\psi_2 - \sin^2\psi_1)} \left\{ -(2\theta_2 - 2\theta_1)\frac{\cot\theta_1}{2} + (2\theta_2 - 2\theta_1)^2 \frac{1 + 2 \cdot \cot^2\theta_1}{8} \right\} \tag{2}$$

$\frac{1}{2}s_2$ is a constant of proportionality, which for some combinations of material and wavelength can be approximated by the macroscopic constants of elasticity

$$\frac{1}{2}s_2 = \frac{1+\nu}{E} \tag{3}$$

For accurate stress measurements $\frac{1}{2}s_2$ has to be measured by using known loading stresses. The value of $\frac{1}{2}s_2$ is sensitive to plastic deformation as shown by FANINGER [11] and TAIRA et al. [12]. In the present tests the same value has been used for all measurements. Table II summarizes data for the X-ray stress measurements.

TABLE II. X-ray data.

X-ray tube	Target: Cr Voltage: 30 kV Current: 40 mA
Detection	Filter: Va Detector: Proportional Pulse-height discrimination
ψ-angles	0 and 45°
Intensity line	(211) at $2\theta = 156°$
Constant of proportionality	$\frac{1}{2}s_2 = 5.0 \cdot 10^{-6}$ m²/MN

The irradiated area of the specimen was approximately 1 mm times the width of the specimen (6 mm), and the measuring accuracy of notch stresses was $\pm$ 20 MN/m².

In microscopically heterogeneous materials a plastic strain creates microstresses, even if the loading stress is uniform. Microstresses are stresses that are in equilibrium over distances of the order of grain diameters. X-ray measurements by KOLB [13], TAIRA and YOSHIOKA [14], BOLLENRATH et al. [15] and others have shown, that microstresses both broaden the intensity lines and shift the whole line on the 2θ-scale in the same way as macrostresses. Whenever plastic strains are involved it is therefore not always possible to distinguish between macro- and microstress in an X-ray stress measurement.

The broadening effect of microstresses is due to the microscopically inhomogeneous deformation. Some crystal areas have large strains, while others have small. Each crystal area contributes a small intensity that is shifted an angle according to the strains in the area. When summing all the small intensities to the total reflected intensity, the result is an increase in line breadth.

Since microstresses are in equilibrium over small distances compared with the irradiated area, the line shifts from all small areas might be expected to annihilate each other. MACHERAUCH |16| explained the shift to be due to the selectivity of the X-ray measurements. Only crystal planes oriented near the correct reflection position as determined from the Bragg eq. (1) contributes to the reflected intensity. Therefore, all reflecting planes have nearly the same orientation in relation to planes of maximum shear stress in the material, where dislocation movements are most intensive.

Fig. 5 shows microstresses measured on the surface after plastic deformation without stress gradient on the material used in these tests. That the stresses really are microstresses is evident from fig. 6, which shows residual stress versus depth. A macro residual stress would have caused the measured stress to decrease with increasing distance from the original surface. The result in fig. 6 disagrees with results from KOLB |13|, who found a steep stress gradient at the surface. Possibly a difference in specimen shape explains the disagreement, the cross section being rectangular 6x20 mm in these tests and cylindrical in the tests by Kolb. The stresses in fig. 6 were measured on the narrow side of the specimen.
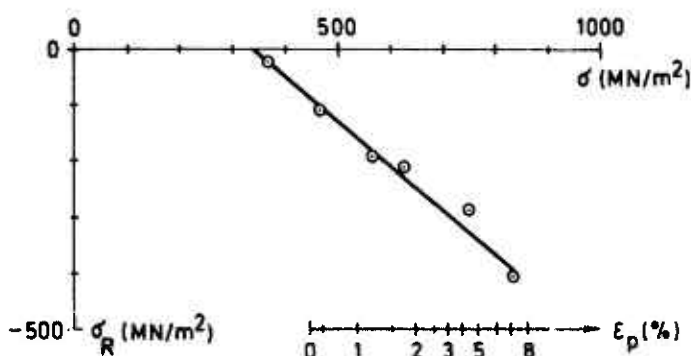
Fig. 5. Residual stresses measured on the surface after plastic loading.
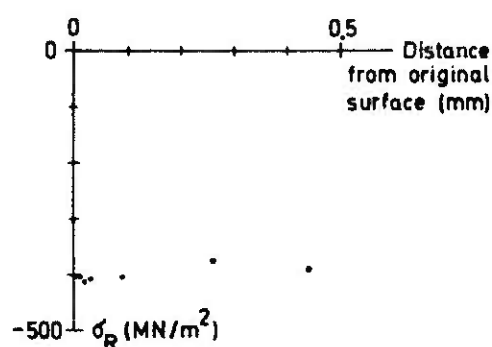
Fig. 6. Stress distribution in depth measured after removing surface layers by electro polishing.

MATERIAL AND SPECIMEN

The material was a Swedish carbon steel B14 (appr. SAE 1064) for which appropriate data are given in table III. After a softening heat treatment, the specimens were machined according to fig. 7 with exception of the notch. The specimens were then given a normalizing heat treatment in protective atmosphere to avoid decarburizing, and the notches were milled. Finally, an electropolishing removed 200 μm of surface material with stresses from the milling. The resulting roughness depth was appr. 1 μm in the notch.

TABLE III. Material data.

Chemical composition	0.7%C, 0.25%Si, 0.30%Mn, <0.035% P and S	
Macro yield stress	440 MN/m^2	
Engineering breaking strength	870 MN/m^2	average of two specimens
True fracture stress	1100 MN/m^2	
Area reduction	18 %	
Vickers hardness	240 ± 15	

The notch factor had to be kept relatively small to minimize stress variation over the irradiated area.

The specimens were milled and electropolished in randomized sequence. Also the allocation of specimens to different fatigue load combinations were randomized to avoid bias in the results.

As nearly always in these kinds of tests the purpose of heat treatment, machining, and electropolishing was to make identical specimens free from residual stresses. This was not quite succeeded as seen on fig. 8a, which shows residual stresses on specimens after fabrication. Before electropolishing residual stresses were greater than 500 MN/m^2. Thus the electropolishing removed most of the residual stresses from the machining.

Reversing the order of machining the notch and normalizing might be expected to give smaller residual stresses, but some tests with reversed order doubled the mean value and the spread of residual stress. The reason for this is ascribed uneven cooling rates in the specimens in normalizing treatment.
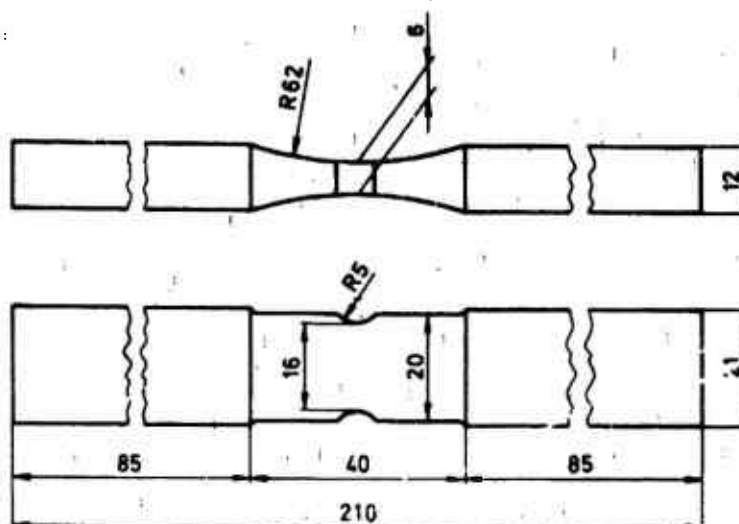
Fig. 7. Specimen used in fatigue tests. $K_T = 1.69$ computed from PETERSON |17|. All measures in mm.

RESIDUAL STRESS AFTER PRELOAD OF NOTCH

To have any effect the preload had to be higher than the highest peak in the loading in fatigue tests in the high cycle range. A preload of $K_T \cdot s = 810$ MN/m^2 was chosen. Table IV tabulates nominal rms-values of stress in the notch, $K_T \cdot s_{rms}$, for which the maximum load is equal to the preload. Preload can only increase fatigue strength for rms-values below the figures in table IV. On account of the relatively small notch factor necessitated by the X-ray measurements the nominal stress s became higher than the yield stress.

TABLE IV. Nominal notch stress $K_T \cdot s_{rms}$ giving the same maximum load as preload.

Stress in MN/m^2	Broad-band	Narrow-band	Constant-amplitude sinusoidal
$s_m = 0$	180	188	573
$K_T \cdot s_m = 255$	123	129	390

Fig. 8 shows histograms of residual stresses σ_R before and after preload. Comparing fig. 8a with 8b it is seen, that preload does not decrease the spread in residual stress though material yielding is generally expected to have a smoothing effect on residual stresses. A plot of σ_R before preload against σ_R after preload showed no correlation at all.
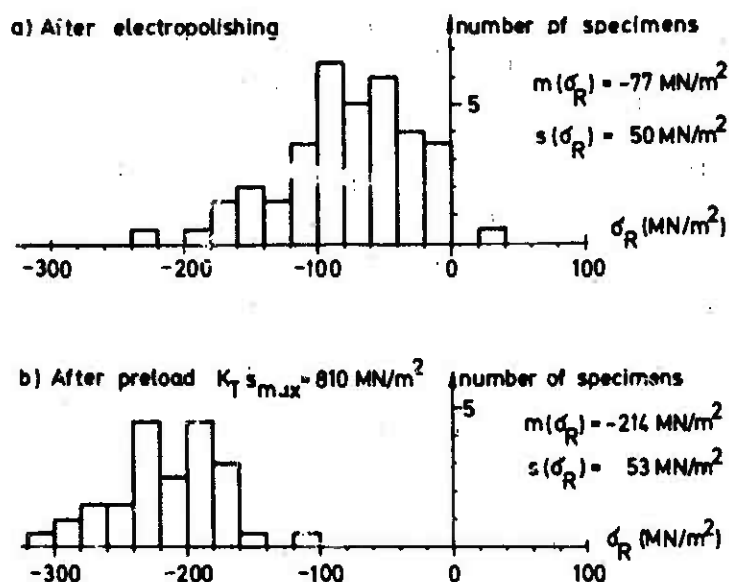
Fig. 8. Residual stresses measured after electropolishing and after preload.

TOPPER et al. |18| proposed a theory for computing local stresses in a notch. They started from a formula given by NEUBER |19| for local stress strain behaviour in a notch

$$K_T^2 = K_\sigma \cdot K_\epsilon = \frac{\sigma}{s} \cdot \frac{\epsilon}{e} \qquad (4)$$

where K_T is the theoretically elastic stress concentration factor, $K_\sigma = \sigma/s$ is the plastic stress concentration factor, σ is the local stress and s is a nominal stress based on the net area, $K_\epsilon = \epsilon/e$ is the plastic strain concentration factor, where analogously ϵ is the local strain and e is a strain corresponding to s.

According to Neuber eq. (4) is valid for an arbitrary stress strain curve. Rearranging eq. (4) gives

$$(\sigma \cdot \epsilon) = K_T^2 \cdot (s \cdot e) \qquad (5)$$

The right hand side of eq. (5) is supposed to be known. By trial and error a point on the stress strain curve is sought where the product of stress and strain equals the right hand side.

IMPELLIZERI |5| proposed a graphical method of solution to eq. (5). In equally spaced points on the stress strain curve of the material, corresponding values of stress σ and strain ϵ is read. The product $\sigma \cdot \epsilon$ is computed and drawn as function of σ (see fig. 9 which also shows the stress strain curve for strains less than 4%). In a notched specimen with given K_T and given s, $s \cdot e$ may be found on the $\sigma \cdot \epsilon$-curve, whereafter $\sigma \cdot \epsilon$ in eq. (5) may be computed. By again using the $\sigma \cdot \epsilon$-curve the local stress σ may be determined.

The residual stress σ_R in the notch after unloading to $s=0$ is

$$\sigma_R = \sigma - K_T \cdot s \qquad (6)$$

if the unloading stress-strain curve is linear. If not, the same procedure as outlined above should be carried out for the unloading curve.

Fig. 10 shows residual stress as function of nominal maximum preload stress, as predicted by the theory above. Due regard has been taken to nonlinearity in unloading. The theory implies that preloading with a nominal stress s just beneath the yield stress gives the largest residual stress attainable.
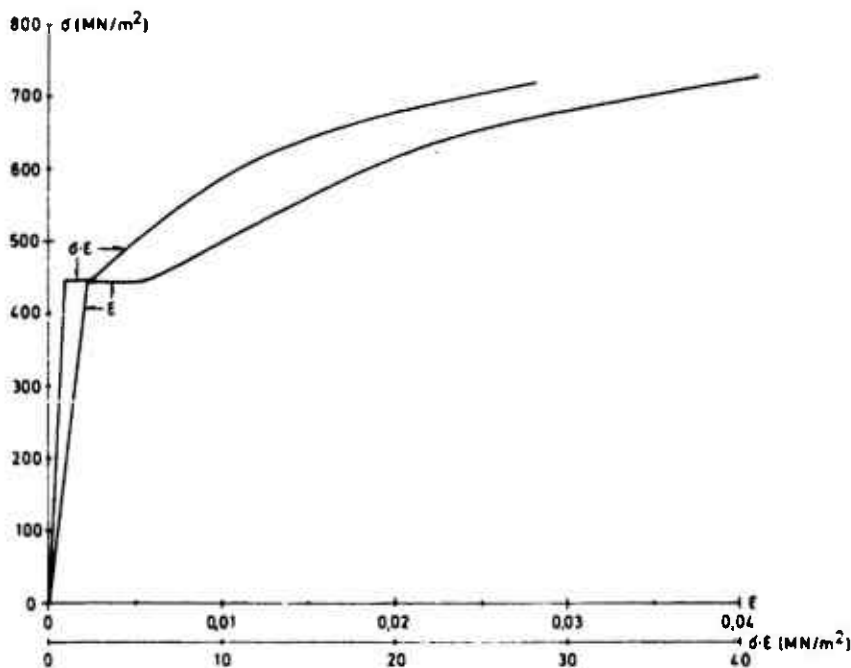
Fig. 9. Part of stress-strain and stress times strain curves.

The use of local overloading of notched details may thus be expected to have the greatest effect for large values of K_T and for materials with linear unloading curves both these conditions giving larger residual stresses.

Residual stresses measured after preloading to various nominal notch stresses are plotted for comparison with the theory on fig. 10. The agreement is reasonable for nominal stresses below the yield stress, but higher nominal stresses give large deviations
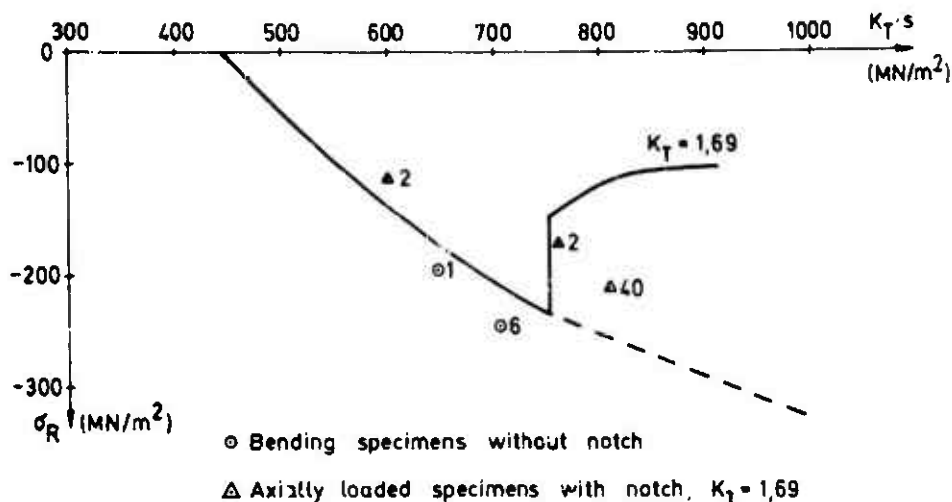
Fig. 10. Residual stress after preload computed from Neuber theory and compared with measured residual stresses. Each measured σ_R-value is an average of i measurements, i being the number besides the points.

from theory because microstresses are created. It is not possible to determine the size of microstress from fig. 5 using the maximum local notch stress, because the reversed plastic deformation during unloading is greater in the notch than on the notch free specimen used on fig. 5.

RESIDUAL STRESSES DURING FATIGUE LOADING

Residual stresses measured during fatigue loading are shown in fig. 11. Each point on the curves is the average of the stresses in the two notches of the specimens.

An arrow at the end of a line indicates a crackfree specimen at the instant of measurement. The line stops either because the specimen later on fractured totally or because the fatigue testing time became prohibitively long. A c at the end of a line indicates that one or more cracks had developed. The abscissa is the number of maxima. In th stochastic loading this number was computed as time in seconds times the frequency of maxima taken from table I.

The stresses in fig. 11a, b and c were all measured after 1, 10, 100 or 1000 periods of noise, each period equalling 200 seconds. Thus the loading stopped in the same place in the signal pattern, causing the material to be in the same place in the hysteresis loop. These measurements are therefore representative for the variation of the mean value of the residual stress.

In fig. 11a, b and d representing tests with preload the measured residual stresses are constant on the average through the fatigue life. Remembering that what is measured is the sum of macrostress and microstress, the residual stress variations during fatigue loading became more complicated. The X-ray measurements showed that the breadth of the intensity lines decreased with increasing number of cycles, i.e. the spread of micro- stress decreased. The decrease of the spread is accompanied by a decrease of the mean value of microstress, which i   easured together with the macrostress, but how fast and to what extent is not yet known. If the Neuber theory correctly describes the stress- strain behaviour in the notch, the macro residual stress can be taken from fig. 10 to be approximately -120 MN/m^2 after preload. Macrostress plus microstress being constant and microstress decreasing during fatigue loading means that the macrostress is increasing. It is not possible to indicate significant differences for the three kinds of loadings, either in mean values or in standard deviations.

Fig. 11c shows the variations in residual stress for the case of narrow-band stochastic loading with no preload. Here one observes a steady increase in residual stress which finally becomes numerically equal to the mean stress in the notch with opposite sign.

Residual stresses measured within 10 seconds from high peaks of the loading in the first period of noise on fig. 11e confirm the following observations:
1) In preloaded specimens loaded with zero mean stress the residual stress drops quickly to zero.
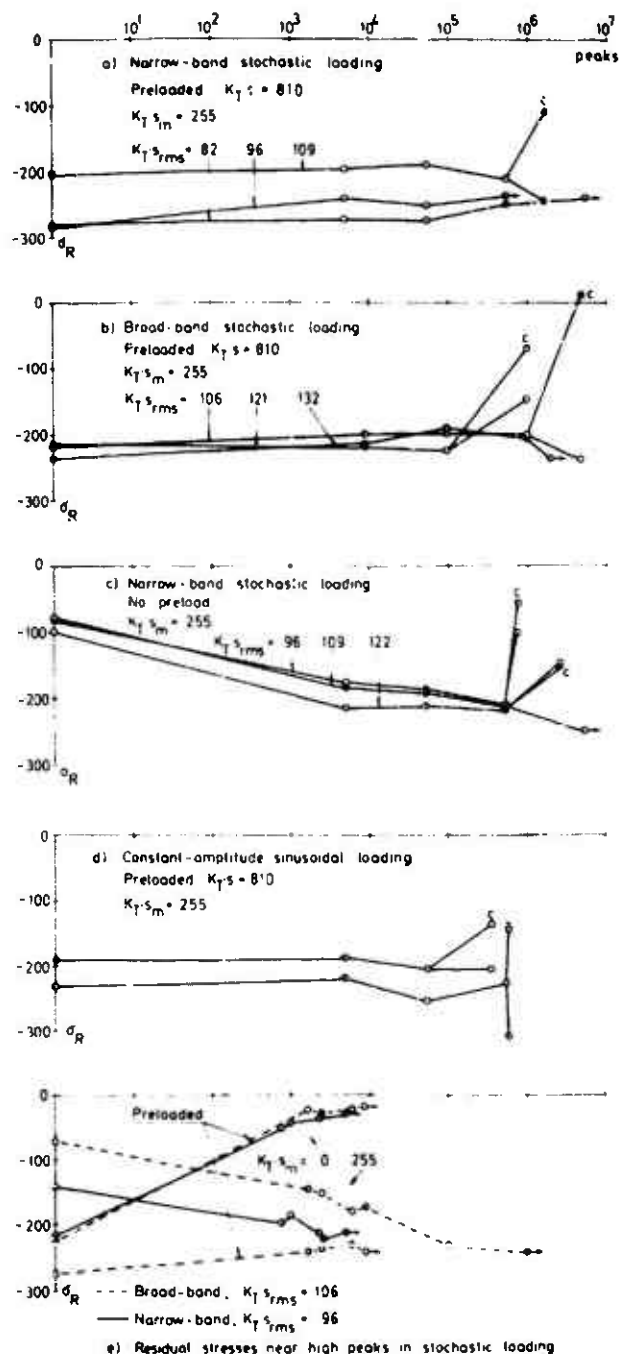2) In specimens with no preload, the residual stress quickly changes to the applied mean stress with opposite sign.

Fig. 11. Residual stresses measured during fatigue loading. All stresses in MN/m².

This means that independent of the applied mean stress the notch material will be loaded with a resulting mean stress (i.e. sum of residual stress and applied mean stress) near zero during the main part of fatigue life.

The rms-levels used in fig. 11e are in the high-cycle range as seen on the s-n-curves on fig. 17.

VARIATION OF RESIDUAL STRESS IN THE HYSTERESIS LOOP

When discussing changes in residual stresses cyclic stress-strain curves are very convenient. The curves were here measured according to a method demonstrated by LANDGRAF et al. [20]. A specimen was loaded with ten blocks of strain-controlled cycles, each block containing 10 cycles with increasing or decreasing amplitudes. Fig. 12 shows the stress-strain behaviour in the 10th block.
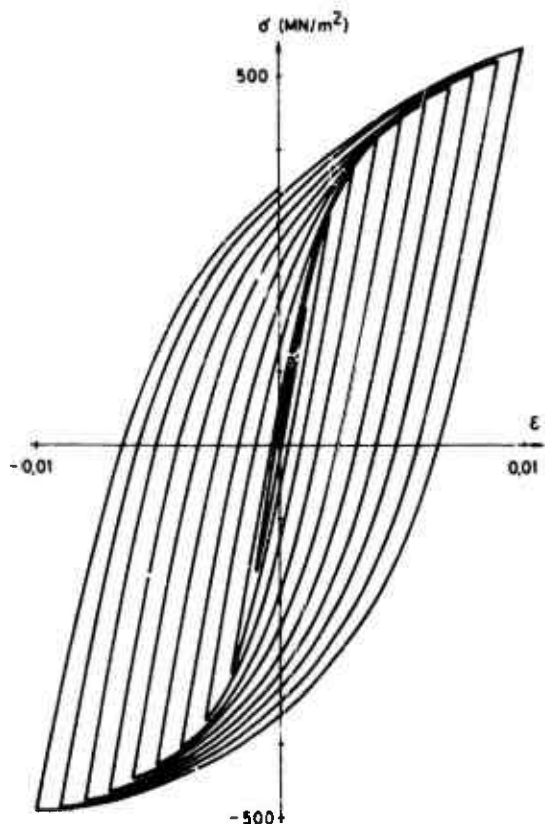
Fig. 12. Hysteresis loops measured on notch free specimen under strain control.
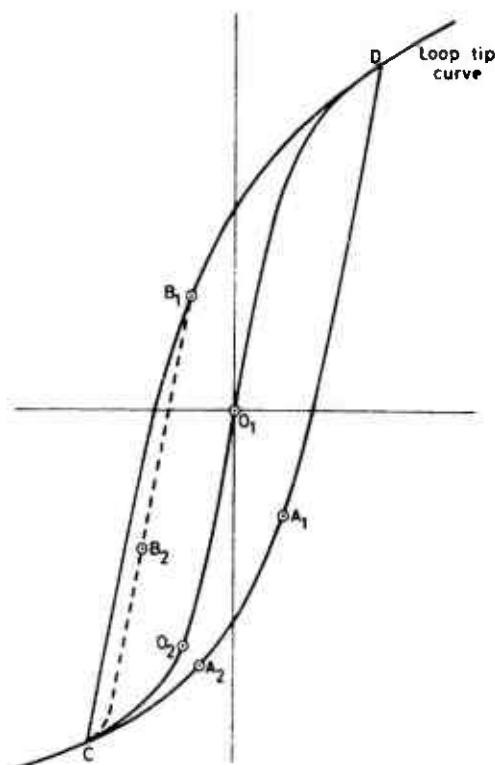
Fig. 13. Single stable hysteresis loop for notch material showing residual stresses after unloading.

When fatigue stresses are high enough to open the hysteresis loops, the residual stress in the notch found upon unloading depends on how the loading stopped.

Let the hysteresis loop in fig. 13 represent a stabilized loop for the notch material loaded with constant-amplitude and zero mean stress. The loop tip curve is a curve through the tip of loops in fig. 12. Depending on the last peak being a maximum or a minimum the residual stress measured after unloading will be either σ_{A1} or σ_{B1}. The point A_1 is found by trial and error such that

$$(\sigma_D - \sigma_{A1}) \cdot (\varepsilon_D - \varepsilon_{A1}) = (\sigma_{A1} - \sigma_C) \cdot (\varepsilon_{A1} - \varepsilon_C) \tag{7}$$

according to the Neuber theory. Point B_1 is found analogously. If the loading stops before the stress reaches a maximum or minimum, the residual stress may attain any value between σ_{A1} and σ_{B1}.

A loading mean stress narrows the range of possible residual stress values. The X-ray measurements showed, that for the material used here, the notch material stabilizes such that the resulting mean stress is zero during fatigue loading, i.e. the same loop as shown on fig. 13 is applicable. When stopping the amplitudes, the sum of residual stress and mean loading stress in the notch therefore again may be anywhere on the curve $A_1O_1B_1$. Unloading the mean stress moves this curve down over $A_2O_2B_2$ to C depending on the size of mean stress and thus decreases the range $\Delta\sigma_R = \sigma_B - \sigma_A$.

To evaluate the range for a stochastic load, a specimen was first loaded for 200 seconds with broad-band loading ($K_T \cdot s_{rms} = 106$ MN/m²) to stabilize the material. Residual stresses were then measured before and after static loading to the maximum and minimum of the fatigue load. Table V summarizes the results. Each measured value is the mean of the stresses in the two notches of a specimen.

In spite of the large possible variations in σ_R as seen in table V the fluctuations in the measured σ_R values in fig. 11e are very small even if these measurements were taken within 10 seconds from the largest peaks.

It is therefore concluded that the material always stops near the center of the loops because the material in random load fatigue continuously shifts from one nearly concentric hysteresis loop to another. This again implies, that all X-ray stresses are measured near the center of the loops and therefore indicate the mean value of residual stress.

TABLE V. Residual stresses after peaks. $K_T \cdot s_{rms} = 106$ MN/m^2. Broad-band.

Stresses in MN/m^2	$K_T \cdot s_m = 0$	$K_T \cdot s_m = 255$
σ_0 after 200 sec. fatigue loading	-14	-242
σ_A after $K_T \cdot s_{max}$	-88	-276
σ_B after $K_T \cdot s_{min}$	101	-174
Range $\Delta\sigma_R = \sigma_B - \sigma_A$	189	102

RELAXATION OF RESIDUAL STRESS AFTER PRELOAD DUE TO NEGATIVE PEAKS

After preload the material in the notch may be in a state corresponding to point A_2 on fig. 13, only the hysteresis loop corresponding to the preload is much larger. A positive loading stress is not dangerous. i.e. it will not make the residual stress more positive, but a negative loading stress is very harmful to the residual stresses because the notch material comes into a more horizontal part of the loop curve.

The relaxation of residual stress due to negative peaks after a preload of $K_T \cdot s = 810$ MN/m^2 was determined theoretically again using Neuber theory and the actual loop curve as is shown on fig. 14. The curve on fig. 14 explains the rapid changes of residual stress measured on fig. 11e in the two cases with $K_T \cdot s_m = 0$. The minimum nominal notch stress was here -420 MN/m^2 giving a complete relaxation of macro residual stress according to fig. 14.
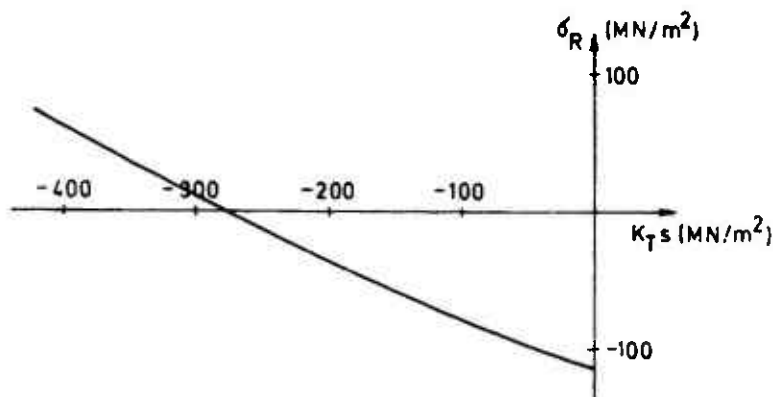
Fig. 14. Relaxation of residual stress after preload due to negative loading stress.

RELAXATION OF RESIDUAL STRESS DUE TO CYCLIC CREEP

In fatigue tests with non-zero mean stresses on unnotched specimens, it is often observed that the mean strains change with an increasing number of cycles. This change is called cyclic creep. In notched specimens cyclic creep alters the residual stresses, because the creep relieves the stresses in the notch.

To describe the relaxation of residual stress due to cyclic creep in sinusoidal loading IMPELLIZERI |5| proposed a relation which using the notation from the present paper is written

$$\frac{d\sigma_R}{dn} = a \cdot \sigma_R \cdot \sigma \cdot \epsilon / F_{ty} \qquad (8)$$

where n is the number of cycles, a is an empirical constant and F_{ty} is the yield stress (0.2% proof stress). Integrating eq. (8) from $n = 0$ yields

$$\frac{\sigma_R}{\sigma_{Ro}} = \exp(-a \cdot n \cdots \epsilon / F_{ty}) \qquad (9)$$

where σ_{Ro} is the value of σ_R at $n = 0$.

The X-ray measurements have shown that the driving force behind changes in residual stress is the sum

$$\sigma_R + K_T \cdot s_m \qquad (10)$$

The residual stress stop changing when this sum becomes zero. When using the sum instead of just σ_R eq. (9) becomes

$$\frac{\sigma_R + K_T \cdot s_m}{\sigma_{R0} + K_T \cdot s_m} = \exp(-a \cdot n \cdot \sigma \cdot \epsilon / F_{ty}) \tag{11}$$

The curves on fig. 11c and two curves on fig. 11e show how the mean value of residual stress build up in originally almost stress free specimens during fatigue loading. In all but one (the one which had $K_T \cdot s_{rms} = 122$ MN/m^2) of these curves, the maximum nominal stress did not exceed the yield stress. The plastic strains were then small, making the microstresses small. The four curves thus show the relaxation of macro residual stress.

To facilitate comparison the curves were replotted on fig. 15 using the left hand side of eq. (11) as ordinate and log(n) as abscissa.

All parameters in the exponent in eq. (11) being approximately equal for all four curves they were gathered in a single parameter

$$K = a \cdot \sigma \cdot \epsilon / F_{ty} \tag{12}$$

To check the validity of eq. (11) for random loads, K was computed such that the theoretical curve fitted the experimental average at $n = 10^4$. The theoretical curve was then plotted on fig. 15 (the dotted curve), and it is seen that the agreement is bad.
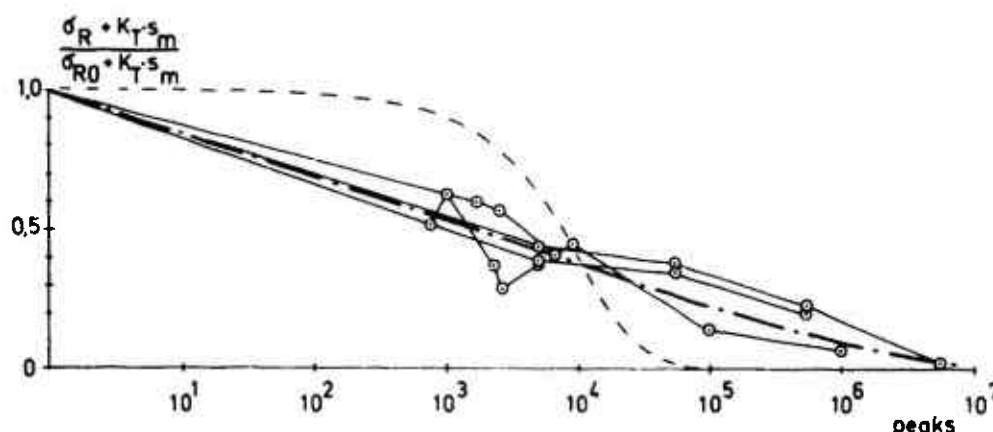
Fig. 15. Normalized relaxation of residual stress.

The measured relaxations suggest another empirical relationship

$$\frac{\sigma_R + K_T \cdot s_m}{\sigma_{R0} + K_T \cdot s_m} = -\ln(\frac{n}{n+K})/\ln(1+K) \tag{13}$$

where

$$K = K(\sigma_{rms}, \epsilon_{rms}, K_T, F_{ty}, C) \tag{14}$$

The function on the right hand side of eq. (13) has the following desirable properties:
1) It is equal to unity for $n = 1$.
2) It approaches zero as n approaches infinity.

To test eq. (13) K was computed to fit the experimental average at $n = 10^4$. When plotted on fig. 15 (the dot-and-dash line) good agreement was obtained. More tests are needed to estimate the function K in eq. (14).

STRAIN GAGE MEASUREMENTS

The variations in residual stress in fig. 11 may be divided into two parts. The first part is due to the highest peaks exceeding the compressive or tensile yield strength. Every time a peak arrives that is higher than the previous peaks there will be a jump in the residual stress. The second part is due to cyclic creep.

To illustrate this fig. 16 shows continuous strain gage recordings from the notch material in narrow-band loading.

The measuring length of the strain gage was 0.75 mm. At four different rms-levels the specimen was first loaded with $s_m = 0$, thereafter with $K_T \cdot s_m = 255$ MN/m^2. Each loading lasted ½ hour. During this time, the mean value of strain was plotted by placing a low-pass filter with time constant of appr. 1 second between strain gage apparatus and plotter.

At the first loading (i.e. $K_T \cdot s_{rms} = 83$ and $s_m = 0$) the change in mean strain is small, because the residual stress before the test was near zero.

In the beginning of all other curves a very characteristic pattern appears. Each time a large peak arrives, the strain increases stepwise. Between the peaks the strain changes smoothly. The rate of change decreases with increasing number of cycles.

The symmetric appearance of curves measured with the same rms-value but different mean-value is due to narrow-band loading being used. The steps in the curves are caused by positive peaks for the case of $K_T \cdot s_m = 255$ MN/m^2 and negative peaks for the case of $K_T \cdot s_m = 0$. But in narrow-band loading positive peaks and negative peaks of nearly the same size are neighbours as may be seen on fig. 3. The time difference between a positive and negative peak is therefore too small to be detected on fig. 16.

At large rms-values the larger cyclic creep is observed for positive mean stress. This indicates, that larger material volumes are loaded high enough to creep.

Measurements of the kind shown on fig. 16 involving both creep and fatigue loading is a critical application for strain gages. There should therefore not be placed too much confidence in the exactness of the strains, although it is believed that they give correct trends. The change in mean strain cannot be used to determine change in residual stresses because the strain variations increase with increasing rms-level whereas the change in residual stress is nearly the same and equal to the change in local mean loading stress for all loadings as shown by the X-ray measurements.
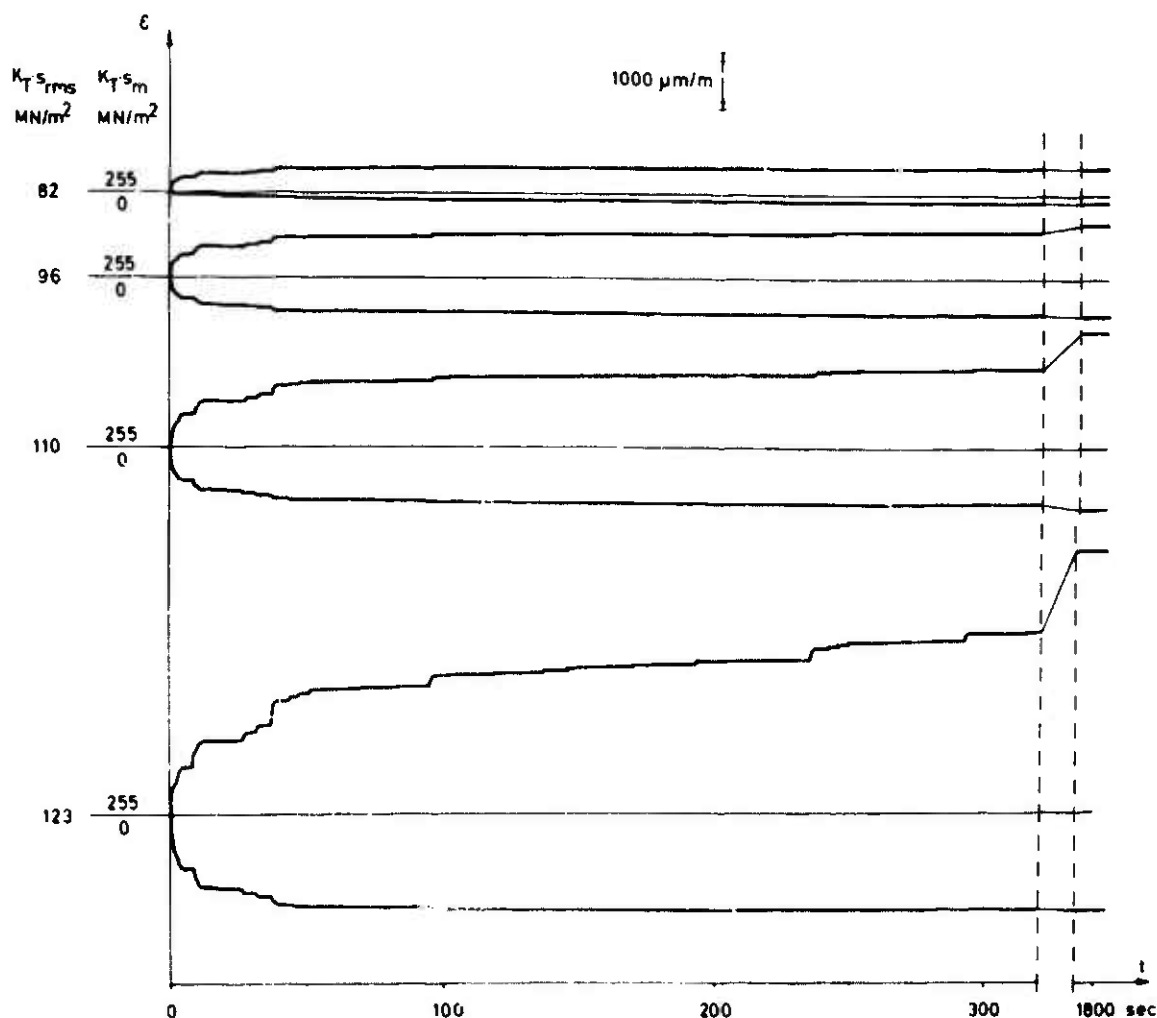
Fig. 16. Strain gage measurements of mean strain variation of notch material during narrow-band loading.

FATIGUE TEST RESULTS

The results from the fatigue tests are shown on fig. 17. The build-in error detectors in the MTS-machine were not sensitive enough to avoid complete rupture of the

specimens. This was undesirable because X-ray measurements were impossible on ruptured specimens. The fatigue tests were therefore stopped by a crack detector working on the Eddy-current principle. The sensitivity of the instrument was adjusted to stop the fatigue loading when cracks of appr. 3 mm length on the surface had developed. The time from a crack of this size had developed and until final fracture, was only a small percentage of the total life time. Therefore, variations in crack length on stopped specimens did not increase the spread in lifetime significantly.

All tests marked with an arrow on fig. 17 indicate that no cracks were observed. These tests were retested at a higher stress-level, but all retests had a lower life than corresponding tests that were not retested. Therefore, the retests were not plotted on fig. 17.

The spread in lifetime were estimated by computing the variance, where two or more specimens were tested with the same loading conditions and same rms-value. Except for one pair in fig. 16c near the fatigue limit, all variances were pooled and a standard deviation of $s(n)=20\%$ was obtained.
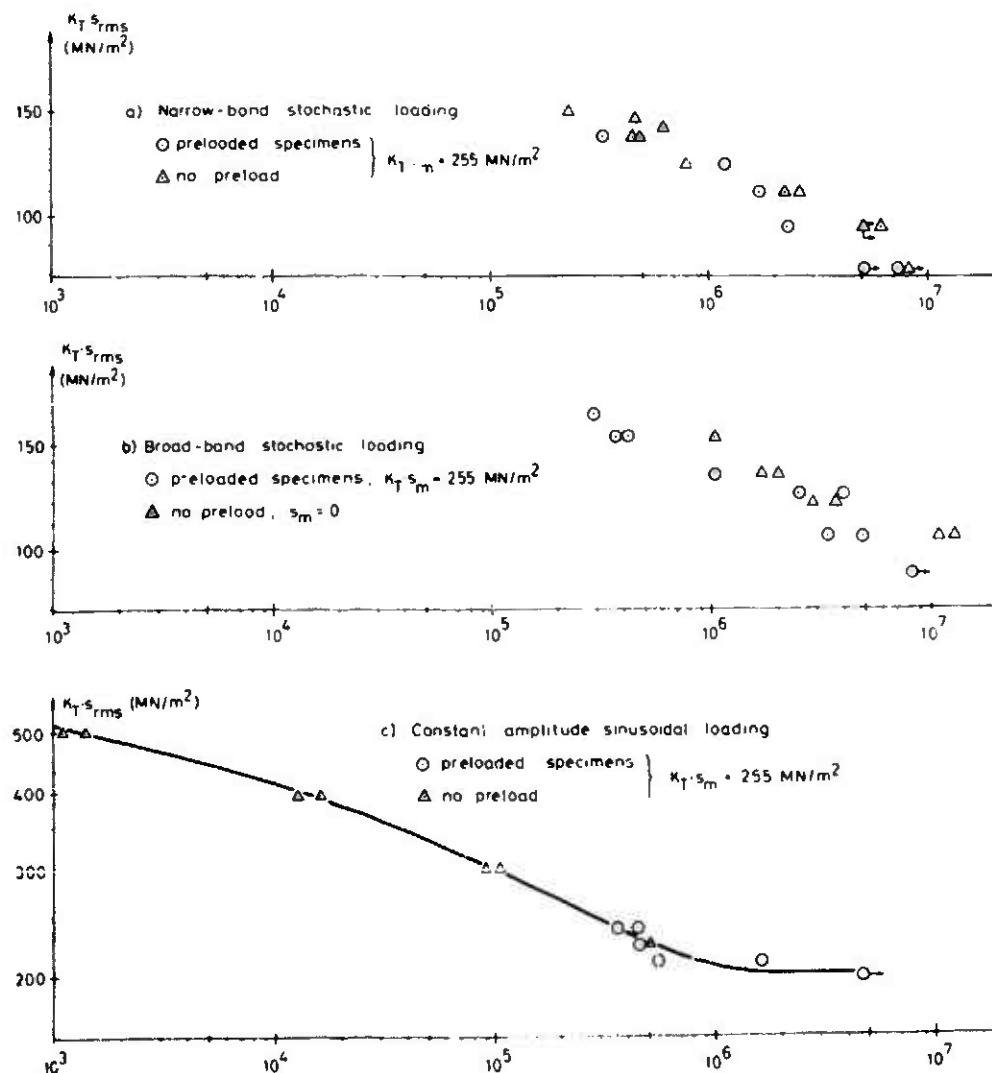
Fig. 17. $K_T \cdot s_{rms}$ versus number of maxima for notched specimens with $K_T=1.69$ on steel B14.

The X-ray measurements done, preload was no more expected to have any influence on the fatigue strength of the heterogeneous steel used here, because the resulting mean stress (i.e. the sum of loading mean stress and residual stress) was near zero during the main part of fatigue life. Test results in fig. 17a and b indicate that preload decreases fatigue life at low stress levels in contrast to what is normally expected. This may be explained by assuming the dislocation mechanisms, which creates the microstresses, to have detrimental effect on fatigue strength. Following this conception, the microstresses created during the preload are a mesure of the detrimental effect of plastic strains. The microstresses themselves cannot explain the shorter fatigue life

because they fade during fatigue life.

CONCLUSIONS

The highest residual stresses after static preload of a notch are attained when K_T is large and when the plastic deformation in the notch is small.

In high-carbon normalized steels the residual stress in a notch changes fast during fatigue loading. The change is such that the sum of residual stress plus mean loading stress is zero during the main part of fatigue life independent of the residual stress prior to fatigue loading. This conclusion applies probably also for other soft materials such as low-carbon steels.

Cyclic creep may change the residual stress more than a single preload.

Residual stress relaxation in a notch during stochastic loading caused by cyclic creep could be described by eq. (13).

Microstresses in high-carbon normalized steels created by plastic strains decrease during fatigue loading.

Plastic strains of a few per cent have detrimental effect on the fatigue strength of normalized high-carbon steels.

ACKNOWLEDGEMENTS

REFERENCES

1	A.L.Esquivel and K.R.Evans; Experimental Mechanics 8 (1968) 496-503
2	D.Munz; Härterei-Technische Mitt. 22 (1967) 52-61
3	D.V.Nelson, R.E.Ricklefs and W.P.Evans; ASTM STP 467 (1970) 228-251
4	R.L.Mattson and J.G.Roberts; 337-360 in
	G.M.Rassweiler and W.L.Grube: Internal Stresses and Fatigue in Metals;
	Elsevier Publ. Co (1959)
5	L.F.Impellizeri; ASTM STP 462 (1970) 40-68
6	W.T.Kirkby and P.R.Edwards; 253-290 in
	E.Gassner and W.Schütz: Fatigue Design Procedures;
	Proceedings of the 4th Symposium (1965); Munich. Pergamon Press (1969)
7	B.D.Cullity: Elements of X-ray Diffraction;Addison-Wesley Publ. Co (1967)
8	A.L.Christenson: The Measurement of Stress by X-ray;
	SAE Information Report TR-182 (1960)
9	E.F.Kaelble: Handbook of X-rays; McGraw-Hill Book Co (1967)
10	R.Glocker: Materialprüfung mit Röntgenstrahlen;Springer-Verlag (1958)
11	G.Faninger; Härterei-Technische Mitt. 22 (1967) 26-36
12	S.Taira, K.Hayashi and Z.Watase;
	Proc. of the 12th Japan Congress on Materials Research (1969), 1-7
13	K.Kolb; Härterei-Technische Mitt. 20 (1965) 228-237
14	S.Taira and Y.Yoshioka;
	Proc. of the Seventh Japan Congress on Testing Materials, Koyoto, Japan (1964) 31-37
15	F.Bollenrath, V.Hauk and W.Ohly; Zeitschr.Metallkunde 57 (1966) 464-469
16	E.Macherauch; Experimental Mechanics 6 (1966) 140-153
17	R.E.Peterson: Stress Concentration Design Factors; John Wiley & Sons (1953)
18	T.H.Topper, B.J.Sandor and J.D.Morrow; Journal of Materials 4 (1969) 189-199
19	H.Neuber; Journal of Applied Mechanics 28 (1961) 544-550
20	R.W.Landgraf, J.D.Morrow and T.Endo; Journal of Materials 4 (1969) 176-188

The Fatigue Life Under Three Different Load Spectra
- Tests and Calculations -

Dr. Ing. Walter Schütz
Industrieanlagen-Betriebageaellachaft mbH
8012 Ottobrunn, Einsteinstraße, Germany

One of the more urgent problems in the fatigue life prediction of military airplanes is caused by the difference between the load spectrum used in the full scale fatigue test and the load spectrum in service. This may have various reaaons:

- The same aircraft is used for different purposes i.e. ground attack, interception (composite spectrum)
- Diffarent squadrcns have different squadron duties
- The spectrum changes during the life of the individual aircraft because the military requirements have been altered.

Complex flight-by-flight tests with two types of notched specimens and a bolted joint simulating a skin-fitting joint were carried out under three different load spectra occurring in service of a German military airplane.

It is shown that Miner's-Rule can be used as a transfer-function ("relative" Miner Rule) to calculate the lives with high accuracy for the notched specimens and with less accuracy for the bolted specimens.

1. Introduction

Military and civilian aircraft are often flown in service under load spectra different from those for which they were designed and to which they were tested. There may be various reasons for this:

- The same aircraft type is used for different purposes, i.e. ground attack, interception etc.

- The spectrum changes at aome point during the life of the individual aircraft - for example, because the military requirementa have been altered. Civilian transport aircraft may also fall into this category: For instance the "Super Constellation", a type originally designed for high altitude, long range flight, was used as an "airbus" for short range flights at low altitude in Germany during the latter part of its service life.

- The service load spectrum was not estimated correctly in the first place; the life calculations and the full scale fatigue test were therefore carried out with the wrong spectrum.

It is obviously not possible to do a new full scale fatigue test in all these cases, but it is necessary to calculate the lives under the different load spectra. For this calculation, at oest the fatigue life under one spectrum is approximately known from a full acale fatigue test or from service experience. Using Miner's rule or a similar cumulative damaga hypothesis as a "transfer function", the life under the different spectra can then be calculated; it is not necessary in this case that the damage sum is unity as postulated by Miner [7], but only that the damage sum is similar for the various spectra ("relative" Miner rule). As long as the spectra are not too different, this assumption might be justified. However it is hard to decide when the difference hecomes too large.

One way out of these difficulties would be to use a more severe spectrum in the full scale fatigue test than can possibly occur in service, resulting, hopefully, in a conservative life estimation. However, this will penalize the structure weight unduly; furthermore the question "what is a more severe load spectrum?" is sometimes not easy to decide. Truncating the high amplitudes in a flight-by-flight gust load spectrum has been shown to decrease the life during the crack propagation phase for the aluminum alloys 2024-T3 and 7075-T6 [2] and for the titaniun alloy Ti6Al4V [3]. But will it also decrease the life before macroscopic cracks are present? On the other hand proof testing surface flawed specimens made of   D 6 A C   did not influence crack propagation under a programmed maneuver load spectrum without ground-to-air cycles, while a similar spectrum containing several higher peaks did have a slightly retarding effect on crack propagation life [4]. Again contrary to these results, some Air Forces limit the load factors of fighter airplanes to extend the fatigue life of their structure, if it is insufficient.

2. Test Program

A certain German military airplane is flown under two distinct load spectra. A number of aircraft is used for pilot training exclusively, resulting in the relatively severe load spectrum A. see Fig. 1. The remaining airplanes are flown to spectrum B according

to flight load measurements. Spectrum C was flown during the first years after the introduction of this airplane into the German Air Force. Some cracks have occured in airplanes flown to spectrum A in the region of the joint between wing skin and the wing-to-fuselage fitting. The full scale fatigue test was carried out at the IABG to spectrum C for about 1000 flying hours, afterwards changing over to the more severe spectrum B. Similar cracks have been found at the identical position as in the service aircraft.

The specimen tests described in the present paper were performed to determine the affect of the three different load spectra A, B and C on fatigue life. The results were to be used for an improved fatigue life estimation of the aircraft under spectrum B, starting from the known fatigue cracks in service under spectrum A and from the results of the full scale fatigue test under the composite spectrum mentioned above.

Three specimen types, shown in Fig. 2, were used; two of them are notched, with stress concentration factors of 2.5 and 3.6 respectively; the third is a bolted joint simulating the region where fatigue cracks were observed in service with regard to type and torque moment of bolts, distance between the bolt holes, and material thicknesses. The material for the notched specimens was 7075-T6, as in the aircraft. For the bolted joint this material was not available; instead Fuchs AZ 74 was used, which is similar to 7075 except for the addition of silver. It is not thought that this change in material specifications would have affected the results. Earlier tests by the author $\underline{/5, 6, 7/}$ have shown both materials to have very similar fatigue properties.

The program for the specimen tests was analogous to the full scale fatigue test, i.e. it was a complex flight by flight program of 803 different flights averaging 100 cycles each and consisting of 143 load distributions, taking into account positive and negative maneuver and gust loads, symmetrical and unsymmetrical maneuvers with and without aileron and flaps, three Mach numbers, three configurations, the change in weight due to fuel burnoff, and taxi loads. The program was repeated after every 803 flights. An example of wing root bending moment versus time during flight No 11 is shown in Fig. 3.

The nominal stress in the $K_t = 2.5$ specimens simulated exactly (with regard to sequence and magnitude) the local nominal stress at the surface of the wing skin at fitting No 3 at the wing station in question, as determined by a strain gauge calibration of the full scale test article. The stresses were reduced proportionately for the $K_t = 3.6$ specimen and for the bolted joint to give about one thousand flights to failure under spectrum A. Fig. 4 shows the stress sequence of two flights. The differences between the load spectra A, B and C were obtained by increasing the frequency and the magnitude of certain load cases for spectra A and B as compared to C.

The test machine, see Fig. 5, was built by the IABG, using a 25 ton Schenck servohydraulic cylinder. It is controlled by a digital computer (PDP-8L), Fig. 6. Details of this highly successful system were reported to the S/M Panel during the 31st. meeting in Tonsberg, Norway $\underline{/8/}$ and have also been published elsewhere $\underline{/9/}$. The testing frequency was about 25 cycles per second, resulting in a testing time of about 50 minutes for one program of 803 flights. As the specimens failed between about 800 and 8000 flights, see Fig. 8, the tests took from 50 minutes to 8 hours each. Buckling of the specimens under compression loads was prevented by steel antibuckling guides with Teflon liners.

3. Results and Discussion

The results of the specimen tests are summarized in Fig. 7; for a statistical evaluation see Fig. 8; for individual results see Tables 1, 2 and 3, which also contain a number of tests at stresses different from the main test series shown in Figs. 7 and 8.

Notched specimens

The number of flights to failure under spectrum A was about 1100 for the $K_t = 2.5$ specimens, which is very similar to the number of flights at which the cracks were observed in service aircraft. The ratio of the geometric mean of the lives under the 3 spectra was

0.7 (A): 1.0 (B): 1.7 (C) for the $K_t = 2.5$ specimens and

0.5 (A): 1.0 (B): 1.5 (C) for the $K_t = 3.6$ specimens.

Next, the life was calculated by a computer program using Miner's rule. The necessary SN-curves[*] were determined in the following way: For the $K_t = 2.5$ specimens they were linearly interpolated using the well-known NASA data with stress concentration factors of 1.0, 1.5, 2.0, 4.0 and 5.0 $\underline{/10 \div 13/}$; for the $K_t = 3.6$ specimen data of the author for the same material and K_t $\underline{/5/}$ were employed. The g.t.a.c. was considered to extend from the minimum stress during taxiing to the maximum stress in the individual flight. The following damage sums $\sum n_i/N_i$ at failure were obtained:

0.56, 0.47 and 0.48 for spectra A, B and C respectively, for $K_t = 2.5$ and

0.28, 0.30 and 0.25 for $K_t = 3.6$.

[*] In fact complete Goodman diagrams were required because of the many different mean stresses of the stress spectra.

These data confirm the well known experience that flight-by-flight tests will usually give $\sum n_i/N_i < 1.0$ at least for maneuver load spectra $/14/$; besides, the results suggest that Miner's rule can be used as a "transfer function"; that is, given the life under one spectrum, determined in a flight-by-flight test, the life under not too different spectra can be calculated, using Miner, with high accuracy. Thus the assumption mentioned in the Introduction ("relative" Miner rule) was verified for the notched specimens. The results also show that spectrum A was indeed the most severe one, giving the lowest life, followed by B and C.

However this is true only for the nominal stresses chosen. Three tests, one under Spectrum C, two under spectrum B, were performed with $K_t = 3.6$ specimens at about 25 per cent higher stresses (i.e. all stresses, including the 1 g stress, were increased by 25 per cent). Surprisingly the life under spectrum B was slightly longer than under spectrum C, see Table 2. The reason is not clear: Although the failures happened at about 400 flights, before one complete program of 803 flights had been applied, this is not the cause for this unexpected result; all high loads above 90 per cent of the maximum load had occured in the correct fraction, i.e. about 0.5 times as often as they occur in a complete program. Rather it seems that just using higher stresses can yield a quantitatively and even qualitatively different result.

This points to the importance of doing even a flight-by-flight test on a simple notched specimen at the correct stresses. Increasing the stresses in order to shorten the testing time can give completely misleading results. This topic will again be discussed in the next section.

Bolted joint

The fatigue performance of the bolted joints is summarized in Figs. 7 and 8, individual results are shown in Table 3. The ratio of the geometric mean of the numbers of flights to failure was 0.4 : 1.0 : 2.3 for spectra A, B and C respectively, provided that only specimens where the critical fatigue crack had started in the cylindrical part of the bolt hole, or at the intersection between the countersink and the cylindrical part are considered for spectrum C. Otherwise the ratio was 0.4 : 1.0 : 2.7, as several fatigue cracks also originated in the countersink portion, under the bolt head, see Fig. 10.

A cumulative damage calculation was again carried out, using the SN-curves for the $K_t = 2.5$ specimens, as no SN-curves for the bolted joint were available. The damage sums $\sum n_i/N_i$ at failure were 0.43, 0.55 and 0.76. Thus the "relative" Miner rule is less accurate for the bolted joint. There may be two reasons for this:

- The SN-curves used are not correct. A shortage of funds unfortunately prevented another cumulative damage calculation to be carried out with appropriately estimated SN-curves, i.e. SN-curves with a lower fatigue limit. However, it is thought that this was not the main reason, as the "relative" Miner rule is relatively insensitive to changes in the SN-curves, as long as the spectra are similar and there are that many load cases.

- The stress amplitudes of medium size cause the two parts of the joint to slip, thus transmitting the loads not by friction but by bearing of the bolt shank against the hole, which gives a low fatigue performance. As spectra A and B contain a larger number of such medium sized amplitudes, this is thought to have caused the relatively lower life under spectra A and B.

Two bolted joints were tested at about 17 per cent lower stresses, giving about 14 000 flights to failure, see Table 3. The fatigue cracks did not originate in the bolt hole any longer, but from fretting between the faying surfaces. This again points to the importance of the selection of a correct stress in a fatigue test, when conclusions regarding aircraft fatigue life are to be drawn. As the bolted joint has two critical sections, at the first and at the last bolt row, the specimens were inspected at the unbroken critical section after the fatigue test. In every case fatigue cracks were present.

Scatter

The scatter was extremely low in most test series, the average standard deviation of number of flights to failure being below 0.07 for the bolted joint, see Fig. 8. This confirms the well known experience that flight-by-flight tests usually will have low scatter. One notable exception was the bolted joint under spectrum B, giving $\sigma = 0.22$ approximately. No explanation can be given for this, except the one mentioned in the preceding paragraph: Slipping between the two parts joined together under medium sized amplitudes may occur in one specimen under spectrum B and not in another, due to different clamping forces. In another test series carried out elsewhere $/15/$ the scatter for the bolted joint under a programmed constant amplitude test (8-step LBF-program) was also quite low (s = 0.1 approximately).

Fracture Surfaces

Some typical fracture surfaces of notched specimens are shown in Fig. 9 and of bolted joints in Fig. 10. The spectra, the nominal stresses and the corresponding numbers of flights to failure are also shown. The macroscopic crack propagation phase was quite short in comparison to the crack initiation phase, judging from visual observation of the hole surfaces during the tests and from the indication of one "crack wire" bonded

to the hole surfaces: it broke after 1076 flights, the specimen failing completely on the 1205th flight. This short interval between the appearance of a macroscopic crack and complete failure is probably due to two reasons:

- The relatively large number of high maximum stresses, typical for maneuver load spectra

- The unfavourable crack propagation and residual static strength properties of the materials used

Fig. 11 shows the fracture surface of a wing box for the aircraft in question which failed after 3351 flights under spectrum B at identical nominal stresses. The similarity of the number of flights to failure to the number for the bolted joint (see Tabel 3), and of the crack surfaces, is quite good.

4. Summary and Conclusions

The results presented in this paper, together with some other results obtained at the IABG, support the following conclusions:

- Using Miner's rule as a transfer function and a flight-by-flight test as a basis from which to "read across" to other, not too different spectra, can yield a considerably improved life estimation compared to the normal cumulative damage procedure, using SN-curves as a basis. For the time being this can only be stated for maneuver spectra. In view of the modern test equipment available it is not a disadvantage any longer that the method proposed requires a complex flight-by-flight test.

- To obtain meaningful results in a fatigue test, it is necessary to simulate the stresses occuring in service as closely as possible with regard to sequence and magnitude.

- If a test must be accelerated, this should not be done by increasing the stresses but by leaving out some small stress amplitudes.

Futher research along the following lines is considered necessary:

- How far can we "read across", in other words, how different can the spectra be and still yield satisfactory results?

- Can the method also be employed for gust load spectra?

- How sensitive is the method to the SN-curves employed, with regard to the slope of the finite life portion and to the magnitude of the fatigue limit i.e. is it really necessary to have actual SN-curves or would it be enough to make an "educated guess" of the SN-curves?

5. References

[1] Miner, M.A.: Cumulative Damage in Fatigue. Journal of Applied Mechanics 12 (1945) 3, S. A 159/A 164

[2] Schijve, J., F.A. Jacobs and P.J. Tromp: Crack propagation in aluminum alloy sheet materials under flight simulation loading. NLR-TR 68117 U, Dec. 1968

[3] Schütz, W. and H. Zenner: Rißfortschritt an Titanblechen im Einzelflugversuch. IABG Report TF-224, Jan. 1972

[4] Wood, H.A. and T.L. Haglage: Crack Propagation Test Results for Variable Amplitude Spectrum Loading in Surface Flawed D6AC Steel. AFFDL Technical Memorandom FBR-71-2, Febr. 1971

[5] Schütz, W.: Zeitfestigkeit gekerbter Flachstäbe aus dem Werkstoff 3.4364.7. Technische Mitteilung Nr. 21/67, LBF Darmstadt, March 1967

[6] Schütz, W.: Zeitfestigkeit gekerbter und ungekerbter Flachstäbe aus 3.4354.7 (Fuchs AZ 74/72, stranggepreßt). Technische Mitteilung Nr. 24/67, LBF Darmstadt, May 1967

[7] Schütz, W.: Zeit- und Betriebsfestigkeit gekerbter Flachstäbe aus 3.4364.7. Technische Mitteilung Nr. 43/68, LBF Darmstadt, Dec. 1968

[8] Schütz, W.: Report to the Agard S/M Panel on Progress in Fatigue in the Federal Republic of Germany, 1968 to 1970

[9] Schütz, W. and R. Weber: Digital computer control of servohydraulic fatigue testing machines. Materialprüfung 12 (1970) Nr. 11, S. 369/72

/T0/ Grover, H.J., S.M. Bishop and L.R. Jackson: Fatigue Strengths of Aircraft Materi-
als. Axial-Load Fatigue Tests on Notched Sheet Specimens of 24 S T-3 and 75 S T-6
Aluminum Alloys and of SAE 4130 Steel with Streas-Concentration Factor of 5.0,
NACA TN 2390

/T1/ Grover, H.J., S.M. Bishop and L.R. Jackson: Fatigue Strengths of Aircraft Materi-
ala. Axial-Load Fatigue Tests on Notched Sheet Specimens of 24 S T-3 and 75 S T-6
Aluminum Alloys and of SAE 4130 Steel with Stress-Concentration Factors of 2.0
and 4.0, NACA TN 2389

/T2/ Grover, H.J., S.M. Bishop and L.R. Jackson: Fatigue Strengths of Aircraft Materi-
als. Axial-Load Fatigue Tests on Notched Sheet Specimens of 24 S T-3 and 75 S T-6
Aluminum Alloys and of SAE 4130 Steel with Stress-Concentration Factor of 1.5,
NACA TN 2639

/T3/ Grover, H.J., S.M. Bishop and L.R. Jackson: Fatigue Strengths of Aircraft Materi-
als. Axial-Load Fatigue Teats on Unnotched Sheet Specimens of 24 S T-3 and 75 S T-6
Aluminum Alloys and of SAE 4130 Steel, NACA TN 2324

/T4/ Crichlow, W.J., A.J. McCulloch, L. Young and M.A. Melcon: An Engineering Evalua-
tion of Methods for the Prediction of Fatigue Life in Airframe Structures. Tech-
nical Report ASD-TR-61-434

/T5/ Schütz, D. and O. Gökgöl: Optimierung der verschraubten Fügung zwischen Flügel-
unterdacke und Anachlußbeschlag eines Militärflugzeuges. Laboratorium für Be-
triebsfestigkeit, Bericht TB 95 (1971)

Table 1: Test Results

Specimen type	Spectrum	Highest maximum Stress in the Spectrum $\bar{\sigma}_{max}$ [1] kp/mm^2	Specimen Number	Flights to failure
Notched $K_t = 2.5$	A	33.1	II C 1 II C 2 II C 3 II C 4 II C 5 II C 6	1 067 953 1 058 1 001 1 095 1 404
	B	33.1	II A 1 II A 2 II A 3 II A 4 II A 5 II A 6 II A 7	1 949 1 899 1 739 1 482 1 727 1 205 1 837
	C	33.1	II B 1 II B 2 II B 3 II B 4 II B 5 II B 6	2 634 2 565 2 388 3 017 3 600 2 658
Notched $K_t = 3.6$	A	26.5	I C 1 I C 2 I C 3 I C 4 I C 5 I C 6	796 768 754 767 1 128 778
	B	33.1	2 3	391 454
		26.5	I A 1 I A 2 I A 3 I A 4 I A 5 I A 6	1 372 1 595 1 153 1 418 1 577 1 638
	C	33.1	1	341
		26.5	I B 1 I B 2 I B 3 I B 4	2 135 2 634 2 035 2 265
Bolted Joint	A	46.2 (32.0)	12 13 14 15 16	809 907 842 1 055 1 290
	B	46.2 (32.0)	6 8 9 10 11	1 155 4 096 2 391 1 632 2 114
	C	38.2 (26.5)	1 3	14 604 14 664
		46.2 (32.0)	2 4 7	8 510 5 580 4 558
		19.8 (13.7)	5	55 000 no failure

[1] The stresses without parentheses are net stresses, within parentheses gross stresses.

Fig. 1: Load Spectra A, B and C

Fig. 2: Test Specimens

Fig. 3: Full Scale Fatigue Test
Flight No 11
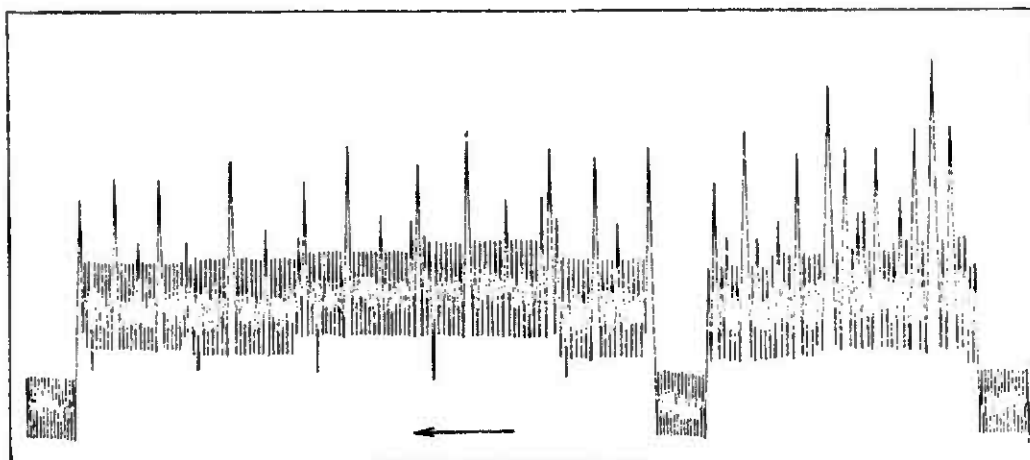
Fig. 4: Sequence of Nominal Stress in the Specimen Tests

Fig. 5: Fatigue Test Machine
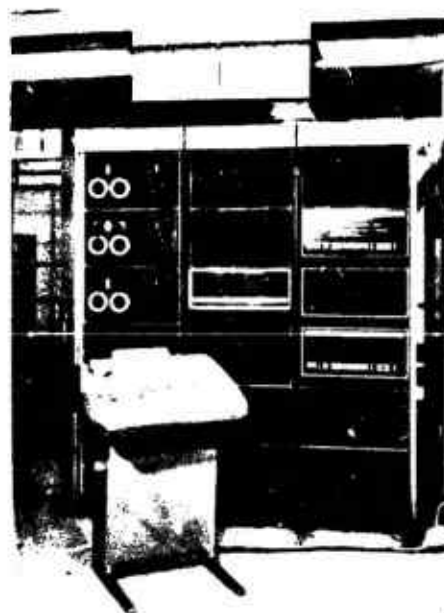
Fig. 6: Digital Computer
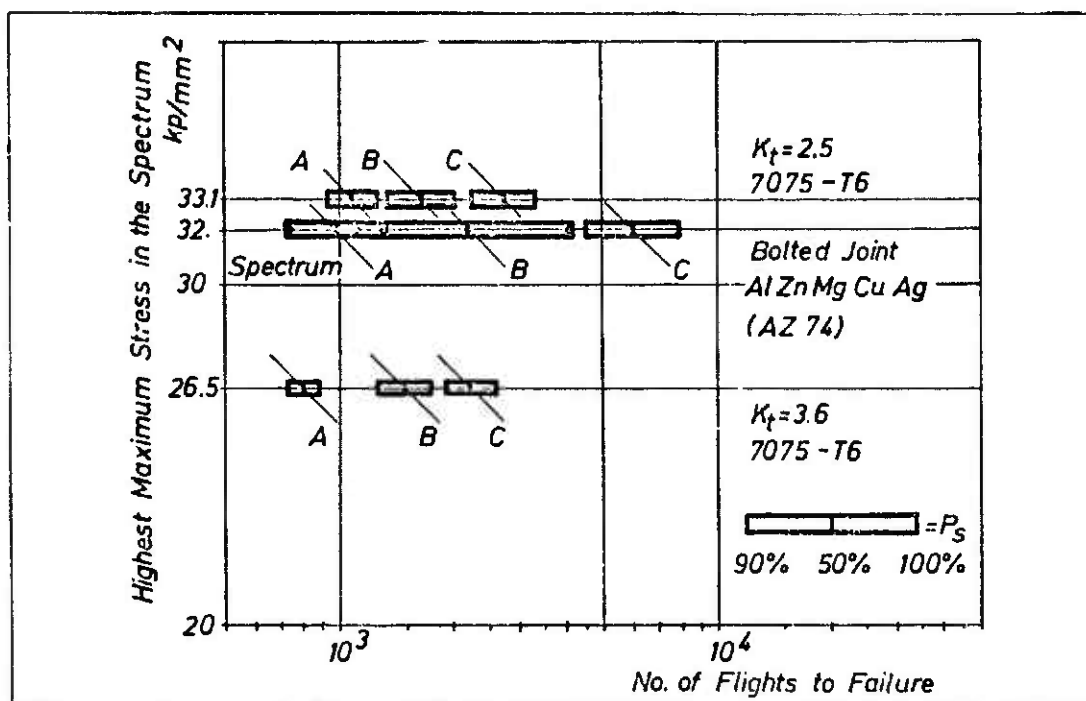
Fig. 7: Results of Flight-by-Flight Tests
under Three Different Load Spectra
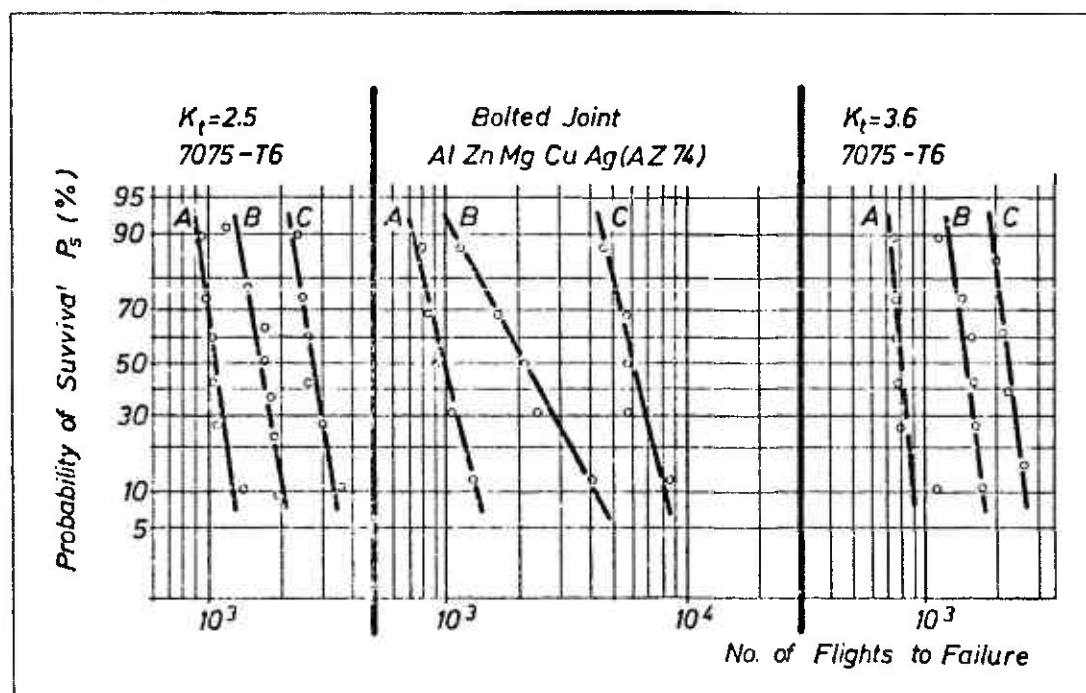
Fig. 8: Statistical Evaluation of Test Results

Notched Specimens

Spectrum: A , S_{max} = 26,5 kp/mm²   A , S_{max} = 33,1 kp/mm²
K_t = 3,6   1126 Flights K_t = 2,5   1058 Flights

B , S_{max} = 33,1 kp/mm²
K_t = 3,6   454 Flights

     B , S_{max} = 33,1 kp/mm²
     K_t = 2,5   1899 Flights

B , S_{max} = 26,5 kp/mm²
K_t = 3,6   1577 Flights

C , S_{max} = 26,5 kp/mm²   C , S_{max} = 33,1 kp/mm²
K_t = 3,6   2035 Flights K_t = 2,5   3600 Flights

Fig. 9: Fracture Surfaces of the Notched Specimens

Bolted Joint

Spectrum: B, S_{max} = 32 kp/mm²   C, S_{max} = 26,5 kp/mm²
2114 Flights   14604 Flights

A
S_{max} = 32 kp/mm²
C, S_{max} = 32 kp/mm²   907   C, S_{max} = 26,5 kp/mm²
5580 Flights   Flights   14664 Flights

Fig. 10: Fracture Surfaces of Bolted Joints

Spectrum B , 3351 Flights

Fig. 11: Fracture Surfaces of the Wing Skin in a
Wing Box Test

A RELATION BETWEEN MEASURED C.G. VERTICAL ACCELERATIONS AND THE LOADS AT THE T-TAIL OF A MILITARY AIRPLANE

by

O. Buxbaum

Laboratorium für Betriebsfestigkeit
61 Darmstadt-Eberstadt
Mühltalstrasse 55
West Germany

SUMMARY

An engineering solution is presented for correlating two different random loads – time histories, based on measurements of C.G. vertical accelerations and loads at the tailplane of an aircraft. The choice of instrumentation for a fleet airplane is described and the measurements of operational loads are related to C.G. acceleration countings.

A RELATION BETWEEN MEASURED C.G. VERTICAL ACCELERATIONS AND THE LOADS AT THE T-TAIL OF A MILITARY AIRPLANE

by

Otto Buxbaum
Laborotorium für Betriebsfestigkeit
61 Darmstadt-Eberstadt
West Germany

SUMMARY

The common equipment for recording operational flight loadings on airplanes, the fatigue lives of which are to be controlled, is still the so-called counting accelerometer because of its reliability and low costs. Problems, however, may arise, if the accelerations as counted e.g. vertically in the center of gravity of an airplane have to be transformed into stresses or strains, as the respective relations are generally complicated. In some cases such a relation cannot be found even by correlating simultaneously recorded in-flight measurements. There exists, nevertheless, a possibility which allows to derive the relation in question with certain assumptions from the respective cumulative frequency distributions. How that can be achieved, is demonstrated on hand of the results of in-flight measurements carried out on the tailplane of a military airplane under normal operational conditions.

1. INTRODUCTION

If the fatigue life of individual airplanes out of a fleet is to be controlled, the amounts of damage must be known, which have been accumulated in the structures during the respective periods of usage. Since there is at this time no general, reliable method available by which the increase of damage in a structure can be measured directly, usually the causes of damage are recorded, i.e. histories of strains, stresses, or of any other parameter, from which they can be derived. The measured values have to be analyzed such, e.g. by counting the number of crossings of given levels (Refs. 1, 2), that the results allow to define the corresponding damage and the remaining life.

This report does not claim to present a complete solution for the complicated subject of fatigue life control of airplanes. It merely tries to summarize the considerations and experiences arisen during such a program for a military airplane and to demonstrate the results obtained on hand of the example of loads acting at the tailplane.

2. INSTRUMENTATION OF FLEET AIRPLANES AND EXAMPLES OF RESULTS

2.1 Some Considerations about the Choice of the Recording System for Fleet Airplanes.

The stress or strain histories recorded at an airplane structure during a period of operation will differ on the location, where they have been measured. This fact made it at first sight appearing desirable to record strains at all airplanes. But beside the difficulty of defining the locations of measurement, which have to be found by a detailed fatigue life analysis supported by full-scale tests, and the significance and order of which may vary from one squadron to the other depending on duties and configurations of the airplanes, mainly economical reasons have been opposing that solution, like costs for suitable recording equipment, for strain gage installation, for periodical calibrations of the structures, for data reduction and analysis, etc. Since also from the engineering point of view it seemed to be justified to relinquish strain gages at all airplanes of the fleet, if one or two airplanes were instrumented to measure loads in all sections of the structure which could be critical with respect to fatigue, it has been decided to count only c.g. accelerations at the fleet airplanes. From competitive counting systems, which have been carefully evaluated (Ref. 3), finally the so-called Fatigue-Meter has been choosen for that purpose (Ref. 4).

2.2. Results of C.G. Vertical Acceleration Countings from Fleet Airplanes.

The counters of the Fatigue-Meters are read after each flight and the results are written down into a form-sheet together with pilot's remarks about airplane configuration, type of mission, duration of flight, etc. The sheets are analyzed by Messerschmitt-Bölkow-Blohm GmbH, Unternehmensbereich Flugzeuge (Ref. 5).

As an example of the results the average cumulative frequency distributions of (gust- and manoeuver-) load factors as experienced by several airplanes in four squadrons are shown, see Figure 1. The numbers of exceedances per 1,000 flight hours differ at $n_z = 2$ between 5.5×10^3 (squadron D) and 3.8×10^4 (squadron C) depending on the type of missions flown. The effect of external stores on the wing can also be observed, if e.g. the number of exceedances per 1,000 flight hours at $n_z = 5$ are compared: In squadron B, where airplanes are flown mainly in clean configuration, that level is reached or exceeded about ten times more than in the other three squadrons.

Beside the differences between cumulative frequency distributions belonging to different squadrons also the variations have to be taken into account existing between those of individual airplanes within a squadron. As an example for the latter variation the distributions of six airplanes of squadron A are shown, see Figure 2, where a ratio of about 1 : 1.5 between the lowest and highest number of exceedances can be observed. If it is assumed, that the load factors encountered by the individual airplanes belong to the same population, a statistical analysis can be performed by plotting the relative number of exceedances into a Gaussian probability paper with logarithmic grid for the variate, see Figure 3. From that graph cumulative frequency distributions can be derived, which are reached or exceeded with a certain probability.

If information of Fatigue-Meter readings of the kind as presented above are to be used for fatigue life control, regard has to be payed to the fact, that the data have been obtained already in form of cumulative frequency distributions, i.e. the original acceleration history has been lost. Therefore a requested relation between c.g. vertical accelerations and the corresponding strains ot a point of the structure has to be based probably on the respective cumulative frequency distributions instead of the original time histories.

3. MEASUREMENT OF OPERATIONAL LOADS FOR INTERPRETATION OF C.G. COUNTINGS

3.1 Aims of the Measurement Program

At the present time it seems to be almost impossible to predict theoretically o relation between c.g. vertical accelerations due to manoeuvers and the corresponding loads ot the tailplane. That, of course, does not refer to a loading condition os used for the static design, where all parameters like airplane weight, configuration, c.g. position, airspeed, flight altitude, manoeuver flap position, angles ond rates of deflections of elevator, aileron, and rudder, etc. are given but to load-time histories under operational conditions, where all the mentioned parameters can vary more or less independently of each other, or with other words, where o peak acceleration of given magnitude can be caused by several possible combinations of the parameters, each combination of which may result in o different load distribution ond load history at the tailplane.

The in-flight measurement of all mentioned parameters may help to define the boundary conditions for the calculation of individual loads ond accelerations, but that does not look very promising either, because o general relation between loads ond accelerations can be obtained in this case only by means of o multi-dimensional analysis. In order to avoid that complicated procedure it seems to be the easiest way to measure loads at the tailplane ond c.g. accelerations directly ond to try to derive the requested relation between them empirically.

When doeing so, the main problem may be expected to orise from the fact, that the vertical accelerations in the c.g. describe only the incremental loads resulting from the translatorical movement of the oirplane in vertical direction, whereas the loads ot the tailplane are caused generolly from movements in several degrees of freedom. Therefore, the results of such o measurement program can be generalized only, if it will be ossumed that the ratia of movements of the oirplane in the vertical to those in other directions will remain in the overage the same. This requirement can be possibly met for the measurement program by distinguishing between flights performed under equal conditions, i.e. flights, for which the porameters as mentioned above ore either constant (like oirplane configuration) or - if o parameter varies within given limits - for which the statistical moments of o parameter ore the same (like e.g. airplane weight). That can be expected to happen, if for each squadran o relation between c.g. accelerotions and loads ot the tailplane will be derived separately, becouse it is very likely that a change of missions or duties will result in a change of the average ratio of vertical airplane movements to those in other directions.

3.2 Instrumentation of an Airplane with Strain Gages and Transducers.

For the measurement of loads at the tailplane on oirplane has been instrumented with combinations of calibrated strain gage bridges (Ref. 6), the cutputs of which were proportional to bending ond torsion moments in different sections of the tailplane. These were in detail, see Figure 4,

- bending moments ot R/H and L/H sides of stabilizer, $B_{S,R/H}$ and $B_{S,L/H}$, respectively
- torsion moment at stabilizer, T_S
- bending moment near root of fin, B_F
- torsion moment af fin, T_F .

The direction of orrows in Figure 4 carresponds with pasitive sign os used in this report.

Beside a transducer for the measurement of c.g. vertical accelerations also transducers for indicated airspeed, pressure altitude, ongle of attock, flap position, stabilizer deflection, angular velocities about X- and Z-axes of the airplane, ond vertical accelerations in the rear part of the fuselage have been installed in the airplane.

The data were commutated ond recorded on 1-inch wide, 14-track mognetic tope together with a time code and the voice of the pilot.

4. ANALYSIS AND DISCUSSION OF RESULTS

4.1 Selection of two Squadrons with Different Missions.

In order to demonstrate the validity of the ossumption, which was made in parograph 3.1 for the relo⁺ion to be derived empirically from measured c.g. vertical accelerations and bending moments at the stabilizer, the instrumented airplane was given to two squadrons, called A ond B. The airplane was flown by several pilots of the two sauadrons in typical routine missions.

But there were differences between the two squadrons not only with regard ta missions but olso e.g. ta the duration of flights, see the statistical analysis in Figure 5, which shows o significant difference between the two squadrons. Further, in squadron A the oirplanes are flown with and in squadron B without external stores.

The different usage of airplanes in the two squadrons shows up also in the respective cumulative frequency distributions of c.g. vertical accelerations per flight, see Figure 6, and that not only in the region of high accelerations, where again the effect of external stores can be observed, compare with Figure 1, but also for the number of crossings of $\Delta n_z = 0$, which corresponds to the 1g-condition; the latter difference does not only result from the above mentioned difference in flight-times but mainly from turbulence encountered by airplanes of squadron A when flying in lower altitudes. [+]

Similar trends as having been observed for the cumulative frequency distributions of incremental load factors can also be read from those of angles of attack, see Figure 7, with the exception, that the distribution for squadron B seems to be clipped at 13 degrees. This is the result of the interaction of a stall warning system.

The cumulative frequency distributions of stabilizer deflections per flight, see Figure 8, are almost identical without regard to a peak value of -16 degrees, which has occurred once during flights of squadron B. This result is at first sight somewhat surprising in view not only of the differences as explained before but also of the distributions of bending moments at the stabilizer, which are not conformable at all, see Figure 9.

4.2 Relations Between Stabilizer Bending Moments and C.G. Vertical Accelerations.

Before conclusions are drawn from the cumulative frequency distributions of bending moments measured at the R/H side of the stabilizer during flights performed in two squadrons, attention has to be payed to the fact, that the distributions in Figure 9 have been obtained by counting level crossings about the bending moment of zero, which designates the loading condition "airplane on ground", i.e. changes of the 1g-bending moment due to different trim conditions, flap positions, etc. have not been treated separately. It only can be noted that, contrary to the previous results for other measured parameters, the cumulative frequency distributions of stabilizer bending moments for squadron B is covered by that for squadron A.

In order to gain as much information from the data as possible, the two bending moment outputs as measured at the R/H and L/H sides of stabilizer, see Figure 4, have been combined for the following analysis to get the symmetrical bending moment, which is defined as $0.5 (B_{S,R/H} + B_{S,L/H})$, and the so-called antimetrical bending moment ($B_{S,R/H} - B_{S,L/H}$).

After having applied a time consuming procedure for separating incremental and 1g-bending moments, it appeared, that the cumulative frequency distributions of symmetrical 1g-bending moments are almost identical except that they seem to be shifted parallel to each other, see Figure 10. The difference in bending moment between these two distributions can be explained by the effect of tip-tanks, which lead theoretically to an increase of the (negative) 1g-bending moment at the section of the stabilizer in question of about -0.07 Mpm (squadron A) if compared with that for the airplane in clean configuration (squadron B). This effect, however, does not explain the difference of the cumulative frequency distributions shown Figure 9. Since it cannot be explained either by variations of the respective distributions of incremental bending moments, as it will be demonstrated later on, see Figures 11 and 12, the original time-histories have been investigated. The solution of the problem was, that about 90 percent of all manoeuvers exceeding a load factor of 3.0 were flown in squadron A with manoeuver flaps down, whereas in squadron B it were only about 40 percent.

The procedure for manoeuver flap setting in squadron A is such, that the flaps are put down for periods of time up to 15 minutes while the periods in squadron B are much shorter. Since a cumulative frequency distribution of countings of a given characteristic occurrence of the respective load time history can give information only about the number, how often the flaps were moved, and not about the periods, during which they were up or down, the two distributions in Figure 10 show accidentally the same cumulative number of occurrences per flight. For a fatigue life estimation, however, also the time has to be taken into account, during which the 1g-bending moment was at a given level, because the incremental bending moments have to be superimposed to them again in an order similar to the actual sequence in flight.

For the presentation of incremental stabilizer bending moments the unsymmetrical (i.e. measured at one side of the stabilizer), symmetrical, and antimetrical parts have been choosen, see the results of the statistical analysis for squadron A in Figure 11. The three distributions are almost symmetrical about the bending moment zero. As it has been expected, the largest deviations from zero occur at a given relative frequency for the increments as measured at one side, the smallest for the antimetrical bending moments. The latter show, however, the highest number of mean (zero) crossings beeing about twice as high as that for the symmetrical bending moment increments. If the relative cumulative frequency of unsymmetrical bending moments, which lies between the two other figures, is said to be 100 percent, then that for symmetrical bending moments is about 80 percent. Hence follows, that about 20 percent of the bending moment increments occurring on one side of the stabilizer have to be regarded as antimetrical moments. The remaining antimetrical moments have to be superimposed thus to the symmetrical ones in order to get the complete cumulative frequency distribution as observed at one side of the stabilizer.

The same remarks as made before refer also to the incremental bending moments of the stabilizer as measured in squadron B, see Figure 12, where only the cumulative numbers of mean crossings per flight are less than those of squadron A, but the ratio of them is similar.

The foregoing, brief discussion of some of the results obtained from in-flight measurements give the basis for the solution of the problem of a relation between c.g. vertical accelerations and loads at the tailplane.

[+] The incremental load factor due to a $\pm$ 50 fps-gust at zero altitude and M = 0.68 is for the given airplane in clean configuration and for an average gross weight $\Delta n_z = \pm 1.6$.

Recalling the remark already made in Paragraph 3.1, that the accelerations allow only to derive incremental loads in the direction and at the point where they have been measured, as a first step a cross-plot of simultaneously occurring values of incremental load factors versus incremental symmetric bending moments at the tailplane has been made, see Figure 13. Although only increments are taken into account and although only symmetrical bending moments are correlated with vertical accelerations, the result might be called by a statistician a low correlation. That is, nevertheless, what one might have anticipated, because the load-time history at the tailplane must not be always in phase with the c.g. acceleration. This is not only due to dynamic effects but results also from the fact that for generating a manoeuvre acceleration in the c.g. of the airplane first e.g. a stabilizer deflection and thus a bending moment increment has to preceed. There may, moreover, be loads at the stabilizer without any measurable response in the c.g. and also c.g. accelerations without any effect on the symmetrical stabilizer loads. This is the reason, why a correlation between c.g. accelerations and bending moment increments at the tailplane will never be successful on a deterministic basis.

That problem can be solved by means of the cumulative frequency distribution, if it is recalled, that during such a statistical analysis the individual peaks, ranges, or whatever has been counted from the load time history are ordered with regard to their respective magnitudes and cumulative numbers of occurrences. If two cumulative frequency distributions are given, the load time histories of which have been recorded simultaneously during a representative period of time, where representative refers here beyond the normal definition also to the condition as postulated in Paragraph 3.1, that the ratio of airplane movements in vertical direction to those in other degrees of freedom will not change, then the conclusion can be drawn, that the ratio between those values of the cumulative frequency distributions, which have occurred with equal relative cumulative number of occurrences, will be constant. This allows to establish a correlation between c.g. vertical acceleration increments and symmetrical bending moment increments from the respective cumulative frequency distributions, see Figures 6, 11, 12 just by plotting those values, which have occurred with the same cumulative frequency per flight, see Figure 14. In order to pay regard to the trend observed in the correlation as shown in Figure 13, negative bending moments have been plotted with positive accelerations and vice versa.

As an example for the application of the correlation shown in Figure 14, the cumulative frequency distributions of symmetrical bending moment increments have been derived from the c.g. counting results as shown in Figure 1 (squadrons A and B), and have been compared with the respective measured distributions, see Figure 15.

4.3 Relations Between Bending and Torsion Moments at Stabilizer and Fin.

As a complement to the results shown in the previous Paragraphs the cumulative frequency distributions are presented for incremental stabilizer torsion moment, see Figure 16, incremental fin bending moment, see Figure 17, and incremental fin torsion moment, see Figure 18. Cross plots of simultaneously occurring values show, that there is a good correlation between the antimetrical stabilizer and the fin bending moment increments, see Figure 19. A still satisfying result is obtained, if increments of torsion versus bending moments at the fin are plotted, see Figure 20. The deviations from the averaging line may be explained by chordwise variations of the center of pressure.

5. CONCLUSION

The presented engineering solution for correlating two random load time histories, which was demonstrated for the example of c.g. vertical accelerations and loads at the tailplane, is based on the present possibilities for a fatigue life control of a fleet of airplanes. It is regarded to be only a step towards more detailed and more exact methods to be developed for an adequate description of the relations between load time histories, which occur at different points of a structure during the same time; it meets, however, the requirement to be asked by any other method applied for fatigue life control, which is, that the results of the measurements have not only to be suitable for fatigue life estimation but give also information for the design of new airplanes.

ACKNOWLEDGEMENT

REFERENCES

1. Schijve, J.: The Analysis of Random Load Time Histories with Relation to Fatigue Tests and Life Calculations. Published in: Fatigue of Aircraft Structures, ed. by W. Barrois and E.L. Ripley. Pergamon Press, 1963, pp 115-149.

2. Buxbaum, O.: Statistische Zählverfahren als Bindeglied zwischen Beanspruchungsmessung und Betriebsfestigkeitsversuch. Laboratorium für Betriebsfestigkeit, Technical Report No. TB-65 (1966).

3. Hahn, P.: Unpublished Reports EWR No. 148-67 and 149-67, Messerschmitt-Bölkow-Blohm GmbH, Unternehmensbereich Flugzeuge, Ottobrunn, 1967.

4. Sturgeon, J.R.: The Use of Accelerometers for Operational Load Measurements in Aircraft. Published in: Conference on Stresses in Service. Inst. of Civ. Engrs., London, March 1966, pp 43-48

5. Hohn, P.: Unpublished Interim Reports No. 1/72 and 2/72. Messerschmitt-Bölkow-Blohm GmbH, Unternehmensbereich Flugzeuge, Ottobrunn, February 1972.

6. Skopinski, T.H.,
   Aiken, J.W.S.,
   Huston, W.B. : Calibration of Strain-Gage Installations in Aircraft Structures for the Measurement of Flight Loads. NACA Report 1178, 1955.

Symbol	Squadron	Total Flight Time - hrs	No. of A/C Observed	Ext. Stores
o——o	A	1224	6	yes
•---•	B	481	4	no
□——□	C	650	4	yes
△——△	D	562	3	yes
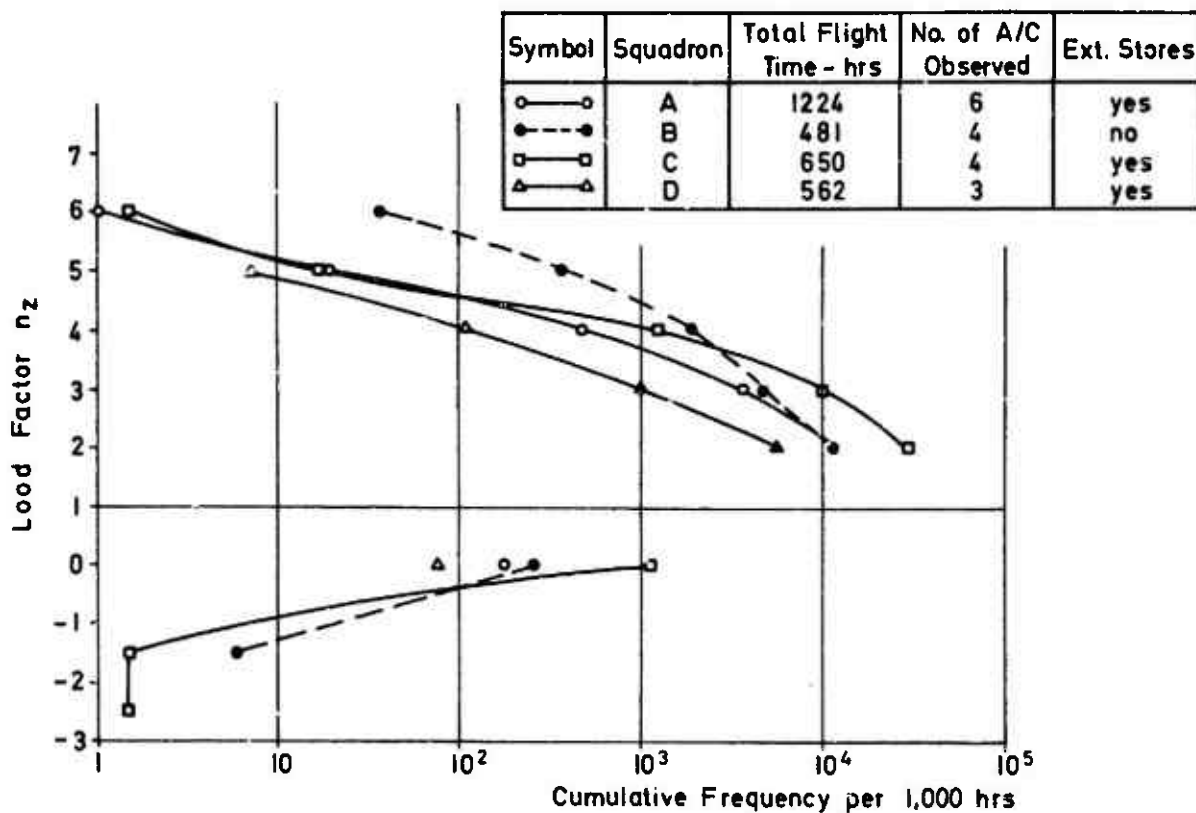
Fig.1 Average cumulative frequency distributions of load factors as experienced in four squadrons with different duties

Symbol	Total Flight Time-hrs
x	275
•	138
△	30
o	494
▲	170
□	147
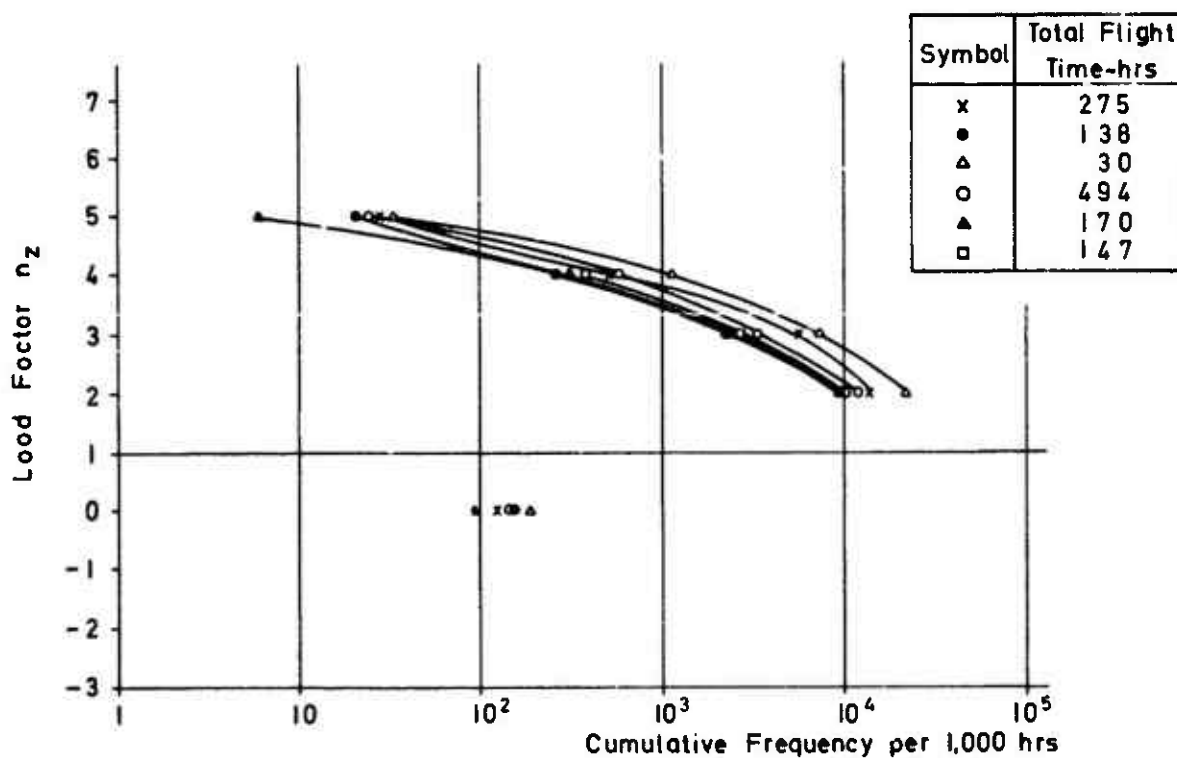
Fig.2 Cumulative frequency distributions of load factors as experienced by individual airplanes within one squadron
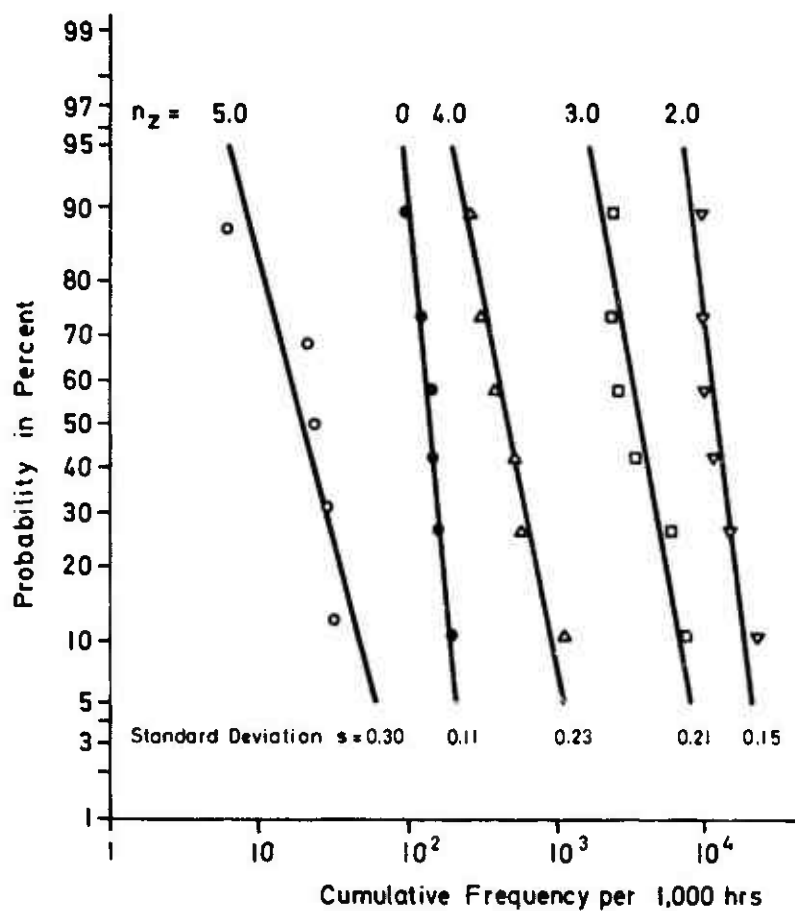
Fig.3   Scatter of cumulative frequency distributions of load factors as experienced by airplanes within one squadron.   (Statistical analysis of results shown in Figure 2.)
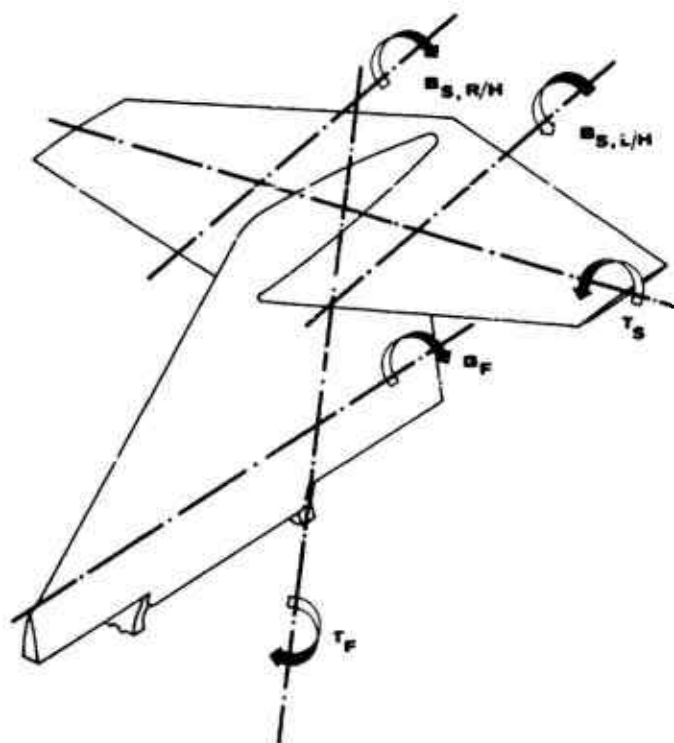
Fig.4   Sections at the tailplane with strain gage installations for measurement of bending and torsion moments
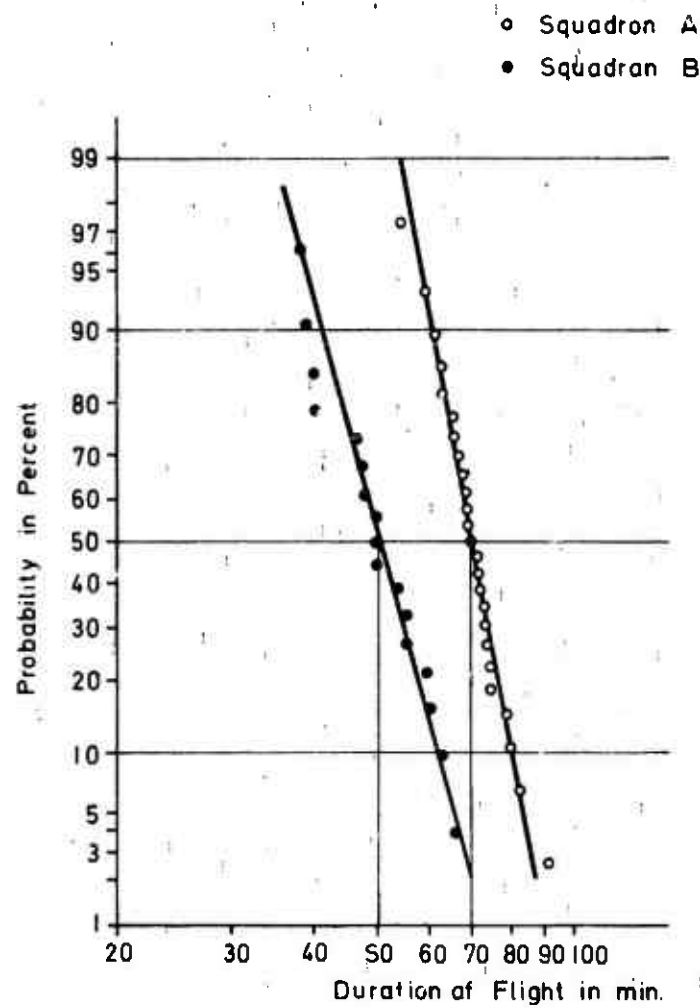
Fig.5   Statistical analysis of flight times of two squadrons
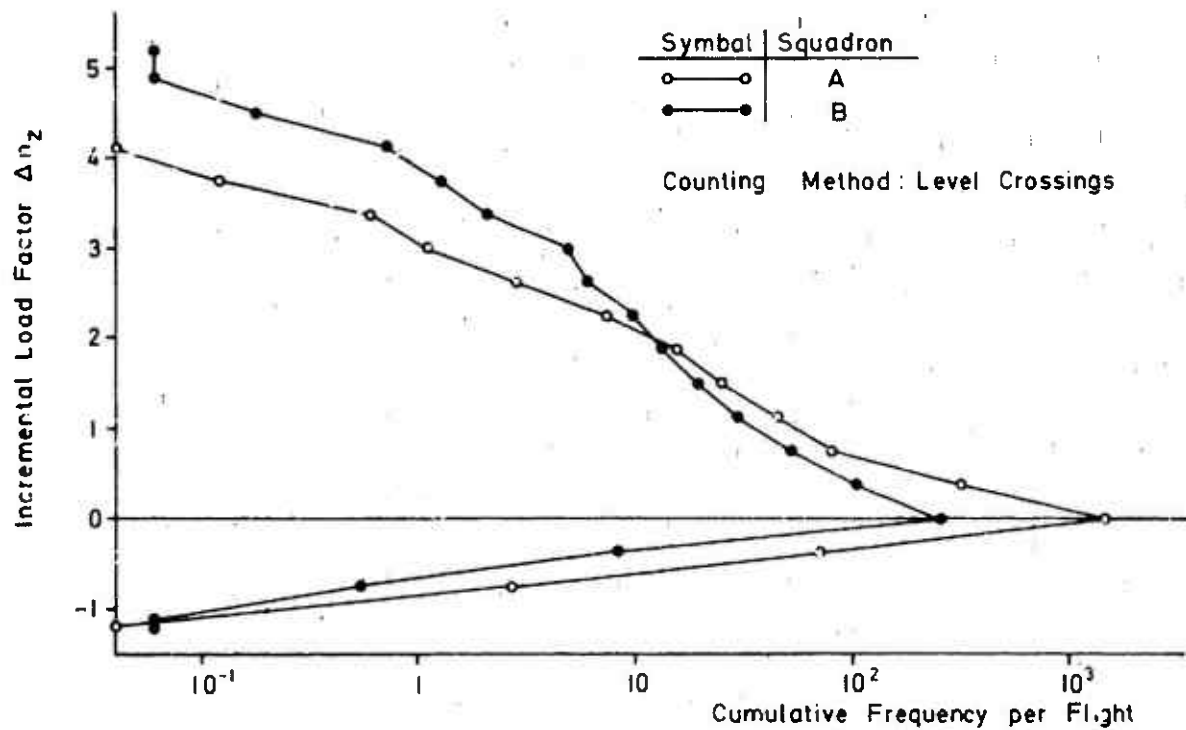
Fig.6   Cumulative frequency distributions of incremental load factors
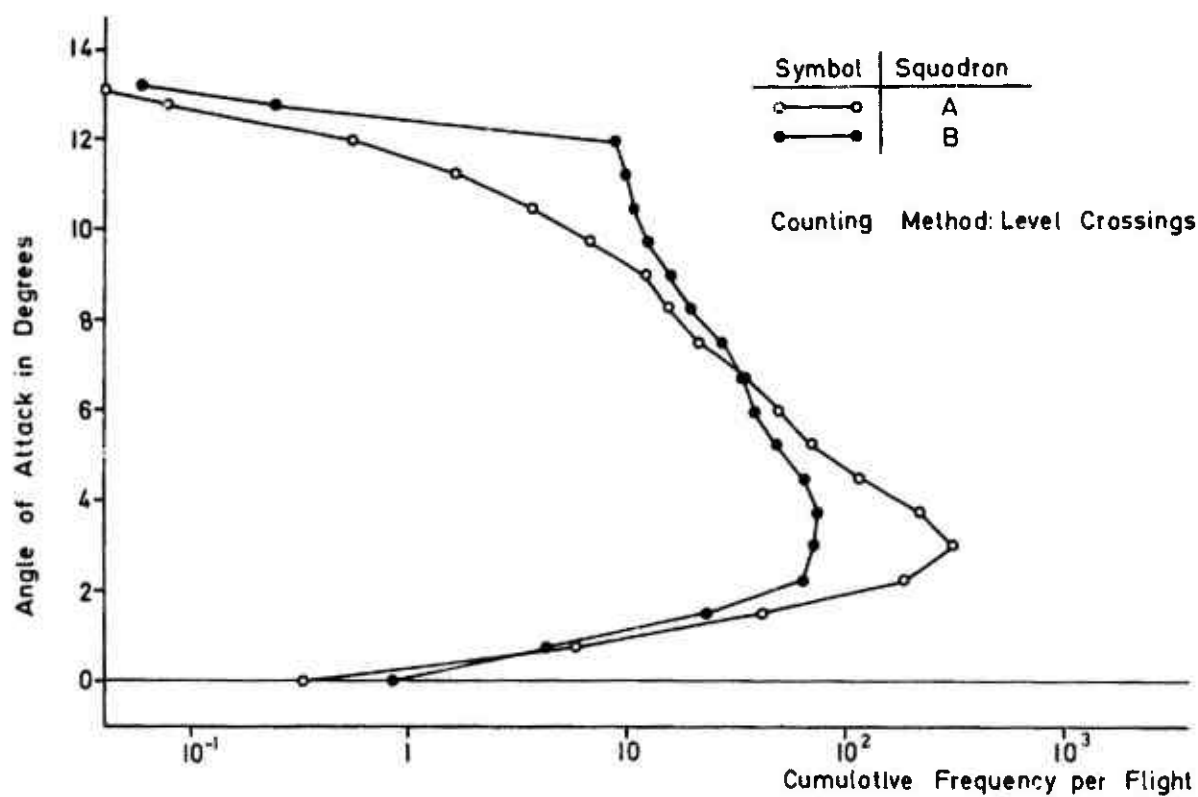
Fig.7   Cumulative frequency distributions of angles of attack
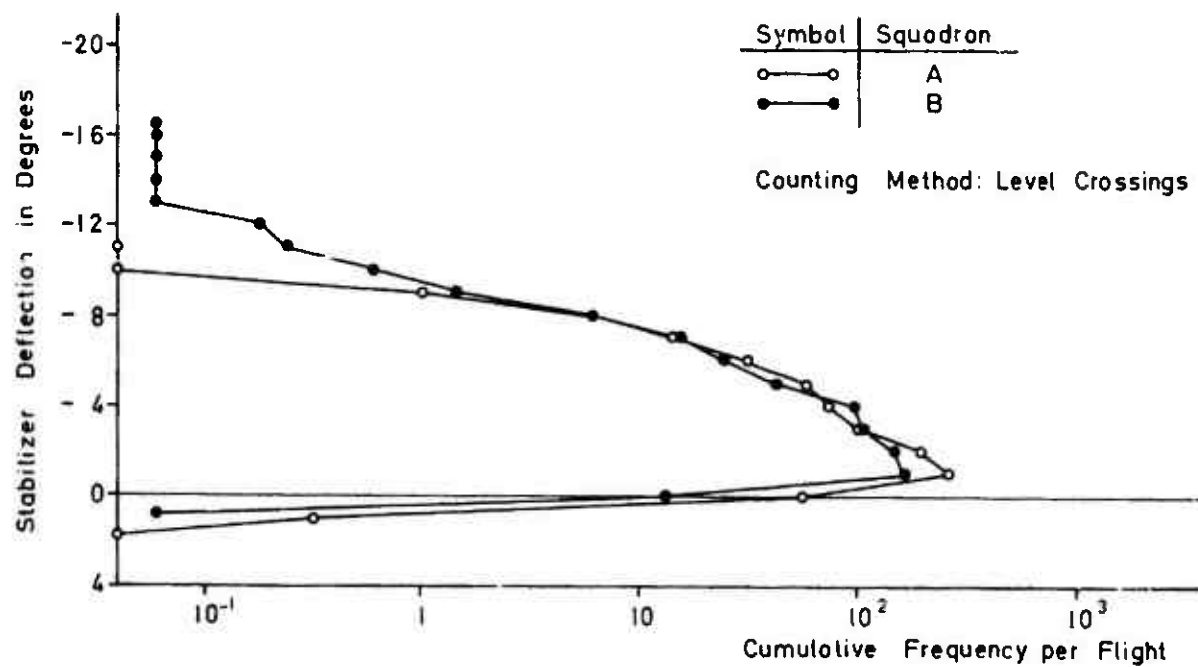
Fig.8   Cumulative frequency distributions of stabilizer deflections
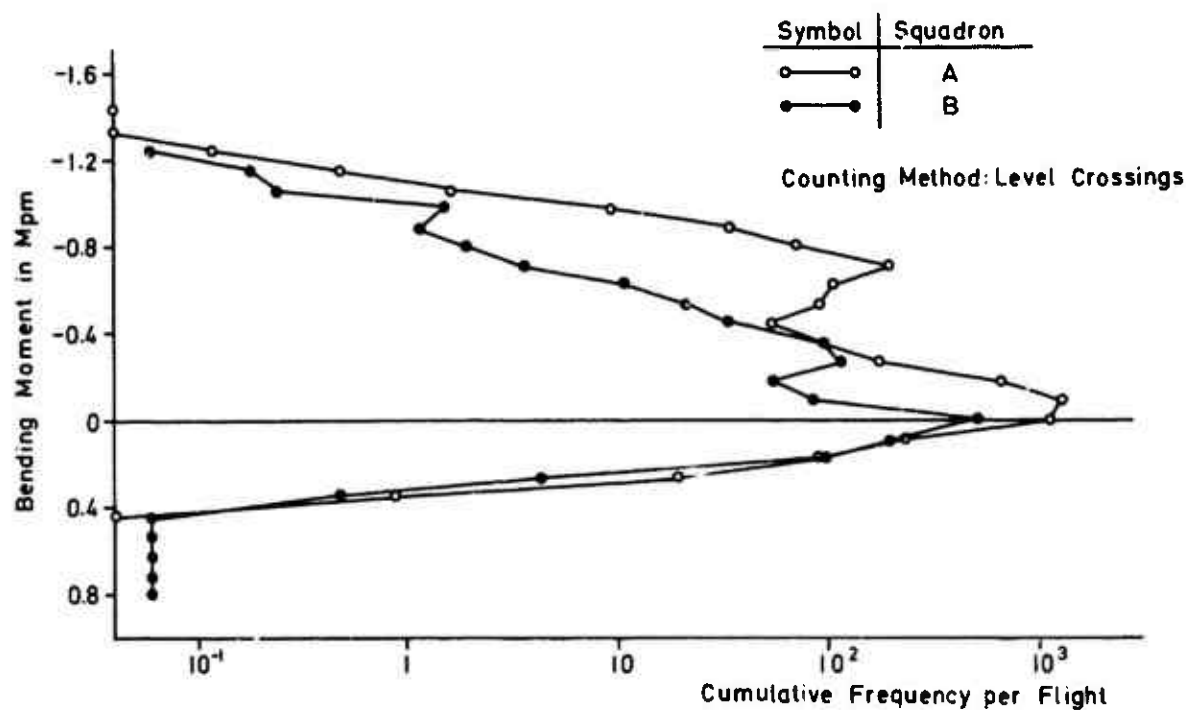
Fig.9 Cumulative frequency distributions of R/H stabilizer bending moment
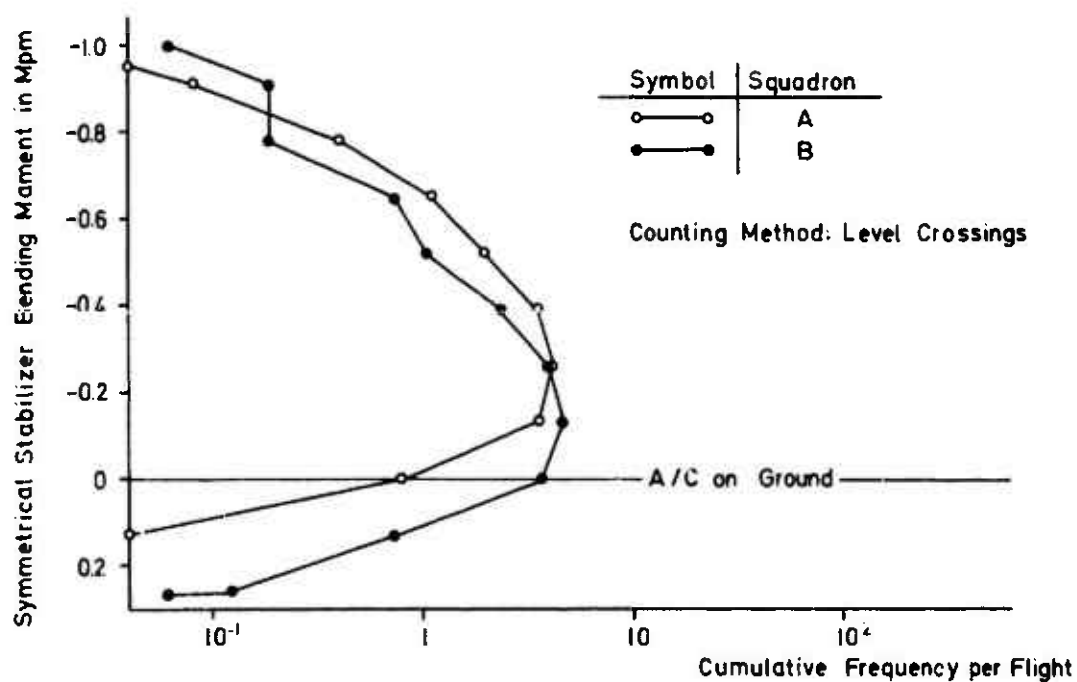
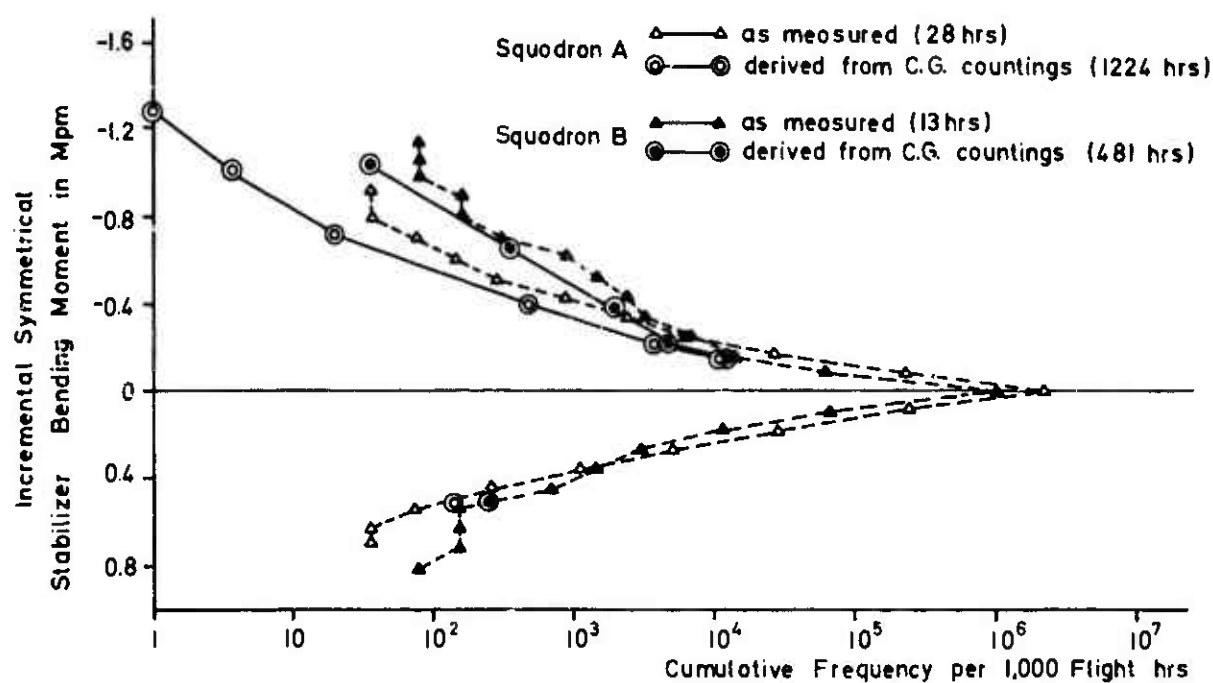Fig.10 Cumulative frequency distribution of symmetrical 1g-bending moment at the stabilizer
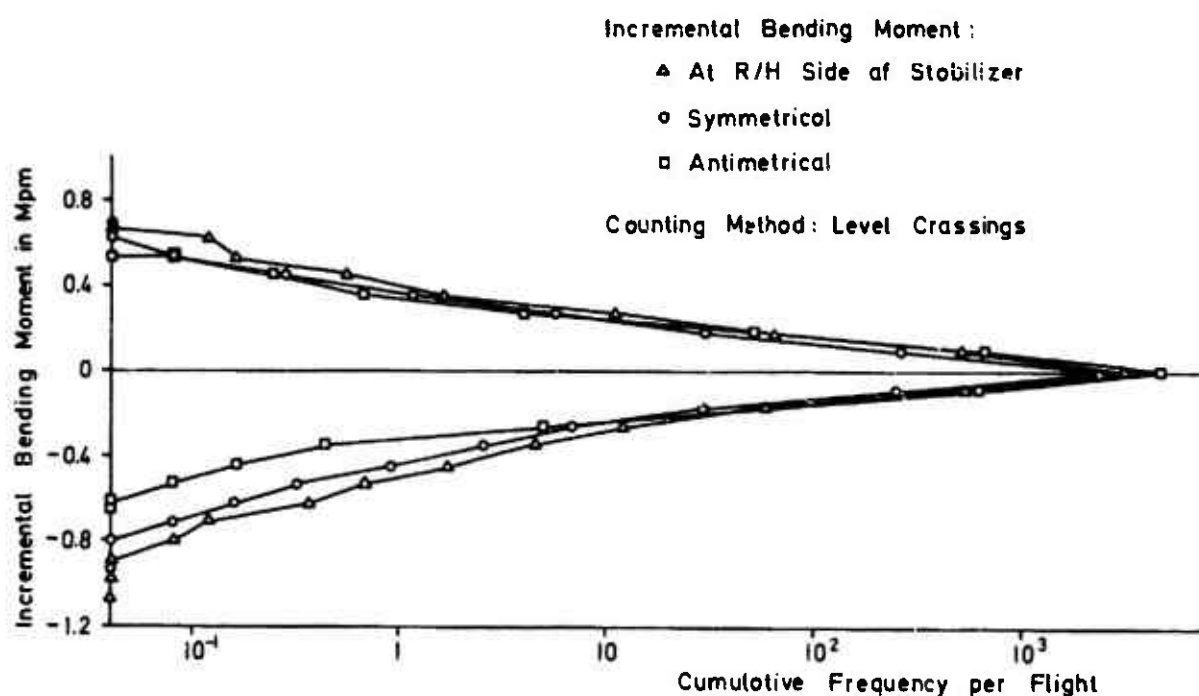
Fig.11 Cumulative frequency distributions of incremental stabilizer bending moments experienced in squadron A
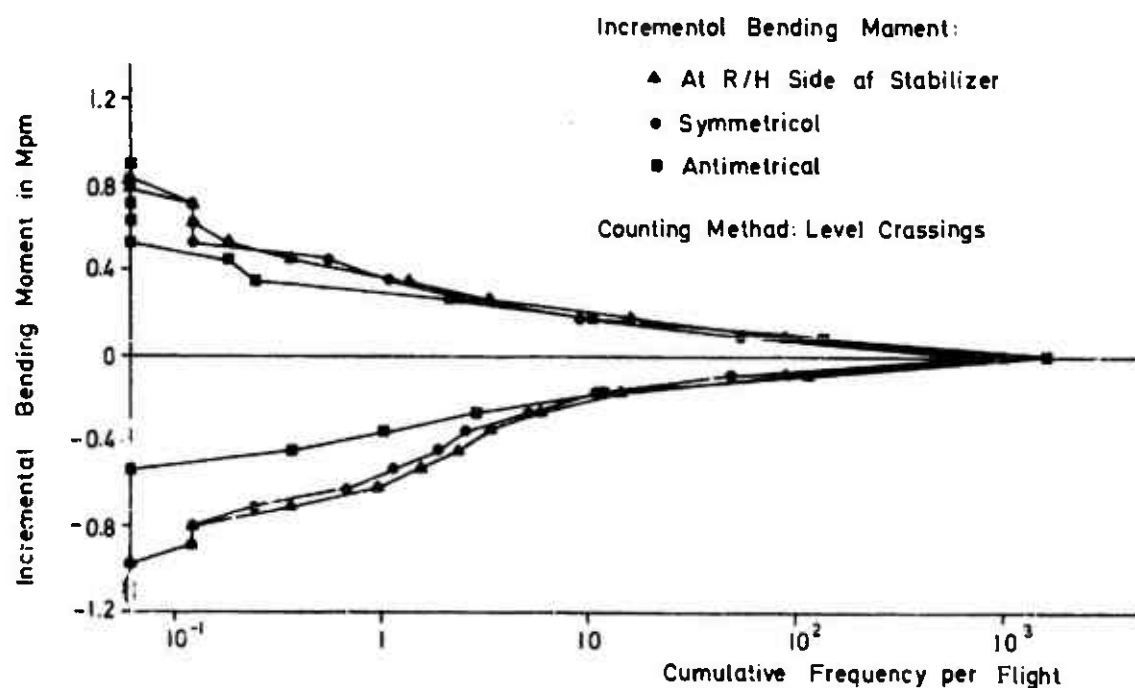
Fig.12 Cumulative frequency distributions of incremental stabilizer bending moments experienced in squadron B
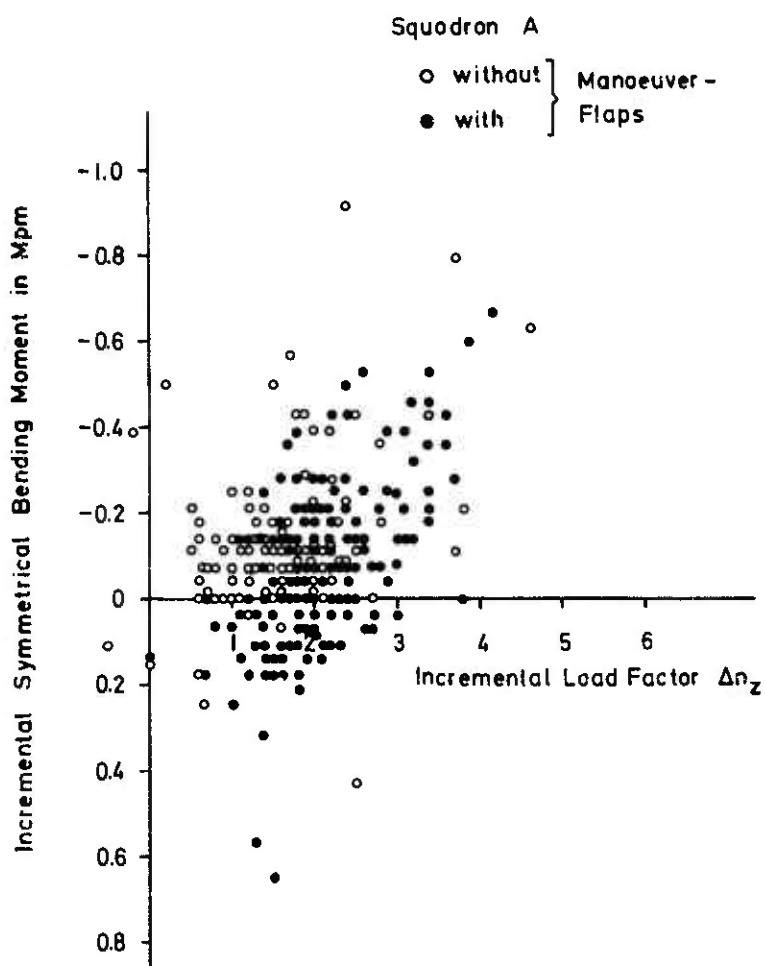
Fig. 13 Simultaneously occurring values of increments of symmetrical stabilizer bending moment and load factor
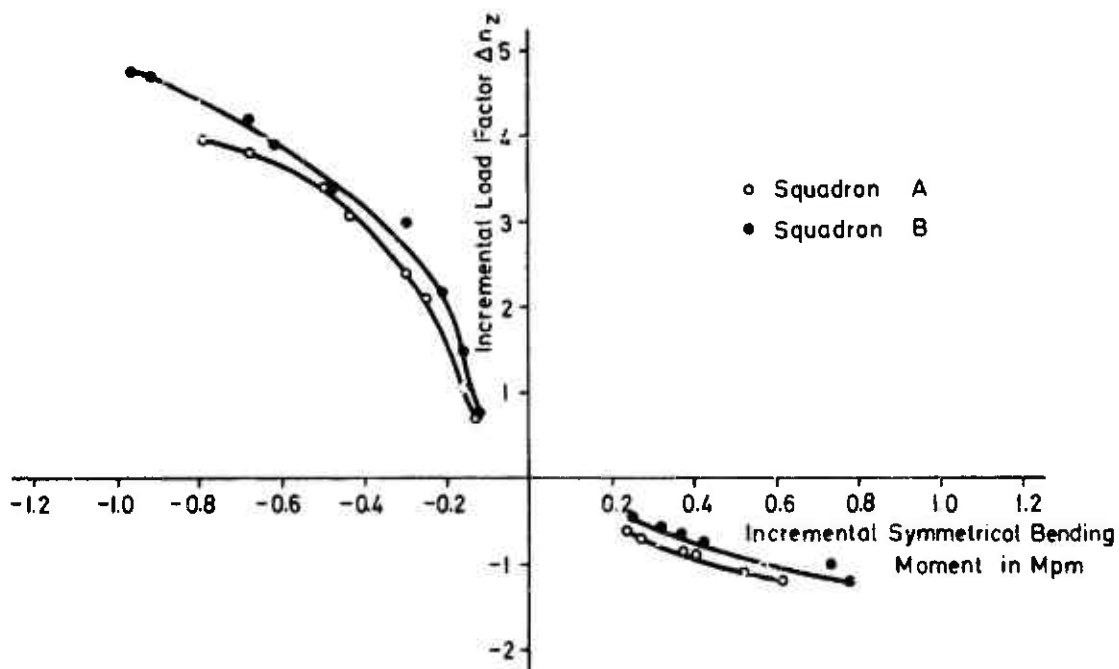
Fig. 14 Incremental load factors versus incremental symmetrical stabilizer bending moments occurring with equal relative cumulative frequencies

Fig.15   Comparison of cumulative frequency distributions of incremental
symmetrical bending moment at the stabilizer
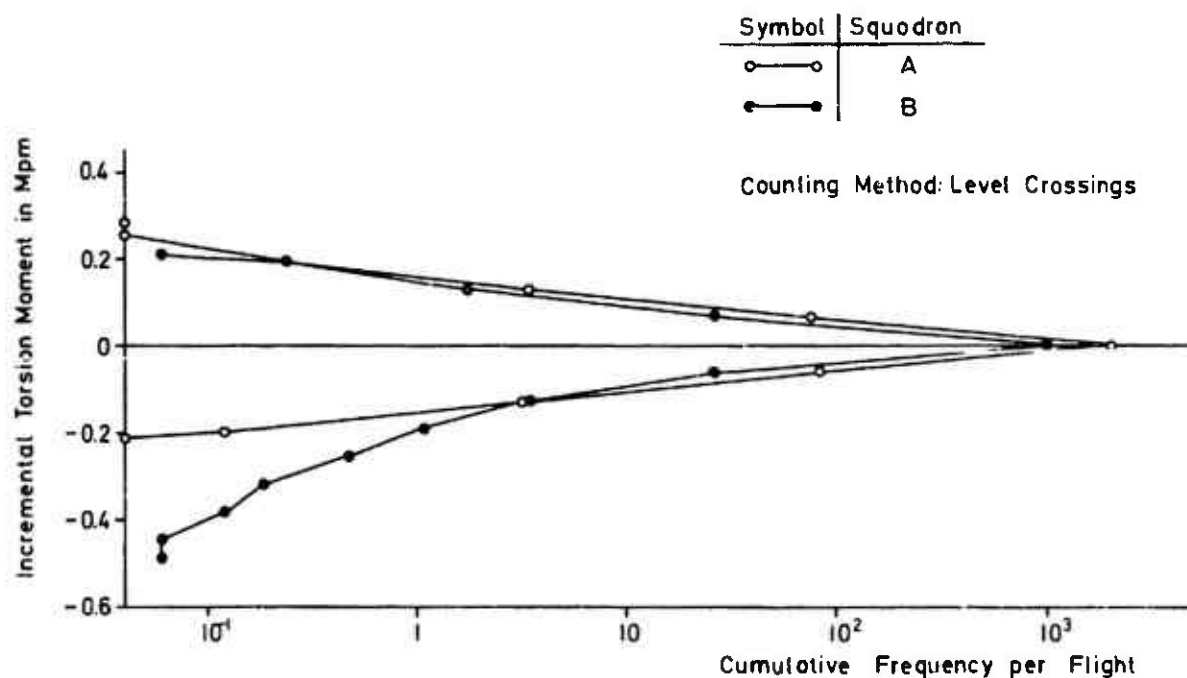
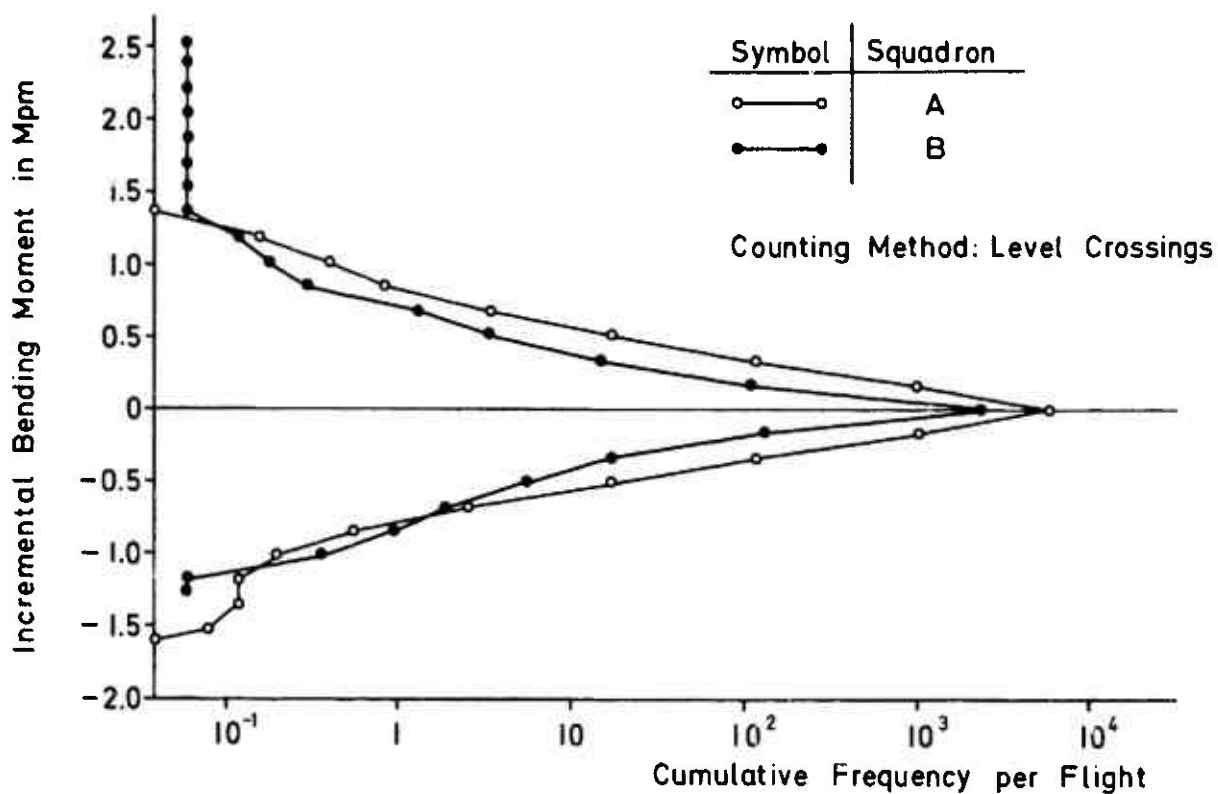Fig.16   Cumulative frequency distributions of incremental stabilizer torsion moments

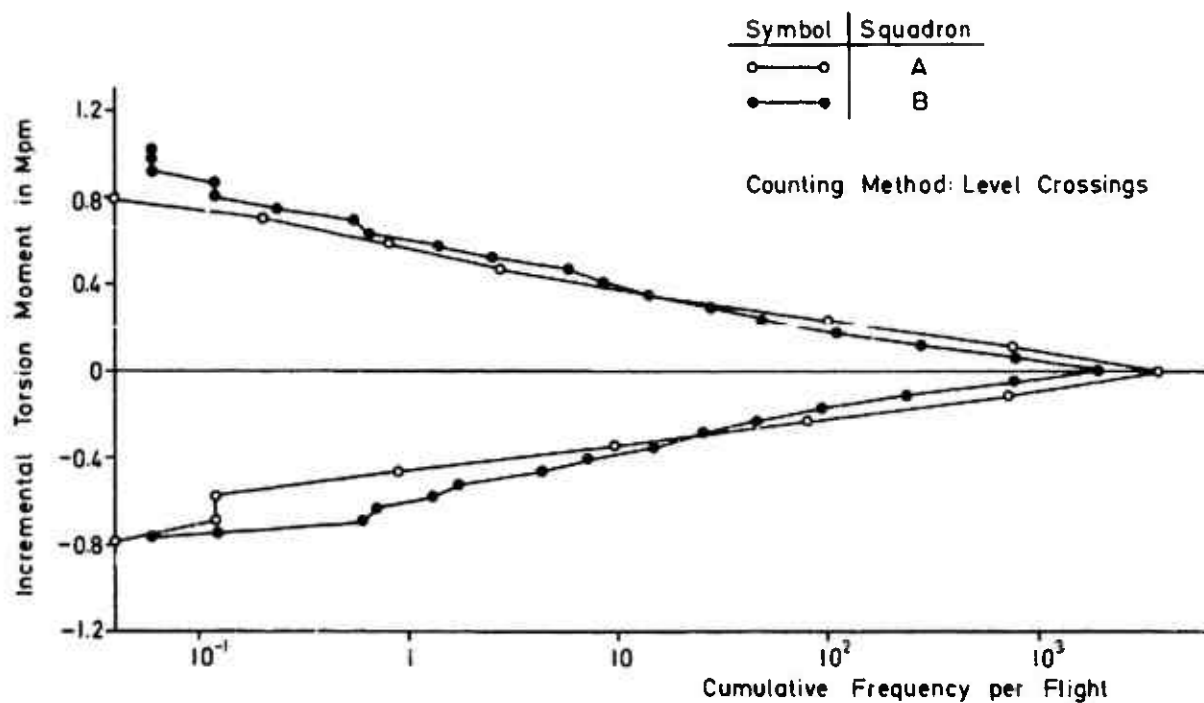Fig.17 Cumulative frequency distributions of incremental fin bending moments

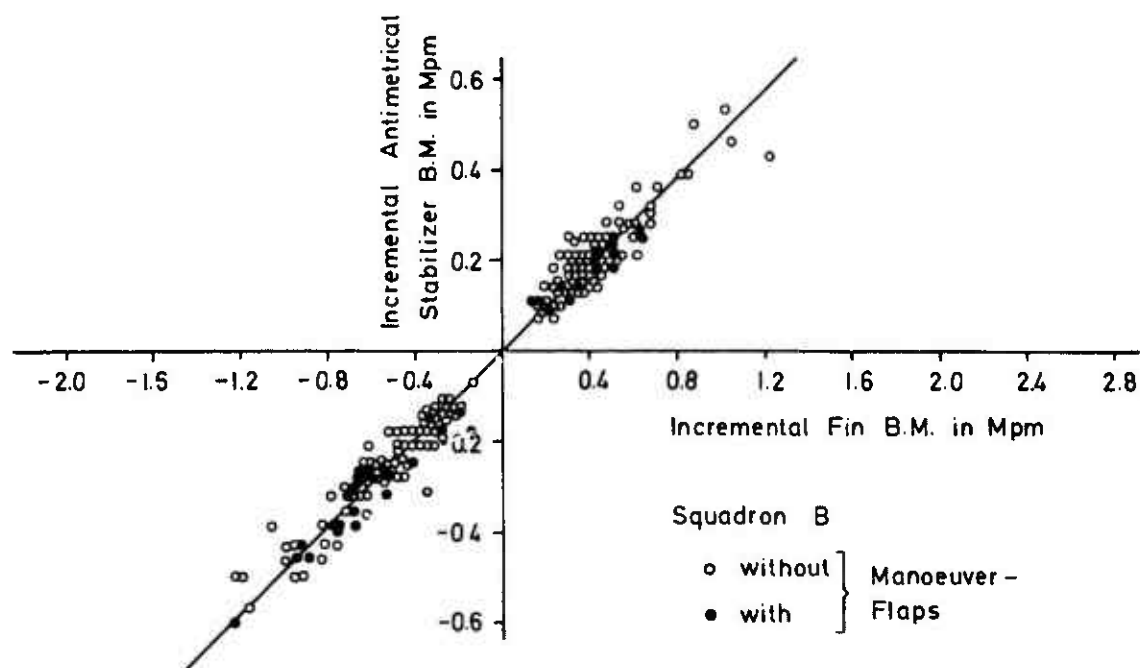Fig.18 Cumulative frequency distributions of incremental fin torsion moments

Fig.19 Simultaneously occurring values of increments of antimetrical
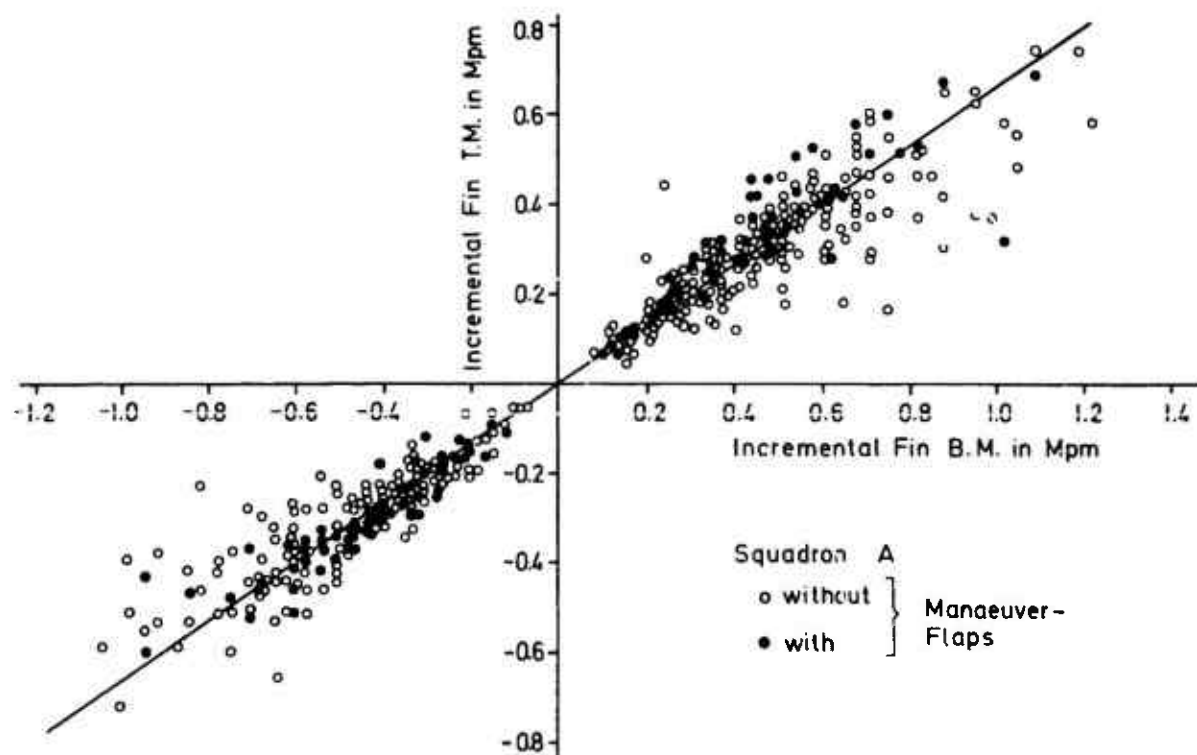stabilizer and fin bending moments

Fig.20 Simultaneously occurring values of increments of fin torsion and fin bending moments

Fatigue test procedures are discussed and comparison is made with service failures with a description of critical factors such as varying load spectra, differences in random load-time histories, spectrum changes during the life of an aircraft, etc.

Methods for predicting the fatigue life of aircraft structures are reviewed and recent achievements for improved life estimation are reported.

Papers presented at the Structures and Materials Panel 24th Meeting held in Lyngby, Denmark, 13 April 1972.

Fatigue test procedures are discussed and comparison is made with service failures with a description of critical factors such as varying load spectra, differences in random load-time histories, spectrum changes during the life of an aircraft, etc.

Methods for predicting the fatigue life of aircraft structures are reviewed and recent achievements for improved life estimation are reported.

Papers presented at the Structures and Materials Panel 34th Meeting held in Lyngby, Denmark, 13 April 1972.

Fatigue test procedures are discussed and comparison is made with service failures with a description of critical factors such as varying load spectra, differences in random load-time histories, spectrum changes during the life of an aircraft, etc.

Methods for predicting the fatigue life of aircraft structures are reviewed and recent achievements for improved life estimation are reported.

Papers presented at the Structures and Materials Panel 34th Meeting held in Lyngby, Denmark, 13 April 1972.

Fatigue test procedures are discussed and comparison is made with service failures with a description of critical factors such as varying load spectra, differences in random load-time histories, spectrum changes during the life of an aircraft, etc.

Methods for predicting the fatigue life of aircraft structures are reviewed and recent achievements for improved life estimation are reported.

Papers presented at the Structures and Materials Panel 34th Meeting held in Lyngby, Denmark, 13 April 1972.

AGARD Conference Proceedings No.118
North Atlantic Treaty Organization, Advisory Group
for Aerospace Research and Development
SYMPOSIUM ON RANDOM LOAD FATIGUE
Published October 1972
246 pages

AGARD-CP-118

539.43

Eight papers were presented at this Symposium.
Physical aspects of fatigue damage accumulation and
the significance of theories for the calculation of
fatigue damage accumulation are reviewed. Influence
of test frequencies on crack propagation rates,
measurements of residual stresses in notched speci-
mens, etc. are reported.

P.T.O

AGARD Conference Proceedings No.118
North Atlantic Treaty Organization, Advisory Group
for Aerospace Research and Development
SYMPOSIUM ON RANDOM LOAD FATIGUE
Published October 1972
246 pages

AGARD-CP-118

539.43

Eight papers were presented at this Symposium.
Physical aspects of fatigue damage accumulation and
the significance of theories for the calculation of
fatigue damage accumulation are reviewed. Influence
of test frequencies on crack propagation rates,
measurements of residual stresses in notched speci-
mens, etc. are reported.

P.T.O.

AGARD Conference Proceedings No.118
North Atlantic Treaty Organization, Advisory Group
for Aerospace Research and Development
SYMPOSIUM ON RANDOM LOAD FATIGUE
Published October 1972
246 pages

AGARD-CP-118

539.43

Eight papers were presented at this Symposium.
Physical aspects of fatigue damage accumulation and
the significance of theories for the calculation of
fatigue damage accumulation are reviewed. Influence
of test frequencies on crack propagation rates,
measurements of residual stresses in notched speci-
mens, etc. are reported.

P.T.O

AGARD Conference Proceedings No.118
North Atlantic Treaty Organization, Advisory Group
for Aerospace Research and Development
SYMPOSIUM ON RANDOM LOAD FATIGUE
Published October 1972
246 pages

AGARD-CP-118

539.43

Eight papers were presented at this Symposium.
Physical aspects of fatigue damage accumulation and
the significance of theories for the calculation of
fatigue damage accumulation are reviewed. Influence
of test frequencies on crack propagation rates,
measurements of residual stresses in notched speci-
mens, etc. are reported.

P.T.O.

NATIONAL DISTRIBUTION CENTRES FOR UNCLASSIFIED AGARD PUBLICATIONS

Unclassified AGARD publications are distributed to NATO Member Nations
through the unclassified National Distribution Centres listed below

BELGIUM
Coordinateur AGARD – V.S.L.
Etat-Major Forces Aériennes
Caserne Prince Baudouin
Place Dailly, Bruxelles 3

CANADA
Director of Scientific Information Services
Defence Research Board
Department of National Defence – 'A' Building
Ottawa, Ontario

DENMARK
Danish Defence Research Board
Østerbrogades Kaserne
Copenhagen Ø

FRANCE
O.N.E.R.A. (Direction)
29, Avenue de la Division Leclerc
92, Châtillon-sous-Bagneux

GERMANY
Zentralstelle für Luftfahrtdokumentation
und Information
Maria-Theresia Str. 21
8 München 27

GREECE
Hellenic Armed Forces Command
D Branch, Athens

ICELAND
Director of Aviation
c/o Flugrad
Reykjavik

ITALY
Aeronautica Militare
Ufficio del Delegato Nazionale all'AGARD
3, Piazzale Adenauer
Roma/EUR

LUXEMBOURG
Obtainable through BELGIUM

NETHERLANDS
Netherlands Delegation to AGARD
National Aerospace Laboratory, NLR
P.O. Box 126
Delft

NORWAY
Norwegian Defense Research Establishment
Main Library,
P.O. Box 25
N-2007 Kjeller

PORTUGAL
Direccao do Servico de Material
da Forca Aerea
Rua de Escola Politecnica 42
Lisboa
Attn of AGARD National Delegate

TURKEY
Turkish General Staff (ARGE)
Ankara

UNITED KINGDOM
Defence Research Information Centre
Station Square House
St. Mary Cray
Orpington, Kent BR5 3RE

UNITED STATES
National Aeronautics and Space Administration (NASA)
Langley Field, Virginia 23365
Attn: Report Distribution and Storage Unit

*   *   *

If copies of the original publication are not available at these centres, the following may be purchased from:

Microfiche or Photocopy	*Microfiche*	*Microfiche*
National Technical Information Service (NTIS) 5285 Port Royal Road Springfield Virginia 22151, USA	ESRO/ELDO Space Documentation Service European Space Research Organization 114, Avenue Charles de Gaulle 92200, Neuilly sur Seine, France	Technology Reports Centre (DTI) Station Square House St. Mary Cray Orpington, Kent BR5 3RE England

The request for microfiche or photocopy of an AGARD document should include the AGARD serial number, title, author or editor, and publication date. Requests to NTIS should include the NASA accession report number.

Full bibliographical references and abstracts of the newly issued AGARD publications are given in the following bi-monthly abstract journals with indexes:

Scientific and Technical Aerospace Reports (STAR)
published by NASA,
Scientific and Technical Information Facility,
P.O. Box 33, College Park,
Maryland 20740, USA

United States Government Research and Development
Report Index (USGDRI), published by the
Clearinghouse for Federal Scientific and Technical
Information, Springfield, Virginia 22151, USA